POLITECNICO
MILANO 1863

SCUOLA DI INGEGNERIA INDUSTRIALE
E DELL'INFORMAZIONE

a2a
LIFE COMPANY

Potentialities of the floating offshore wind market in the Meditteranean

Tesi di Laurea Magistrale in
Energy Engineering - Ingegneria Energetica

Author: **Lisandru Giordani**

Student ID: 963789
Academic advisor: Prof. Paolo Silva
Company advisor: Sg. Davide Colzani
Academic Year: 2022-23

Acknowledgements

With this thesis my academic career comes to an end, and I must conclude it with a genuine testimony of gratefulness towards the many people who accompanied me along the way and offered me an essential support.
First of all, I must thank my amazing family who supported me so much. To my parents, thanks for having always encouraged me to follow my own path and doing everything you could to offer me the better. Your examples of hard work and goodwill guided me in my studies and more generally all along my life. To my dear sister then, thank you for the beautiful and inspiring person you became, we spent our whole life together and whatever what the future holds I know you will stand by my side. To my grandparents then (I briefly switch to French so they can understand this), merci pépé et mémé pour tous ce que vous avez fait pour moi et pour votre amour inconditionnel, vous êtes de vrais exemples pour moi. Finally, I would like to thank my girlfriend for this years by my side and the constant encouragements that have brighten up this academic path.
Then, I would like to strongly thank Mr. Davide Colzani for giving me the opportunity to lead this work in such a stimulative environment as A2A, for its gentleness and most of all for its availability and its constant yearning for help. Your critical mind, engineering knowledge and rigour helped me shape this thesis, and I hope will influence me in my professional career. I would also thanks the great A2A innovation team that welcomed me during 6 years, I learned a lot from you.
Obviously, I would like to thank Professor Paolo Silva for its time and for supervising my work on this promising field, as well as for its master courses that triggered my strong interest on the offshore wind sector.
To all my friends who have accompanied me on this long path, either in Ajaccio, Lyon or Milan: you have made this university stage unforgettable. I will have a particular thought for Slim and Andrea whose support during complicate phases made my Milanese journey easier.

Thanks to all,
Lisandru.

Abstract

Offshore wind is gaining momentum and will represent a strong asset for the world green transition challenge thanks to its great features in terms of production, power density, landscape impact and grid friendliness. Yet, classical fixed-bottom technologies fail to unlock the wide potential offered by stronger and more constant offshore winds since the potential sites are limited by seabed depth. Floating offshore wind (FOW) solves this issue thanks to technological solutions suited for deep waters. FOW offshore wind is a young but promising sector. After years of R&D and POCs on floating substructures notably, pre-commercial scale farms have been commissioned and an important pipeline of projects, counted down and analysed in this work, is announced. The challenge of FOW sector is now to develop its supply chain and to optimise its production costs. The capital expenditures (CAPEX) of FOW projects are at the base of this work and the main cost drivers – Turbines, Floaters, moorings and anchors, connection to grid, inner-array cables and installation – have been identified and deeply analysed. Many factors will generate cost reduction, among which the introduction of ever bigger turbines which will have a positive impact on floaters and mooring devices. These last two elements can currently be considered as the critical elements of FOW and the forecast of their specific cost evolution with commissioning year have been supported by a physical model based on external loads mitigation. This model study the two main floaters technologies identified: tension leg platforms (TLP) and Semi-submersibles (SS). In the Mediterranean, FOW will face lower wind resources and higher depths than in main zones of development (North sea for example). Yet, the drops in CAPEX, alongside others phenomenon, will make FOW competitive by 2035 and the sector can become a strong asset for Mediterranean countries. This economic viability analysis is supported by levelized cost of electricity (LCOE) calculations. In this development path of FOW, the control of the visual impact on landscapes and the use of TLP, well suited for the high Mediterranean depths, will be primordial.

Keywords: Offshore wind, Floating, CAPEX, LCOE, Forecast, External loads mitigation

Sommario

L'eolico offshore sta guadagnando slancio e rappresenterà una forte risorsa per la sfida mondiale della transizione verde, grazie alle sue ottime caratteristiche in termini di produzione, densità di potenza, impatto paesaggistico e facilità di connessione alla rete. Tuttavia, le classiche tecnologie a fondo fisso non riescono a sbloccare l'ampio potenziale offerto da venti offshore più forti e costanti, poiché i siti potenziali sono limitati dalla profondità del fondale marino. L'eolico offshore galleggiante (EOG) risolve questo problema grazie a soluzioni tecnologiche adatte alle acque profonde. L'EOG è un settore giovane ma promettente. Dopo anni di R&D e POC sulle sottostrutture galleggiante, sono stati messi in funzione parchi su scala pre-commerciale ed è stata annunciata un'importante pipeline di progetti, contati e analizzati in questo lavoro. La sfida del settore FOW è ora quella di sviluppare la propria supply chain ed ottimizzare i costi di produzione. Le spese in conto capitale (CAPEX) dei progetti EOG sono alla base di questo lavoro e i principali fattori di costo - turbine, struture galleggiante, ormeggi e ancoraggi, connessione alla rete, cavi interni e installazione - sono stati identificati e analizzati in profondità. Molti fattori genereranno una riduzione dei costi, tra cui l'introduzione di turbine sempre più grandi che avranno un impatto positivo principalmente sulle strutture galleggiante e sui dispositivi di ormeggio. Questi ultimi due elementi possono essere considerati come gli elementi critici del EOG e la previsione dell'evoluzione dei loro costi specifici con l'anno di messa in servizio è stata supportata da un modello fisico basato sulla mitigazione dei carichi esterni. Questo modello studia le due principali tecnologie di galleggiamento identificate: le Tension leg platforms (TLP) e i Semi-Submersibles (SS). Nel Mediterraneo, l'EOG deve affrontare risorse eoliche inferiori e profondità più elevate rispetto alle principali zone di sviluppo (ad esempio, il Mare del Nord). Tuttavia, la riduzione del CAPEX, insieme ad altri fenomeni, renderà il FOW competitivo entro il 2035 e il settore potrà diventare una forte risorsa per i Paesi del Mediterraneo. Questa analisi di redditività economica è supportata da calcoli del costo livellato dell'elettricità (LCOE). In questo percorso di sviluppo dell'eolico, il controllo dell'impatto visivo sul paesaggio e l'uso del TLP, ben adatto alle alte profondità del Mediterraneo, saranno primordiali.

Extended abstract

Introduction

In recent years, there has been growing interest in the development of renewable energy sources to reduce the world's dependence on fossil fuels and decrease greenhouse gas emissions. The offshore wind industry is one of the fastest-growing sectors in renewable energy and appears as a strong asset for countries yearning at a complete decarbonation of their energy sector in the decades to come. For the last twenty years, offshore wind sector development relied on fixed-bottom substructures, but this technology fails to unlock the whole potential of offshore wind power since only shallow sites are suited for this type of projects. By offering a solution to this limitation, floating offshore wind (FOW) technology has attracted significant attention in the recent years. The Mediterranean Sea, and even more particularly Italy, with its vast coastline and relatively deep waters, may benefits from this FOW development that could allow the development of an offshore wind sector in zones where fixed-bottom solutions were out of questions. This master thesis work being developed in collaboration with A2A s.p.a, a particular emphasis on this zone will be put.

The aim of this master thesis is to assess the potentialities of FOW technology in general and more specially the Mediterranean, taking into account the technical, economic, logistical and Nimby aspects. The thesis will explore the current state and future potential evolution of FOW technology and market (main industrial players and domestic markets will be presented). A deep assessment of CAPEX (capital expenditures) for FOW projects will be led, allowing the identification of main cost drivers and generating a detailed forecast of their evolution with time. This CAPEX model will then be used as a base for the analyse the economic feasibility of FOW projects in the Mediterranean. This economic feasibility assessment, materialised through the estimation of the levelized cost of electricity (LCOE) of various hypothetical projects, will also rely on considerations related to site characteristics (bathymetry and wind resources notably), operation and maintenance (O&M), financial aspects and visibility impact on landscapes.

The findings of this research could contribute to a better understanding of the potentiali-

ties of FOW technology as well as the challenges to face in the Mediterranean and provide potential valuable insights for policymakers, industry stakeholders, and investors. The results of the study will also contribute to the ongoing discussion on the role of renewable energy in achieving a sustainable energy future for the region and beyond.

Methodology

The research methodology for this master thesis is based on a combination of desk-based research, insights from hypothetical benchmark case studies and results obtained from in-house developed numerical models. To a lower extent, this work has also been supported by discussion with A2A specialist and industrial players interviewed within the framework of my internship in A2A.

Desk-based research will involve a comprehensive literature review of existing academic and industry literature on floating offshore wind technology to support the numerous assumptions and discussion performed in this work. The academic knowledge summoned in this study is wide since FOW is composed of numerous sub-fields and will be mainly obtained from online academic platforms opened by Politencico di Milano access. To nourish the physical based model used for CAPEX predictions or for wind production assessment, more global academic knowledge on wind power, mechanic of structures and hydrostatic will be cited. Then, the industrial knowledge will be used as a based for CAPEX model generation as well as for site impact assessment, O&M and financial hypothesis. In particular, this knowledge will be used to choose technological solution or farm configuration over another in our hypothetical benchmark project generation. This industrial knowledge will mainly be obtained thanks to private consulting agency or European industrial association gathering information from industrial players and field experts to create holistic reports on the subjects. Some of these contents are freely available to ease the diffusion of these important insights while other have been obtained through A2A. Let's note that the industrial knowledge on fixed-bottom solution, way more advanced regarding the maturity of the field, has been an important contribution to this fields since many links could be find with FOW. Similar reports on more global subjects (from the IEA for example) have also been used to characterise FOW within the global green transition context and to compare it with other energy sources for example. Other interesting sources for industrial knowledge on technology used, sites impact and future evolution were the documentation disclosed by project leaders in order to cope with public authorities requirements in terms of environmental impact and connection to the national grid (Italian and French ones notably).

Then online tools as national geo-portals for bathymetry information as well as wind atlas

and wind velocity online dataset were useful to simulate real life projects characteristics. The data collected for every site of interest will be controlled and sharpen in order to be the most representative possible of real life conditions.
Some of the results of desk-based research will support the elaboration of benchmark projects in the CAPEX evaluation model that will thus be representative of project for given time and site characteristic. The idea of this benchmark analysis process is to obtain concrete and insightful results of the CAPEX of a project with a maximum number of parameters entering in consideration. This wide rage of parameters allow us to work with a flexible model allow to give sensitive results and that will be then be suited to various site conditions later on. Yet, since the study here tends to deliver general insights and does not focus on one particular project, every single parameter impacting the cost and productivity of a FOW project will not be integrated to the model. For sake of representativeness and simplicity as well, some more precise consideration belonging to project-specified pre-studies will not be discussed in this project and general assumptions, backed-up by industrial and scientific data, will thus cemented the model.
The data collected or generated from benchmark analysis will sometimes have to be retrieved, analysed, transformed and reported in a way to highlight the useful insights. To do so, the software of business intelligence will be used Tableau will be used.

The proceeding of the work is set to be logically coordinated in order to finally be able to answer the global problematic of the master thesis. It will be divided in 3 distinct chapters, distinction being based on logical proceeding more than discussion length. Indeed, since the choice has been made to develop an holistic and strongly supported by physical and industrial background CAPEX model, the chapter 2 dedicated to this work will be significantly longer than the other ones. Yet, it would have few semantic sense to cut it in different smaller chapters. First, offshore wind is inserted and discussed within the green transition issue and its advantages of are presented and explained through physical aspects. Then the FOW market is widely discussed allowing to identify the main players and most of all the main domestic markets that will help us constitute representative benchmark projects later on. Then, main cost drivers are identified and deeply analysed for typical FOW projects. The development of a static based model allows us to generate a forecast on the dimensions of different floater types in different external conditions that will thus allow to predict the CAPEX evolution of the floating substructures. This dedicated model for floaters and moorings and anchors will then be inserted in a global CAPEX model from which insights on the CAPEX breakdown evolution of FOW with different parameters will be obtained and discussed. Finally, this CAPEX model will be used to assess the economic viability of benchmark floating projects in the Mediterranean.

The characteristics of the sites of interest where projects are simulated are included in the LCOE calculation which allow us to discuss the effective potentialities offered by future FOW in this zone.
As the thread of discourse proceeds, the methodology used may evolve. In chapter one, classical desk-based research is used to list the physical and engineering characteristics of FOW. A manual count down of existing announced FOW projects is notably performed and the data relatives to these projects are processed and reported via Tableau.
The overall objective is to develop a holistic CAPEX model able to take various input parameters in consideration to generate insightful information of the main cost drivers of a FOW project. Since floating platforms and moorings and anchors are the most critical and specific parts of a floating project (in comparison with classical fixed-bottom technology), a particular emphasis will be put on these elements. Thus, to predict their evolution in sizing with external conditions and the introduction of bigger turbines, a static model will be developed for the two typologies of turbines previously identified as the most interesting ones. The two block diagrams displayed here after describe a little more precisely how the physical static model is computed (first block diagram) and then inserted in the more global CAPEX model (second block diagram), the two being important pieces of this work. On the static model block diagram, the difference of nature between the parameters considered in the model can be seen: the inputs in blue are set by the user while in purple some constants are assumed thanks to academic and industrial data. Two distinct optimisation process are performed one the parameters highlighted in orange, one for the floaters and one for the moorings. The optimisation process, performed in Excel, is a combination of Excel solver and manual process and leads to desired outputs on dimension of platforms and size and numbers of the moorings lines.
The global CAPEX model includes even more inputs parameters, some will be used as input parameters of the static model, and the outputs of this one will be integrated to the global static model. The interest of the block diagram representation is to distinguish the inputs set by the user from the constants of the model but also to bring to light the direct and indirect impacts of one parameter to another until reaching the outputs of the model. As previously explained these two models are supported by academic and industrial results.

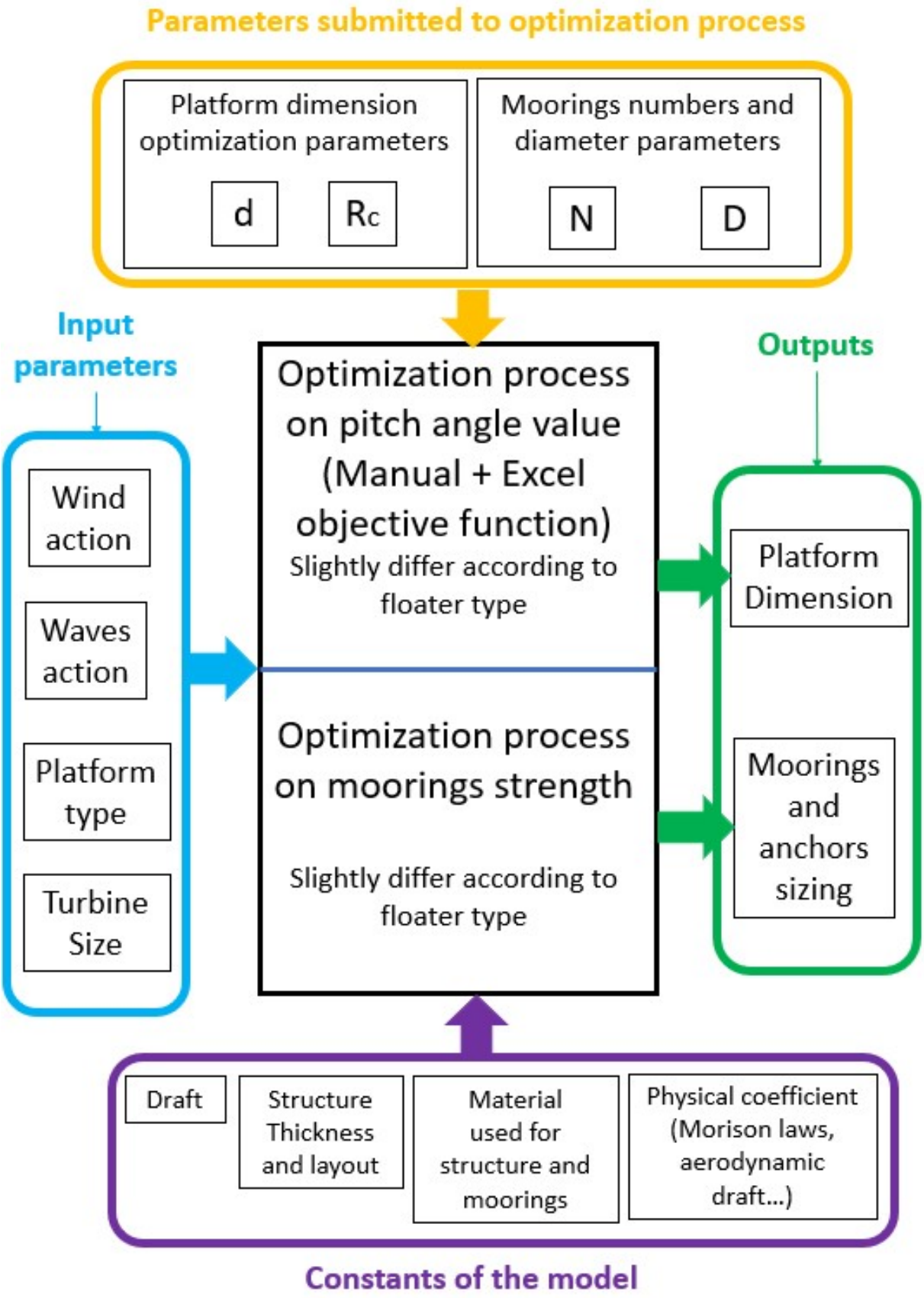

Inputs and outputs of the computed static model, cf figure 2.43

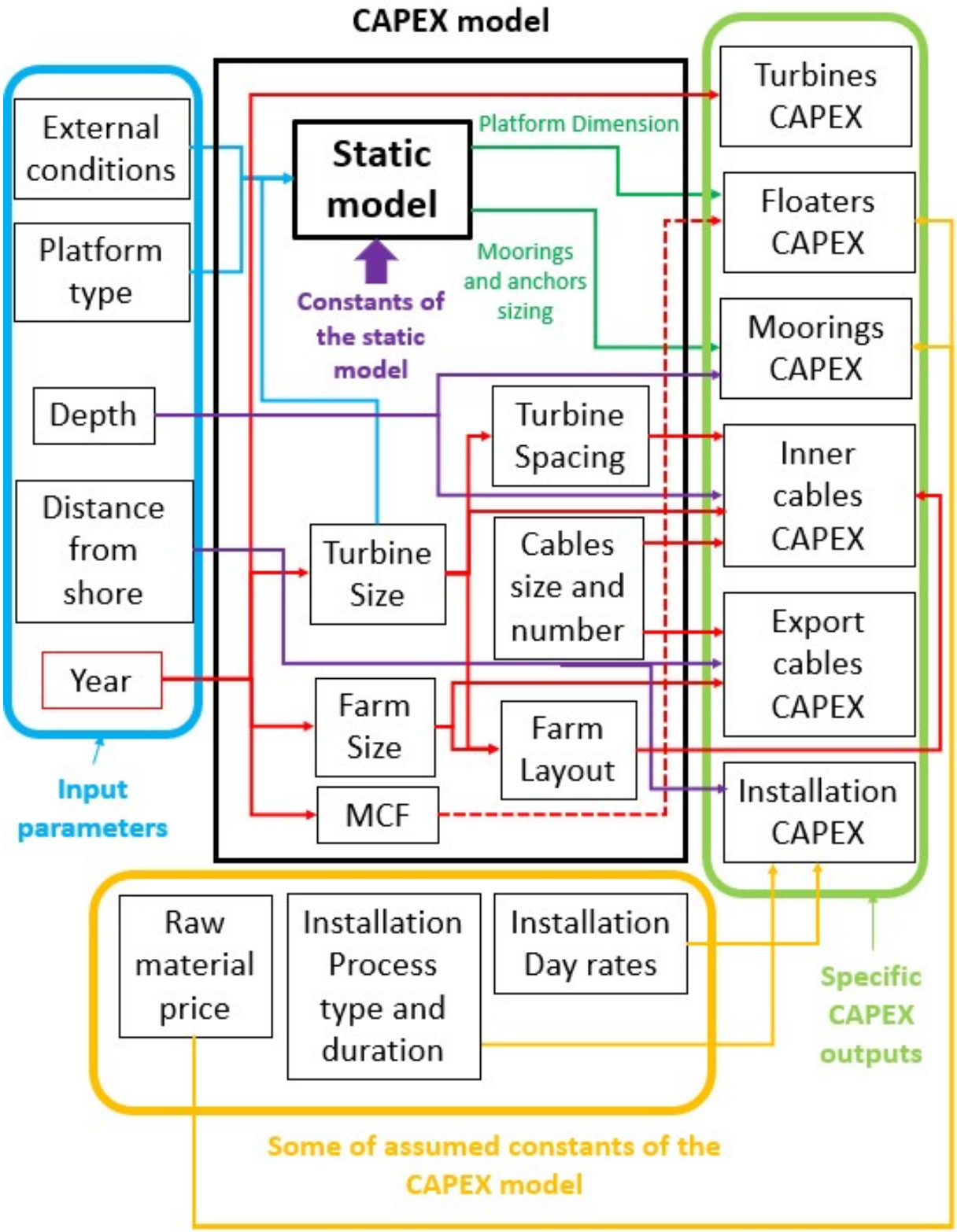

Inputs and outputs of the whole CAPEX model, cf figure 2.112

Sensitivity analyses on the inputs parameters will then be conducted and the results will be analysed and discussed along chapter 2.

Finally, third chapter is room to benchmark analysis on various hypothetical projects located in various zones chosen to be representative of FOW projects, and more particularly of Mediterranean and Italian FOW projects. The zones will be chosen mainly based on wind resources and existing or announced projects as well. Since an objective of this operation is to able a global site impact assessment, a diversity of site in terms of location, bathymetry and wind resource is yearned for. A particular emphasis will be put on the estimation of the productivity of these sites; that is why the wind dataset used for this scope will be sharpen and adjusted, accordingly to proven academic methodology, to be the more representative of real life condition.
The importance of visual impact of these projects will be regarded as a key elements of FOW projects, that is why a visibility impact evaluation framework will be built to be able to quantify this factor and take it in consideration in our analysis.
The LCOE will then be used as the criteria for evaluating the economic viability of each hypothetical project considered. The creation of a LCOE model, still computed on Excel, will thus be required and will consider many inputs parameters as the CAPEX results from chapter 2, the site impact assessment previously done but also O&M and financial related elements. The impact of losses, that can evolve with input parameter, will be included through VBA coding in Excel. Finally, adapting a LCOE estimator developed by A2A (based on the Excel solver) for renewables projects to our work, LCOE values will be generated for various sites and years. Sensitivity analyses on the inputs parameters will then be conducted and the results will be analysed and discussed. Comparison with other types of renewables sources will feed the final discussion on the global problematic of the work.

In the the study will use a mixed-methods approach to provide a comprehensive analysis of the potentialities of floating offshore wind in the Mediterranean. The methodology will be designed to provide a robust and reliable analysis of the technical, economic, and environmental factors that influence the feasibility of FOW projects in the region.

Results and sensitivity

Let's now have a glance to some of the main results obtained applying the methodology described above. The results presented here follow the chronological order of the thesis and only general comments on these will be made, further explanations being obviously available in the core of the thesis. In order to remain general and not overcharge the discourse of this extended abstract, representative charts and figures from the analysis have been extracted and will consist in the main support of presentation of the results. An important part of the results presented here after come out sensitivity analyses on the input parameters of the CAPEX and LCOE models.

Let's begin with insights from the FOW market overview led in chapter 1. To the pivot date of 01/01/2023, 98 projects have been counted and analysed in 15 different countries. In this list, the most ancient project is operating since 2010, and time-scope ranges until 2034 in terms of announced operating year (cf figure 1.28). Over this timescale, the global worldwide pipeline currently announced is 55,142 GW. Yet, the majority of these projects are still in planning phase and nowadays (01/01/2023) the global installed floating power capacity is about 115 MW, mainly located in UK via the two pre-commercial wind-farms and another 3 turbines farms of 25 MW located in Portugal. The 10 remaining MW are distributed between Norway, France and Japan through pilot projects developed by floater manufacturers. Plus, in the months to come, about 300 MW in cumulative capacity of projects under construction mainly in France, Norway and UK are set to increase the global park.

The following graph displays a forecast of power to be installed in the years to come, with countries of installation highlighted as well. The main insight from this graph is the expected skyrocketing from yearly installed power in the years to come, with a maximum of over 14 GW commissioned in 2031. Let's precise that the decrease after 2031 is not due to a slow of the market but to the fact that many projects are not disclosed yet. From this graph, we can point out that the years 2025-2026 are expected to become huge milestones for the field with what could be regarded afterwards as the pivot towards commercial state. Then, the commissioning dates for some of the planning stage projects must be taken with precaution, mostly for countries as Italy that announce a huge pipeline while having few experience in the fixed-offshore field.

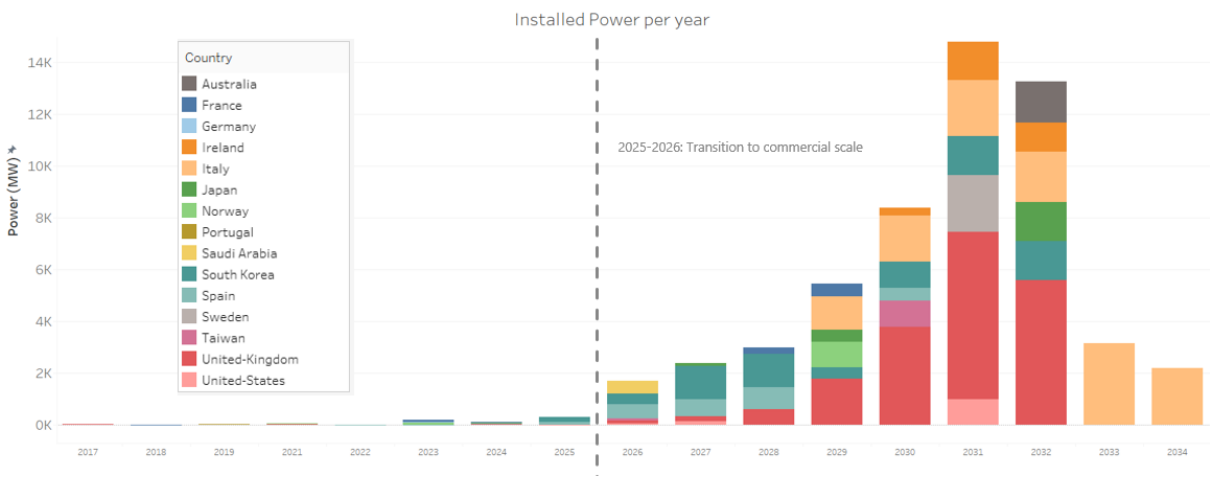

Yearly installed capacity forecast, cf figure 1.28

If getting insights from projects in early planning stage can be hazardous, the following map displays the countries with operating or under construction projects. This representation allow the identification of most ready domestic markets for FOW, that could be regarded as pioneers of the floating field. Alongside United-Kingdom, home of the two biggest operating farms, France appears as the other great pioneer of floating wind. Globally, the sector development is concentrated in Europe, Portugal, Spain and Norway following up. Finally, Italy and south Korea, while having huge announced pipelines, are yet to effectively enter the market, Italy has not even real experience in fixed-bottom offshore wind.

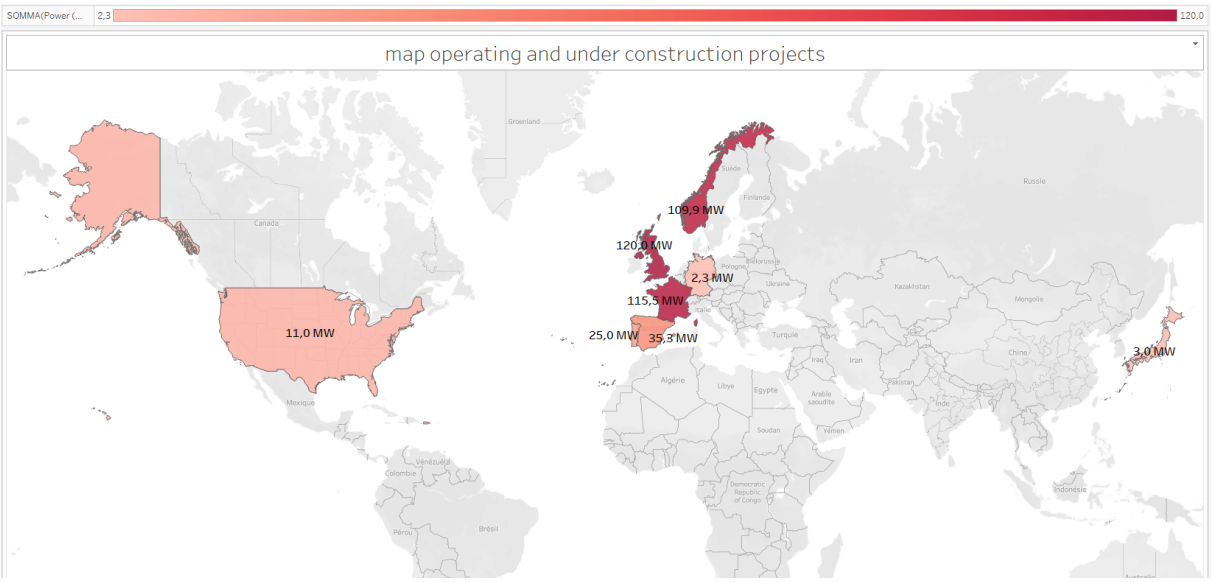

World map of most ready projects, cf figure 1.30

Let's now enter the an important share of the work performed in this master thesis: the creation of a CAPEX model for FOW projects described in chapter 2. This economical model will be organised into six different cost drivers as illustrated on the next figure. These six inner fields have been identified as the main cost drivers of the CAPEX of a FOW project. These six cost drivers, already presented the block diagram displayed in methodology section, will be technologically analysed and their impact will be discussed and predicted as well. Gathering the elements on these six fields will allow us to obtain a holistic CAPEX model. Let's precise that a particular emphasis will be put on the floating specifics, so as to say the moorings and anchors and most of all floating platforms. In addition, it will be obtained that the expected introduction of bigger turbines along the years will foster interesting economies of scale. These drops in cost will heavily assessed throughout chapter 2.

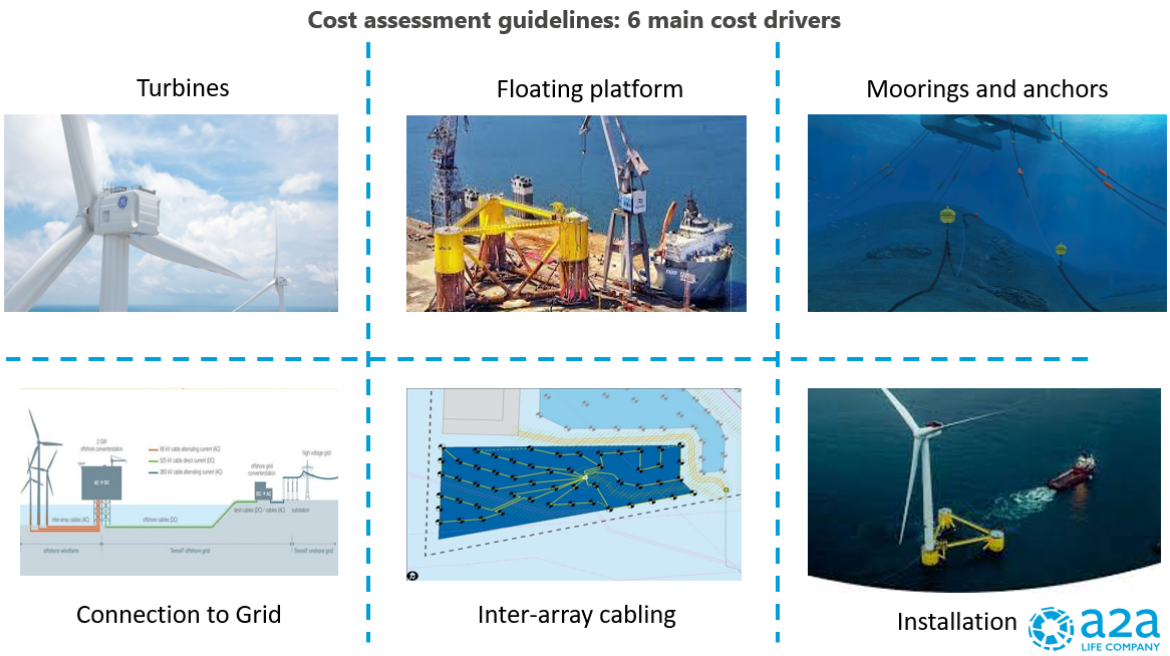

Different cost drivers for offshore floating projects, cf figure 2.1

Let's now focus on the static model computed for floaters through some outputs of the model displayed in the two graphs to come. The section 2.3.3 features many graphs and analysis related to the outputs of the static model for different external condition (representative of Mediterranean or oceanic conditions) and different floaters typologies, semi-submersibles (SS) and tension leg platforms (TLP) being the two typology analysed in the model. Let's precise that other typologies exist and are presented in chapter 2 yet, focus has been put on the two technologies considered as more promising ones (arguments in section 2.3). In this extended abstract, only an extract of these outputs is displayed

with here after the graph presenting the evolution with turbine size of external loads a SS platform is submitted to in Mediterranean conditions.
In Mediterranean conditions, unlike oceanic ones, wave and wind actions are comparable. The total external load remain almost proportional to the turbine power (in pink on specific external moment graph here after). Specific loads per power actually have opposite trends, such that wind contribution overpass wave one for huge turbines. In Mediterranean condition, specific wave moment has a decreasing trend with power but this decreasing effect is compensated by the wind behaviour. These results on external loads will feed the optimisation process (the whole static model is presented in subsection 2.3.2) that will be performed for different turbine size leading to the dimension of the SS floater in the Mediterranean. Same reasoning will be made for both external conditions types and both platform typologies as well.

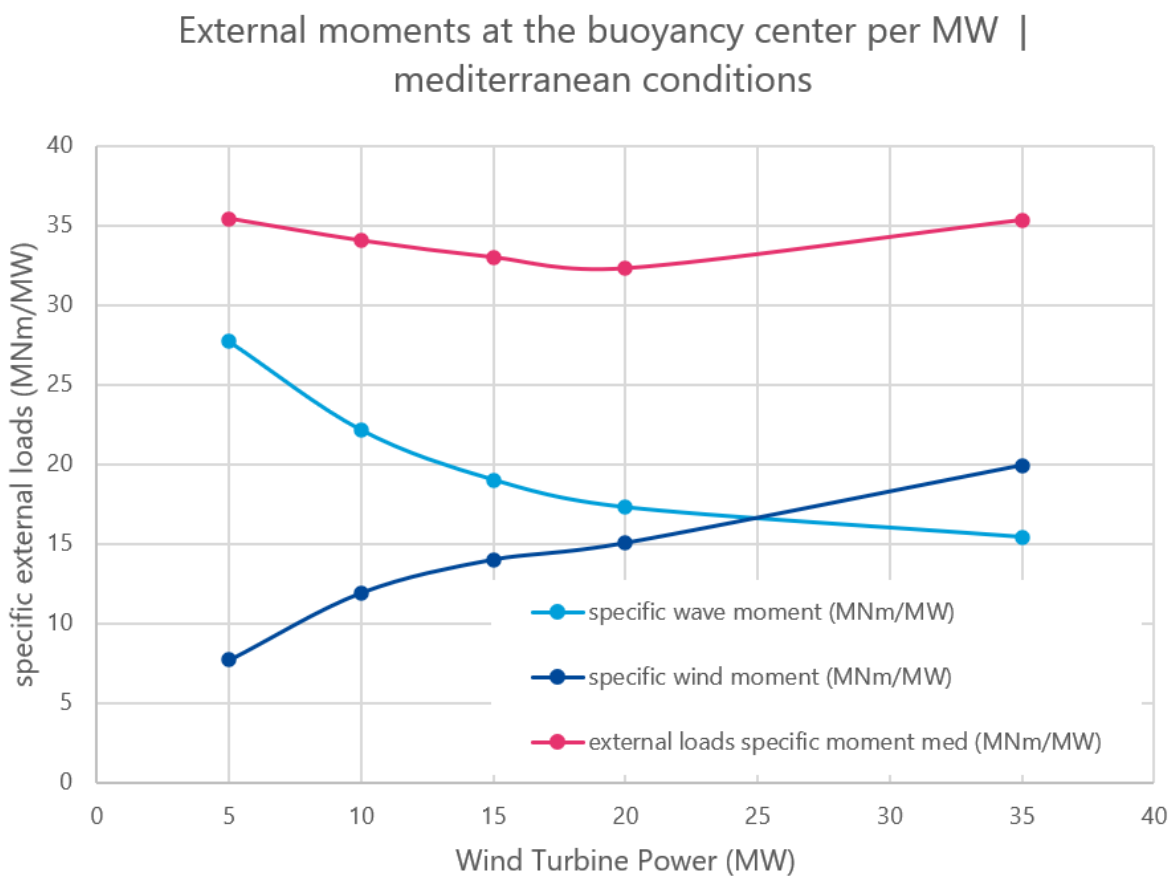

Specific External moments per power Mediterranean conditions for SS, cf figure 2.50

The outputs of the optimisation process for floaters are the dimensions of the platform, from which the weight of the structure (that will be directly linked to its cost through the introduction of manufacturing complexity factors) is obtained. The results for SS

platforms in Mediterranean and oceanic conditions, alongside the same forecast performed by BloombergNEF (which results on the FOW field, obtained through the collaboration between A2A and BNEF, will be used often in this work) that is coherent with the results of our model. The main insights from the weight forecast graph for SS displayed here after are the important drops in specific weight with the introduction of bigger turbines and the economies fostered by the softer external conditions of Mediterranean sea. Similar work will be performed for TLP floaters.

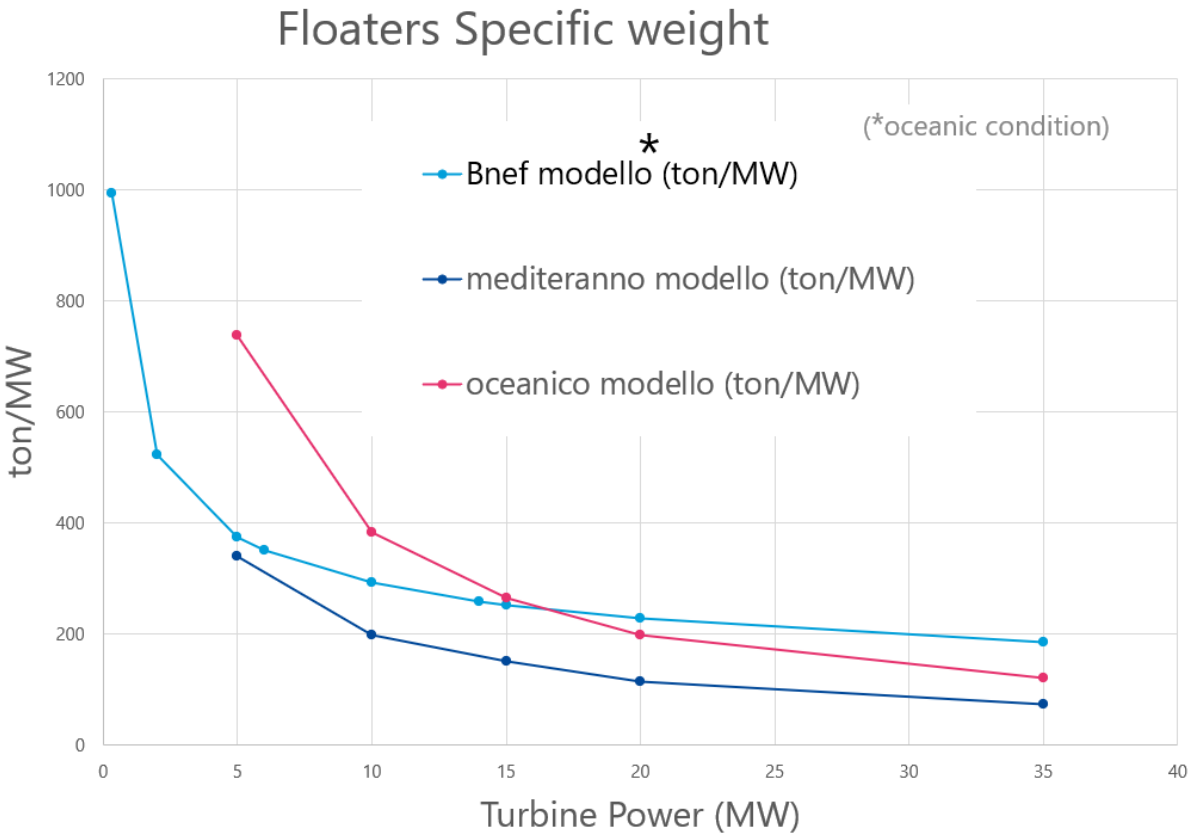

Semi submersible specific weight evolution with turbine size, cf figure 2.54

In section 2.4 similar results are displayed for moorings sizing. A more interesting insight to discuss in this extended abstract would be the impact of depth of on typology of moorings used, which will influence the type of floating substructure as well. Indeed, the two main mooring configurations are taut and catenary ones, where moorings are constantly under constraint or let in suspension respectively. Typically, and this will be assumed in our CAPEX model, SS will feature catenary moorings while TLPs will feature taut moorings. Besides, the figure here after shows what are the depth ranges in which each mooring configuration is more suited (both for economical and physical consideration). We thus get that shallower waters will be suited for SS solutions, currently more mature.

Yet, for deep waters (over 500 meters deep, typical depth of Italian seas), TLP solutions may appear as the most suited (and even only possible at even bigger depths) solution. The figure also presents the possibility of using chain-wire-chain catenary configuration to increase the range of catenary (and thus SS) solutions.

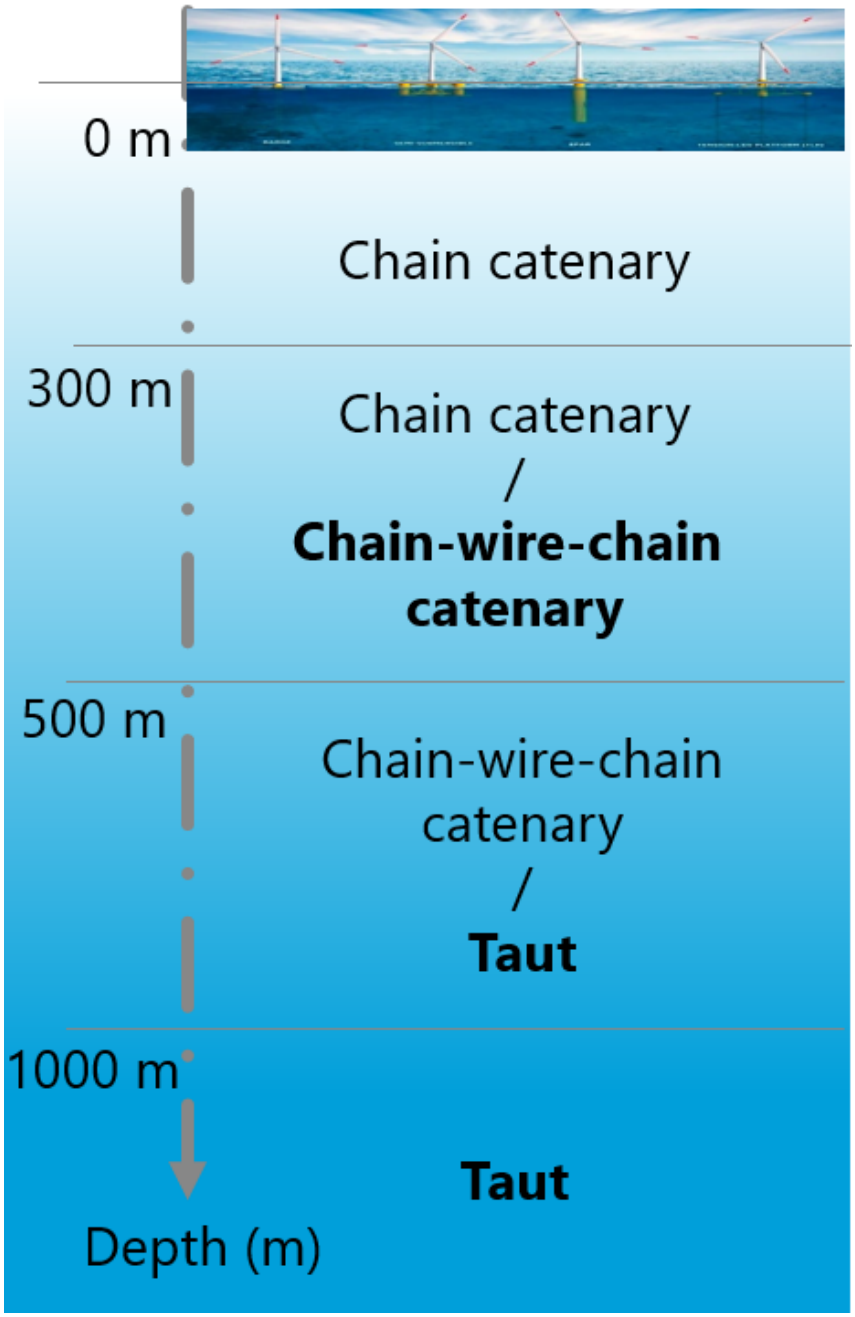

Most suited mooring solution evolution with depth, cf figure 2.72

Let's switch to the global CAPEX model outputs discussed in section 2.8. First let's keep working on the comparison between TLP and SS solutions from a CAPEX perspective,

the figure to come being an insightful support to this.
TLP solutions nowadays are less mature than SS ones as explained in sections. Yet, the CAPEX model outputs presented here above confirm the potential cost savings offered by TLP solutions. In order to deal with this question, on figure displayed here after is displayed a graph presenting the cost savings offered by TLP solution regarding SS catenary solutions in percent (negative values will mean that TLP solutions are most expensive). CAPEX estimation have been made assuming a distance to shore of 50 km. With this representation, it's easier to spot in which cases and to what extent TLP are cost effective solutions in comparison with SS catenary ones. Two clear phenomenons are highlighted by this graph: first, TLP solutions offer bigger cost reductions for smaller turbines and then TLP solutions offer ever bigger cost reductions with increasing depth. On graph 2.112 the two indicative common depth range of application (cf previous figure) of the two technologies have been represented. On cost side, it can be seen that our CAPEX model confirm these results. At high depth TLP solutions are indeed way cheaper than SS ones with more than 12% of total savings in CAPEX for a 15 MW turbine assumed to be used for projects commissioned in 2030. At such depths, catenary SS technologies are whatever out of question even for technological and environmental impact considerations. Yet, even at the "frontier" between the two zones located at 500 meters depth, TLP solutions offer CAPEX reductions of about 8% for 15 MW turbines (2030 projects) and 4.3% for 20 MW turbines (2035 projects). Eventough TLP development is currently lagging behind SS one (as taken in consideration in the model), the cost saving discussed here concern projects that would be disclosed 7 or even 13 years from now, offering time to platform manufacturers to close the technological gap between the two solutions. For the yet to born Mediterranean market that as it will be deeply discussed in chapter 3 features big depths, the TLP solutions could make FOW competitive and viable for more sites.
For smaller depths (100 or 200 meters) located in the indicative SS depth range, the cost savings offered by TLP solutions are smaller, and even negative for huge 35 MW turbines. In this zone, it is unlikely that this solution will be chosen over SS catenary ones since the low cost savings may not compensate the higher risks and lower investors trust in the technology. SS and TLP thus really appear as complementary solutions that would both have a place in the future development of the FOW market in the Mediterranean.

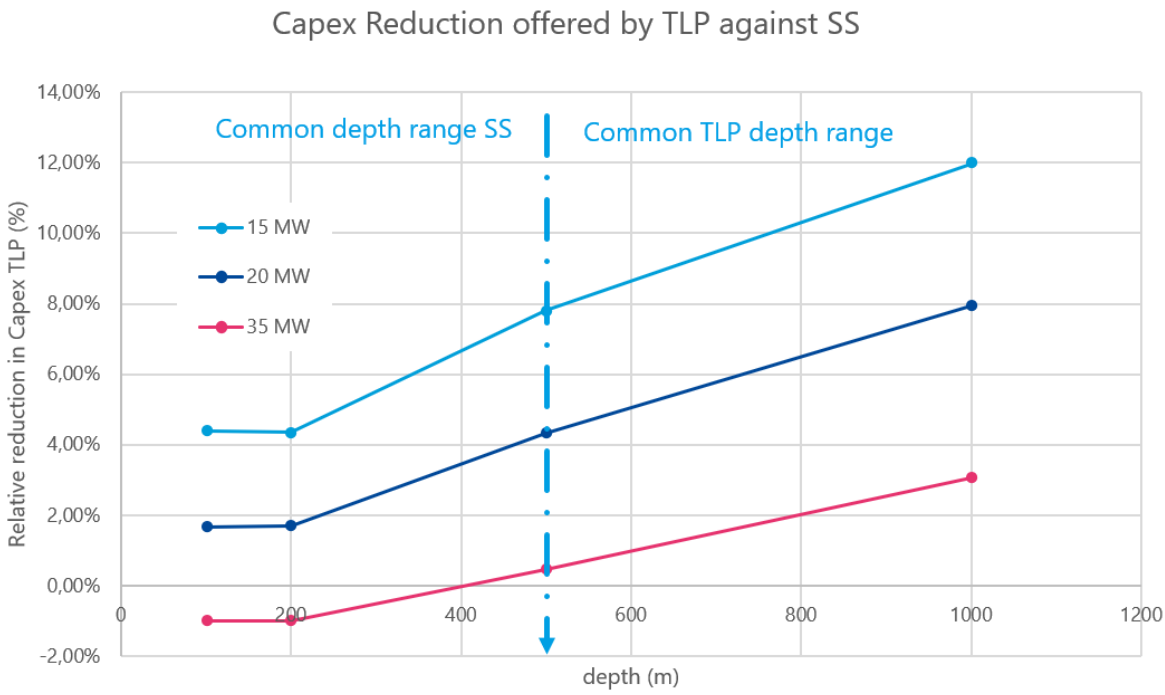

CAPEX Reduction offered by TLP over SS (platform + mooring and anchors) against SS in % for Mediterranean conditions, cf figure 2.114

The outputs of the of the CAPEX model are not only absolute values but also feature pie charts representation that can be very insightful for a clear understanding of the cost breakdown evolution with the different inputs of the model. To reach these results, various hypothesis all listed in the core of the thesis have been made and discussed. Let's precise that, in addition to the six cost drivers previously identified and for each a colour has been attributed, a constant 20% share of the final CAPEX is assumed to be dedicated to other costs, mainly project management, contingency and insurance. The pie chart here after corresponds to a 2030 SS project featuring 200 meters depth, 50 km distance from shore and Mediterranean conditions. This inputs can be seen as representative of what the first commercial scale Mediterranean projects could look like (expected by the end of the decade in France and Spain). The colours attributed to each cost driver will always remain equal, allowing comparison in shares for different model inputs, as it will be seen with next figure. Let's finally precise that the specific CAPEX value for this project is 3.01 $M/MW.

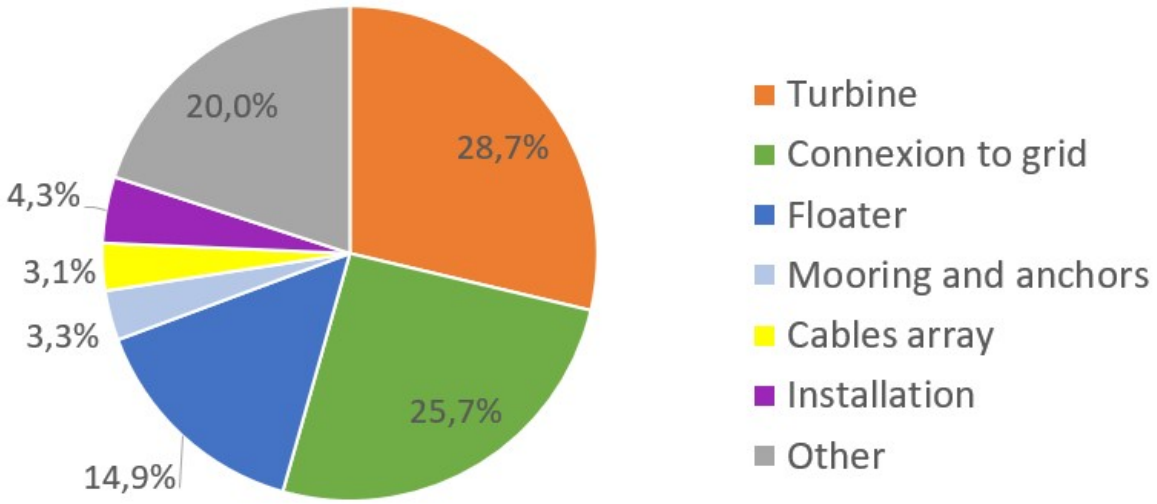

Pie-chart representation of CAPEX model breakdown for a 2030 SS project featuring 200 meters depth, 50 km distance from shore and Mediterranean conditions, cf figure 2.111

More than the global absolute CAPEX values, the share of each cost driver in the total cost breakdown is interesting to analyse. To support this analysis, cost breakdown pie charts alongside the specific CAPEX value in [$M/MW] will be represented represented. On the figure here after for example, different pie charts for combination of year parameter (2030, 2035 and 2040) and of floater/meteo configuration (Med TLP; Med SS and ocean SS) are displayed. To compare these cost breakdown one to another, the two other parameters, depth and distance to shore, are maintained fixed for every pie chart respectively at 500 m and 50 km. Except the grey part corresponding to the "other" module described every parts evolve with commissioning year for different floater/meteo configuration. A deep analysis of these evolution is made in section 2.8.

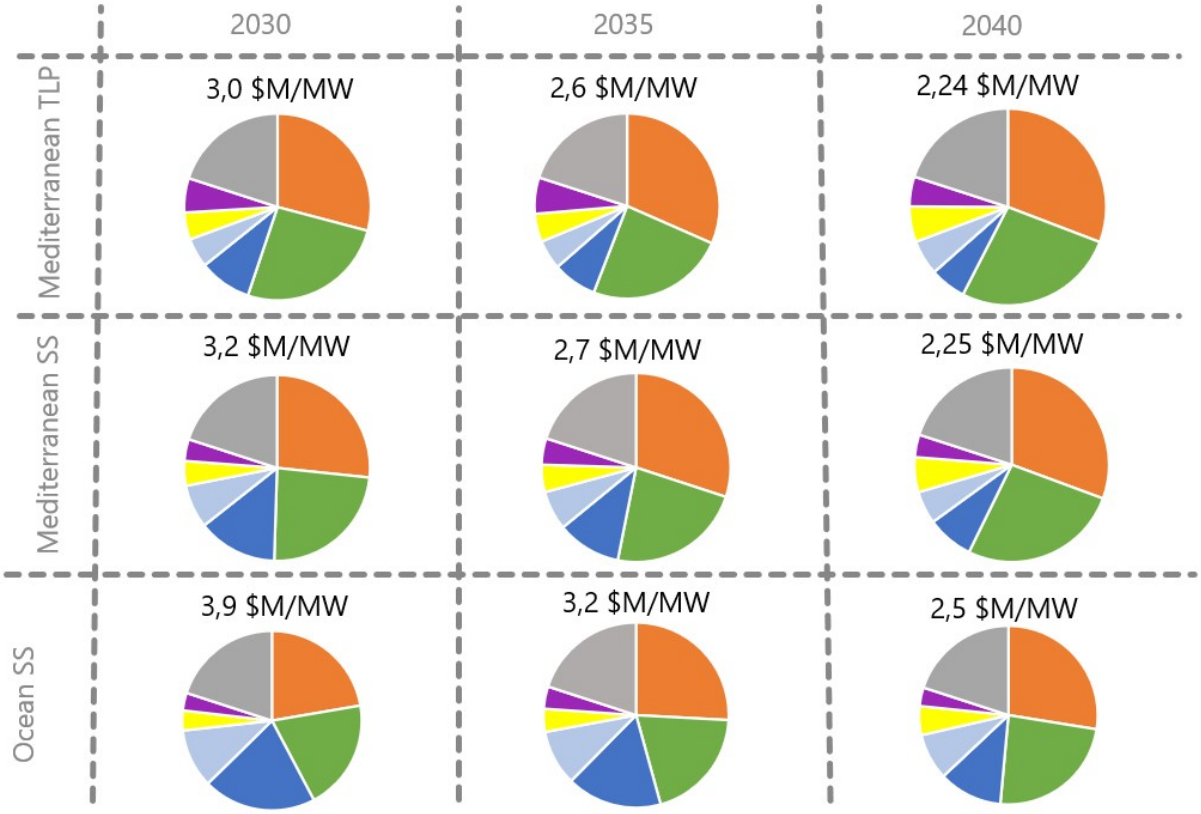

CAPEX breakdown evolution with commissioning year and floater used. Depth = 500 m ; Distance to shore = 50 km, cf figure 2.115

Let's now briefly present some of the main results and insights from chapter 3, the last chapter of this master thesis dedicated to the assessment of site characteristics on the viability of a FOW project and to the calculation of the LCOE for different representative benchmark projects.

To perform this analysis, various sites of interest where hypothetical projects will be studied have been chosen. The identification of this sites was driven by reality of FOW pipeline as well as by win resources obtained from the global wind atlas tool developed by DTU. Accordingly to the global problematic, sites have been chosen to be representative of the Mediterranean and more particularly Italian sea potentialities for FOW development. Thus, 9 out 12 sites are located in Italy, when the other Mediterranean one is located in the Golfe du Lyon (GDL) where France is set to develop its pioneers projects. Two additional located in united-kingdom vicinity (where oceanic conditions will be applied) completes the panel and will give an interesting comparing point. The following map displays the sites of interest identified alongside the equivalent hours - measuring the productivity of the sites - computed for this sites. The process of calculation of the productivity based on wind datasets is described in subsection 3.1.2. The following map

shows that globally, Italian sites are less windy than 3 other sites considered. Yet, the equivalent hours calculated are still almost 75% higher than the value obtained onshore in Italy.

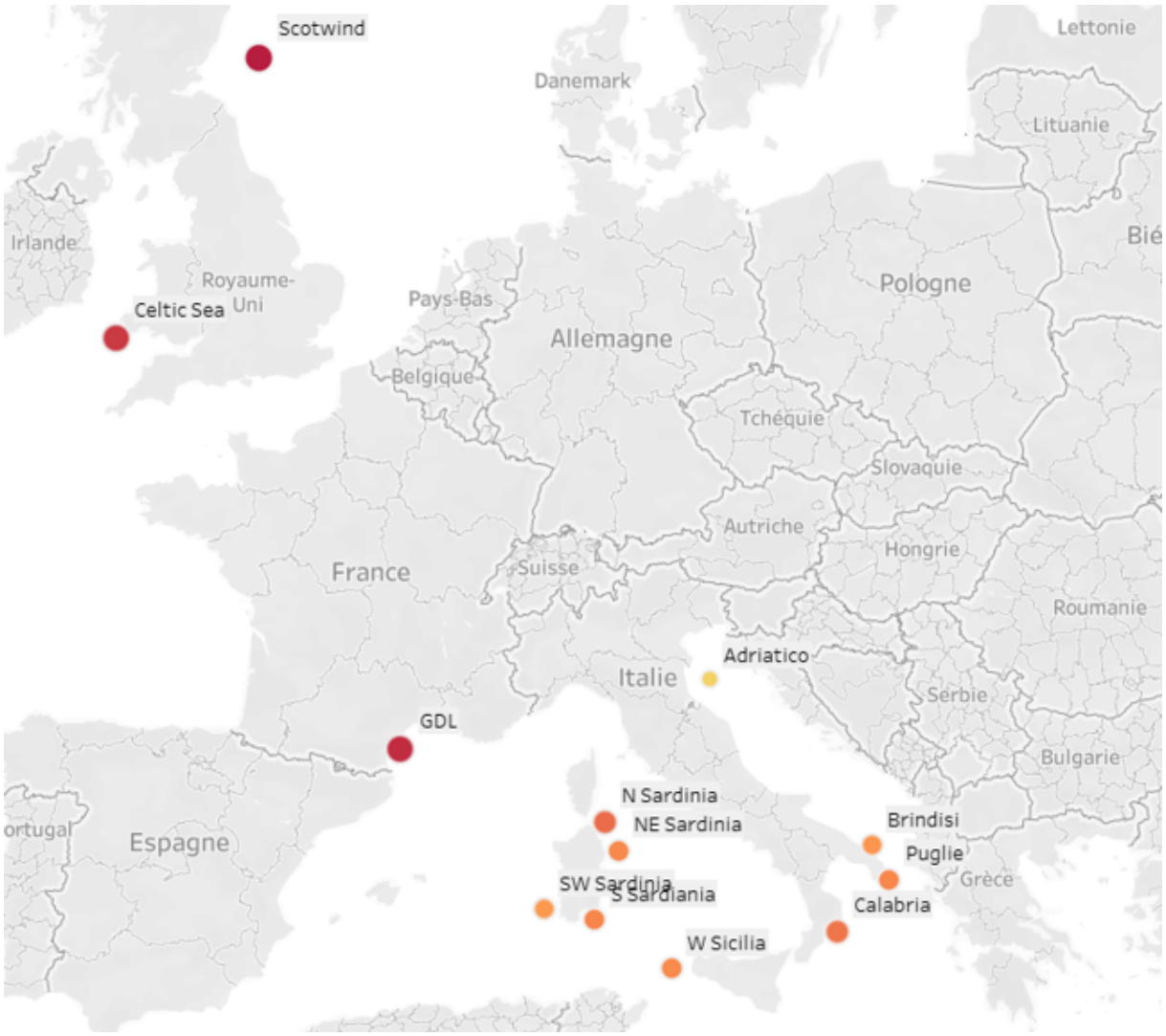

Sites of interest, colour scale indicates the equivalent hours from yellow (lower h_{eq}) to red (higher h_{eq}), cf figure 3.2

As explained in subsection 3.1.4, the potential detrimental impact of FOW farms on landscapes can be an important brake to FOW development in Italy, even more considering that the potential sites of development are for the most located in touristic zones known for their remarkable landscapes (NIMBY phenomenon). This tremendous parameter has to considered in our analysis, and thus had to be quantified. To do so, a visibility model linking the visual impact with distance from shore and turbine height has been created. The "useful" effect of earth curvature that tend to hide objects at a given distance of the

shore has been included in this model. It end up with an acceptable visibility framework described on the following figure. The upper frontier is the distance at which, for a given turbine height, the farm would be entirely hidden for an observer located at sea level on the shore, meaning that going further from shore than this frontier would not bring any improvements on the visual impact side. The lower barrier corresponds to visibility socially accepted for an offshore wind-farm in St-Nazaire, France.
The yearn for mitigating the visual externality generated by FOW projects thus tend to push projects far from shore. Yet, this come with CAPEX - and thus LCOE - increase from a direct and indirect phenomenon (cf chapter 2). First, connection to grid related costs increase with distance from shore. Then, as explained in subsection 3.1.5, the bathymetry profile of the Mediterranean, and more particularly of Italy, is sharp. Thus going further from shore usually mean reaching higher depths, which will have impacts on many CAPEX drivers listed in chapter 2. These impacts are summarised on CAPEX block diagram displayed in methodology section and in figure 2.112.

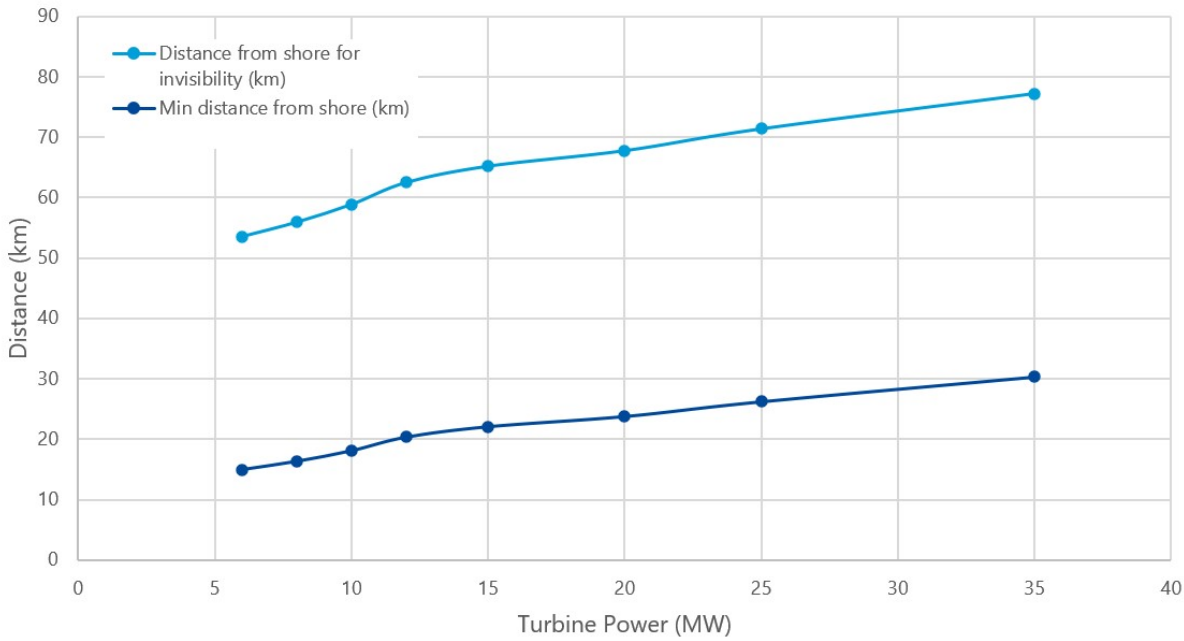

Evolution of minimum distance from shore to obtain limited visual impact with turbine size, cf figure 3.13

The LCOE model has then been computed and its outputs have been analysed and discussed in section 3.3. In particular, an insightful discussion have been led on the impact of landscape preservation on the LCOE in different sites. To support this discussion, on the following figure LCOE evolution with turbine power (here strictly linked to commissioning year) and in different configuration have been displayed for three sites. The green

curves representing "invisible" conditions correspond to the higher barrier where turbines start to be fully hidden by earth curvature and the red ones represent "visible" conditions corresponding to the lower visual barrier. AS expected, for every site and for both technologies, important LCOE drops are generated when going from the invisible frontier to the visible. These drops are heavily linked to bathymetry profiles. Indeed, the drops are more important for N Sardinia than for W Sicily, it self more impacted than GDL site. And while the GDL seabed depth profile remains for long distance from shore more or less constant to 200 meters, for W Sicily and even more N Sardinia going further from shore to decrease the visual impact implies to development of projects in deeper water that will be more costly. When bathymetry is not flat, the diminution have a double detrimental impact on CAPEX and then LCOE: from distance from shore and from depth point of view. The harsher the seabed depth profile of site will be, the more the developers will be encouraged to neglect the visual impact of their projects: it's "easier" from an economic to respect landscapes in Western Sicilian sites than in Northern Sardinia ones (or than Puglie ones for example).

The impact of floater technology used, less important than landscape preservation one, is also highlighted by these charts. When the visual impact in non negligible (red curves) the projects considered feature relatively low depths (200 meters) and thus TLP and SS globally presents similar costs. On the contrary, when harsh seabed depth profile are considered, the preservation of visual impact (green curves) make industrial players developing projects in deep waters where TLP offers interesting drops in CAPEX over SS solutions, which lead to LCOE reduction for TLP invisible witnessed in West Sicily and even more in North Sardinia.

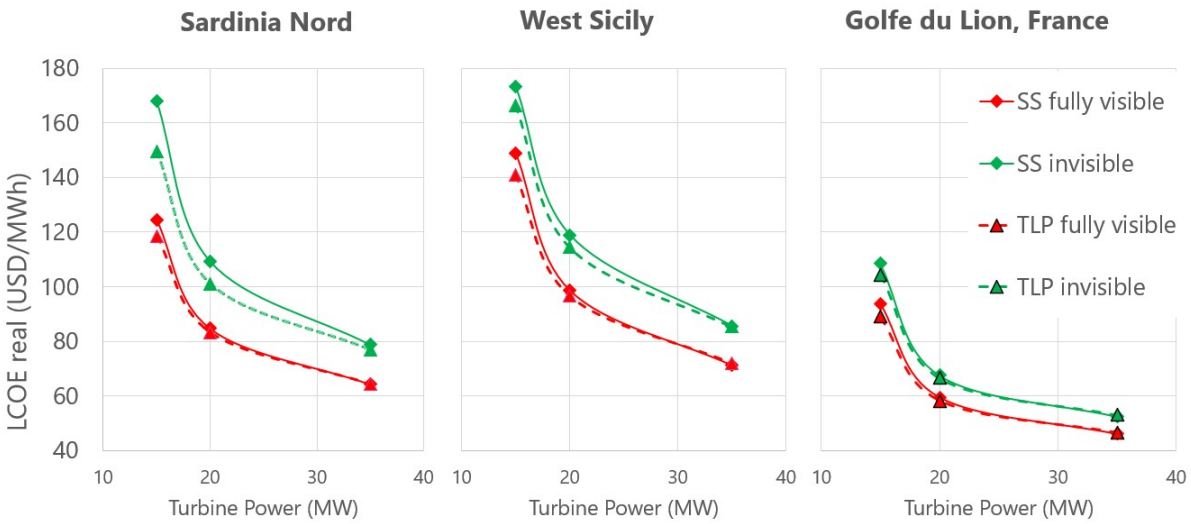

LCOE evolution in terms of turbine power and thus commissioning year that are here assumed to be coupled for different floater typologies and visual impact levels, cf figure 3.28

Landscape visual preservation and use of Tension leg platforms could thus be seen as dependant issues for Italian FOW development. More globally, an important insight of this global work is the strong asset TLP technology could represent for FOW development in the Mediterranean and especially in Italian surroundings. Indeed, the seabed profile of the zone, harsher than "classical" zone of offshore development, will require solutions suited for high depths in order to be place further enough from shore. Seemingly, the Mediterranean market could appear as a good opportunity for TLP manufacturers to gain share, which could close the technological gap with more mature SS technologies.

Sensitivity analyses have been performed through the analyses of different inputs to the model. Yet, many hypothesis for fixed parameters have been made along the process and further sensitivity analysis could have strengthen even more the results. For example, a conservative value for the raw cost of steel have been made which drastically influence the CAPEX of the projects. These various assumptions, explained along the core of the thesis, has an influence on absolute values but less on global trends that still are very insightful.

Conclusions

The driving problematic of this thesis was the potentialities of the floating offshore wind market in the Mediterranean. It end up that, eventough the bathymetry as well as the wind resources in the Mediterranean, and more specifically in Italy, are not always as well suited to offshore wind as in the North sea for example, regarding the important depth of the Mediterranean FOW appears as the only solution for Mediterranean countries to unlock their offshore wind potentialities. Plus the combination of economies of scale expected generated by the introduction of bigger turbines, technological breakthroughs, supply chain optimisation and diminution of the risk related to FOW investments is set to enhance important LCOE drops making FOW competitive by the mid 2035's in the Mediterranean. This economic viability coupled to the excellent comparative features of offshore wind in terms of power density, land occupation and grid friendliness regarding other fatal renewables sources could make FOW plants strong assets for Mediterranean governments yearning for decarbonation of their energy mixes.

Alongside this sensitive work, many assumptions have been made to evaluate the CAPEX of FOW and then the LCOE of hypothetical projects. Eventough these hypothesis have always been supported by scientific sources and argumentative reasoning, when forecast are at stake absolute results must be analysed with caution. Instead, the trends, relative importance of various cost drivers and technological insights as for example the huge potential of TLPs for Mediterranean applications or the importance of visual impact in project design will be regarded as the main take away information from this thesis work. The idea here was to remain global and to deliver general insights, but if a given FOW is under study, deeper and more precise considerations on the wind resource of the site, the platform technologies and dimensions (dynamical behaviour in particular would have to be further assess), external loads, supply chain and local content use as well as environmental impact would have to be performed. Plus, some aspects as the supporting policies from EU or countries (Feed in tariff, financial incentives etc...) or the potential revolution of offshore electrical grid composed of various hubs have not been integrated to the discourse. The FOW is still a young but very promising market and many results of this study will be sharpened thanks to the industrial feedbacks to come.

Contents

Acknowledgements **i**

Abstract **iii**

Sommario **v**

Extended abstract **vii**

Contents **xxix**

List of Figures **1**

List of Tables **9**

Introduction **11**

1 Chapter one: offshore wind power market and potentialities **13**

1.1 Wind power potential and net zero objectives 13

1.2 Going offshore 17

1.2.1 Physical and engineering preamble 17

1.2.2 Extrinsic offshore advantages 19

1.2.3 Intrinsic offshore advantages 22

1.3 Offshore wind market overlook 30

1.4 Floating offshore wind: holistic market analysis 40

1.4.1 Floating potentialities 40

1.4.2 Global market and projects pipelines 42

1.4.3 Focus on main industrial actors 49

1.4.4 Focus on main domestic markets 53

1.5 Chapter conclusion 62

2 Chapter two: Floating offshore wind projects CAPEX estimation **63**

2.1 Foreword . . . 63
2.2 Focus on wind turbines . . . 64
2.3 Focus on floating platforms . . . 69
2.3.1 Floaters technological and market overview . . . 70
2.3.2 Physical model . . . 85
2.3.3 Model outputs analysis . . . 129
2.3.4 Floaters future and innovative concepts . . . 147
2.4 Focus on moorings and anchors . . . 151
2.4.1 General overview . . . 151
2.4.2 Catenary moorings . . . 156
2.4.3 Taut Moorings . . . 162
2.4.4 Model outputs for moorings and insights . . . 168
2.4.5 Future development and innovative concepts . . . 174
2.5 Focus on connection to grid . . . 178
2.5.1 Export cables . . . 179
2.5.2 Offshore substation . . . 184
2.6 Focus on inner-array cabling . . . 188
2.7 Focus on installation . . . 195
2.7.1 Turbine installation . . . 196
2.7.2 Platform installation . . . 197
2.7.3 Moorings and anchors installation . . . 198
2.7.4 Export and inner array cables installation . . . 199
2.8 CAPEX summary and cost breakdown of FOW projects . . . 201
2.8.1 CAPEX model explanation and summary . . . 202
2.8.2 CAPEX model global outputs and FOW cost breakdown . . . 209

3 Chapter three: Site impact assessment and LCOE estimation 217
3.1 Site Impact assessment for zones of interest . . . 217
3.1.1 Identification of sites of interest . . . 217
3.1.2 Wind resource assessment and equivalent hours estimation . . . 219
3.1.3 Port infrastructures issue . . . 227
3.1.4 Distance from shore and visual impact . . . 232
3.1.5 Bathymetry . . . 236
3.1.6 Review of Italian projects . . . 241
3.2 A Word on Operation and Maintenance (O&M) . . . 245
3.3 LCOE calculation . . . 250
3.3.1 Losses assessment . . . 251

3.3.2 Financial and project life-cycle related hypothesis 255
3.3.3 Results for sites of interest 259

Conclusion **269**

Bibliography **273**

List of Figures

1.1 Main components of 3 blades HAWT 14
1.2 Energy-related and process CO2 emissions, 2010-2050 and temperature rise in 2100 by scenario (IEA world energy outlook 2022) 15
1.3 Renewables are now the cheapest source of new bulk power generation in countries comprising 66% of world's population (BloombergNEF 1H 202 2 LCOE update) 16
1.4 Rotor Power coefficient by tip speed ration λ for different wind turbine technologies, from [1] 18
1.5 Power curve of a wind turbine 19
1.6 specific power forecast onshore and offshore (BNEF) 20
1.7 Riot against onshore wind power project in Canada 21
1.8 Part of world population living within 100 km of the coast 22
1.9 Blades weight increase with length and material use from [2] 23
1.10 General electric Haliade-X real size 12 MW prototype in St-Nazaire, France 24
1.11 Higher average wind speed and faster wind shear development [3] 25
1.12 Variations of wind speed and power due to wind shear from [4] 26
1.13 Global Ocean Wind Energy Potential from NASA Earth observatory . . . 27
1.14 Range of mean hour-to-hour variations in output by technology, based on 2018 weather data, from [5] 28
1.15 average weekly capacity factors for new offshore wind and solar PV projects by region , based on 2018 weather data, from [5] 29
1.16 Brief history of the offshore wind market development 31
1.17 Annual offshore wind capacity addition by region, 2010-2018, from [5] . . . 32
1.18 4cOffshore Offshore wind project map, Europe 33
1.19 4cOffshore Offshore wind project map, China 33
1.20 Levelized offshore wind prices, from [6] 35
1.21 Annual ex China installation by manufacturer, from [6] 38
1.22 Annual China installation by manufacturer, from [6] 39
1.23 Global cumulative offshore installation forecast, from [7] 40

1.24 fixed-bottom vs floating substructures 41
1.25 First 2.3 MW floating wind turbine 44
1.26 Kincardine floating windfarm, Scotland 45
1.27 Project advancement overview 46
1.28 Yearly installed capacity forecast 47
1.29 Global pipeline world map 48
1.30 World map of most ready projects 49
1.31 Most ready energy companies 50
1.32 Energy companies with biggest pipelines 50
1.33 Most ready project developers 52
1.34 Project developers with biggest pipelines 53
1.35 Map of Scottish projects awarded via Scotwind lease process from [8], Floating projects are evidenced in Blue 55
1.36 Map of french projects from [9], floating projects are framed in blue. Distinction is made commercial and pilot projects 57
1.37 floating wind projects LCOE evaluation in Korea from [10] 59
1.38 floating wind projects in Korea from 4C offshore 60
1.39 Logical scheme for VIA (environmental impact valuation), from [11] 61

2.1 Different cost drivers for offshore floating projects 64
2.2 BNEF turbine capacity forecast onshore vs offshore, from [2] 65
2.3 IEA turbine size forecast, from [5] 66
2.4 BNEF specific weight division forecast, from [2] 67
2.5 BNEF total wind power installed capacity per year 68
2.6 Specific cost forecast for wind turbines 69
2.7 Main floaters types 70
2.8 Windfloat SS floater by PrinciplePower 72
2.9 SS strengths and weakness summary 73
2.10 Damping pool Barge by Ideol 74
2.11 Barge strengths and weakness summary 75
2.12 SparBuoy by equinor and Technip 76
2.13 Spar buoy strengths and weakness summary 77
2.14 TLP floater by SBM Offshore 78
2.15 TLP strengths and weakness summary 80
2.16 Comparison of different technologies based on seven criteria of interest . . 81
2.17 Division of counted floating concepts based on typology 82
2.18 Division of counted floating concepts based on base material used 83

2.19 Year of first commercial scale project of mapped platforms concepts. 84
2.20 Main floating platforms field development milestones 85
2.21 Forces taken in consideration in the static model 86
2.22 Thrust force on rotor 88
2.23 Drag force on Tower 89
2.24 Linear wave model explanation 91
2.25 Range of Morison's laws application 92
2.26 Morison laws application framework 94
2.27 Deep wave configuration results 95
2.28 Inertia and drag Morison's force time evolution from [12] 97
2.29 Methods of stabilisation of platform types from [13] 99
2.30 Righting moment equation explanation 101
2.31 Water-plane area stabilisation method explanation 102
2.32 Second moment of area 103
2.33 Ballasted stabilisation method explanation 105
2.34 TLP stabilisation method explanation 107
2.35 Map showing the 100-yr return levels for the North Atlantic Ocean and North Sea from [14] 111
2.36 Seasonal wave height in Mediterranean 112
2.37 Turbines dimensions of interest for physical model computation 114
2.38 Pitch to feather VS Pitch to stall regulation for wind speed higher than rated one 117
2.39 Classical V-shape 3 column Semi-submersible upfront view 119
2.40 Classical V-shape 3 column Semi-submersible lateral view 121
2.41 Free-floating 10 MW size TLP 3D view with dimensions in operation from [15] 122
2.42 Free-floating 10 MW size TLP 2D upfront view from [15] 124
2.43 Inputs and outputs of the computed static model 125
2.44 Steel price evolution from BNEF 126
2.45 Manufacturing complexity factor for different platform typologies and material from [16] 127
2.46 Manufacturing complexity factor used in cost model from 2020 to 2050 . . 129
2.47 External moments Oceanic conditions for SS 130
2.48 Specific External moments per power Oceanic conditions for SS 131
2.49 External moments Mediterranean conditions for SS 132
2.50 Specific External moments per power Mediterranean conditions for SS . . . 133

2.51 Specific External moments per power Mediterranean VS Oceanic conditions for SS . . . 134
2.52 Specific column radius R evolution with power for SS . . . 135
2.53 Specific column distance to center d_c evolution with power for SS . . . 136
2.54 Semi submersible specific weight evolution . . . 137
2.55 Semi submersible specific cost evolution . . . 138
2.56 External moments Oceanic conditions for TLP . . . 139
2.57 Specific External moments per power Mediterranean conditions for TLP . 140
2.58 Specific External moments per power Mediterranean VS Oceanic conditions for TLP . . . 141
2.59 Specific dimensions R/P and d_c/P evolution with power for TLP . . . 141
2.60 Specific loads on moorings in oceanic condition . . . 142
2.61 Specific loads on moorings in Mediterranean condition . . . 143
2.62 TLP specific cost evolution . . . 144
2.63 Specific weight comparison SS vs TLP . . . 145
2.64 Specific cost comparison SS vs TLP for Oceanic condition . . . 146
2.65 Specific cost comparison SS vs TLP for Mediterranean condition . . . 147
2.66 3.6 MW Tetra-spar pilot launched in 2021 in Norway . . . 148
2.67 Modularity of Stiesdal design for an onshore assembly . . . 149
2.68 Eolink small scale pilot in France . . . 150
2.69 X1 wind small scale pilot in Canaries (Spain) . . . 150
2.70 Twin wind concept from Hexicon . . . 151
2.71 Different mooring system for floating platforms from [17] . . . 152
2.72 Most suited solution evolution with depth . . . 155
2.73 Catenary Mooring arrangement from . . . 157
2.74 Anchoring Radius R over depth evolution with depth, industrial data from Oil&Gas sector gathered in [4] . . . 158
2.75 Catenary chain characteristics extrapolated from data gathered in [18] . . . 160
2.76 Drag embedment anchors . . . 161
2.77 Taut Mooring arrangement . . . 163
2.78 Polyester ropes characteristics from Bridon-Bekeart catalogue [19] . . . 166
2.79 Drag suction anchors . . . 167
2.80 Catenary mooring specific cost evolution with depth . . . 169
2.81 Anchors specific cost evolution with turbine size . . . 169
2.82 Taut mooring specific cost evolution with depth . . . 170
2.83 Comparison total specific cost of taut VS catenary solutions for oceanic conditions . . . 171

2.84 Comparison total specific cost of taut VS catenary solutions for med conditions . . . 171
2.85 Summary of TLP pros and cons . . . 173
2.86 TLP failure configuration . . . 174
2.87 GICON TLP concept with gravity anchor . . . 176
2.88 Gazelle TLP concept with counterweight mooring concept . . . 177
2.89 Saitec Barge concept with single point mooring system . . . 178
2.90 General floating offshore farm layout . . . 179
2.91 HVDC and HVAC connection technologies, from [5] . . . 180
2.92 HVDC and HVAC OSS weight, from [17] . . . 181
2.93 Transmission losses for HVDC and HVAC technologies . . . 182
2.94 General characteristics of export cables based on industrial survey led by BNEF, extracted from [17] . . . 183
2.95 Bottom fixed offshore substation cost per nominal power in the UK, from [17] . . . 185
2.96 Fukushima floating OSS pilot, 2015, Japan . . . 187
2.97 BW Ideol damping pool floating OSS concept . . . 188
2.98 Layout of the general electrical array considered . . . 189
2.99 Number of turbine per strings depending on cable size, from [17] . . . 190
2.100 Components of dynamic cable system . . . 191
2.101 Optimised vertical profile of a dynamical . . . 192
2.102 W shaped profile for dynamic cables . . . 193
2.103 Static cables costs from [20] . . . 194
2.104 Cost model outputs for inner array . . . 195
2.105 Turbine onshore assembling for tetra concept by Stiesdal [21] . . . 196
2.106 Towing of pre-assembled floating structure on site, from [22] . . . 198
2.107 Anchor Handling Tug Supply (AHTS) vessels . . . 199
2.108 Cable Laying Vessel . . . 201
2.109 Fixed Bottom LCOE breakdown from [23] . . . 203
2.110 Example of CAPEX model breakdown for a 2030 SS project featuring 200 meters depth, 50 km distance from shore and Mediterranean conditions . . . 205
2.111 Pie-chart representation of CAPEX model breakdown for a 2030 SS project featuring 200 meters depth, 50 km distance from shore and Mediterranean conditions . . . 206
2.112 Inputs and outputs of the whole CAPEX model . . . 208
2.113 CAPEX evolution with turbine power for depth of 200 meters and 1000 meters, at a fix representative distance to shore of 50 km . . . 210

2.114 CAPEX Reduction offered by TLP over SS (platform + mooring and anchors) against SS in % for Mediterranean conditions 211
2.115 CAPEX breakdown evolution with commissioning year and floater used. Depth = 500 m ; Distance to shore = 50 km 213
2.116 CAPEX evolution with depth for SS and TLP projects, 2035 Mediterranean projects are considered 214
2.117 CAPEX breakdown evolution with depth and floater used, 2030 Mediterranean projects are considered, and distance from shore is maintained at 50 km 215

3.1 Wind resources in the Mediterranean at 100 meters height from [24] 218
3.2 Sites of interest 219
3.3 Renewable Ninja Interface, from [25] 222
3.4 Power Curve of a 9.5 MW offshore wind turbine, based on Vestas V164/95000 model 224
3.5 Mean wind speed evolution with nacelle height 225
3.6 Equivalent hours of site of interest for different turbine sizes 227
3.7 Construction port and towing route for Tetra demonstrator from Stiesdal [21] 228
3.8 Eiffage Metal building site of Fos-Sur-Mer in France 229
3.9 Review of Italian industrial ports and compatibility with FOW port operations 231
3.10 Earth curvature effect on visualisation from long distance 233
3.11 Geographical evaluation of the visual impact on landscape of FOW project called Minervia and located in south Italy (Calabria) 234
3.12 Offshore turbine visual impact example for French project 235
3.13 Evolution of minimum distance from shore to obtain limited visual impact with turbine size 236
3.14 North sea bathymetry, from [26] 237
3.15 Map of the bathymetry of Italian surroundings, from [27] 238
3.16 Bathymetry and distance from shore table for 12 zones of interest 240
3.17 Overview of the potential impact on landscape of announced FOW Italian projects 243
3.18 Overview of the mean depth and floater technology currently considered for announced FOW Italian projects 245
3.19 Diagrams of different maintenance strategies from [28] 247
3.20 Drone inspection of wind turbines 249

3.21 Annual O&M costs forecast in the world, from [5] 250
3.22 Wake phenomenon 253
3.23 Offshore wind turbine maintenance operation 254
3.24 VBA code implemented in the LCOE calculation to model the transmission losses 255
3.25 Real and nominal discount rate 258
3.26 Inputs to the LCOE calculator and characteristics of selected sites of interest 260
3.27 LCOE values for selected sites of interest alongside visual impacts 261
3.28 LCOE evolution in terms of turbine power and thus commissioning year that are here assumed to be coupled for different floater typologies and visual impact levels 263
3.29 LCOE evolution of different energy sources from DNV [29] 264
3.30 LCOE evolution of fixed-bottom offshore wind from IEA [5] 266
3.31 Potential advantage of using smaller turbines for different sites 267

List of Tables

1.1 IEC Wind turbines classes 20

2.1 Turbine dimension per power 66
2.2 Turbine specific characteristics 68
2.3 Value of physical coefficient adopted 116

Introduction

Man kind is collectively facing a global crisis that will define its future. Our relations towards the earth and its resources must be heavily rethought and, in order to mitigate the effect of the inevitable climate crisis, the greenhouse gases emissions must be drastically reduced.
This challenge must be assess both at individual level improving our behaviours and at global and political level. In this horizon, an ever greater number of countries pledge to reach net-zero emissions by mid-century or soon after. Yet, to reach the two flagships goals fixed by the scientific community and the successive COP which are the net zero emissions and an increase in global temperature lower than 1.5 °C, concrete and pragmatic plans must be engaged. Among all the requirements at stake, the electrification of the energy sector coupled to a decabornation of the electricity production appears as the prerequisite for an hypothetical overcome of the global crisis.

Wind energy is set to play a key role in this transition. It has been exploited by men for hundreds of years, and the first wind turbine dedicated to electricity production goes back to the late XIXth century. Yet, before the 90's wind energy contribution to the global electricity mix was negligible. Then, a rise in concerns related to fossil energies alongside technological breakthroughs and political incentives led to a constant increase in wind energy facilities throughout the world. Indeed, the amount of electricity produced by wind has skyrocketed in the last two decades, going from 30 TWh in 2000 to about 2000 TWh in the year 2021. This expansion is expected to keep on and even accelerate in the net-zero by 2050 scenario.

Wind power was born onshore but its present and future also belong to the seas. Indeed, after years of researches and tests, offshore wind power plants achieved commercial in the late 2000's and represent now 7% of the installed power. This share is set to increase in the years to come thanks to the greater size of the offshore farms are and the fewer limiting factors for sites identification than onshore.
The last major breakthrough in the field is the dawn of floating offshore facilities which,

since less limited on site depth, could unlock access to a tremendous quantity of wind. For example, it could allow countries boarding the deep Mediterranean sea to consider the offshore wind solution. This issue will guide our whole study.

1 | Chapter one: offshore wind power market and potentialities

1.1. Wind power potential and net zero objectives

Wind energy is an indirect source of solar energy: roughly 2% of the incident solar radiation is continuously transformed in kinetic energy of the air masses on earth through a conversion process assimilable to a Joule Brayton Cycle. [3]
This wind energy is then mainly converted into electricity using wind turbines, which now stand, alongside large hydro power plants, as the most mature technology in green electricity production field. In this work, focus will be made on the most mature and widespread wind turbine type: the horizontal axis 3-blades wind turbine, of which the typical main components are displayed on figure 1.1. Other configurations of wind turbines exist and present pros and cons compare to the 3-blades HAWT (horizontal axis wind turbine) such as VAWT (vertical axis wind turbines) which are worth the analysis for offshore application [3] [5]. Still, HAWT are more ahead both in market size and technological aspects for large power capacities [5] and present higher power performances as figure 1.4 shows.

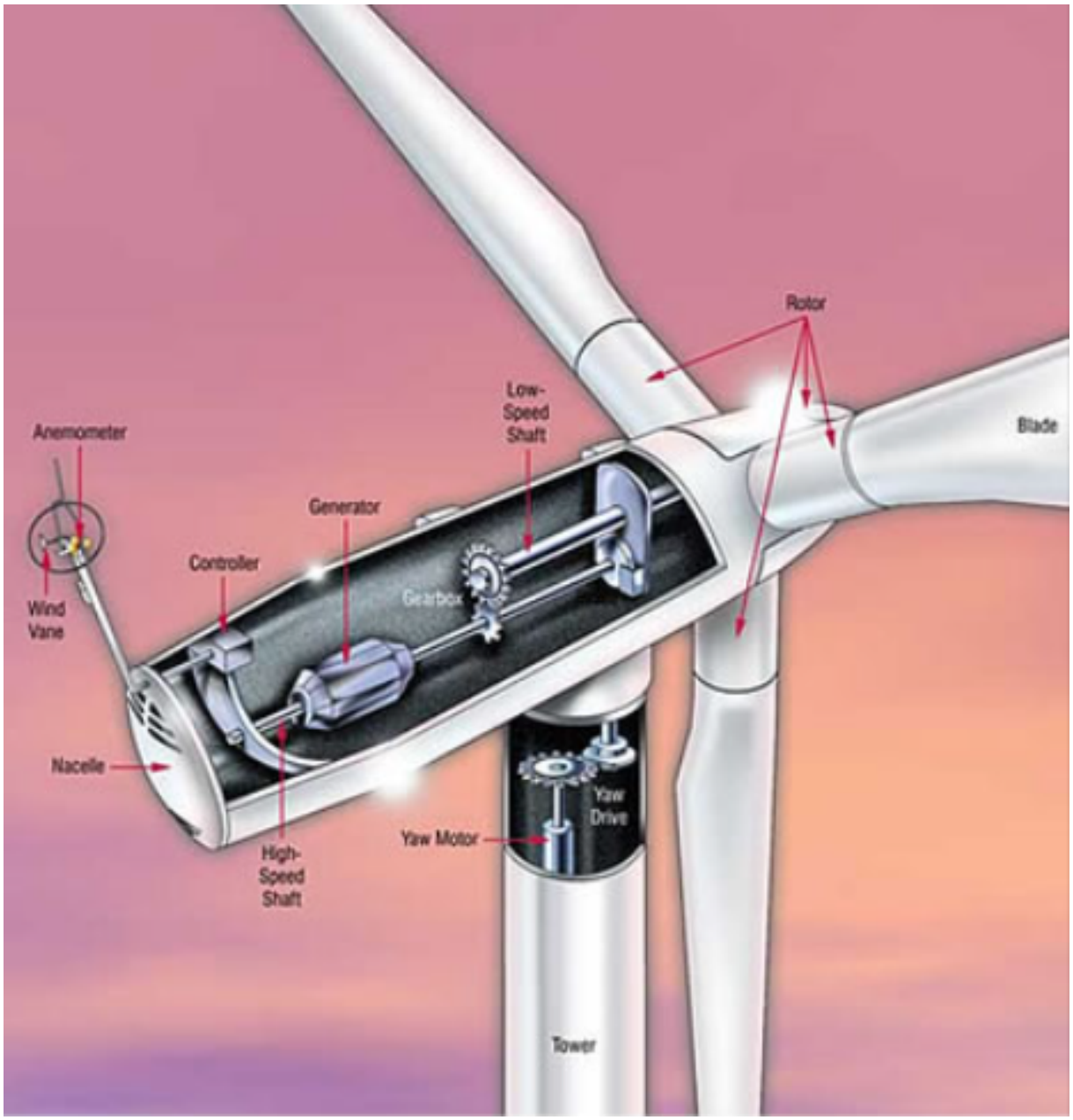

Figure 1.1: Main components of 3 blades HAWT

This maturity is the result of decades of technological breakthroughs and market scaling. This development has been also fostered by incitive policies led throughout to world in order to cope with the Co2 emissions reductions objectives. These objectives have been collectively set by the countries members of the successive COPs that for example led to the Paris agreement of 2015. This legally binding international treaty on climate change was adopted by 196 Parties and its main goal is to limit the the global increase in temperature below 1.5 °C by 2050 compared to pre-industrial level [30]. By 2020, signatory countries submitted their plans for climate action known as nationally determined con-

tributions (NDCs). These plans described the short and long term action that will be conducted in order to enhance the required economic and social transformation. Countries also communicate in the NDCs actions they will take to build resilience to adapt to the impacts of rising temperatures.
The International energy agency (IEA) incorporates these policies in their hollistic energy forecast, defining various energy scenario among which the net zero by 2050. The last version of their outlook also take in consideration the latest huge energy shocks related to the pandemic and the War in Ukraine [31]. According to this report, additional policies are yet to be implemented to reach the net zero by 2050.

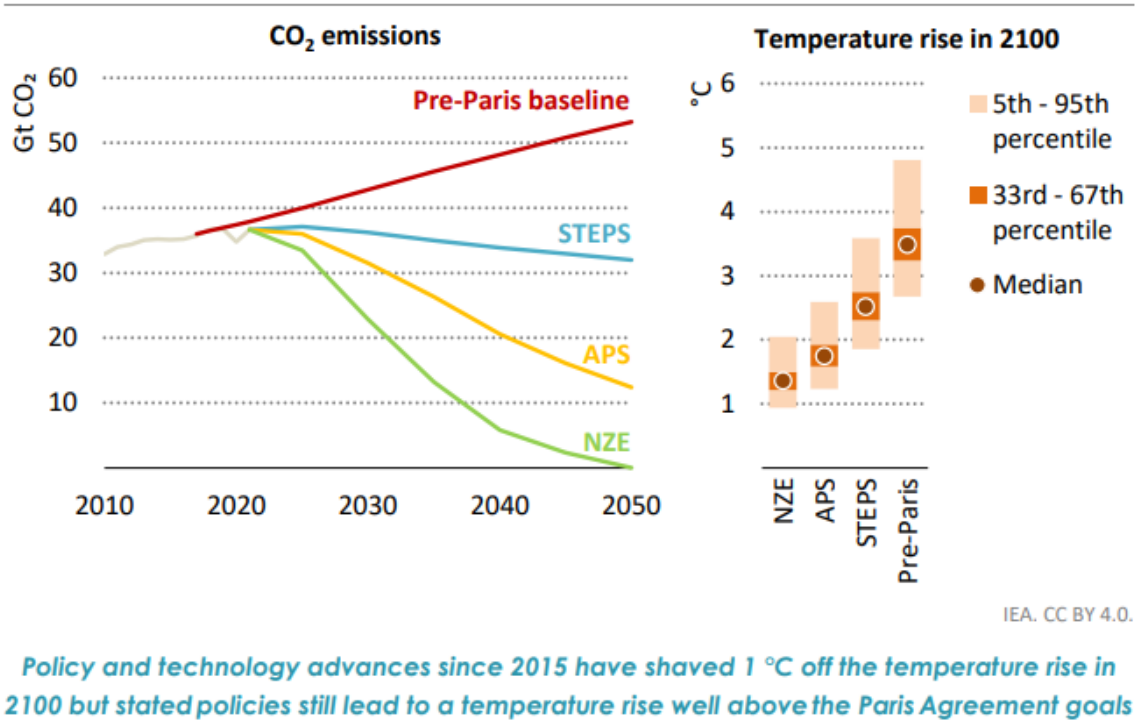

Figure 1.2: Energy-related and process CO2 emissions, 2010-2050 and temperature rise in 2100 by scenario (IEA world energy outlook 2022)

However, every scenario, every evolution, will feature an electrification of the total energy supply coupled to a necessary decarbonation of the electricity production. Nowadays, the world electricity penetration, i.e.the part of electricity in final energy consumption, is only 20%, and 63% of electricity generation still come from unabated fossil fuels [32]. Indeed, the electricity sector accounted for 59% of all the coal used globally in 2021, alongside 34% of natural gas and 4% of oil. Plus 52% of all renewables and nearly 100% of nuclear power were linked to electricity production. At the end, it accounted for over one-third of all energy-related CO2 emissions in 2021. To cope with 2050 objectives, a

nearly 90% decarbonised electricity sector coupled to an electricity penetration of 50% would be required.

Alongside and complementary to solar energy, wind energy exponential development will be the cornerstone of this electricity sector transition. All the more so as these technologies are now competitive regarding fossil fuel based ones. An interesting tool to compare different sources in terms of economic competitiveness is the levelized cost of energy LCOE measured in USD/MWh [33], its exact mathematical definition will be presented and used later on in section 3.3. The levelized cost of energy can be thought of as the average minimum price at which the electricity generated by the asset is required to be sold in order to offset the total costs of production over its lifetime.

The following map show to what extent renewables are now the cheapest solutions for in many areas. This economic argument, even over the green one, is set to multiply tenfold the installation of such types of plants throughout the world.

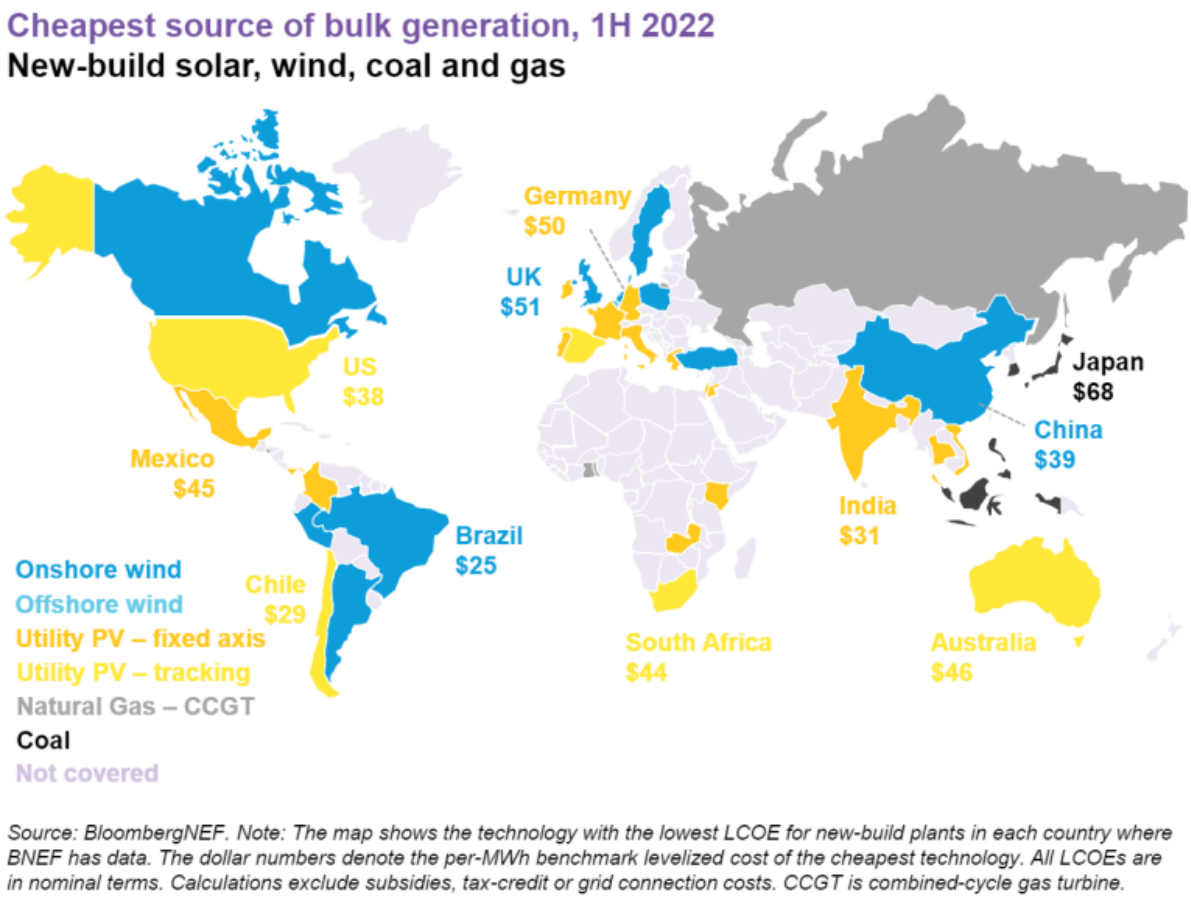

Figure 1.3: Renewables are now the cheapest source of new bulk power generation in countries comprising 66% of world's population (BloombergNEF 1H 202 2 LCOE update)

Another advantage offered by these renewables technologies compared to the classical

ones is the energy autonomy they offer. Unfortunately, the latest crisis has shown how geopolitics could impact the disponibility and the cost of energy [31]. These events consolidated the wish of countries to be less and less dependant on fuel importations, which should foster the increase of the renewables share in the energy mixes.

Wind power is a thus a mature, non carbonate and competitive sector. For decades, it belonged to shore. But in order to fully exploit the potential of this energy source, and to overcome various issues as well, it is now time to go offshore.

1.2. Going offshore

1.2.1. Physical and engineering preamble

As exposed in the introduction, offshore wind sector has been on the rise for the last two decades. This could arouse interrogations: why going offshore rising obvious issues of investment, installation and maintenance difficulties and technological challenges. The arguments for offshore wind are multiple and summarised here after.
The arguments listed here after are for the most physic based. To expose them, even if the purpose of this first chapter is to remain generic and market oriented, let's introduce a simple yet tremendous equation (physical aspects will be deepen in the chapters to come). The power available at the turbine shaft is given by:

$$P = \frac{1}{2}\rho.\pi.\frac{D^2}{4}.C_p.v^3 \tag{1.1}$$

The process to obtain (1.1) is described in [34] where ρ is the air density (which can depend on the altitude), v is the wind velocity at the nacelle, D is the rotor diameter of the turbine and C_p is the Power coefficient. This power coefficient is the parameter on which the power regulation is made since it depends on the blade profile that can be twisted by motor action. When the maximum power must be extracted from a given airflow of velocity v, this coefficient is maximised thanks to a regulation on ω the rotation speed of the rotor [34]:
If a rotor rotates too slowly, "too much" wind to pass through undisturbed, and thus not enough energy is extracted from the airflow. On the other hand, if the rotor rotates too quickly, it appears to the wind as a large flat disc, which creates a large amount of drag and lower the performances.
In order to easily model these behaviour, a non dimensional number is introduced: The rotor Tip Speed Ratio (TSR) λ :

$$TSR = \lambda = \frac{rotor - tip - speed}{wind - speed} = \frac{\omega.\frac{D}{2}}{v} \tag{1.2}$$

The range of TSR at which interesting values of C_p depends on the blade airfoil profile used, the number of blades, and the type of wind turbine [34]. In general, a three-bladed HAWT operates at a TSR of between 6 and 8, with 7 being the most widely as graph 1.4 shows.

Graph 1.4 also shows how the use of TSR allow to compare the performances of different types of wind turbines. Three-blades HAWT is the technology bringing power coefficient closest to the Betz limit of $\frac{16}{27}$ described in [34], hence their massive use. For well designed state of the art turbines, a classical value of maximum C_p is 0.5.

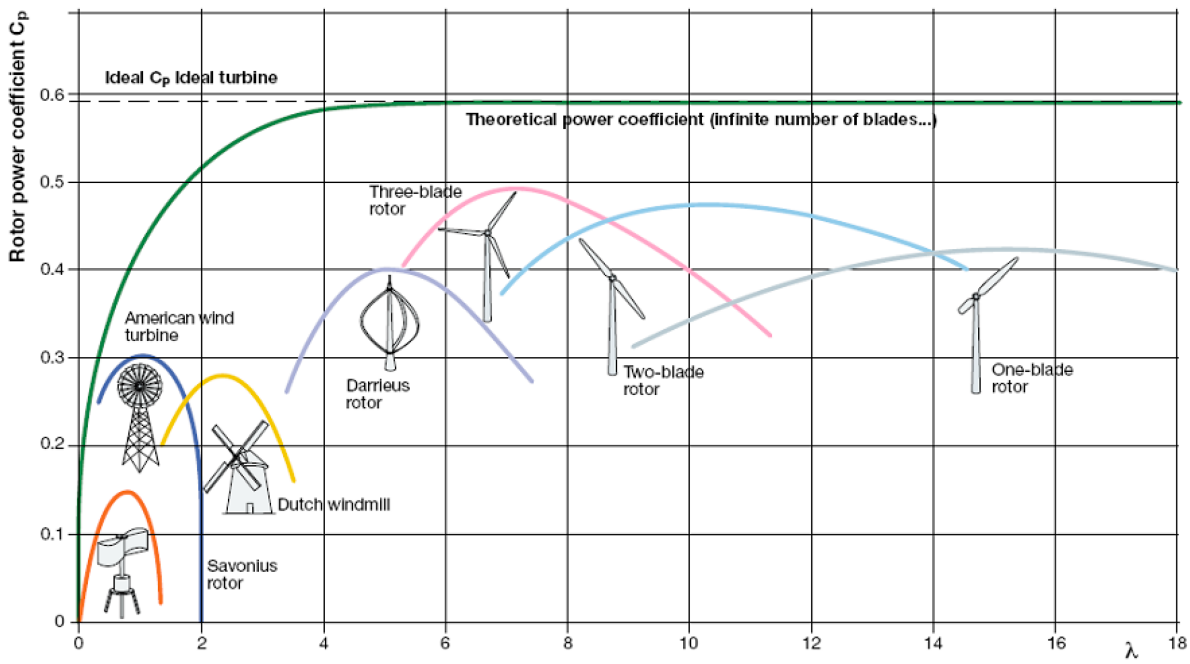

Figure 1.4: Rotor Power coefficient by tip speed ration λ for different wind turbine technologies, from [1]

Finally, let's have a glance to a a classical wind turbine power curve in function of wind speed displayed on figure 1.5. This curve shows that, due to motor restriction, maximum power is not extracted from the wind flow for high wind velocities. Instead, a regulation on C_p via a motorisation of the blade profile allow to remain at rated power, decreasing the value of C_p far from the 0.5 value that can be obtained with HAWT. This process comes from a techno-economic optimization: invest in bigger and more expensive motors would not be worth in order to exploit wind velocities with rare occurrence.

Hence, mean wind velocity is not enough to evaluate the power output of a turbine. To put that simply, for a rated speed of 12 m/s for example, a turbine will produce more energy from a constant wind at 12 m/s than from a wind oscillating between 9 and 15 m/s. More stable winds is also preferable from the mechanical design point of view. Ideal sites for wind energy projects thus present strong but also stable wind flows.

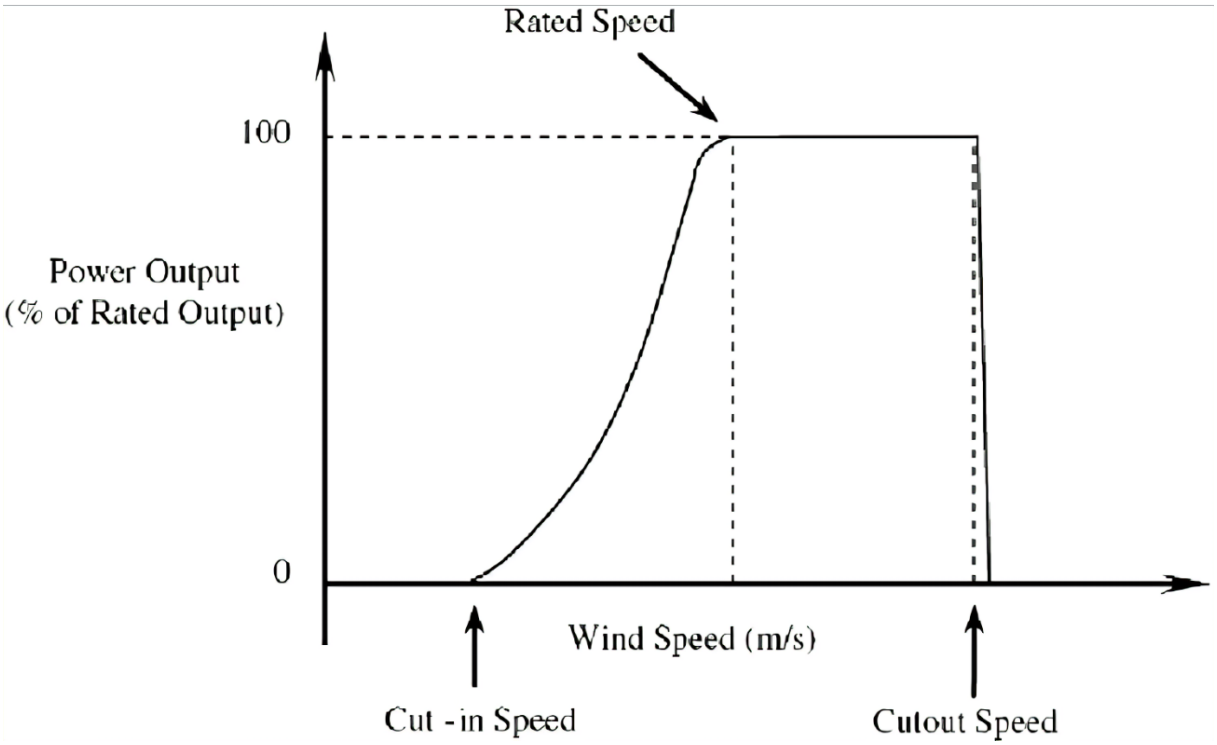

Figure 1.5: Power curve of a wind turbine

1.2.2. Extrinsic offshore advantages

Let's close, for now, these preamble physical parenthesis and explain why the wind power sector is spreading beyond the shores.

Going offshore appears as a solution to extrinsic issues of the technology when installed onshore. First, especially in dense areas such as Europe, a saturation of the zones is witnessed. Indeed onshore the topography, the urban and agricultural areas and the preserved areas tend to limit the available sites for wind power plants. As matter of fact, [2] explains that in many countries the majority of geographically adapted and windy sites have already been invested. Onshore, an evolution of the technology towards lower wind technology is thus witnessed, leading to the emergence of different class of turbines defined as follows in the IEC classification of the wind turbines:

parameter	class I	class II	class III
Reference wind speed (m/s)	50	42.5	37.5
Annual average wind speed (m/s)	10	8.5	7.5
50-year return gust (m/s)	70	59.5	52.5
1-year return gust (m/s)	52.5	44.6	39.4

Table 1.1: IEC Wind turbines classes

Less windy sites require lower class to effectively exploit the kinetic energy from the wind. To do so, bigger than required rotor diameters, and thus more expensive and complex turbines, are required to produced the same power and compensate the loss due to wind velocity decrease in the equation (1.1). Higher classes are thus characterised by lower specific power and thus less competitive turbines. Yet, [2] explains with graph 1.6 how the saturation in onshore wind project will tend to generally decrease the mean specific power for every classes in the years to come. This phenomenon could slower and complicate the future skyrocketing of onshore wind projects.

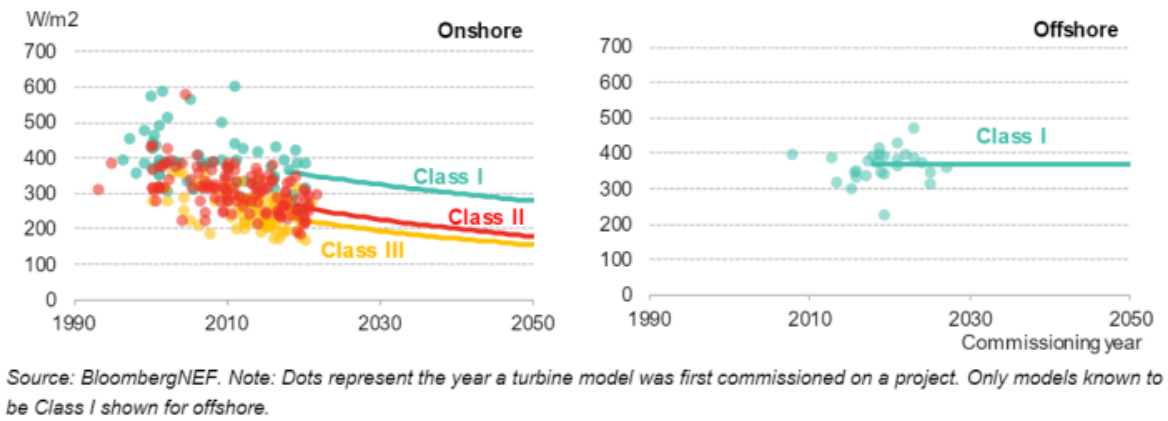

Figure 1.6: specific power forecast onshore and offshore (BNEF)

Unlike onshore case 1.6, offshore topography and sites exploitation are way less constraining and saturation id far from being achieved. Plus, the development of lower classes is not necessary yet.

Then, the main obstacle to the rise of onshore wind project is the so called NIMBY (not in my backyard) effect, described in [35]. This phenomenon lead to a global disapproba-

tion of a part of the public toward the development of wind project near their habitation zones. This Nimby phenomenon is is also present for other types of projects but onshore wind is by far the more concerned sector nowadays. This subject can also find national political resonance in the public debate, which can damage the dynamism of the sector which as previously said rely in a way on government policies.
If as previously explained onshore wind is a tremendous asset for the necessary energy transition, its impact on environment and landscape at local scale is undeniable. Indeed, this technology need space to reach utility scale since for efficiency issues that will be discuss later two wind turbines cannot be to near one to another. Plus, as showed in [2] turbines used onshore are for the most between in a 2-5 MW range, hence an important number of turbines for large scale plants able to "replace" the classic fuel based ones. The civil work required for construction can thus damage the biosphere of a site. Then, a typical 3 MW turbine already tops the 120 m in maximum height [5], with rotor diameter about 90 m. This make these turbines visible from far, especially since they are more likely to be installed in plan areas where winds are more stables. To this damageable impact on landscapes must be added a noise issue that can be tremendous in populated areas. These considerations make the identification of potential sites ever harder, endorsing the previous argument on saturation.

Figure 1.7: Riot against onshore wind power project in Canada

Offshore, nimby phenomenon must also be taken in consideration, and will be further in this work. Yet parts of the problems such as impact on populated areas and landscapes are deleted when selected sites are far from shore. This is largely discuss in CITE CHAPTER. ++ LESS DENSE CF NEXT PARAGRAPH

Last but not least Nearly 2.4 billion people (about 40 per cent of the world's population) live within 100 km of the coast [36], and this share is on the rise. Accordingly, the majority of main industrial and commercial facilities are located in coastal areas. The offshore wind thus relocate the electricity production near the zones of heavy consumption, lightening the burden on distribution networks.

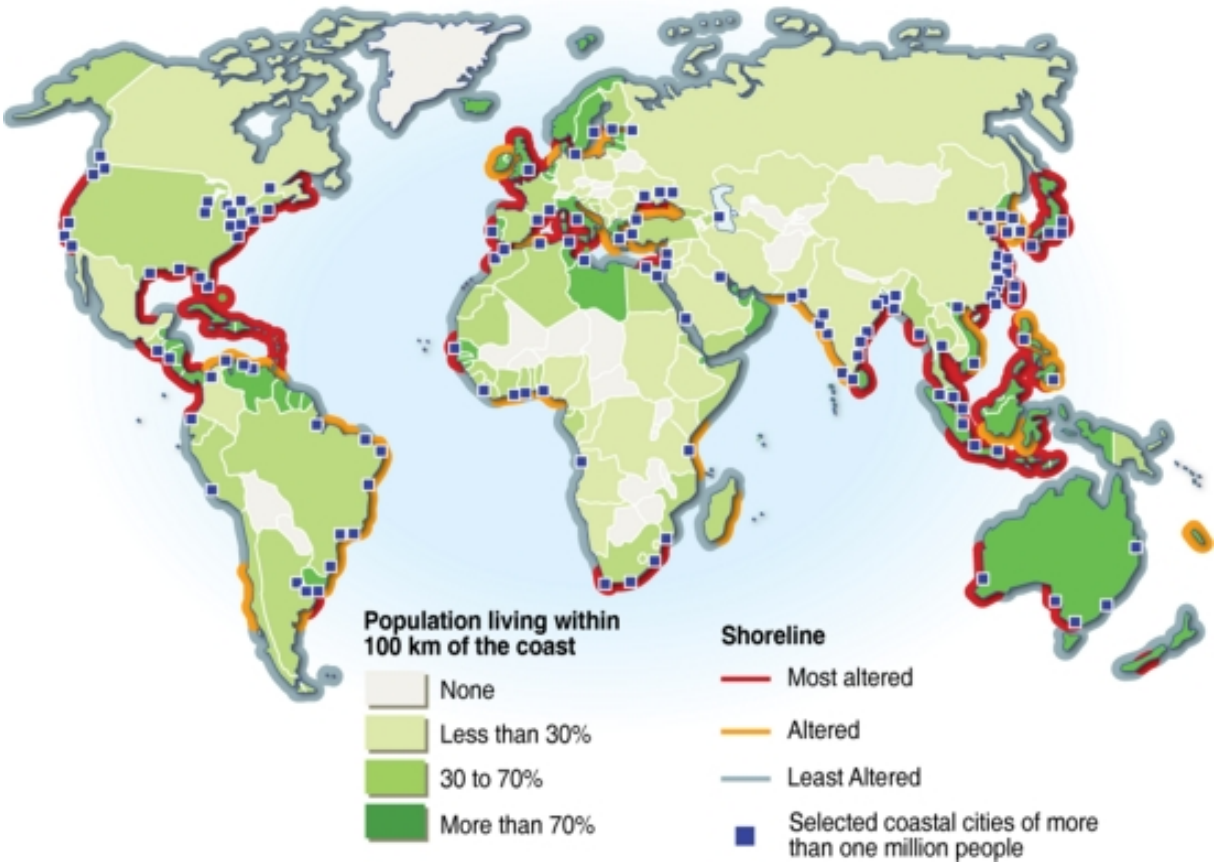

Figure 1.8: Part of world population living within 100 km of the coast

1.2.3. Intrinsic offshore advantages

Let's now discuss the intrinsic physical and engineering aspects making offshore wind a more efficient way to exploit wind energy.

[2] explains how breakthroughs in terms of technology optimisation, material use and installation process rise the bar of maximal turbine sizes. For example the use of glass fibber composite illustrated in 1.9 allows to increase blade length without dramatically impacting blades weight and vibrating behaviour, making these solution viable and competitive.

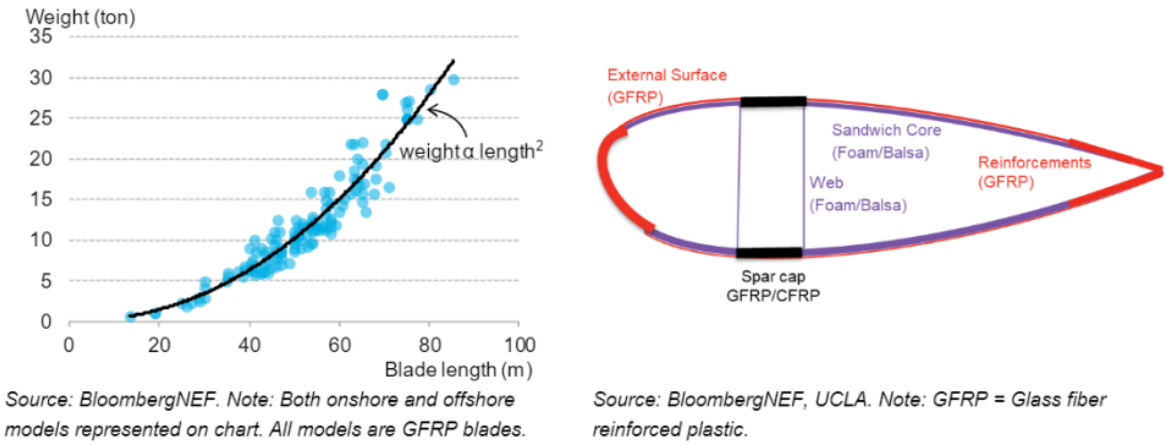

Figure 1.9: Blades weight increase with length and material use from [2]

Equation (1.1) shows that generated power evolves with the square of the blade length, hence the aim to create bigger rotors to capture more kinetic energy. Plus, the use of bigger turbines more dense and competitive plants as it will be largely discuss later while evaluating the cost of floating offshore wind projects CITE.

Thus, the trend in the wind sector is toward ever bigger turbines [2], and offshore this aim can be fully expressed. Indeed, while onshore the NIMBY related issues presented in subsection 1.2.2 are exacerbates with turbines sizes, there are fewer barriers to their installation offshore. Plus, greater rotor diameter tends to increase the shear stress and bending moments on the structure related to wind velocity differences between the lower and higher zones of the rotor. Yet, anticipating on the next argument, the quality of the wind flow is better offshore than onshore as explained in figure 1.11. Hence less design constraints for the development of great rotor turbines offshore.

Noawadays, the biggest turbine ever produced has thus been developed for offshore application and is rated at 12 MW. This is the Haliade-X offshore wind turbine high of 260 m with a rotor of 220 displayed on figure 1.10

Figure 1.10: General electric Haliade-X real size 12 MW prototype in St-Nazaire, France

As exposed by Lynn in his book [4] when listing the advantages offered by offshore applications, the first driver for going offshore is the wind quality: while onshore it's hard to find class I sites (cf table 1.1) with average wind values about 10 m/s, even leading to saturation issues described in subsection 1.2.2, offshore it's common to find sites with average wind speed higher than 11 m/s. A quick glance at the online wind data library wind atlas [24] developed by the well-known wind expert Denmark technical University confirms this statement (this tool will be further presented later on). By the way, this explains why BloombergNEF only considers class I turbines for their evolution forecast in figure 1.6.

This increase in wind quality also come from the sea softness. Indeed, onshore many obstacle at the surface stop the air mass flows, heavily decreasing the wind velocity at low altitude. Because of air viscosity [37], this perturbation due to surface roughness spreads along the z direction, the lower air flow layer "slowering" the upper one, until reaching a maximum undisturbed value at high altitude. Figure 1.11 illustrates this phenomenon. Offshore, this undisturbed value is usually higher than onshore and is reached at way lower altitude.

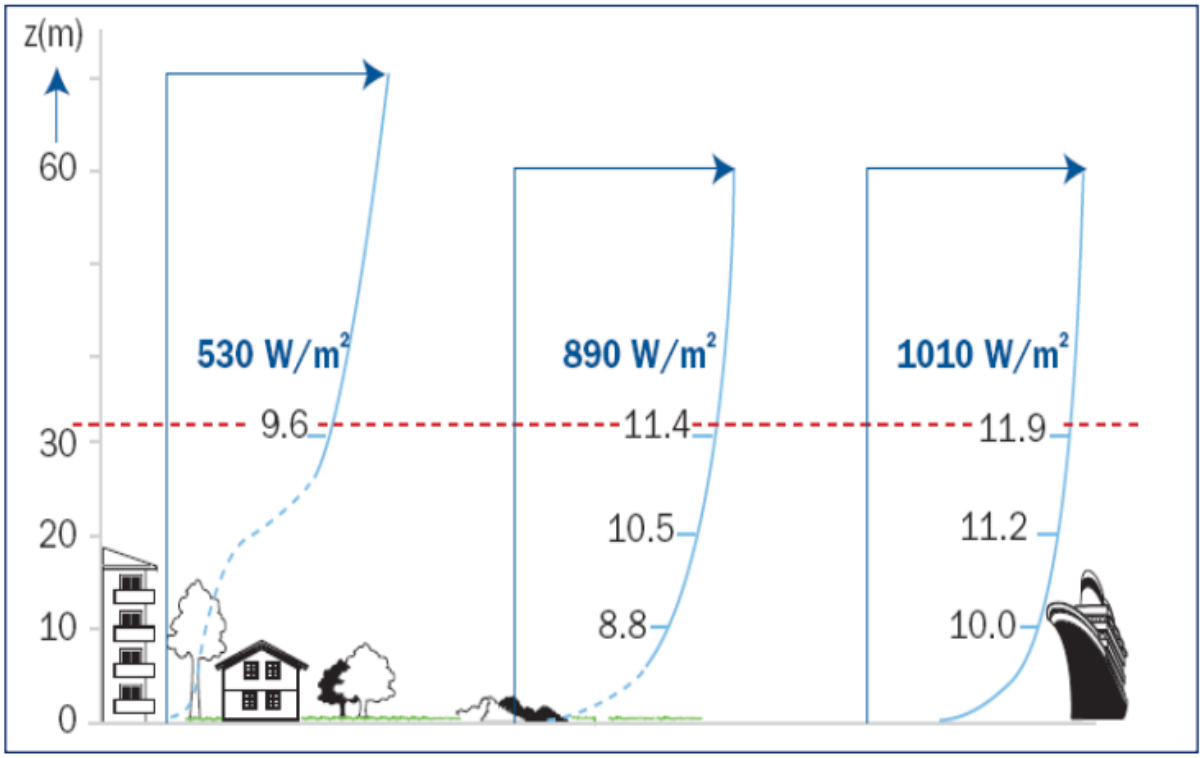

Figure 1.11: Higher average wind speed and faster wind shear development [3]

This wind shear effect lead to a dependence of the wind velocity v on the altitude z that can be approximated according [4] and [37] by this equation:

$$\frac{v}{v_0} = (\frac{z}{z_0})^{\alpha} \tag{1.3}$$

The coefficient alpha depends on the surface roughness. Offshore, a typical value is $\alpha = 0.14$. Onshore it can reach values of 0.3. Thus, the greater dimension of the turbines for offshore application lead to a an additional benefice: higher turbines can exploit faster winds. This aspect cannot be neglected even for low values of α since, combining equations 1.3 and 1.1 we get:

$$\frac{P}{P_0} = (\frac{z}{z_0})^{3\alpha} \tag{1.4}$$

Thus, small height increase can lead to non negligible increase in power. For example, figure 1.12 shows that going from a nacelle height of 100 m to 140 m could increase the power exploitable by about %.

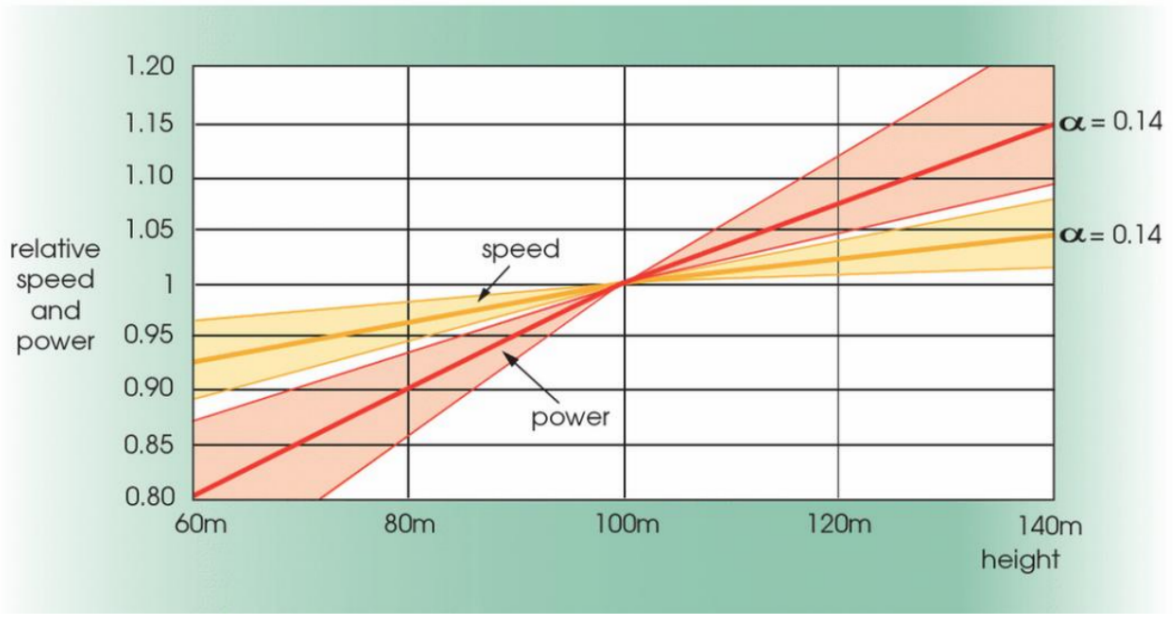

Figure 1.12: Variations of wind speed and power due to wind shear from [4]

In addition, Nasa Earth observatory [38] in addition to the confirmation than offshore wind are stronger, explains that offshore winds are more stable than onshore ones. Indeed seas offering as previously explained obstacle-free environment to the mass flow, less parameters enter in the complex fluid dynamics processes at stake (not studied in this work) leading to more fluid and less gust-made flows. Plus [38] and [3] explains that offshore wind are result of larger scale phenomenon than onshore ones of which variations can results from local topographic linked phenomenon. This last argument support the stability idea and make offshore winds intrinsically easier to predict, which also stands as a pros for an energy application optic.

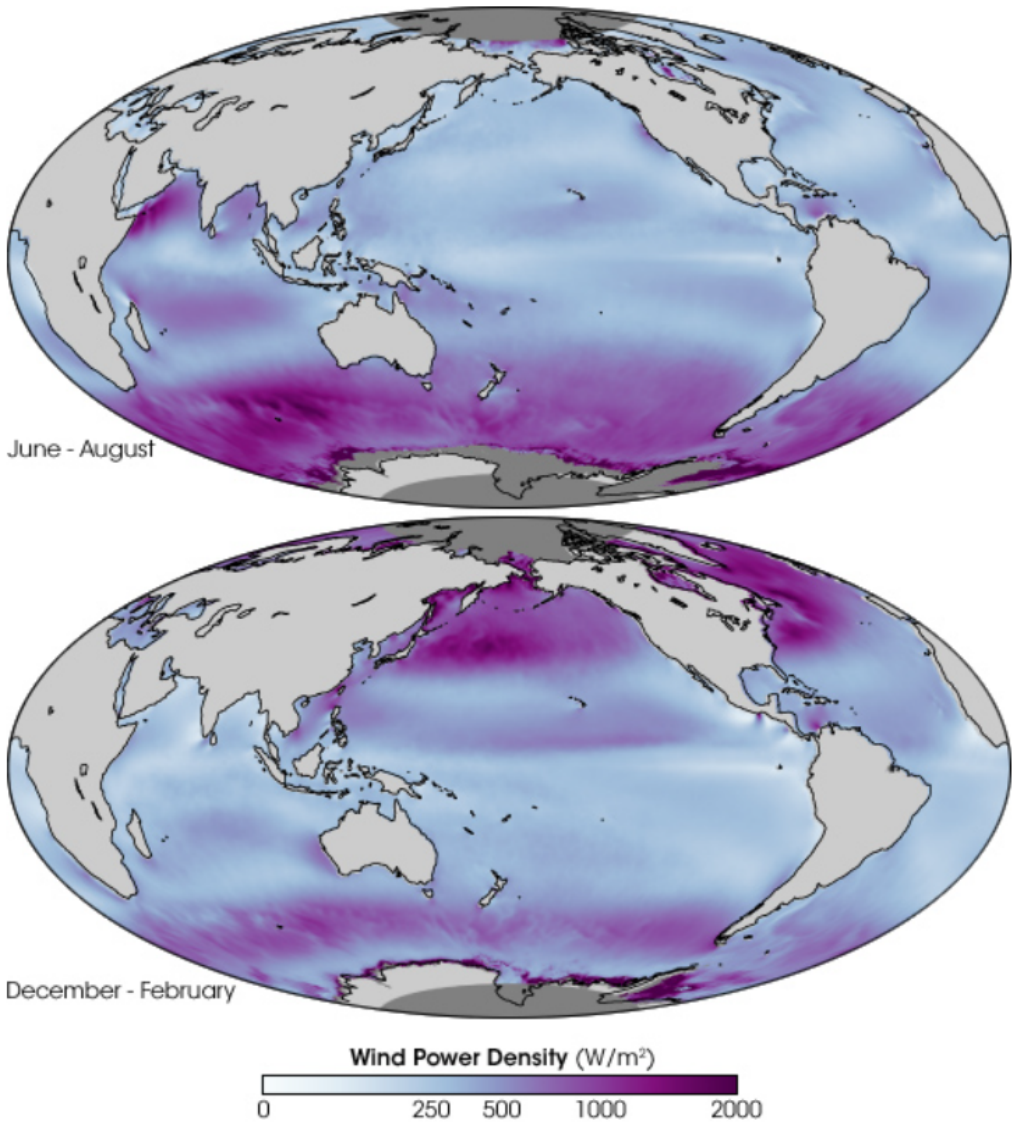

Figure 1.13: Global Ocean Wind Energy Potential from NASA Earth observatory

[5]

The consequence of this accumulation of arguments is a higher capacity factor for offshore wind than for onshore wind. The capacity factor is an important notion that link the rated power of a plant to its real energy production. Indeed, a 10 MW turbine does not always produce 10 MW as figure 1.5 tells us. The capacity factor, or Load factor LF, over a period T is thus defined for a plant of rated power P as:

$$LF = \frac{energy - produced - during - T}{P.T} \tag{1.5}$$

In the end, offshore wind provides higher capacity factors than other variable renewables such as onshore wind and solar PV. In 2018, the average global capacity factor for offshore wind turbines was 33%, higher than the 25% for onshore wind turbines and 14% for solar PV. Looking forward, thanks to design optimisation and technological breakthroughs, new offshore wind projects are expected to have capacity factors of over 40% in moderate wind conditions and over 50% in areas with high quality wind resources. [5] This better load factors allow wind offshore to produce more electricity and thus justify the necessary overcost related to this technology. This economic comparison wil be further assessed later on.

Finally, more stable winds [38] also bring less hourly variation during the day as shown on figure 1.14. Offshore wind thus appears as a reliable energy source for the grid and its characteristics, even if not controllable, are thus closer to the classical fuel based plants from grid point of view.

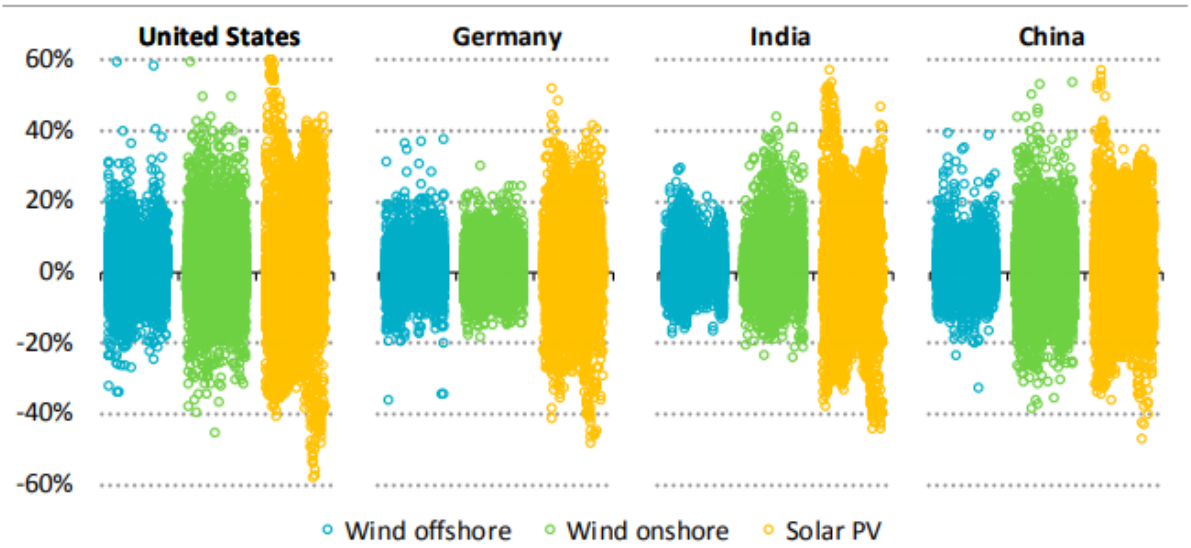

Figure 1.14: Range of mean hour-to-hour variations in output by technology, based on 2018 weather data, from [5]

In addition, as previously said, long term prediction are easier for this technology, easing the work of the TSO that are ever more basing their work on mathematical predictions that try to match the complex meteorological phenomenon that drive the renewables production. Indeed, the french TSO RTE explains [39] that the increasing share of intermittent renewables in the production mix could threat the network integrity. Thus,

its flexibility must follow up and the introduction or more stable and more predictable energy at large scale could ease the burden.
In this optic, the seasonality of the monthly load factors must be assessed. [5] present on figure 1.15 these values for different countries. An very interisting point is that the profiles simulated are complementary to the other main renewable energy source: Solar PV. Thus offshore wind could be a good partner to solarPV in a future fully renewable and balanced mix, decreasing the need for large electrical storages.

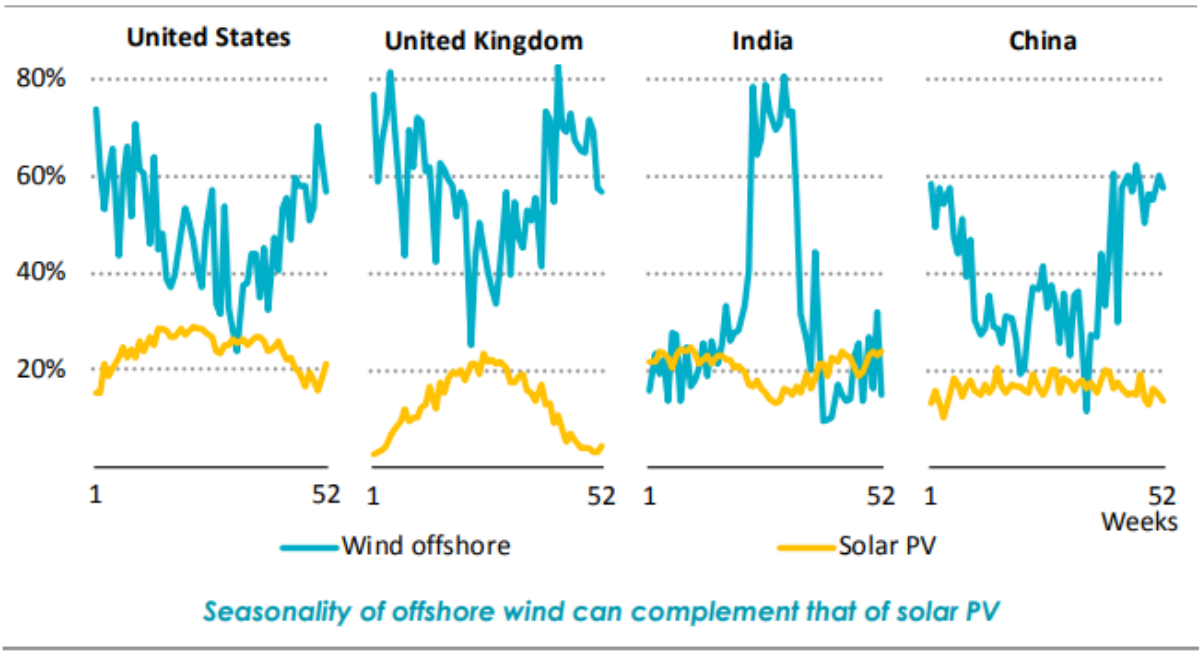

Figure 1.15: average weekly capacity factors for new offshore wind and solar PV projects by region , based on 2018 weather data, from [5]

By the way, [5] states that offshore wind is not subject to the same intermittency limitations as onshore wind and solar PV. The IEA classifies offshore wind as a "variable baseload technology" owing to its high capacity factors and lower variability, as compared with onshore wind and solar PV. Put simply, offshore wind operates, on average, at a higher share of its maximum power output and with less fluctuations. As such, offshore wind can provide more stable power to the energy grid, just as fossil-fuelled plants do, and "has the potential to become a mainstay of the world's power supply."
While energy security; i.e the capacity of the grid to be always balanced and in capacity of always satisfying the demand; appears as one of the major concern of the future energy mix[31], Offshore wind appear as a strong asset to invest in to tackle this issue. Developing offshore wind could thus accelerate our exit of the traditional controllable power plants.

Many arguments in favour the course for offshore has been listed. Along this study, the economical and technological issues related to the development of this technology will also be discuss for floating technologies. To conclude let's cite a last optimistic and motivating data from [5]: Offshore wind's technical potential is 36 000 TWh per year for installations in water less than 60 metres deep and within 60 km from shore. Global electricity demand is currently 23 000 TWh. Moving further from shore and into deeper waters, floating turbines could unlock enough potential to meet the world's total electricity demand 11 times over in 2040.
Let's now have a look to what extent this sector is effectively developing, since this values are slightly ambitious.

1.3. Offshore wind market overlook

Let's precise than in this section, offshore sector mainly concern classic fixed-bottom offshore wind, floating wind being still in its eraly development stage.
The idea to exploit the strong offshore winds is actually old [40], but have been for a long time regarded as too challenging from the technological and economic point of view. Thus, the first offshore wind turbine pilot rated at 220 kW is only installed in 1990 in Sweden. In 1991 the first offshore wind farm made of nine 450 kW turbines is developed in Denmark by the danish company Elkraft, nowadays Orsted, still one of the main leader of the sector.
The 90's have then been a decade of technological breakthroughs and market and legal organisation [41], and the sector really stared to enter commercial maturity in the 2000's, pushed by northern Europe countries such as Denmark, Germany and most of all United-Kingdom that quickly implemented ambitious policies to develop the sector, the supply chain, and make profit from the ideal sites in the north and the Irish sea.
Others milestones of the sector development, such as the entry of the US on the market or the symbolic 8 GW step overcame in Europe, are displayed on the timeline 1.16

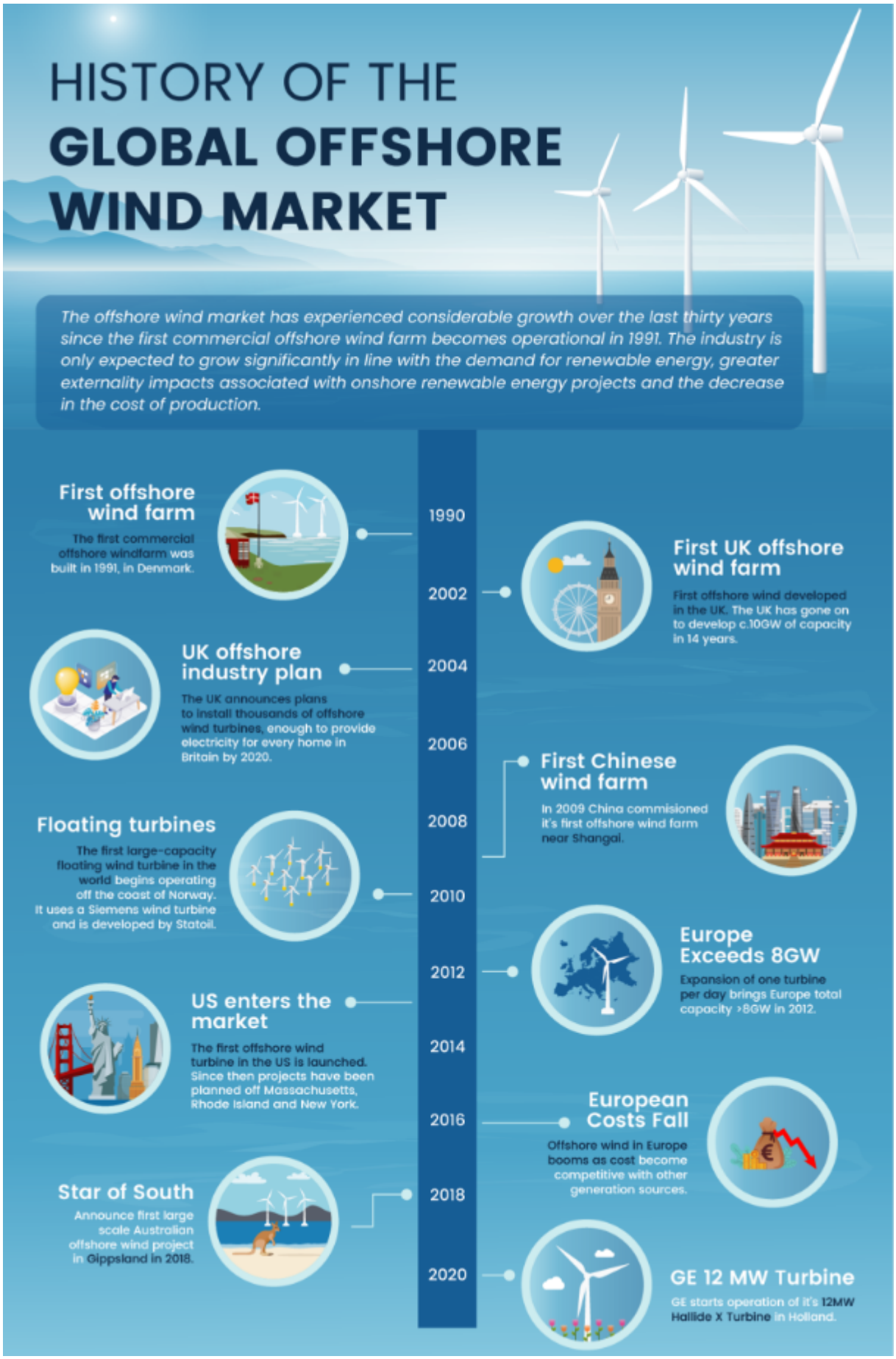

Figure 1.16: Brief history of the offshore wind market development

The epicentre of development of offshore wind has thus been northern Europe, and continues to be the centre of gravity of the sector (cf figure 1.18). This is the consequence of strong winds coupled to low profundity of the sites. Yet, in 2009 China disclosed its first offshore farm and has since appeared has one of the main development contributor in the last decade, as figure 1.17 shows. Some of its asian neighbours as South-Korea and Japan are also starting to enter the market (cf figure 1.19).
The graph 1.17 points out the exponential trend in offshore wind capacity addition between 2010 and 2018. During this period, UK, Germany and China for the most have installed more than 20 GW, among which 8 GW for only 2017 and 2018.

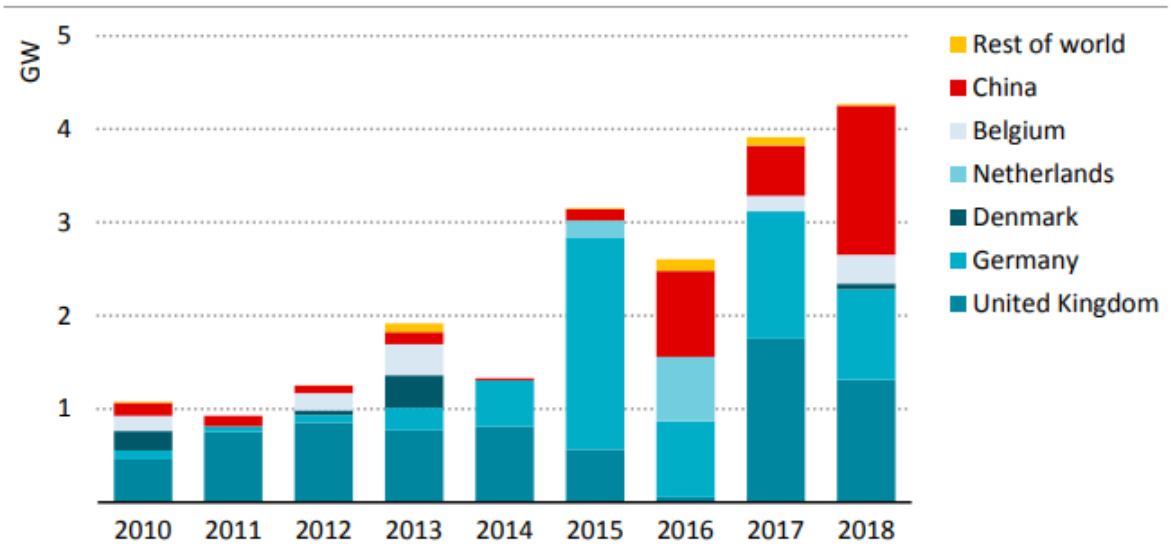

Figure 1.17: Annual offshore wind capacity addition by region, 2010-2018, from [5]

A useful tool to visualise and quantify the extent of offshore wind deployment is the interactive map [42] developed by 4C offshore. Indeed, geographical zones occupied by existing or future offshore wind farms throughout the world are highlighted on this map. Plus, some basic information about the size and the owners of the farm are detailed for most of the cases. The existing wind farms are displayed in green and the one under construction in orange or in yellow according their degree of advancement. Then, future project are displayed from blue to dark purple according their degree of advancement in the pre-project phase. The two screenshots 1.18 and 1.19 shows that the purple sites in early planning stages represent the majority of displayed projects. Even if these projects will probably not all come to an end, this fact gives us a good indication on the expected explosion of the sector in the years to come. Even if few information are available on the projects. This useful tool shall however be used knowing that it may not be fully updated (mostly for floating wind projects), may lack some information and could indicate non

exact data, mostly for future project that may evolve in their size for example.
The two screenshots 1.18 and 1.19 from this interactive map [42] present the current two main zones of interest for offshore wind: northern Europe and china as previously discussed.

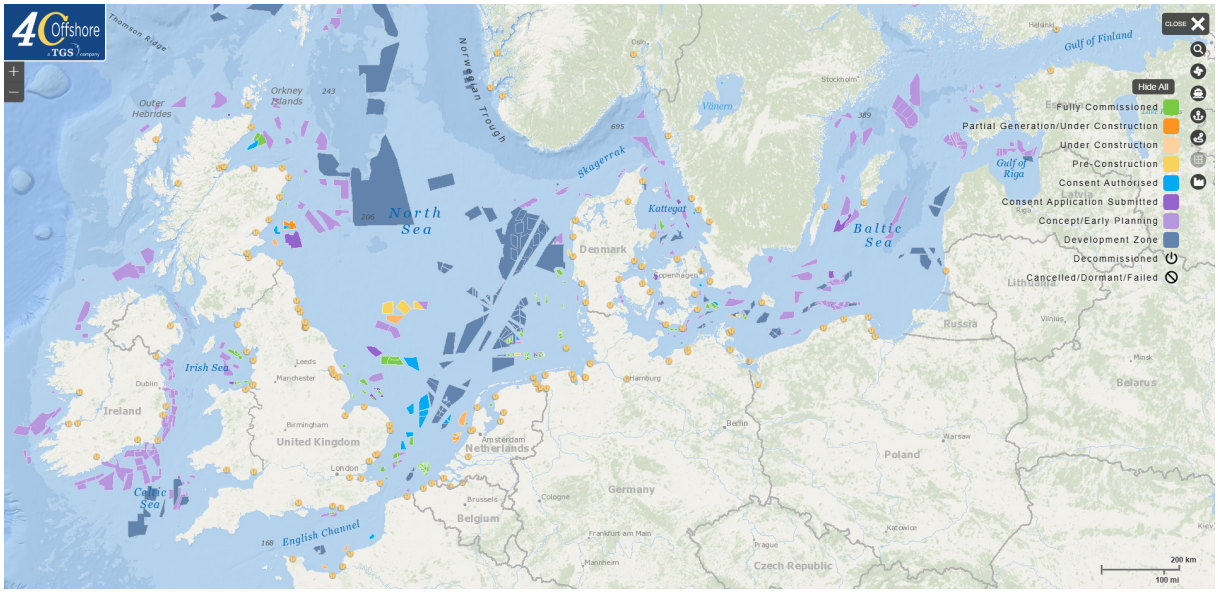

Figure 1.18: 4cOffshore Offshore wind project map, Europe

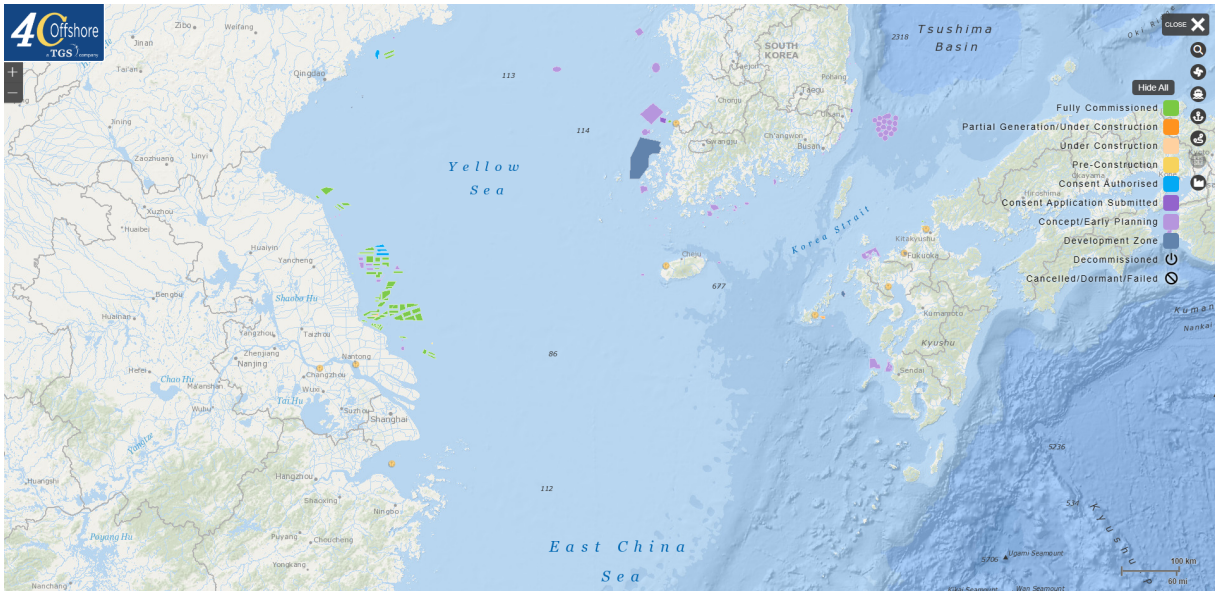

Figure 1.19: 4cOffshore Offshore wind project map, China

Global offshore wind energy in 2021 had a record year for deployment with 17,398 MW of new projects commissioned. At the end of 2021, the 50 GW bar was topped, reaching a

total installed capacity of 53 GW [43]. This growth was largely attributed to China, which commissioned 13,790 MW—more capacity in 1 year than the entire world has installed in any single previous year.
Macroeconomic and geopolitical events have raised the level of market uncertainty in 2022. The extended impact of monetary policy, the COVID-19 pandemic, and the ongoing conflict in Ukraine have created macroeconomic volatility, supply chain disruptions, and inflationary pressures. [43] This unexpected events have slowed down a little the sector increase, delaying some commissioning and frightening some investors. Yet, the 60 GW has still be overcame in 2022. Plus, if the effects of pandemic and geopolitical crisis have been detrimental on short term, the effects on long term deployment of the industry could appear as beneficial and strenghten the development pace. Indeed, the global energy crisis the wordl is currently facing as described in [31] led to huge increases in fossil fuels prices and shed light on the advantages of renewables sources both in term of cost and autonomy.

As previously explained, the main driver for the good health of the sector remains in its recent economical competitiveness (cf map 1.3) in comparison with other energy sources. This competitiveness is the result of the market development described above, supported by green policies and incentives, and off course from its numerous assets described in 1.2. As previously said, a good tool for valuating the competitiveness of a project is its LCOE. The various reports this study is basing some its discourse on, wheter they are elaborated from private cabinates as BloombergNEF [7] or DNV [29] or from public authorities as IEA [5] or NREL [44] converge toward the same insight:this LCOE is on a clear decreasing trend. Yet, the hypothesis and the calculus methodologies differ from one one approach to another thus, for now, the trend is more insightful that absolute values. Plus, offshore wind is really a sector where LCOE values are drastically impacted by sites characteristics such as wind intensity, deepness and distance to shore, as it will be discussed later on. In every cases, the decreasing trend observed in costs for signed projects as well as multiplication of contracts signed in recent years cannot be denied and is showed by fig 1.20. Floating offshore projects must not be considered in this trend and have thus been highlighted on this graph.

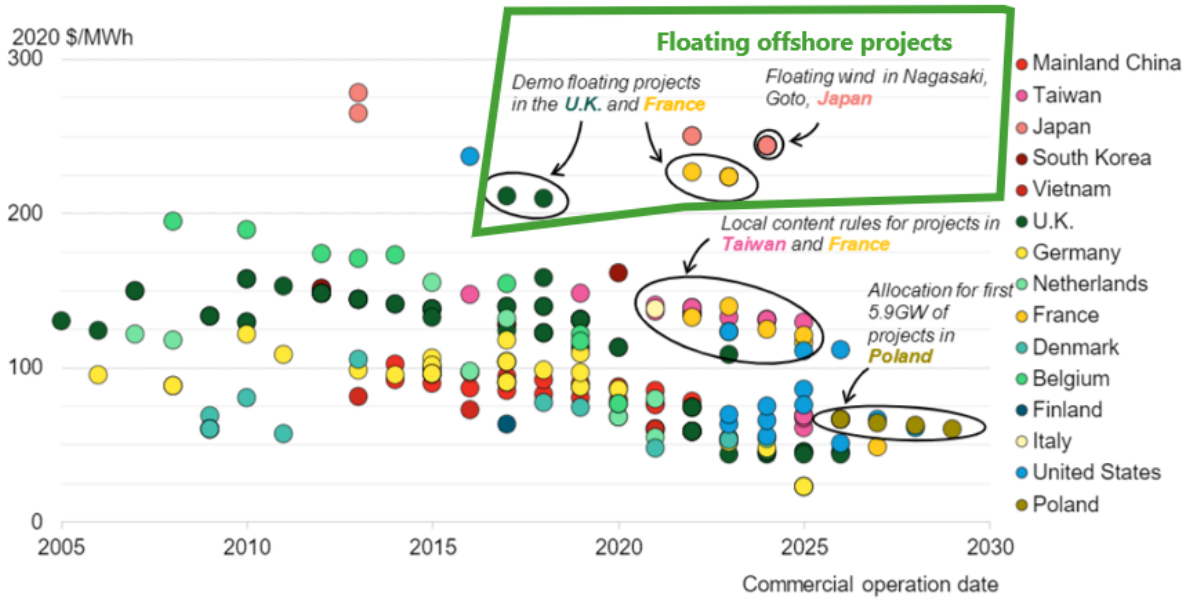

Figure 1.20: Levelized offshore wind prices, from [6]

The offshore wind market also rely on the strategy adopted by each country. Indeed, as BNEF explains in [6] two main conceptions for the management of the sector development can be adopted by government.

- On one hand, the mechanisms for awarding contracts is centralized: the state performs the site identification as well as the pre-sizing of the future plant and the impact studies required. Once the site is identified, a call for bidders is disclosed and companies present their solutions. In this case, the state take in charge a large part of the development risk but, doing so, they can have a better overview of their energetic planning and can easily attract investors. For example, the last call for tender disclosed by France in 2022 for 1 GW project located in the English channel received about 12 applications, among which 6 consortiums made of different size companies, have been pre-selected. All the information relatives to the french call for tenders are available on the dedicated website from french government [9], where gloabl view as well as specific information on each project can be found. The french case (see more in section 1.4) is also interesting since it easily illustrates the increase in competitiveness discussed right above. Indeed, in order to sustain and incentivize the offshore wind development in France, a feed-in-tariff (FIT) mechanism has been established to reassure the project leaders. This FIT is a contractual value at which the MWh of electricity generated by a plant will be sell, the difference with the real electrical market price will be covered (or absorbed) by the state, reducing the risk for investors. Thus, the decision from the call for tenders relies on the FIT value

on which both terms agreed. In 2012 when the first 5 french fixed-bottom offshore projects were attributed on FIT values around 140 €/Mwh. In 2020, EDF win the tenders for the Dunkirk project a FIT value of 49 €/Mwh [9], which mean the LCOE for this project has been evaluated at an even lower value.
The main other countries adopting this kind of centralized strategy are Netherland, Belgium, Germany and Denmark [6]. Yet, going in details, strategies can differ from one country to another: for example some countries as France ask use of local content to winning bidders in order to develop the supply chain and create jobs in the fields. Plus, in this configuration, the winners are generally not in charge of connection to grid of the plants, which is then let at the responsibility of the local transmission system operator (TSO). We will see during the cost analysis that this can drastically affect the elaboration of a project. Let's precise that Denmark is an exception to this last rule.

- On the other hand, contracts can be awarded by countries on a so called developer-led approach. The development risk are here taken by project leaders that must wholly define their projects. The projects are then generally chosen after an auction for site leasing where the consortium will develop their solutions. This is the case for US market with lease auctions organised by states (Maine, Ney York or California for example [43]) and United Kingdom, with the huge Scotwind tender for Scotland, described in government website [8], which will be analysed in section 1.4. The newborn italian market currently seems to also adopt this mechanism, a detailed analysis of this not yet developed floating market will be performed in 1.4 and later on in this study. More than providing the lease amount, developers must then provide all the environmental and social impact studies asked by the authorities. In this configuration, governments does not directly endorse the responsibility of the sector development and thus national TSOs are not taking in charge the connection to grid related investments.
  Other notable countries adopting this contract awarding mechanism are Poland and Taiwan.

Both approach coexist, some hybrid ones are even chosen by some asian countries, while Japan for example is considering switched from the second to the first one in the next years [6]. It depends on the place offshore wind take in the politics of the country but also on various political and economical factors that will not be further discussed in this study.
Let's precise that the chosen approach is not correlated to the country ambition in offshore wind development: for example UK has been a real pioneer in the development and

still has one the biggest portfolio in the world while adopting a developer-led approach. Their ambition is thus seen via financial incentives and supply chain development policies.

The offshore wind sector is technologically challenging and thus rely on a large amount of specialised company constituting its economical ecosytem. Actually, from this point of view floating and fixed bottom projects are quite different sine the actors of floating are not intrinsically common to the classical offshore sector: the needs in terms of foundation structure, cabling and installation are not the same. Thus, only the floating sector actors will be presented in section 1.4 and later on in this work.
Yet, floating and fixed-bottom share a common preponderant subsector which is turbine manufacturing. This field is still dominated by three of the common wind-turbines manufacturing giants:

- Siemens Gamesa (Germany/Spain) became pioneers of the sector the sector 30 years ago installing the world's first offshore wind power project, Vindeby, in 1991 and still lead the sector with more than 70% of market share in Europe[45]. In addition, the company has the most extensive installed base and the largest order book in the industry. Its cumulative installed capacity tops 15 GW.
- Vestas (Denmark) is the main wind turbine manufacturer onshore and entered the offshore market [46] with Tunø Knob in 1995, the industry's oldest commercial offshore installation still in operation. Vestas has a track record of +8 GW and +1,500 turbines installed across 46 projects , covering markets in the UK, Netherlands, Belgium, Sweeden, Denmark, and Germany - and already have floating experiences in markets like Portugal and Scotland.
- General Electric (France/Spain) [47] (GE) has invested more than USD 400 million to develop the most powerful offshore wind turbine (cf its Haliade newest design in figure 1.10). An investment set to drive down offshore wind farms' levelized cost of energy (LCOE), helping make offshore wind energy more competitive for their customers [47]. Their current installed power is about 7 GW installed worldwide, they lead the promising American market.

This three giants have been sharing the large majority of the occidental market since its beginning and have thus been strong market and technological actors of offshore wind development. Their knowhow, their credibility and their supply chain development make them hard to beat for potential newcomers, and thus they are set to keep their leadership in the dynamic European and the new born American market as figure 1.21 shows.

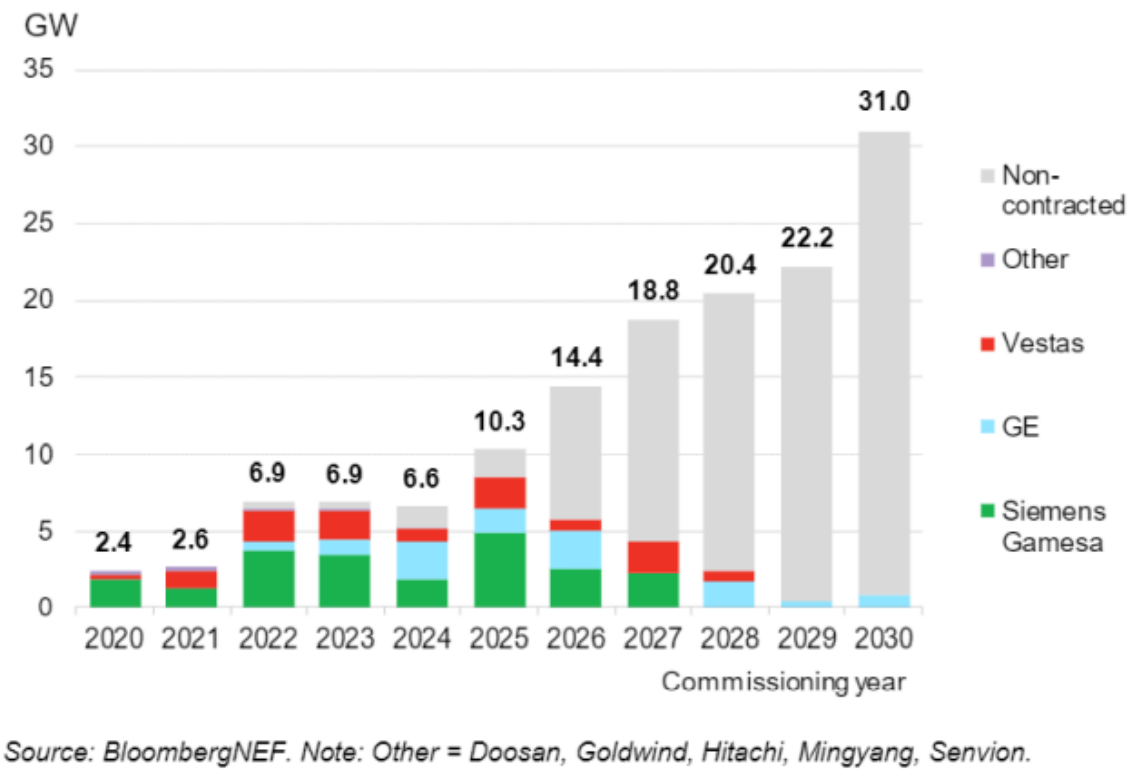

Figure 1.21: Annual ex China installation by manufacturer, from [6]

Yet as already discussed China is nowadays the most dynamic market worldwide and these three European giants are yet to win contracts in China, exclusively composed of Chinese companies [6]. Thus, Chinese manufactures such as Goldwind, Shangai electric and Mingyang have seen their comprehensive park skyrocket in the recent years, making of Mingyang's park the second most important in the world.
This figure also highlights that the Chinese market is more fragmented than the European one. Yet, knowing that the Chinese sector is set to follow its exponential trend (cf figure 1.23) and that these companies now even yearning for occidental markets, it would not be surprising if Chinese companies take the global lead in offshore turbine manufacturing in the years to come.

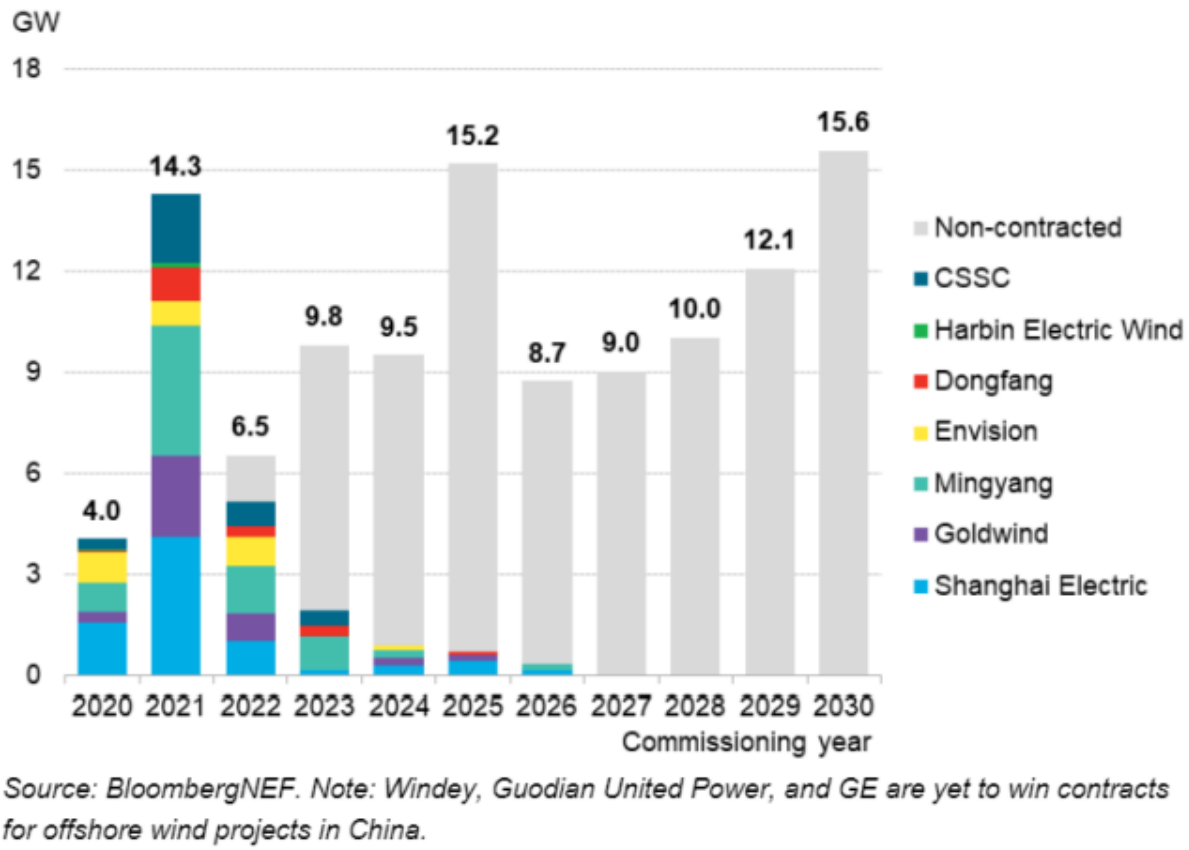

Figure 1.22: Annual China installation by manufacturer, from [6]

In section 1.1, 2050 was erected as the pivot year for internationals emissions reductions policies. As explained over here, offshore wind can represent a major asset of this upcoming energy transition.

In this optic and based on the current trends, public announcements and projects pipelines, BNEF has performed a forecast on global installed offshore capacity by countries until 2035 in their latest rapport from 2022 first semester [7]. This forecast is summarised by graph 1.23.

The main insight from this forecast is the huge increase expected in cumulative installation. Indeed, from 53 GW installed in 2021, the expected installed capacity by 2035 would be 504 GW. The Chinese market is as previously seen expected to become the main market with more than 100 GW by itself. Then, the pioneer united-kingdom would still represent the second main market in the world, offshore wind would then represent a tremendous part of the british energy mix. Then, USA are set to heavily enter this market, as [43] explains, getting the third installed capacity of the sector by 2035.

Let's note that in the same BNEF report from the first semester of 2021, the value by 2035 was only 400 GW: the trend appears more and more fast every year.

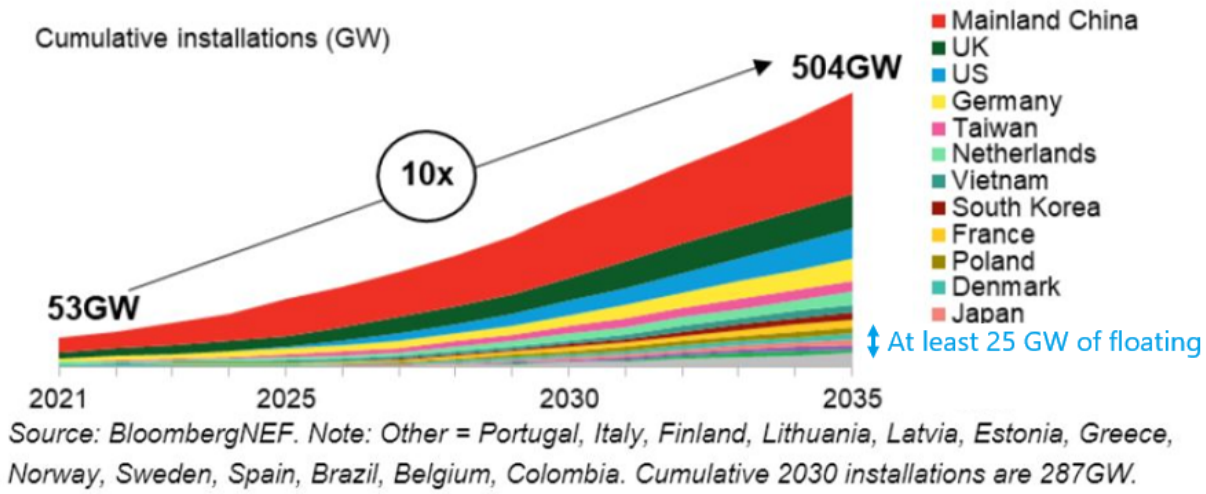

Figure 1.23: Global cumulative offshore installation forecast, from [7]

According to [7], and as highlighted on graph 1.23, floating offshore is expected to reach commercial scale before 2035, and thus at least 5% of the installed capacity by 2035 will be related to floating plants, i.e 25 GW.
The trend concerning floating wind are really difficult to read and to learn from since the sector is really young, and thus this value can appear conservative and under-evaluated (between the 2021 and 2022 report, the floating forecast by 2035 has risen by 25%).
The next section 1.4 will thus be dedicated to refine and precise this forecasts performing a holistic and global market overlook exclusively centered on floating offshore wind sector.

1.4. Floating offshore wind: holistic market analysis

1.4.1. Floating potentialities

Floating offshore wind has the potential to unlock deep water sites that were previously inaccessible. Floating turbines are mounted on top of the floating foundations anchored to the seabed by mooring lines. The difference between this types of technology with the fixed-bottom ones is displayed on figure 1.24

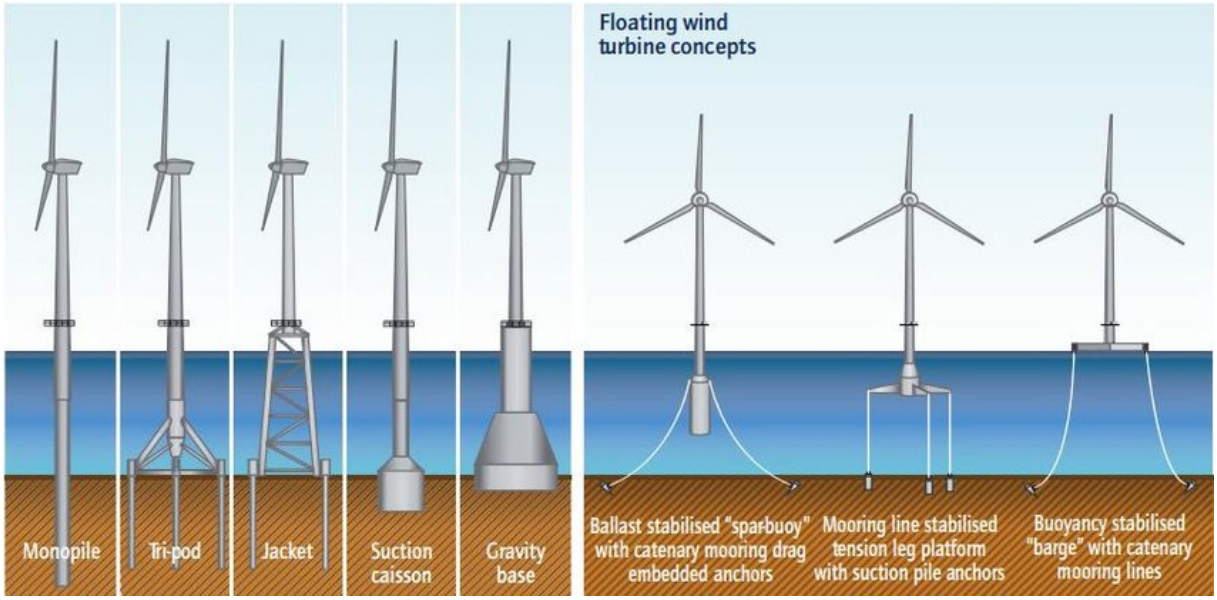

Figure 1.24: fixed-bottom vs floating substructures

This technology is rapidly gaining momentum around the world as the major driver of growth in the offshore wind industry and has several advantages that make it vital to delivering decarbonation of the global power sector. Here are listed some pros of floating technology against fixed bottom ones. These characteristics will be largely discussed in the techno-economics analyses to come.

- The Ability to be placed further offshore allows greater siting flexibility, increases project efficiency, and maximises value.
- Can more easily be placed further from shore since less sensitive to depth, reducing visual impacts, which are particularly important for tourist destinations.
- Floating wind Minimised environmental disruption due to less invasive mooring systems and allows for greater flexibility in terms of location.
- Floating wind offers more streamlined operations, maintenance (return to port for large correctives) and decommissioning, ultimately increasing local supply chain opportunities and reducing costs.

Globally, floating offshore wind represents an opportunity to access a much larger ocean area with high quality wind resources in waters that are deeper (greater than 60 m) than where fixed-bottom foundations are feasible. [43] In the United States, the majority of the total technical offshore wind resource lies over water depths greater than 60 m, and in Europe that number is estimated to be 80% [48]. This ideas are corroborated by the values discussed in the conclusion of section 1.2.

1.4.2. Global market and projects pipelines

The floating wind market as previously explained in section 1.3 is still at its dawn. Few projects are already existing, thus few economical and industrial data are available to perform global studies and forecast such as the one previously cited for the global offshore market ([6], [7], [5], [29]). Thus, the market assessment performed for this subsection rely on personal researches led project by project, actor by actor, country by country. The large majority of the incoming information come from official websites of the numerous actors that will be enumerate. As complemented tools to be sure not forgetting any projects, the 4C offshore map [42] and the non detailed list from [43] has been used. Plus, the well informed online specialised review offshorewind.biz [49] has been a useful tool for the listing of projects performed. Then, since this projects have to go through various administrative procedures such as environmental impact assessment, public concerting with local authorities and population and connection request to TSOs, public authorities usually share key information on the davancement of the projects. A look at the governmental websites of some dynamic countries has thus also been usefull. To close this short preamble on the methodology used for this market overview, let's precise that every following graph have been used using the business intelligence software Tableau.

To the pivot date of 01/01/2023, 98 projects have been counted and analysed in 15 different countries. In this list, the most ancient project is operating since 2010, and time-scope ranges until 2034 in terms of announced operating year (cf figure 1.28). Over this timescale, the global worldwide pipeline currently announced is 55,142 GW.
Regarding the technological challenge coupled to the financial risk (these will be discus later), the huge majority of projects are led in consortiums between different industrial actors. Over 150 different industrial actors have been counted and, for every projects, these stakeholders have been identified and ranked by type as follow:

- Energy companies: These are the different entities that will end up owning the offshore wind plant and operating it. In some cases, various energy companies can have stakes in the same projects in order to share the financial risk. That is for example the case for the Orkney project led jointly by Vattenfall and Fred Olsen Renewables in the E2 zone of the Scotwind (cf 1.4.4). This term gathers 3 main types of companies: Oil&Gas multinational giants aiming to develop their green assets such as Shell, ENI or Equinor anciently Statoil; National energy companies such as EDF or Vattenfall and independent renewable enrgy producers such as Falck

Renewables or Qair.

- Project Developers: These are the one in charge of project development and sizing from its early planning stage to its commissioning. These companies are experts in the (floating) offshore sector and will be missioned by project owners to manage every phase of project development and face every technological, economical or administrative issue. According to governmental strategy (cf section 1.4) the environmental impact survey and site identification is also part of their tasks. More than 90% of counted projects present the classical configuration where a project owner (energy company) let a project developers expert in floating wind sector build the plant.

- Platform manufacturers: These are the one providing the floating substructures for turbines. These are key players since these floaters are the key distinctive and challenging element of the sector. Nowadays, as it will be discuss later, no industrial consensus have been reached on which technology adopt, and very parameters are not fixed yet. The market is thus fragmented with various solutions that will be presented in the techno-economic analysis part. Over the listed presented here, floaters manufacturers are often not disclosed yet since, for the late incoming projects, developers wait to see how the market and different propositions evolve with the beginning of commercial phase.

- FEED and construction companies: These companies can be part of projects as technological support on particular point of the project development according on their different know-how (consulting role) and to realise the complex installation processes that demand specialised skills. The realisation of the platforms can also be concerned.

- Investment funds: To share the financial risk, some energy companies are supported by external investment groups. Quantum Energy partners or Macquarie are two of the main funds involved in the field. In this study, these financial actors will not be further discussed.

- Electrical array and connection companies: Since, as it will explained later, these two points are tremendous and challenging points of a floating offshore projects, the industrial players in charge of this particular question can be disclosed early in the project development.

In few cases companies are hard to be classified in this way since their implication in the projects are hybrid, yet, a clearer overview of the various actors is enables by this

system. These industrial actors will be further analysed in the next subsection 1.4.3. The complete result of this work consisted in an excel tab of 150 rows that was not suitable for display here.

The floating market is young and has not yet experimented its commercial transition. The first floating turbine of big size, 2.3 MW, is installed in 2010 (cf figure 1.25) in the Norwegian sea by Equinor, a Norwegian state-owned multinational energy company headquartered in Stavanger. It is primarily a petroleum company, operating in 36 countries with additional investments in renewable energy.

Figure 1.25: First 2.3 MW floating wind turbine

The same Equinor installed the first pre-commercial floating wind farm in 2017 in Scotland. Named Hywind, this farm features 5 turbines rated at 6 MW and uses the spar-buoy technology (these technologies will be heavily discussed in the second section).
In 2021, still in Scotland, the Kincardine windfarm overtook the Hywind farm reaching an installed capacity of 50 MW. Owned by Cobra group, it is located 15 km from the Aberdeen cost and features five 9.5 MW Vestas wind turbines. The semi-submersible technology is here used for substructures, as displayed on the following picture 1.26

Figure 1.26: Kincardine floating windfarm, Scotland

Nowadays (01/01/2023) the global installed floating power capacity is about 115 MW, mainly located in UK via the two already presented pre-commercial wind-farms and another 3 turbines farms of 25 MW located in Portugal. The 10 remaining MW are distributed between Norway, France and Japan through pilot projects developed by floater manufacturers. Plus, in the months to come, about 300 MW in cumulative capacity of projects under construction mainly in France, Norway and UK are set to increase the global park. In the following graphs, the operating and under construction projects will be put together to qualify the readiness of some actors or countries to enter the floating market.

Yet, as graph 1.27 shows, the very large majority of projects counted in the global pipeline are neither operating neither under construction. 87% of the pipeline in terms of capacity are actually in an early stage defined as planning stage. In this stage, economic partnerships are sealed, sizing is performed, authorisation are asked and environmental and social impact assessment are made. This pre-work is reduced when mechanisms for awarding contracts is centralized by the country as explained in subsection 1.4. That is the case for the call for tenders in France (cf subsection 1.4.4) where two call for tenders worth of 250 MW and 500 MW are considered "near financial close" eventough every industrial players have still not been chosen. Thus, this category of project, representing 12% of the global pipeline, is defined by the ending of the sizing and permitting phase: industrial partners and subcontracting are chosen and the total budget is valuated and dedicated to the project via legal contracts. These projects can be seen as more concrete than the

permeating one which represent a yearn of industrial actors to develop projects but could still face many challenges before the effective commissioning of the plants.
Graph 1.27 shows that the vast majority of floating turbines are yet to be active and corroborate the fact that, as previously explained, the floating market is newly born and thus not fully constituted yet. Let's precise that the choice of representing installed power in ordinate of these graph tend to accentuate this disproportion since the operating and under construction projects are of course of smaller size than the huge commercial wind-farms announced for the future. For example, Shell and Iberdrola won a lease in the Scotwind auction in UK (zone NE7, cf subsection 1.4.4) for a huge 3000 MW farm, expected by 2032. This is the biggest project disclosed by now and, even if it is far from being comissioned, ot shows the huge development path that the field is expected to walk in the decade to come.

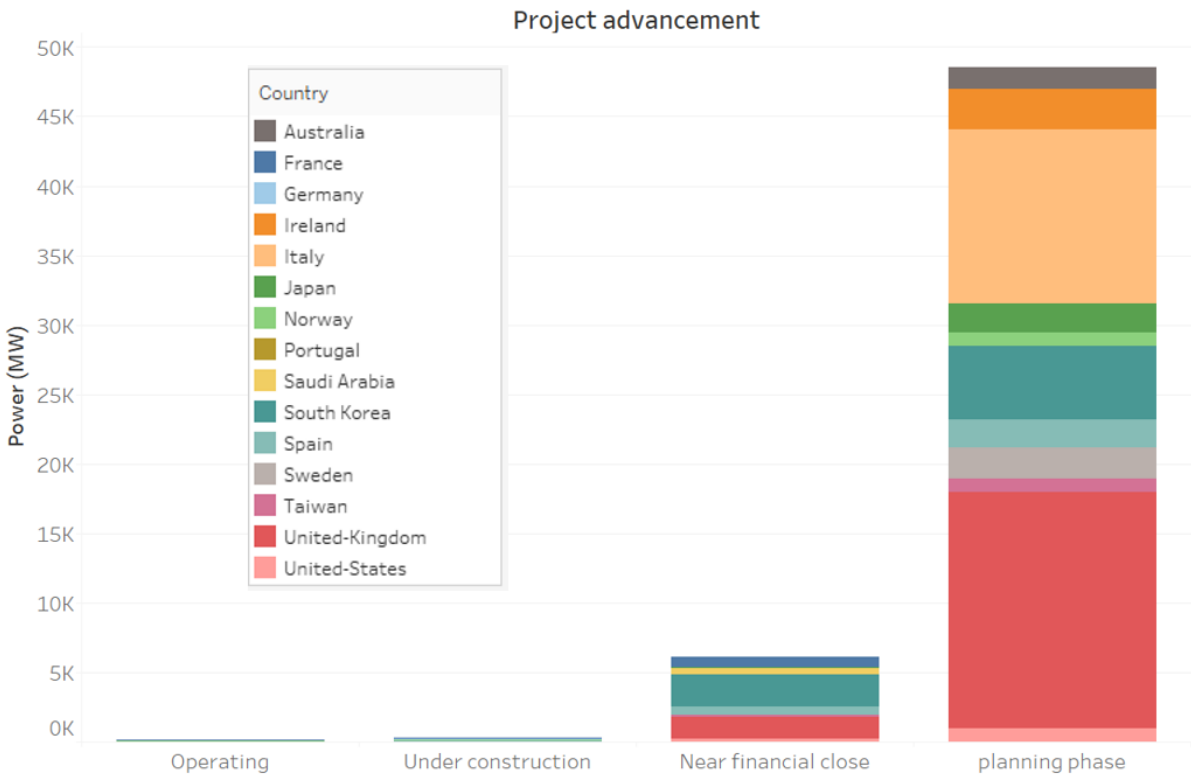

Figure 1.27: Project advancement overview

By encroaching sources (project websites, owners announcements, government policies) and by valuating the trends the expected commissioning years of every counted have been compiled. The yearly installed power per year is displayed on graph 1.28 until 2034. The main insight from this graph is the expected skyrocketing from yearly installed power in the years to come, with a maximum of over 14 GW commissioned in 2031. Let's precise

that the decrease after 2031 is not due to a slow of the market but to the fact that many projects are not disclosed yet.
From this graph, we can point out that the years 2025-2026 are expected to become huge milestones for the field with what could be regarded afterwards as the pivot towards commercial state. Then, the commissioning dates for some of the planning stage projects must be taken with precaution, mostly for countries as Italy that announce a huge pipeline while having few experience in the fixed-offshore field. Delays have been introduced in the forecast to take this in consideration, so to say that the trend itself remains more insightful that the absolute values. Every domestic market has its particularities and the most interesting ones will be discussed in subsection 1.4.4.

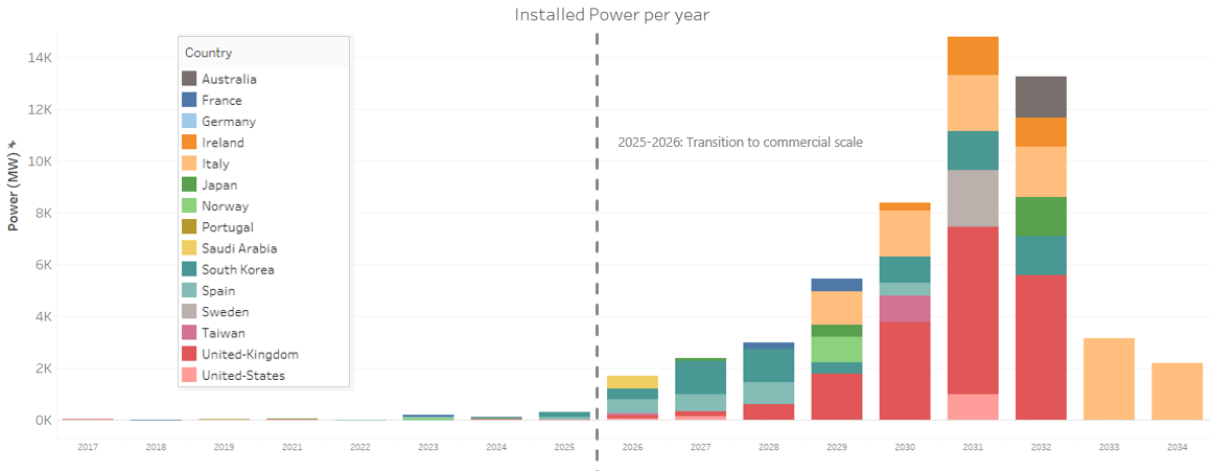

Figure 1.28: Yearly installed capacity forecast

On the two precedent graph, some countries emerge as main domestic markets for floating wind. Every country with an announced pipeline is colourised on the map 1.29, darker colours mean bigger pipelines. On this map, United Kingdom, South Korea and Italy end up as the countries with the bigger pipelines counted with respectively 18.687 MW, 7.620 MW and 12.552 MW. The share of italy is very important eventough the country suffers delay for its entry in the field, and this fortwo reasons: on one hand Italy has a full developer-led approach which mean many projects can be announced without Italian supervision. To limit this, as it will be explained later, only the project having already passed the scoping phase and with full VIA (valutazione impatto ambiantale) have been taken in consideration. On the other hand, a particular attention has been payed towards the Italian market since this study is developed in collaboration with A2A s.p.a. More projects have thus logically been detected in this zone.
On contrary, the share of countries as Spain, Japan and US impact could be underestimate since, eventough Government annouced ambitious goals, less projects have been officialy

annouced by industrial partners. For example, the Spain government alongside the Canary Island authorities announced 2GW by 2035 only in the Canaries, with only "small" projects of maximum 300 MW announced until now, bringing the canarian pipeline to 0,8 GW. Same for continental part of Spain.

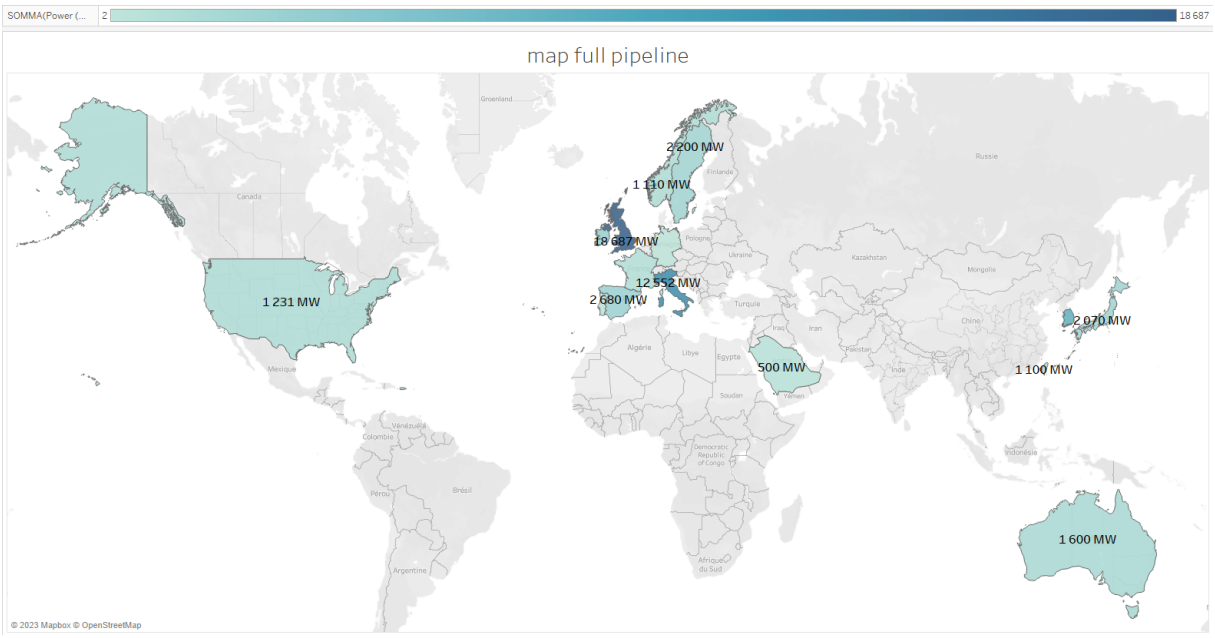

Figure 1.29: Global pipeline world map

Global pipeline is a key parameter of this study, but this only element might shade the locations where the market is effectively dynamic and which actors are currently helping the field pursue its commercial transition. To do so, the next map 1.30 is similar to the previous one but only colourised countries with "ready" fields, that's to say operating or under construction projects.

The world division is then drastically modified: alongside United-Kingdom, home of the two biggest operating farms, France appears as the other great pioneer of floating wind. These two important dynamic markets will be further discussed in subsection 1.4.4. Globally, the sector development is concentrated in Europe, Portugal, Spain and Norway following up. Finally, Italy and south Korea, while having huge announced pipelines, are yet to effectively enter the market, Italy has not even real experience in fixed-bottom offshore wind.

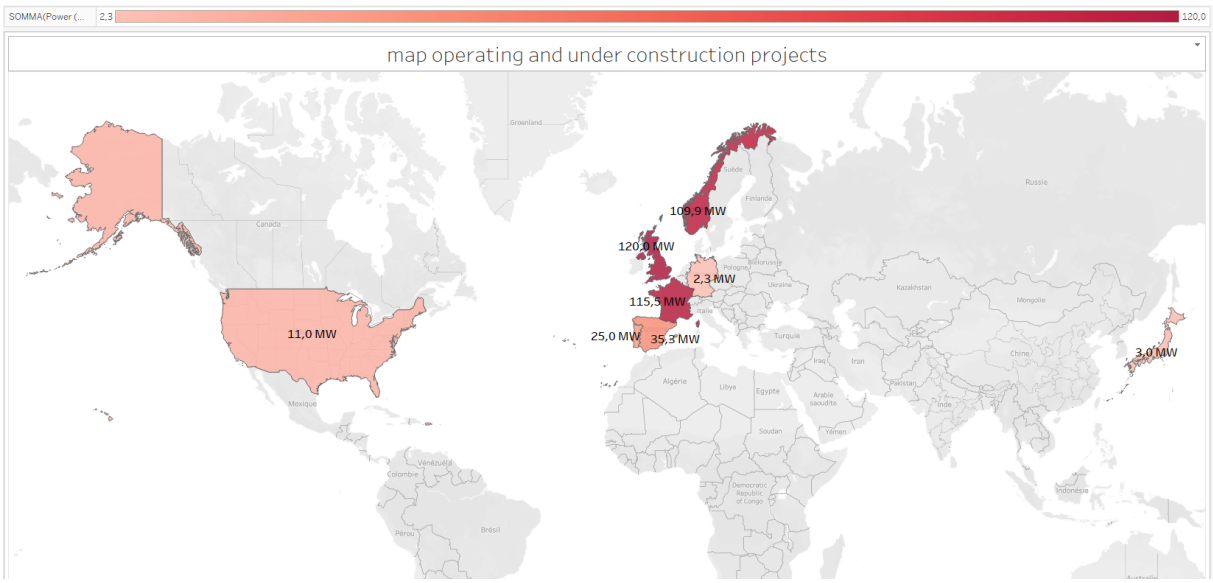

Figure 1.30: World map of most ready projects

1.4.3. Focus on main industrial actors

In this part main actors of the field will be highlighted. The two main actors on which focus will be put are two usual and almost mandatory parts of a classic consortium: energy companies (project owners) and project developers. Let's begin with energy companies. Graph 1.31 shows the first energy companies to have enterred the sector with as previously presented Equinor leading the way with 120,3 MW. This graph also the already discussed Cobra Group owner of the current biggest windfarm and then the owners of the 4 pilots projects under construction in France (cf subsection 1.4.4) Shell, Qair, EDF and last but not least OceanWinds that also owned the first pilot windfarms using semisubmersibles platforms (installed in 2021 in Portugal).
Looking at the same representation for the global pipeline on graph 1.32, the same names appear with Shell, OceanWinds and Equinor all trusting the top 5 in terms of announced pipeline. Yet, a newcomer take the first place: the independant italian producer FalckRenewables. Then, other giants such as Iberdrola and TotalEnergy are set to extand their pipelines in the years to come.

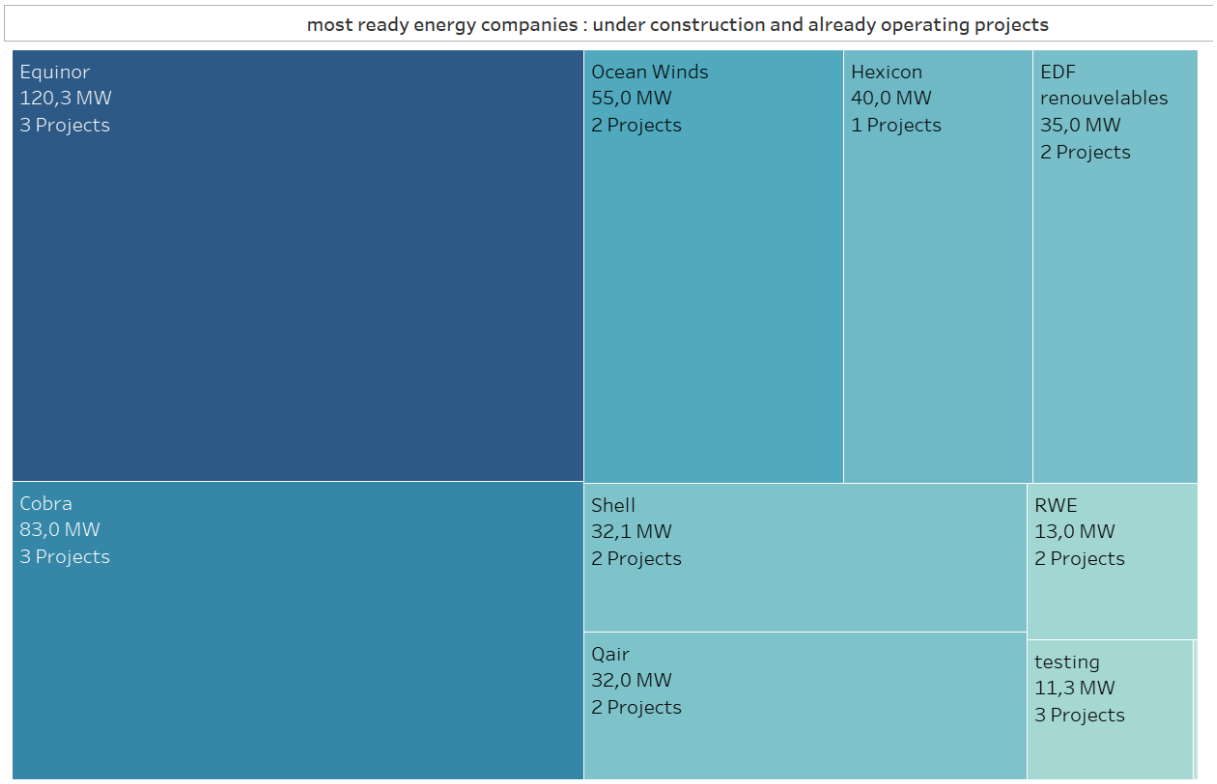

Figure 1.31: Most ready energy companies

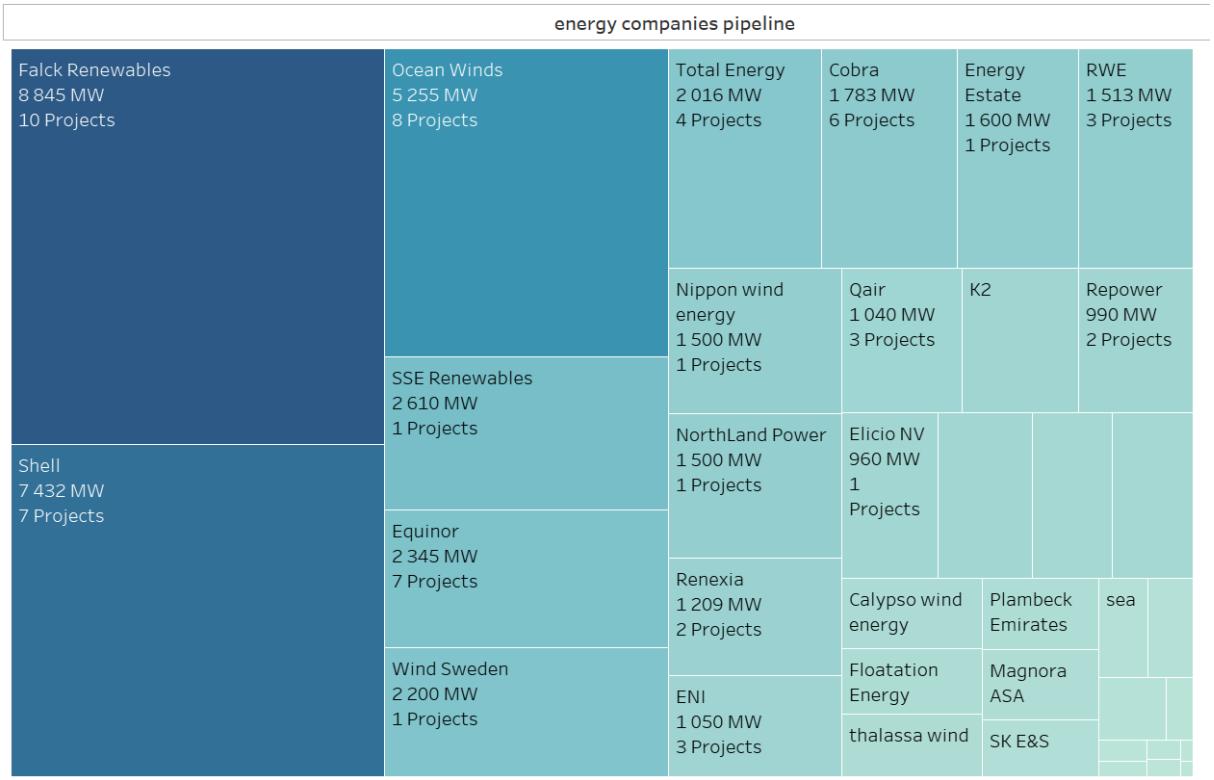

Figure 1.32: Energy companies with biggest pipelines

Thus, to summarise these graphs, the 4 main energy companies currently shaping the floating wind market are:

- Shell : Shell plc is a British multinational oil and gas company headquartered in London, England. This huge energy player already own many fixed offshore farms and announces a global pipeline of 7,5 GW by 2035. Plus many others projects are in the tubs, with MoUs (memorandum of understanding) signed with different players in Korea, Japan, Europe and USA. Nowadays, they already enterred the market investing in 3,6 MW Stiesdal Pilot already operating and via the 28,5 MW pilot farm in south Brittany, France under construction. They buy in 2021 Eolfi, project developers 100% dedicated to FOW projects, and one of most promising players of the field. Finally, they finance intern R&D and participate to many flagship projects in Europe.
- OceanWinds (OW) : Oceans Winds (OW) is an international company dedicated to offshore wind energy and created as a 50-50 joint venture, owned by EDP Renewables and ENGIE. Their global announced pipeline tops 5,25 GW by 2035 via 8 projects disclosed, developed with Various partners. Plus, huge MOUs have been discussed for projects in Canary islands and USA. They own the first semi-sub commercial-scale Pilot wind farm in Portugal (25 MW) and 30 MW pilot farm Lion Golf under construction. This will become the first Mediterranean commercial scale pilot wind farm. As Shell, Intern R&D and participation to academic researches are also part of their plan for floating wind development.
- Equinor :As already discussed, the state-owned Norvegian company is the real pioneer of floating offshore wind. Real experts of the field, they developed in house the floaters used for their first windfarm, and even announce a new technology used for their future projects in Asia. Their global pipeline is about 2,4 GW.
- FalckRenewables : Italian IPP specialized in Renewables projects. Their global announced pipeline reaches 8,5 GW by 2035, the biggest one on the map, while being not fully entered on the market. As it will seen later, they team up with BlueFloat for every projects, helping Bluefloat becoming the main developer mapped. Main Bidder in Scotwind with 4GW over 3 projects, with one of them innovative since dedicated to green Hydrogen synergy with offshore wind. Finally, they are expected to become the field leaders for Mediterranean and especially for Italy.

Let's be more concise regarding project developers. Graph 1.33 shows the developers of the first rising floating offshore wind projects. Technip leads the race thanks to its collaboration with Equinor on their two first projects. Then, floatation energy emerges

as the developer of the biggest floating windfarm, Kincardine. Actually, many of these first low size pilot and pre-commercial projects did not require the expertise of dedicate developers since these were not all driven by cost effetiveness objectives but more by pilot demonstration.

The graph 1.33 is thus more insightful and display the most important developers in the world, with Bluefloat working on a huge amount of 15 projects in 6 countries, for a total pipeline of 12,7 GW, the biggest by far. Then, 7 seas, owned by CIP (Copenhagen Infrastructure Partners) are set to participate in 7 projects for an important pipeline of 5,6 GW. CIP today is the world's largest dedicated fund manager within greenfield renewable energy investments and a global leader in offshore wind, and thus own this development company dedicated to floating offshore working in Asia, in Europe and even in the Mediterranean.

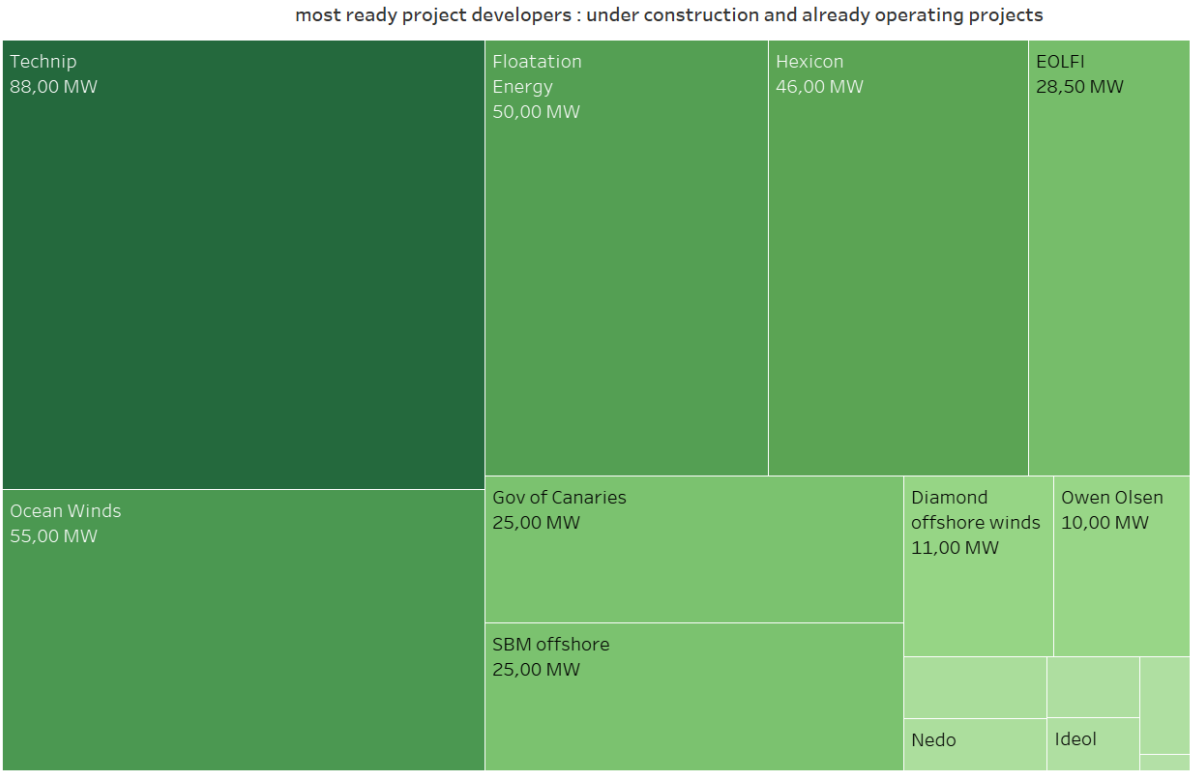

Figure 1.33: Most ready project developers

Figure 1.34: Project developers with biggest pipelines

1.4.4. Focus on main domestic markets

From precedent subsection 1.4.2 United Kingdom, France and South-Korea appear as three important markets for floating wind development. Italy as well has a particular place in this analysis that will be thus further analysed here.

Let's start with home country of the first ever floating wind-farm and the biggest one in terms of counted pipeline: United-Kingdom. Real pioneer of fixed-bottom offshore wind (cf section 1.4), United-Kingdom is set to endorse the same role for floating wind sector. This prior experience on offshore wind of course fosters floating wind development in UK since parts of supply chains and legislation are similar. Furthermore, UK is starting experiencing the saturation issue due to its ambitious politic made to take advantage of their favourable offshore wind conditions (relatively low seabed deepness and strong winds [24]). Indeed, according to [50], the UK government articulated its commitment to supporting renewable energy sectors through The Ten Point Plan for a Green Industrial Revolution published in late 2020. This plan pledged to mobilize over $15 billion in support of the green industrial revolution with hopes that the private sector could be persuaded to match this threefold. Advancing offshore wind is the first tenet of this plan

and outlines a goal of 50 GW by 2030 [7], sufficient to power every UK home with offshore wind by 2030. 10 to 20% of these objective is set to be achieve thanks to floating projects basing on UK government

Among the 18,7 GW british pipeline of projects, the huge majority of huge commercial-scale projects have been formulated and accorded through the Scotwind leasing process located in Scotland. Indeed, according to Crown Estate Scotland entity [8], whose responsibilities include awarding leases and other types of agreements to organisations who want to build offshore wind farms, the leasing rounds awarded for 17,5 GW of floating offshore wind projects in 2022 for a total scottish leased surface of 8,600 km2. Without going too deep in contractual details, the rules of these leases are detailed in [51] and explains that winners must begin the construction within ten years (thus by 2032 for the latest), that hierarchy of projects have been built upon leasing fees, that ranged from £2,000/km2 to £100,000/km2. Plus, a minimum project size of 100 MW was asked as well as various financial and environmental guarantees.

Map 1.35 displays the location of the 19 awarded projects for a total pipeline of 27,5 GW of offshore wind projects. 13 out of these 19 projects are floating, representing 65% of the expected installed capacity and highlighted in blue on the map. These make United kingdom the biggest floating domestic market in the world. Similar leasing round are expected in the late 2023 to select project in the British part of the Celtic Sea, which could further increase this huge pipeline.

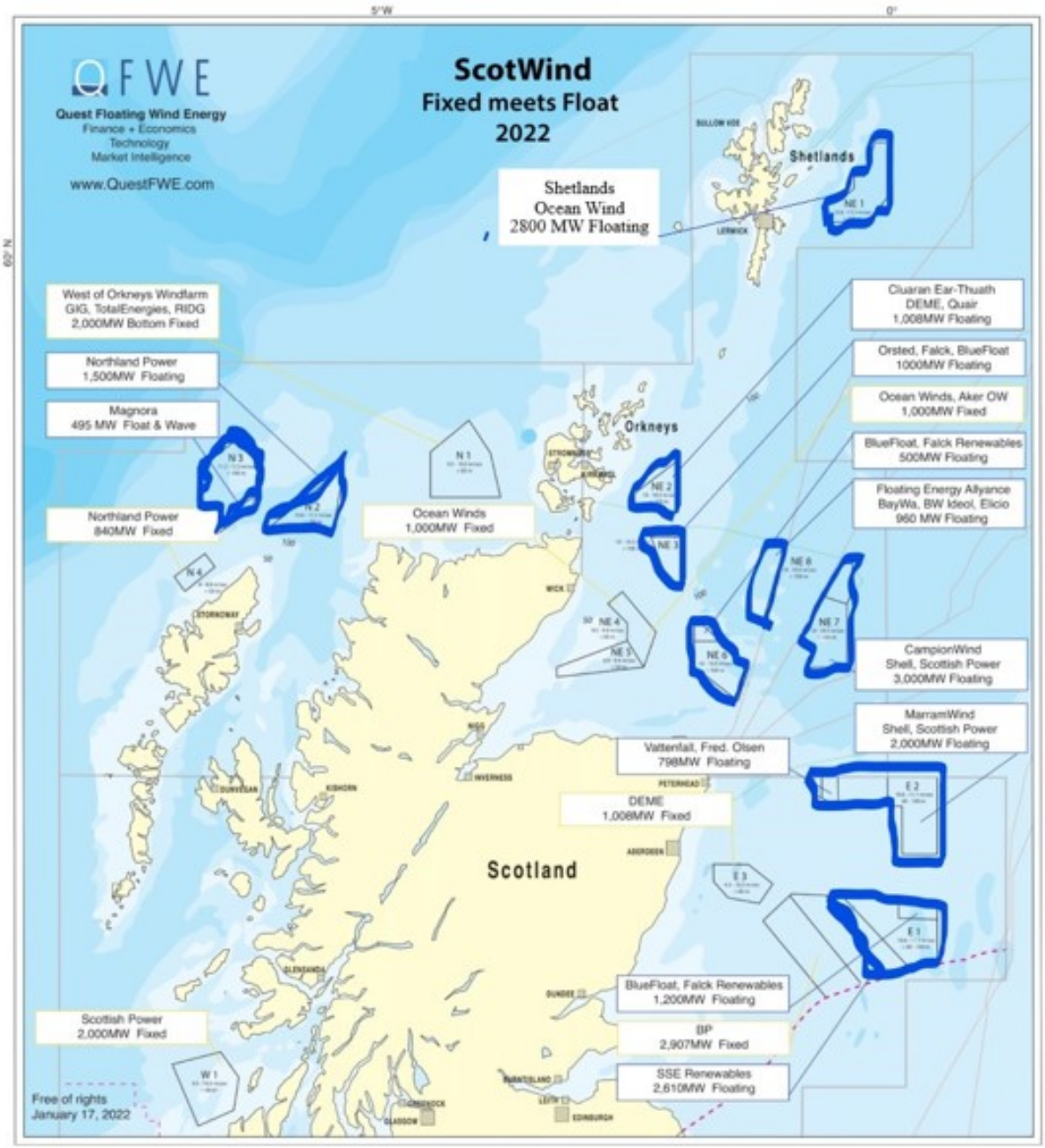

Figure 1.35: Map of Scottish projects awarded via Scotwind lease process from [8], Floating projects are evidenced in Blue

Then, France can be seen as previously explained as the tied pioneer of floating with UK thanks to many company specialized in the sector as Ideol, Eolfi or Eolink (cf 1.4.3 and even more thanks to the biggest pipeline of under construction pipeline. Four pre-commercial floating pilots farms are indeed expected by the end of 2023, the four of size with between 25 and 30 MW. France is the epitome of centralised strategy as explained

in section 1.4 and has anticipated these projects for a long time, backing them up with important social, supply chain development and environmental background. The whole legislative framework has also evolved to allow these field to grow and will benefit in this sens of the prior development of fixed-bottom offshore in the country, that initially suffer legal and Nimby related delays that strengthen the global framework. From France point of view, offshore wind will play a key role in their electricity transition toward greener sources and a diminution of nuclear dependence. French ministry for green transition [52] tells that 40 GW are expected by 2050 in order to assume 20% of the country final electricity production, and floating will for sure have a place in this projects since the topography of France seabeds does not offer many suited sites for fixed bottom offshore. These four pilots are actually the initial step before the deployment of three farms of 250 MW, one located in south Brittany and the others two in the Mediterranean. All these projects, amongside the fixed-bottom ones, are displayed on map 1.36. Let's precise that these projects, currently under tenders, will eventually double in size according on the evolution of the field.

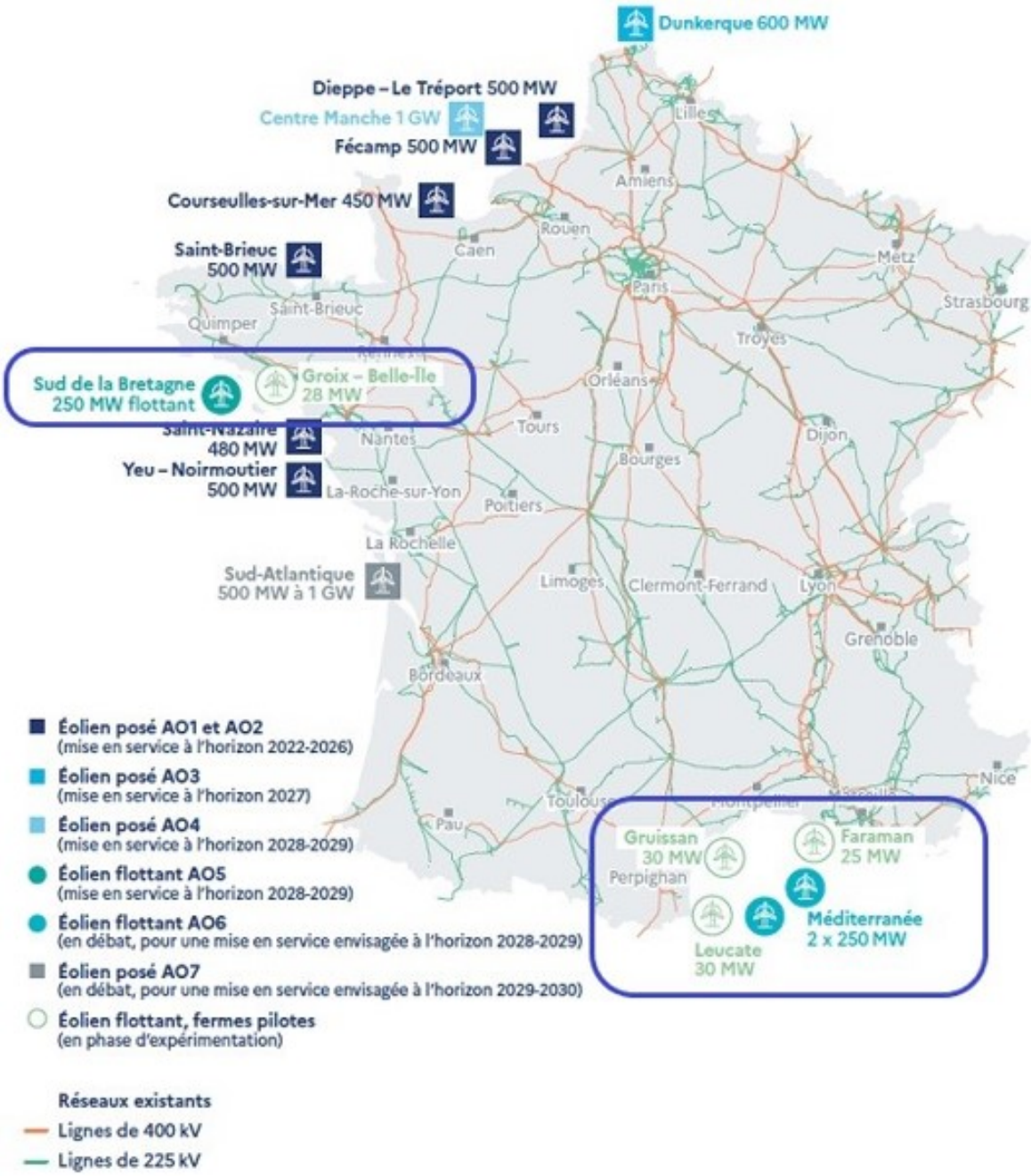

Figure 1.36: Map of french projects from [9], floating projects are framed in blue. Distinction is made commercial and pilot projects

The Korean government released in 2019 the Renewable Energy 2030 Implementation Plan (RE3020). RE2030 outlines how the government aims to increase the level of renewable energy capacity in a country historically heavily dependant on fossil fuels [32]. Yet, Korea suffers delay on their Green new Deal objectives and thus aims at fastly entry on the offshore wind Market: Korean state bets on 6 GW floating wind operational by 2030 as

part of the Korean RE2030 Plan according to [10] and [43]. Indeed, figure 1.37 shows the potentialities offers by floating wind in the region.
Yet, as shown on map 1.30, Korea does not belong to floating wind pioneers. In order to catch up this delay and match these ambitious objectives, they will be first build on a solid offshore experience with already 150 MW fixed offshore wind installed in May 2021. Then, a Free-Market model, with subsidies and pre-studies led or sponsored by Korean State has been adopted [10]. Plus, legal framework is set to fasten the processes.
On map 1.38, project locations are displayed and shows a logical concordance with zones highlighted on figure 1.37. Ulsan will be the center of interest.Consortium between state-owned Korean producer (KNOC, Wind Power Korea) and big western players such as Equinor, Ocean Wind and Shell have been signed, leading to a global pipeline of 7,6 GW until 2032. Then, MoUs until 3 GW, not counted here, are expected to increase the pipeline. Depending on forecasts, South Korea could even outpace UK to become the center of gravity of offshore by 2030-2035.

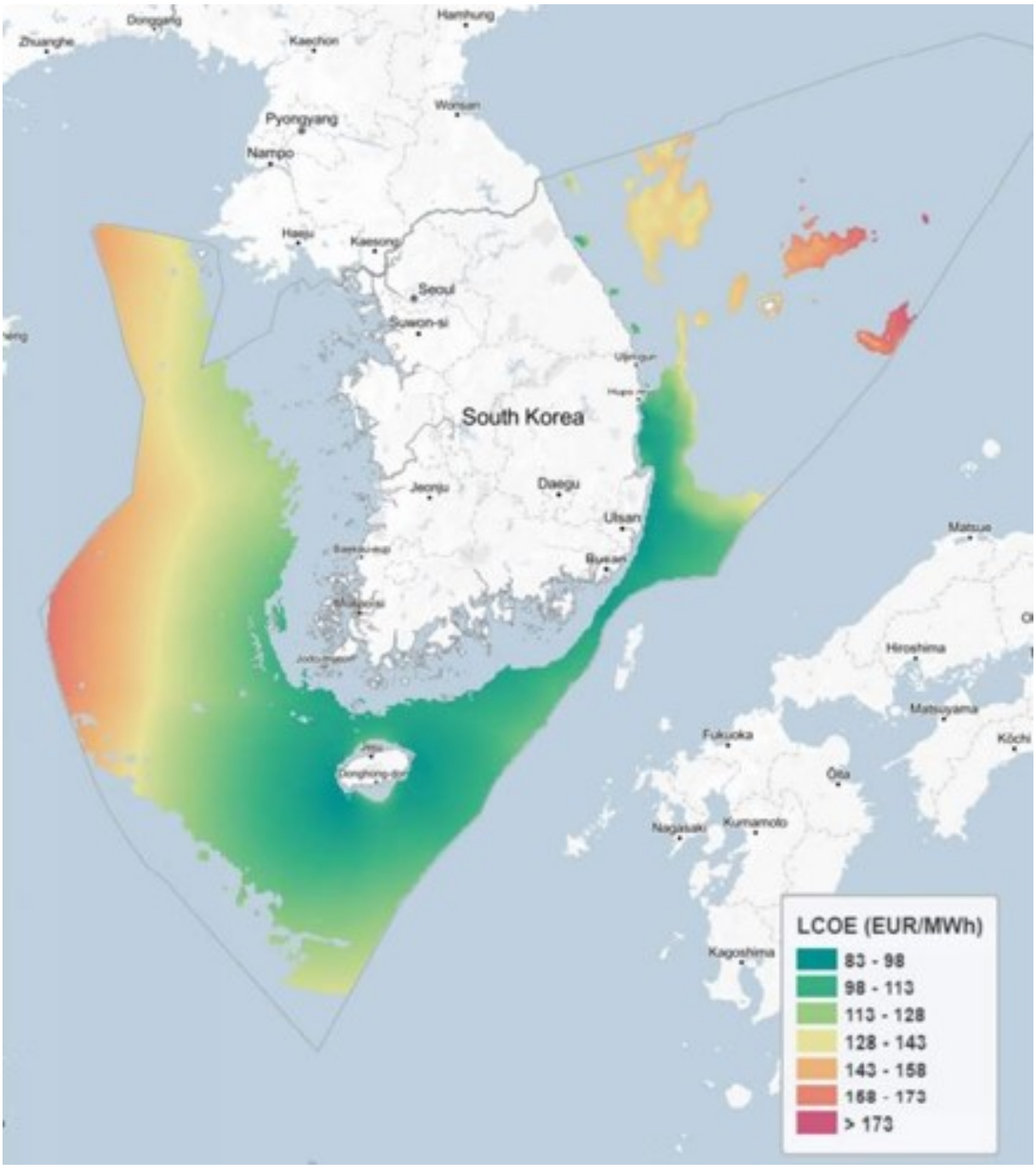

Figure 1.37: floating wind projects LCOE evaluation in Korea from [10]

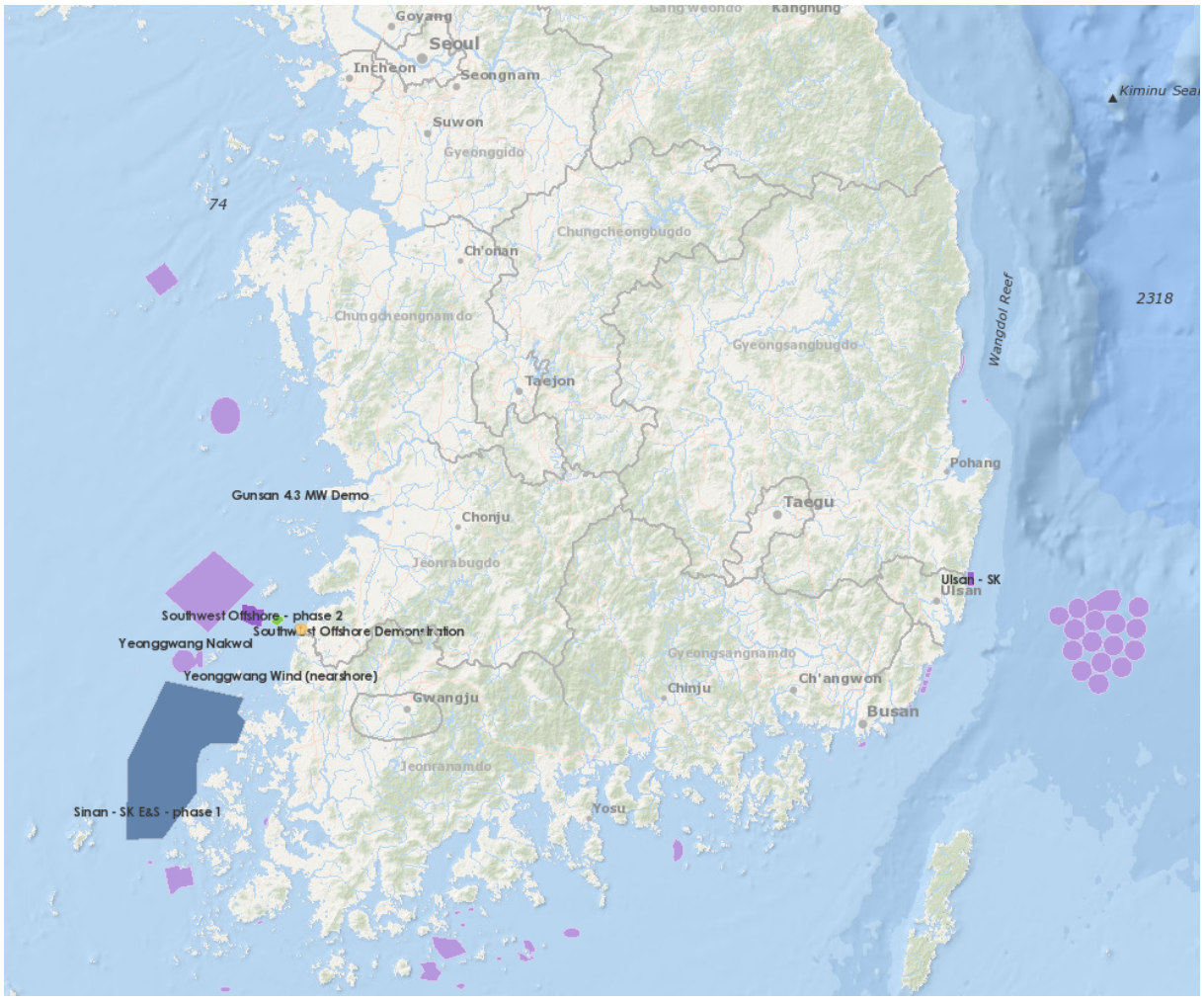

Figure 1.38: floating wind projects in Korea from 4C offshore

Last but not least, let's have a glance to the Italian case, to will be even further analysed later in order to get technological and economical insights. Italy has a developer-led strategy where sites and sizing are identified by industrial players. Eventough few pilot projects or ambitious development policies have been released, many projects are imagined and have entered early planning and development stage. A good indicator in such a kind of developer-led market is the connection requests sent to the TSO, here named TERNA. And, in a press release of the late 2022 [53], TERNA announced a total of almost 95 GW divided in over 50 projects. It is precised than 80% of this requests come from the South of Italy and from the main islands (this will be explained later). Let's precise that this pipeline only overpass the italian objective of 70 GW added power from green sources from green sources [53]. Of course these projects are very far from turning concrete and a large part have not even been officially disclosed, and for now, TERNA only accepted 22 GW of connection to the grid.

In the scope of this study and to be representative of realistic trends, focus have been made on more advanced projects. The italian ministry for green transition keeps a list of projects under scrutiny [54]. There are listed 45 projects currently under SIA ("studio impatto ambiantale" = "environmental impact study") process, alongside large documentation made by project leaders that will be analysed later. 27 of these projects are waiting for their final VIA procedure response while the 18 others are still in the scoping phase [54]. The difference and the chronology between these processes is described by italian government in [11] and resumed on the following scheme 1.39.

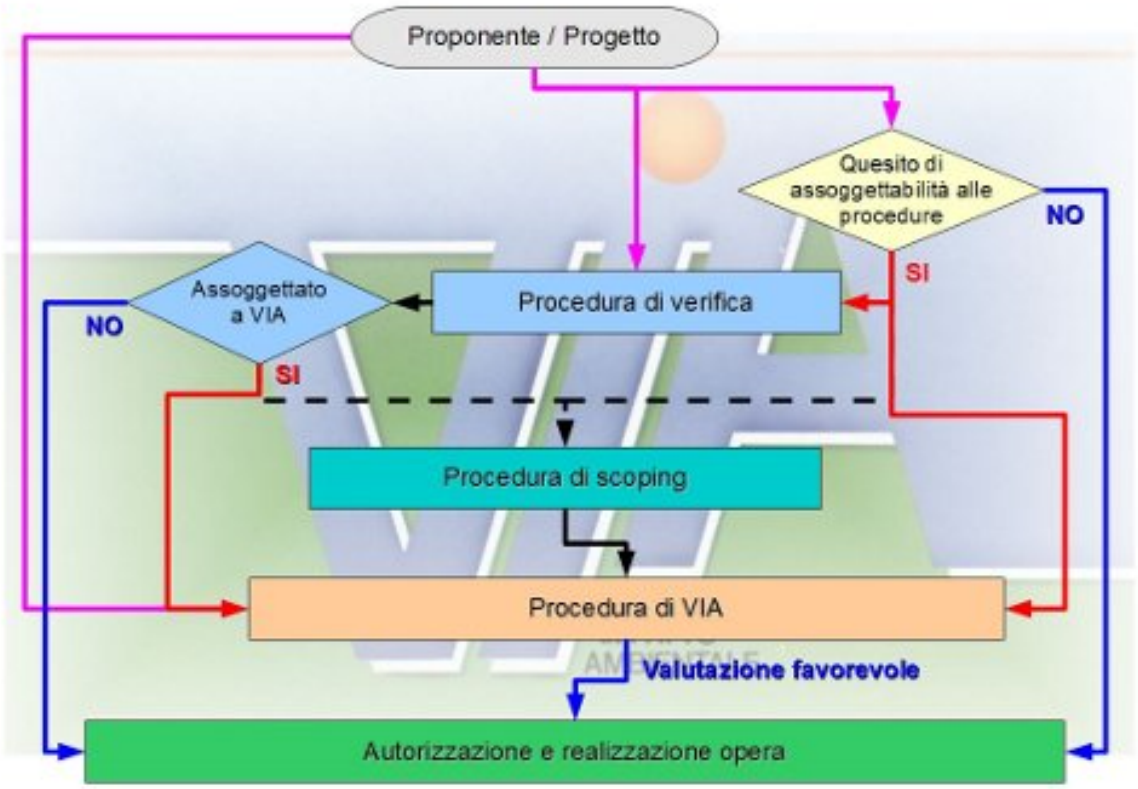

Figure 1.39: Logical scheme for VIA (environmental impact valuation), from [11]

The 18 projects counted in the forecast presented in 1.4.2 and 1.4.4 have been selected in this list since appearing as the most advanced and thus more concrete so. Thus, only the projects in the final stage of the final VIA procedure (i.e the one with a "concluded" state of the demand in [54]) have been incorporated in the study, leading to an Italian pipeline of 12,5 GW with expected operating dates ranging from 2029 to 2034. Delays could be suffered due to Nimby or legislative projects mostly for projects situated near from the cost as it will be seen later.

1.5. Chapter conclusion

Both the important perspectives offered by offshore wind and more specifically floating offshore wind and the development of the field have been heavily discussed in this chapter. Yet, in order to answer the global question of this study the cost and challenges of floating wind must be further assessed in order to help potential players to valuate the viability or not of developing floating wind assets.

Thus, in the next chapter, the various cost drivers of a floating project will be listed, analysed and modelled and a tool for CAPEX (capital expenditure) of floating projects will be provided.

2 | Chapter two: Floating offshore wind projects CAPEX estimation

2.1. Foreword

In this chapter, every aspect of a floating project will be techno-economically analysed in order to evaluate the contribution of each cost driver to the global capital expenditure, CAPEX, such kind of project requires. The final idea is to create a complete cost model that, based on physical principles, strong hypothesis and industrial data, can deliver a good estimation of a cost of project with known characteristics. The many parameters that enter in consideration for the design (floater type, depth, turbine sizes etc...) will of course impact the final cost and will thus be taken in consideration in the study. Plus, commissioning date will also be taken in consideration since the main idea of this analysis is to analyse the cost, and thus the viability, of floating projects at commercial scale, since pilot projects suffer over-costs that will be discussed later on. Thus, forecasting will be introduced in the model and will be based on hypothesis made along the analysis.
In order to predict commercial scale cost evolution, physical models will be introduced since the structures behaviours with bigger turbines are not documented, very few commercial projects existing today. The economic model will thus be based on a physical one for floating characteristics specific to the field.
The two main legs of the model will be be in one hand this physical model for floating specifics characteristics and o n the other hand known data from the well known fixed-bottom offshore field since some characteristics are shared between the two fields.

In the end, the economical model will be organised into six different cost drivers illustrated on figure 2.1. These six inner fields will be technologically analysed, their impact will be discussed and predicted as well. In the end the results from these six particular analysis will be gather and the results of the model will be presented. Let's precise that

a particular emphasis will be put on the floating specifics, so as to say the moorings and anchors and most of all floating platforms.
The cost will generally not be expressed in absolute values but in specific cost per installed power, i.e USD/MW, in order to be able to compare and add costs from different cost drivers.

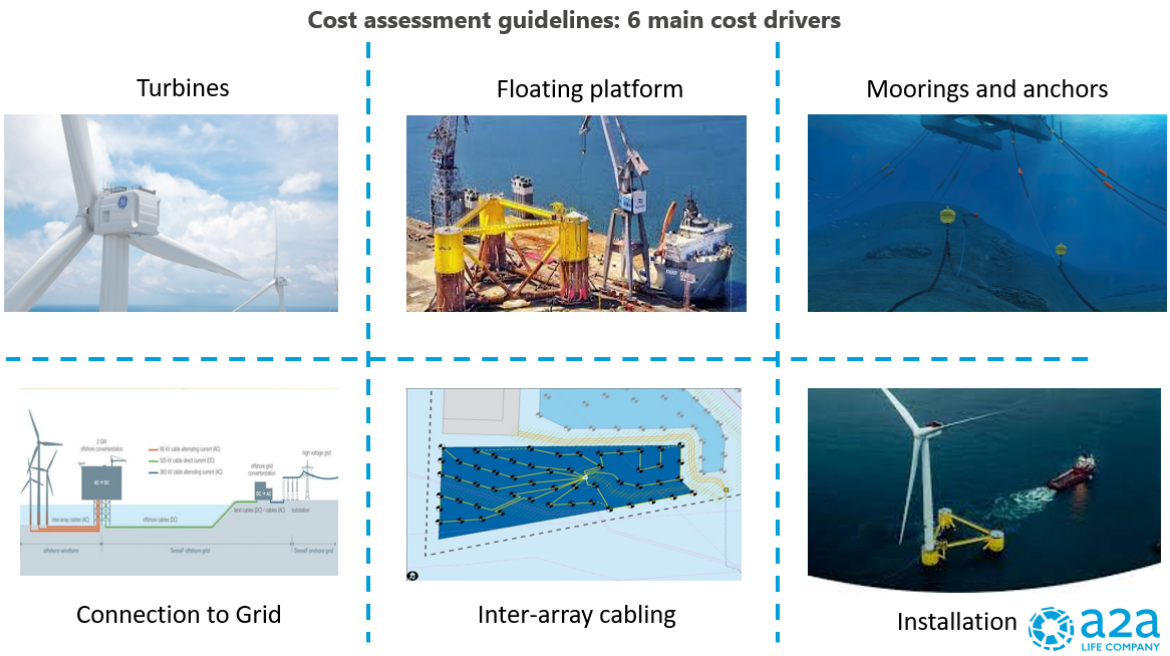

Figure 2.1: Different cost drivers for offshore floating projects

2.2. Focus on wind turbines

Wind turbines are obviously an important part of floating offshore projects CAPEX, and it has both a direct and indirect impact. Indeed, more that the turbine cost itself, the turbine size, and capacity influences substructures dimension and costs, cables sizing, number of installation processes required and globally every single specific cost of others elements.

As explained in [29], wind turbines cost and size for floating projects - eventough currently a little higher due to the small market size and the small adaptation required - will soon be the same as for fixed-bottom projects. This hypothesis will be made all along this study and allow us to use data relative to offshore wind turbines in general.

The main insight regarding offshore wind turbine evolution their evolution in capacity and thus in size. The physical principles explaining the advantages of getting bigger turbines

were detailed in subsection 1.2.2, and lead to a clear trend for both offshore and onshore projects display on graph 2.2.In this graph extracted from [2], the fact already mentioned in subsection 1.2.2 than mainly higher class turbines (cf table 1.1) are considered for offshore projects is confirmed. In the end, while bigger turbines nowadays top 10 MW (cf 1.10), 15 MW are expected by 2025, 20 MW ones by 2030 and even 35MW models could be on market by 2050. Through this chapter, the economies of scale in terms of specific cost offered by this increase in capacity will be analysed.

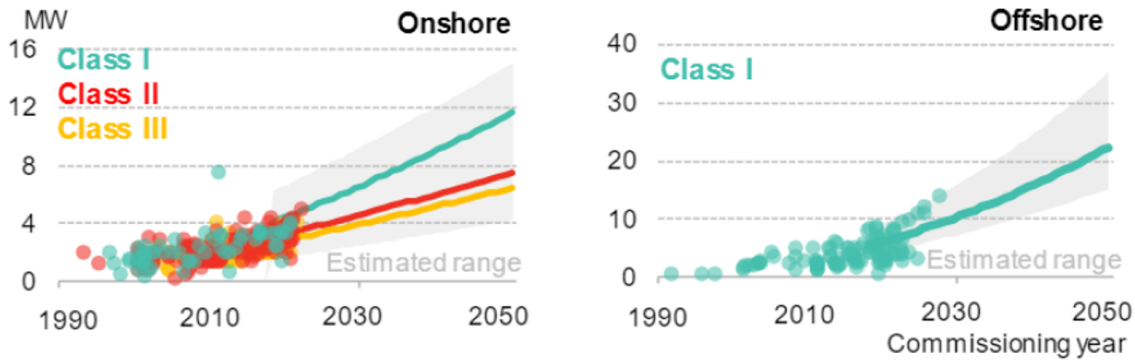

Figure 2.2: BNEF turbine capacity forecast onshore vs offshore, from [2]

Thus, technology innovation has led to an increase in turbine size in terms of tip height and swept area, and this has raised their maximum output [5]. The tip height of commercially available turbines increased from just over 100 metres (m) in 2010 (3 MW turbine) to more than 200 m in 2016 (8 MW turbine) while the swept area increased by 230% (cf equation 1.1. The larger swept area allows for more wind to be captured per turbine. A 12 MW turbine now under development is expected to reach 260 m, or 80% of the height of the Eiffel Tower displayed on figure 2.3. The even larger 15-20 MW turbines targeted for 2030 . This increase in turbine size and rating has put upward pressure on capital costs as larger turbines pose construction challenges and require larger foundations, but it has also reduced operation and maintenance costs, ultimately leading to lower LCOE [5], and this trend is set to keep on as it will be seen. The average turbine size used in offshore wind farms increased from 3 MW in 2010 to 5.5 MW for projects completed in 2018). In the same period, annual capacity factors for new projects increased from 38% to 43%. Compared to smaller units, a bigger turbine can achieve a capacity factor improvement of two to seven percentage points given the same site conditions.[5]

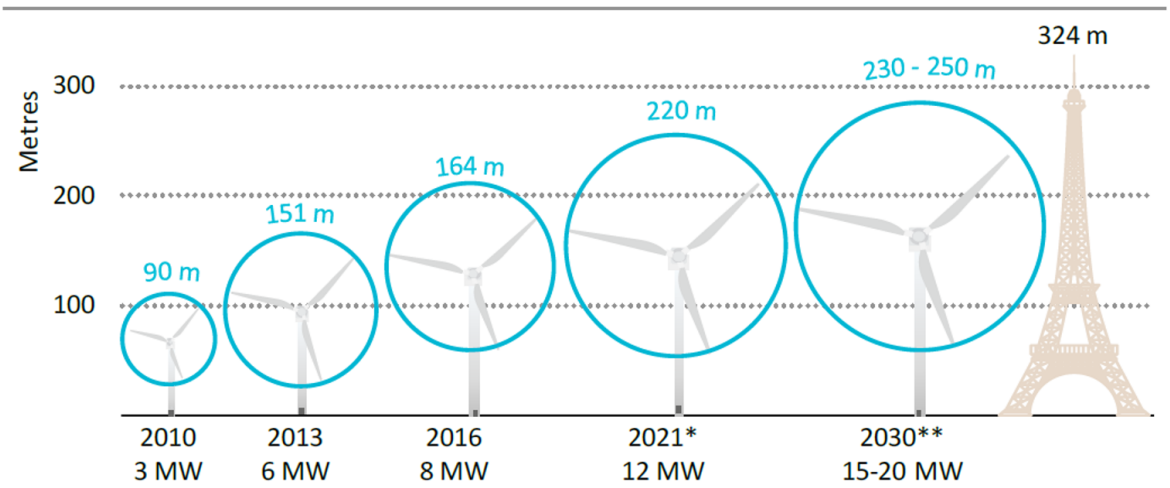

Figure 2.3: IEA turbine size forecast, from [5]

When the same class is considered all along, there is direct link between turbine capacity and rotor size (cf 1.1). When in addition a classical tip clearance value - i.e. the minimum distance between the sea surface and the blade tip - od 25% of rotor length is adopted [2], nacelle height, rotor length and capacity are linked. (Note: the tip clearance value is trade-off between over costs due to nacelle height and disturbance in wind shear development, cf figure 1.11. For offshore application and for big turbines, this tip clearance value could be lower than 25% since wind shear effects are less important offshore as explained in subsection 1.2.2. Yet, to remain conservative, this potential cost and weight saving will not be taken in consideration in this study and in our model of section 2.2).
In the end, the wind turbines dimension hypothesis retained for our study are summarised in table 2.1 and based on NREL typical 5MW wind turbine described in [44] and extrapolated following the Power-rotor and tip-clearance-rotor rules previously described.

Turbine capacity (MW)	**Rotor diameter (m)**	**Nacelle height (m)**	**maximum height**
5	126	95	158
10	184	138	230
15	230	172.5	287.5
25	250	187.5	312.5
35	330	248	413

Table 2.1: Turbine dimension per power

Of course, this increase in size will impact turbine weight and wind surface area, that will

be important parameter in the physical model of floating platforms developed in section 2.2. Graph 2.4 gives us interesting information on specific weight as well as material composition of offshore wind turbines in terms of commissioning year, and thus indirectly in terms of power capacity. As expected, steel is the main weight driver, alongside electronic scrap ad fibbers for blades (cf figure 1.9). The main message from this graph is that specific weight remains more a less constant with turbine size: a 20 MW turbine is set to be twice as heavy as a 10 MW. To be conservative, the specific weight value used in the floater model (cf section 2.2) will be common to every turbine and will be 100 tons/MW. [55]

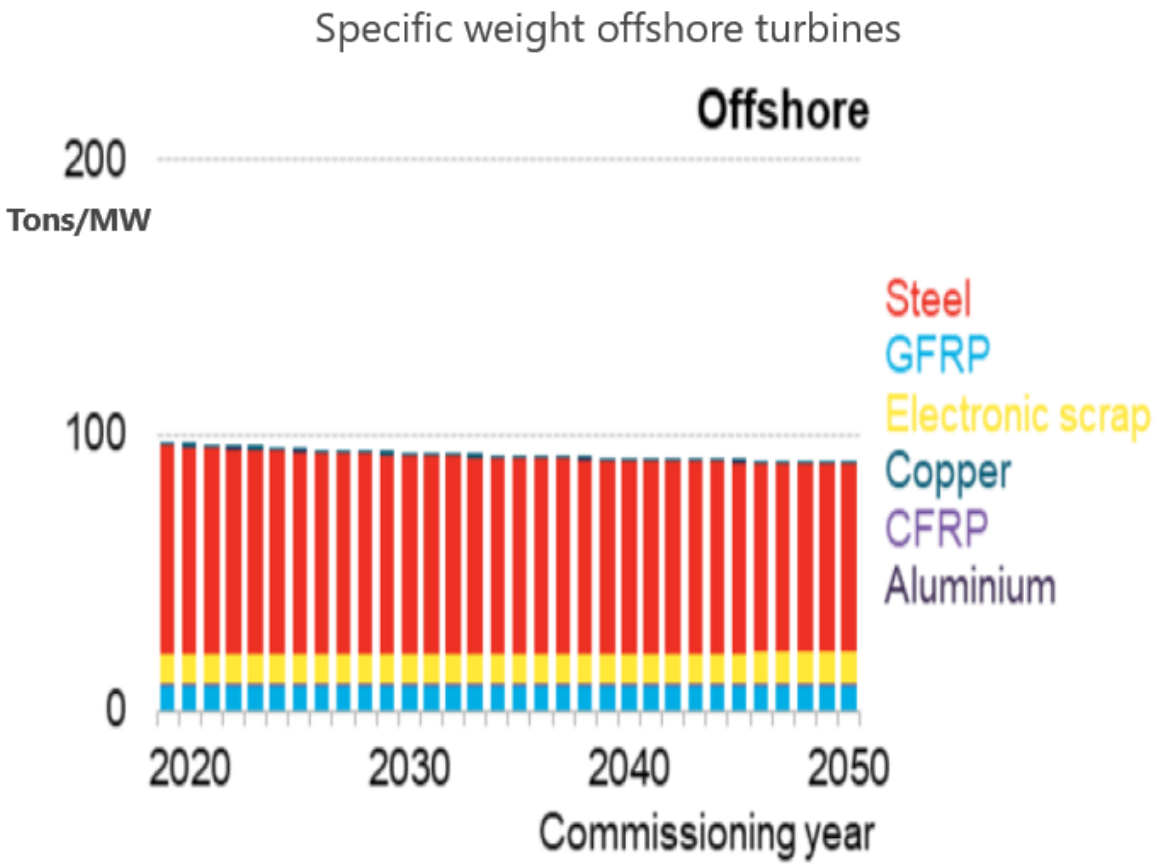

Figure 2.4: BNEF specific weight division forecast, from [2]

Let's anticipate a little the physical model for floating structures of section 2.2 and describe the hypothesis made to describe wind turbines. The center of gravity (COG) - an imaginary point in a body of matter where, for convenience in certain calculations, the total weight of the body may be thought to be concentrated - of the turbines has to be implemented in the model. The following table 2.2 gathers the elements required for its

calculation in the model and the values hypothesised. The calculation will then assume these characteristics does not depend in turbine size evolution displays in table 2.1.

Turbine characteristics	value taken
Turbine specific weight (ton/MW)	100
Nacelle specific weight (ton/MW)	50
Rotor specific weight (ton/MW)	7.5
tangent of conic angle of tower profile	0.009 rad

Table 2.2: Turbine specific characteristics

Since specific material demand does not evolve with capacity, and since turbine costs are strongly linked to this demand, no clear economies of scale are witnessed due to increase in turbine size, fact corroborate by [29] and [7]. [29] precises that the increased turbine size is not expected to play a major role in the turbine cost reduction and that the biggest cost reductions are expected to come from innovation and optimisation of the turbine design. Plus, increase of offshore market is set to lead to increase volume thus leading to assembling and supply chains economies of scale. These phenomenon has driven the onshore field to constantly decrease their cost over the last few years has explained in [56]. The volume of offshore turbines is still way lower the onshore one as shown on graph 2.5, but the gap is starting to reduce.

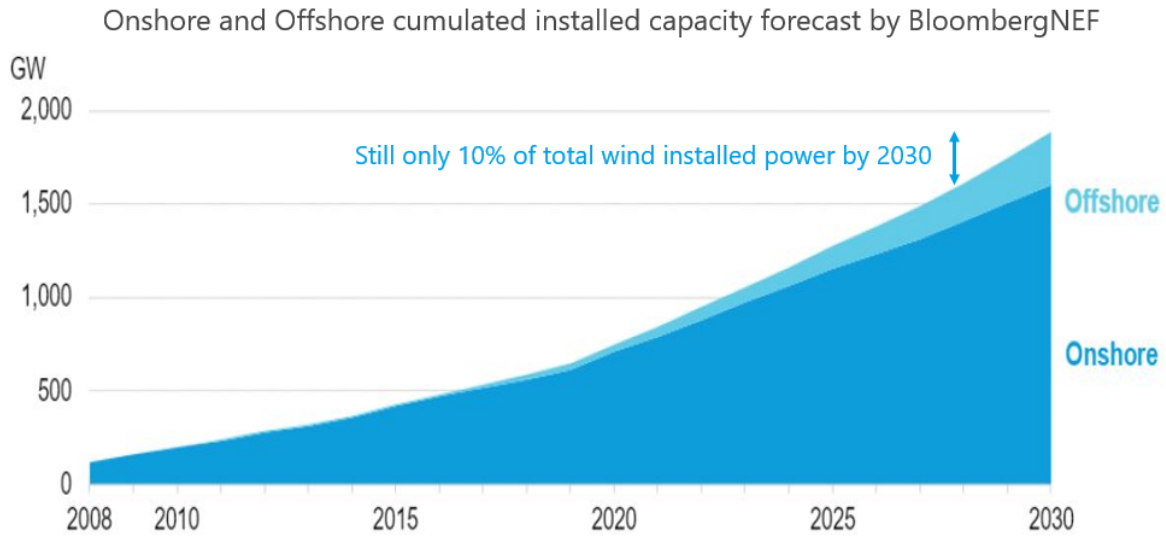

Figure 2.5: BNEF total wind power installed capacity per year

Thus, this difference in volume lead to higher specific costs for offshore as shown on graph

2.6 where offshore turbines cost predictions from [17] are compared with the trend for onshore ones from [56].
Important reductions are expected for offshore turbines that could close the gap with onshore turbines before 2050. Let's precise that these cost values from [17] will be used in our cost model.

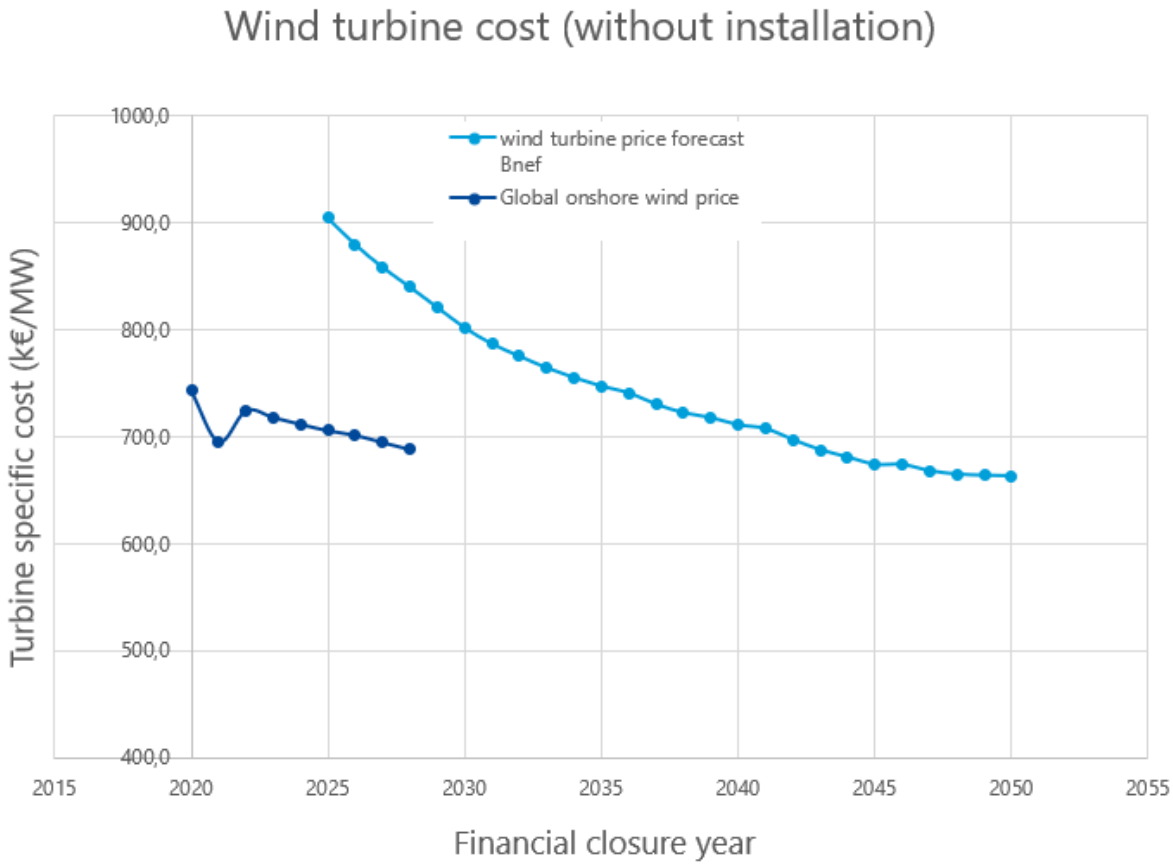

Figure 2.6: Specific cost forecast for wind turbines

2.3. Focus on floating platforms

This element is characteristic of FOW and lead to new questioning on an economical and technological aspect. Indeed, even if floating substructures were also a challenge for some offshore oil&gas operations - which explain the interest in FOW of some former oil&gas specialists as Equinor, SBM or even Shell - [57] explains that the cost issue was not fundamental in these cases. Indeed, only one superstructure was required for a project and the techno-economical optimisation of the structure was thus less of subject. Plus, for such huge substructures, the actual physical effects at stake are not quite similar.
Thus, the focus on floating platforms will thus be particularly complete and will less rely

on industrial data from fixed-bottom offshore projects. Let's begin this floating platforms analysis with an overview of technologies and of players before going deeper in the physical part in subsection 2.3.2 with the model computation.

2.3.1. Floaters technological and market overview

The majority of the existing floating wind hull concepts can be clustered depending on the main hydrodynamic stability mechanism as either a barge, semisubmersible, spar, or tension leg platform (TLP) [29]. These four technological types are here displayed on figure 2.7. Let's precise that, as it will be discussed soon, Barge and SS floaters rely on similar physical effects to ensure buoyancy, which lead some experts to gather them in a same group as it is done in a very complete Carbon trust study for the Scottish government [58].

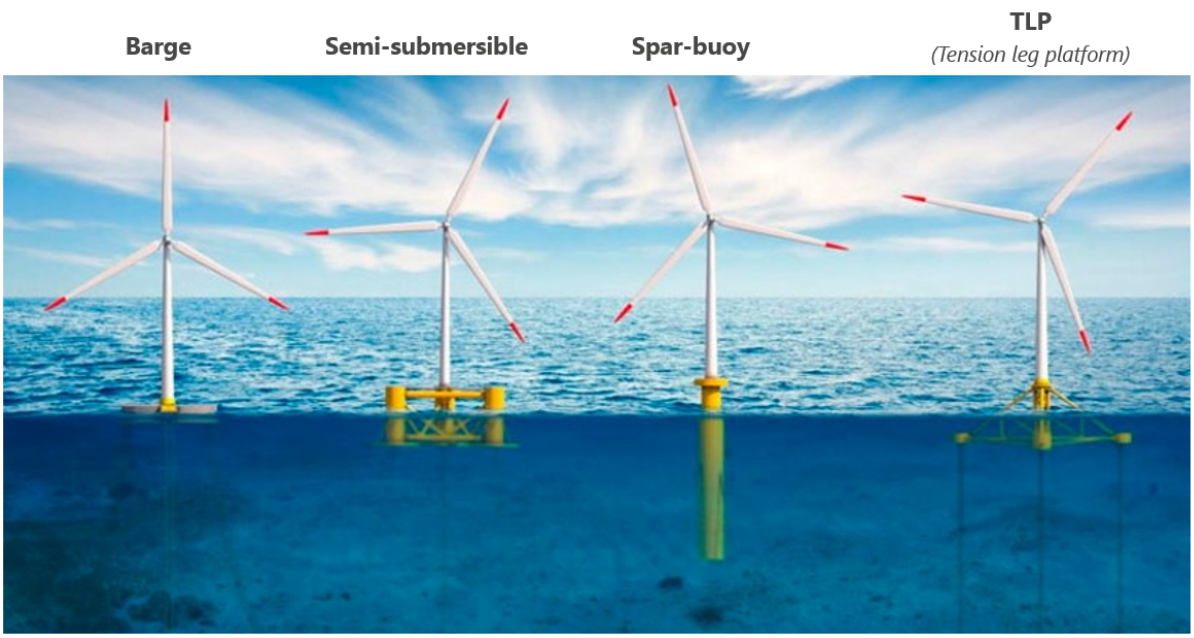

Figure 2.7: Main floaters types

Nowadays, no clear consensus has been found on which technology is the best one, and this consensus may actually never be found since every technologies present different pros and cons that can make them more suited to a situation and less to another. Let's describe each technology. These description are essentially based on experts independent FEED agencies or consultancy companies specialised in FOW such as DNV [29] which seal of approval has a huge impact in the FOW sector for floating concepts; Carbon Trust [58] a British company expert in renewable transition projects that for example collaborate

intensively with the Scottish government for the elaboration of Scotwind projects; and ORE Catapult [59] which has a strong link with industrial players constituting the offshore wind field and elaborate complete cost and technological related reports on the sector. The facts displayed here after are also corroborated by project-particular documentation available for french or Italian projects respectively in [9] and [54].

- **Semisubmersible (SS) :** Semi-submersible floating substructures typically comprise three or four buoyant columns that are secured into a platform formation with connective bracing. Stability is primarily achieved through buoyancy tanks contained within the columns, though the columns may also contain either passive or active ballast systems (varying from design to design). Some designs also include a horizontal heave plate to create a drag force that resists heave motions due to wave and wind effects. Due to its inherent stability, as with spar or barge platforms, the principal function of a semi-submersible's mooring system is to provide station keeping, and therefore catenary mooring configurations can be utilised, as it will be further discussed in subsection 2.4.
  A very good example of such kind of structures is displayed on picture 2.8 with the windfloat SS platform by principle power. This floater is by far the more advanced one of its type, with a first pilot launched in Portugal in 2019 followed by its utilisation for the Kincardine floating windfarm in 2021 (cf 1.26). Plus, one of the four french pilots under construction. (Leucate Le barcares, cf 1.4.4) will use this technology The designer and pre-FEED company Principle Power [60] explains that the concept is wind turbine agnostic and delivers optimal motion performance for increased power production and revenue generation thanks to many patented innovations.

Figure 2.8: Windfloat SS floater by PrinciplePower

The many specific features of windfloat described in [60] are a little out of the scope of this study. Indeed, the model developed here after in subsection 2.3.2 is based on general buoyancy principles in a static approach and thus the specific damping phenomenon linked to dynamic behaviour will not be analysed. Yet, the windfloat main advantages can are shared by every SS concepts and are summarised in the following table 2.9. The high TRL (Technology readiness level scaled to 1 to 9 to describe concept readiness [57]) of these solution, as demonstrated by the windfloat concept combined to easy installation and possible modularity are opposed to backsides linked to complexity and high structural mass leading to potential over costs.

Strenghts	Weakness
✓ Wide seabed depth range	× Mass: higher material consumption (steel)
✓ Aassembled in port and towed to site	× Complexity: Higher manufacturing cost
✓ Platforms with high TRL	× Catenary mooring lines: larger footprint (not suited for depths >500 m)

Figure 2.9: SS strengths and weakness summary

- **Barge :** Though they share a number of characteristics with semi-submersible substructures, barges are a simpler structure with a large waterplane (cf subsection 2.3.2) area and buoyancy compartments distributed throughout the platform. . Ideol's Damping Pool platform [61] – the most advanced barge design at the time of writing – includes a moonpool at the center of the structure to help counteract wave induced loading and provide further stability. The pilot demonstrator of the concept with a 2MW turbine released in France in 2018 is displayed on picture 2.10. Another pilot of 3MW size has also been developed in 2020 in Japan, proving interesting results in Japanese typhoon conditions [61]. One of the four french pilots under construction. (Eolmed, cf 1.4.4) will use this technology. The main characteristics of barge concepts are actually dictated by this ideol dampingpool concept. A

Figure 2.10: Damping pool Barge by Ideol

Usually, barges have the lowest draft of the four typologies (typically <10 metres) and thereby offer greater flexibility, both in terms of the choice of the assembly facility, as a deep-water quayside is not required, and the range of wind farm locations, as barges can technically be installed in shallow water sites (<40 metres). In comparison to semi-submersible platforms, barges are simpler to manufacture and install. A principal drawback of the barge design is that its large waterplane area makes it more susceptible to wave loading, which may require careful consideration when selecting the platform's mooring system. Furthermore, barge designs, which are currently predominantly concrete, generally require a higher structural mass in order to achieve buoyancy and are less predisposed to high industrialisation of manufacturing and assembling. These pros and cons, similar to the SS ones, are as previously summarised in the following table 2.11.

Strenghts	Weakness
✓ Large depth range of application (only solution for shallow waters)	× High structural mass to provide stability. Even more when concrete is used.
✓ High towability, complete port side assembly before installation	× Concrete casting can be time consuming and less suited to industrial pace.
✓ Well suited to the use of concrete instead of steel	× Catenary mooring lines: large footprint and not suited for big depths (>500 m)

Figure 2.11: Barge strengths and weakness summary

- **Spar buoy :**

  Spar floating substructures are typically of a cylindrical design that in many ways resembles the monopile foundations commonly utilised in bottom-fixed offshore wind farms. Conventional spars have a large draft – the substructures can be up to 100 metres in height, with the majority of the structure submerged – and are therefore most likely to be deployed in water depths of >100 metres. The spar is a ballast-stabilised design where seawater, or a combination of concrete and seawater, is used to lower the structure's center of gravity to below its center of buoyancy, thereby creating a natural righting motion when the platform is subject to pitch and roll motions. As for SS and barge, the primary role of a spar substructure's mooring system is therefore to provide station keeping, and catenary mooring configurations can be used.The spar's favourable natural stability is supplemented by its relatively narrow cross-sectional area, small waterplane area and cylindrical form, meaning that it is less susceptible to wave loading than other FOW substructure designs. The classical spar designed is quite simple, which explain it has been the technology chosen for the first equinor's pilot in 2010 and windfarm with Hywind in 2018 previously described in 1.4. This classical design used for Hywind farm and developed by Equinor [62] with the consultancy of technip is displayed on following picture 2.12.

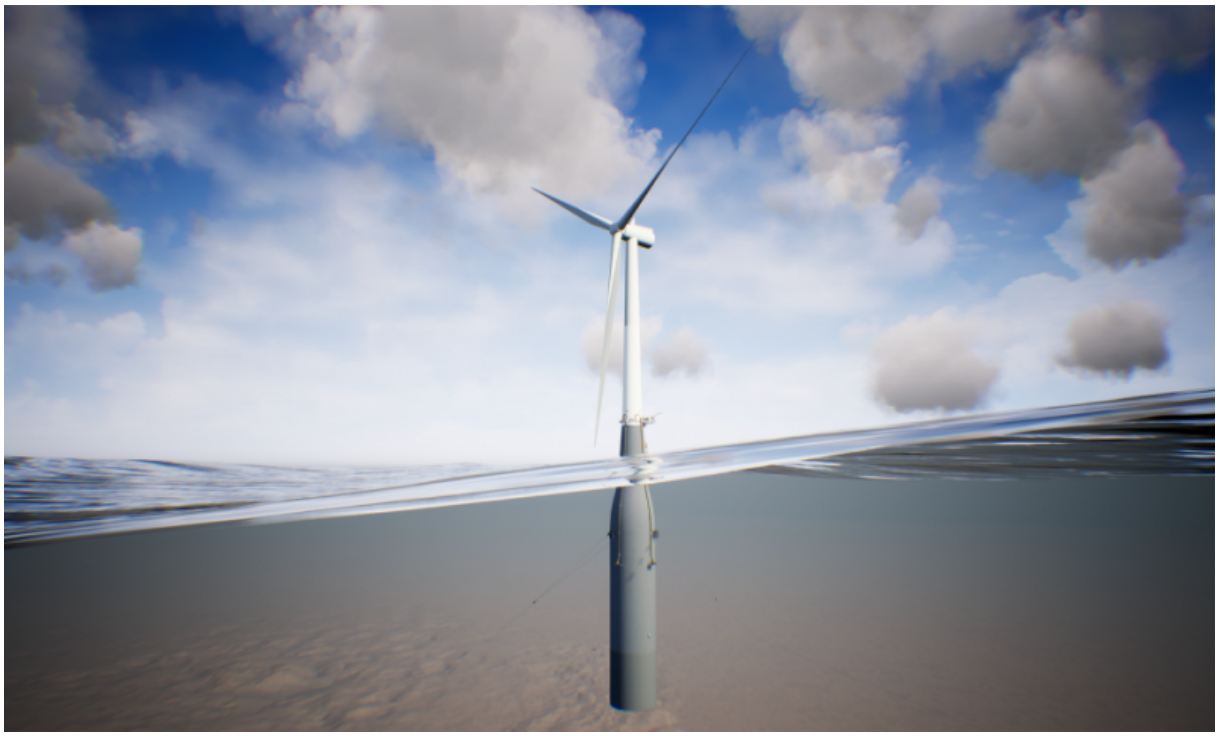

Figure 2.12: SparBuoy by equinor and Technip

If the simplicity of its design, which includes relatively few active systems or welds , improves the ease of fabrication, the principal drawbacks of conventional spar designs generally relate to the large draft. This presents particular challenges related to assembly and installation, as shallow water port facilities are not suitable for assembly, and shallower sites (<100 meter depth) cannot be considered for FOW farm development using spar designs. Likewise, options will likely be limited – both in terms of port facilities and route to port – should a FOW turbine need to be disconnected and towed to port for maintenance.
These pros and cons are as previously summarised in the following table 2.13.

Strenghts	Weakness
✓ Simple design with few moving parts.	× High draft (until 150m) make it inappropriate for shallow waters
✓ Cheap material used for ballasting	× offshore assembling
✓ High TRL, various proven concepts.	× Catenary mooring lines: large footprint and not suited for big depths (>500 m)

Figure 2.13: Spar buoy strengths and weakness summary

- **Tension leg platform (TLP) :** The key distinguishing characteristic of the Tension Leg Platform (TLP) is that it derives its stability from its moorings, which generally comprise three to six anchored tendons that run either vertically or at a slight incline directly to the seabed. A typical TLP configuration includes a central column or frame upon which the turbine is installed, with a series of arms or surrounding lattice frame that connect to the mooring tendons. This typical configuration is illustrated by the SBM offshore TLP concept Float4WindTM of figure 2.14. To develop this innovative concept, SBM offshore [63] used its know-how in offshore Oil&Gas operation to adapt concepts used in this mature sector to the youg FOW one. One of the four french pilots under construction. (Provence Grand Large, cf 1.4.4) will use this technology, making of SBM offshore the pioneer of TLPs for floating wind application and potentially will boost the utilisation of this promising floating typology.

Figure 2.14: TLP floater by SBM Offshore

A TLP's buoyancy tank, or tanks, exerts a buoyancy force that exceeds the weight

of the platform, thereby establishing continuous tension between the platform and its anchors. We will talk about "overbuoyancy". This tension in the mooring system is set to provide excellent stability for operational turbines, resisting pitch, roll, sway and yaw motions from wave and wind loading. Plus, stability offered by tendons allow the water area to be reduced in comparison with SS or barge, enhancing stability by reducing the effects of wave loading. Yet, let's precise that wave dynamics of shallow water sites are still expected to be challenging for TLP designs, these dynamics behaviour will not be analysed in the model described in 2.3.2 but make TLP's solution better suited for deeper sites. The seabed deepness also has an importance on tendons pre-tension that are complex mechanical phenomenon out of the scope of the projects.

Then, taut mooring configuration means that the TLP has the smallest mooring footprint of the four substructure typologies as it will be explained in 2.4. The platforms also usually have smaller dimensions – and therefore lower weight and material requirements – than the other substructure typologies. The TLP's shallow draft would provide developers with greater flexibility when considering assembly facilities, as a deep-water site would not be required.

The main issue with TLPs is that eventough a wealth of experience of TLP applications in the oil and gas sector, it is currently the least commercially advanced FOW platform concept. Some key design challenges still require addressing, particularly related to the mooring system. The mooring tendons and anchors must be able to withstand the higher and continuous stresses that they would be subject to throughout a wind farm's lifecycle. Higher grade materials, either steel or synthetic, will therefore be required, and designers may opt to include additional redundancy in the moorings in order to counter the higher risk of failure. For this reason, developers would be less likely to select TLP platforms when developing wind farms in locations that are subject to seismic activity. Furthermore, as TLP substructures are not inherently self-stable, the tow to site and installation process is likely to be more complex and potentially costly, this last argument will heavily influences our model described in 2.3.2.

Strenghts	Weakness
✓ Low motion of the platform which tend to increase machine performance.	× Onshore assembling possible but challenging offshore installation.
✓ No theoretical maximal depth	× High criticality and failure rate for these components
✓ No added structural mass required for stability as well as shorter moorings can drive cost reductions	× Relatively low TRL with few proven concepts for offshore wind application
	× Complexity on moorings and anchors design

Figure 2.15: TLP strengths and weakness summary

Each typology thus presents pros and cons that can make them more or less suited to a particular project. That is why project developers can work with different suppliers according on the project. The majority of projects counted in 1.4 have not announced the turbine supplier to evaluate which solution will suit the best the sites requirements, and also to witness the first performances and costs of the solution used in the first pre-commercial projects to come. In the end, a summary of the comparison of different technologies has been performed with figure 2.16, where green means an advantage regarding others solutions, yellow an indifference regarding others and red a downgrade. The seven criteria of comparison are hard to be prioritised which make the final choice appear as trade-off based on economical, local and technological causes.

Typologies comparison

	Port assembly	Supply chain / industrial pace	Structural mass	Depth range	TRL	Design complexity	Pitch compensation
Steel SS			High steel mass	50-500 (max 1000)		Active and passive damping	
Concrete barge		Low industrialization		50-500 (max 1000)			
Spar	Offshore assembly required			Middle			
TLP				500-2000 (min 200)		Deep water operation + High stress on tendons	

Figure 2.16: Comparison of different technologies based on seven criteria of interest

Let's have a look at the young platform manufacturing market to identify technological trends among these actors. In a similar approach to the floating market analysis of section 1.4, 19 platform design companies have been mapped and studied. Out of 19 concepts, some were near TRL 9 while the others where still at conceptual phase. In particular, DNV whose seal of approval is the higher estimated one in the market, presents an overview of concepts in [29] which has been very useful to class them. Then researches on developers websites and moreover their implication in projects mapped in section 1.4 has been tremendous to elaborate a list and highlight the more advanced or promising ones.

The first output of this study is the division of projects between floaters technologies displayed on pie chart 2.16. Semi submersibles technologies currently lead the way. This is even more true if barge technologies, which are similar, are considered as SS. Spar buoys technologies was the first developed but are less fashion. Even Equinor, the fist to develop a spar concept, is now heading toward SS solution for future projects. TLP projects are less advance since some technological challenges already presented are yet to be hundred percent resolved, but could gain shares in the years to come based on their potential cost and material saving and their good performances.

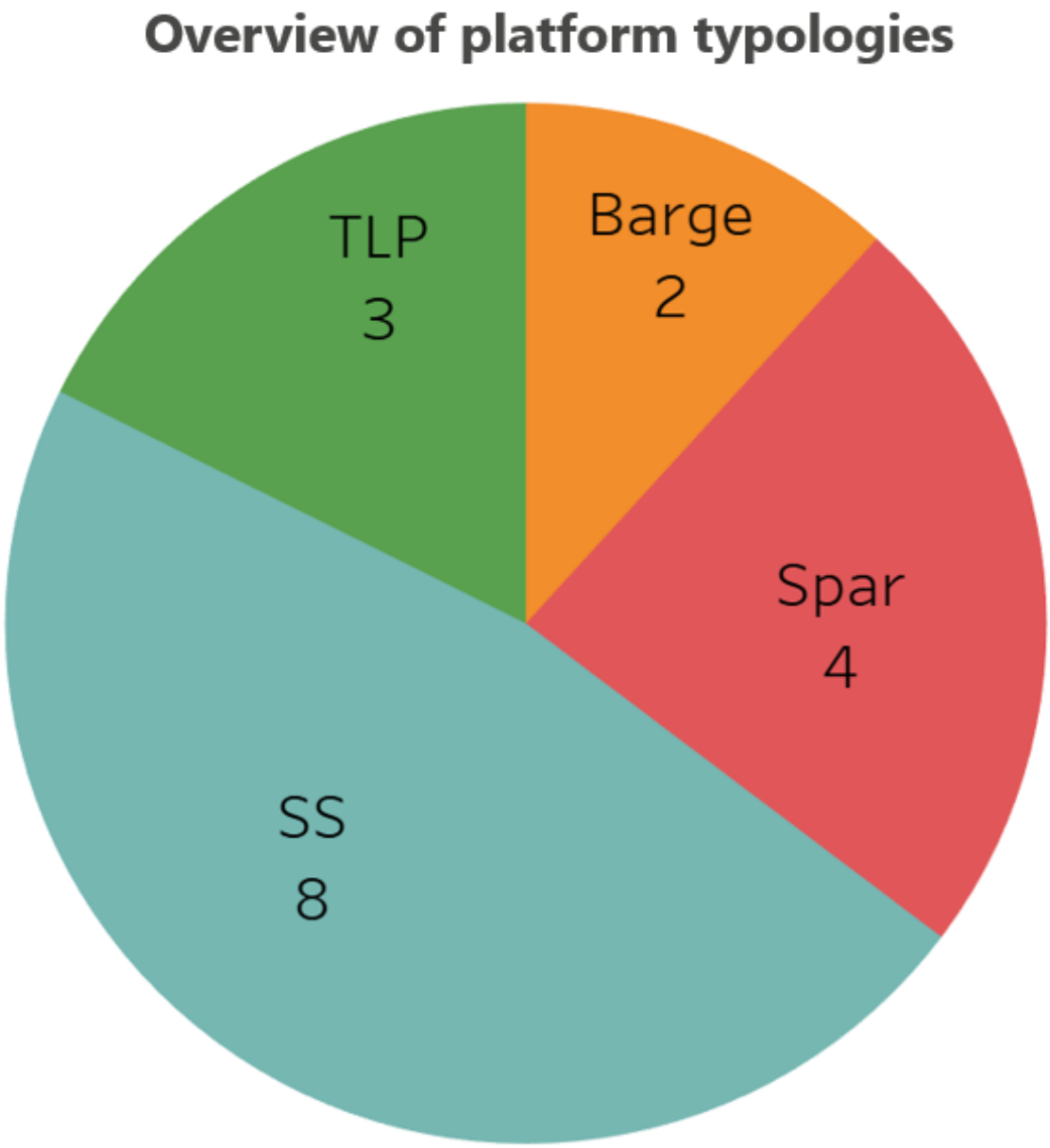

Figure 2.17: Division of counted floating concepts based on typology

A similar pie chart is realised on figure 2.18 showing that Steel is currently by far the most used material. Steel offer good weight to size ratio and is suitable for commercial scale manufacturing: a classical supply chain path could be manufacturing of elemental parts in a factory before an offshore assembling on site requiring less heavy welding and casting facilities on site. The possible high industrialisation rate and modularity offereed by steel solutions is as the based of Stiesdal concepts that will be further presented in section 2.3.4.

Concrete is slowly gaining share. Indeed, it could offer cheaper solution from material solu-

tion and promote local content use: every sites cannot be located near steel manufacturing factories. Yet, concrete used would be less suited to big commercial scale installation from an construction pace point of view. Indeed, videos from Ideol barge 2MW pilot creation in France [61] shows that about 2 weeks of work and important equipment and humans means are required to the realisation of one barge. Plus, these kind of solution would not benefit the same economies of scale offered by industrialisation and supply chain development as for steel based material. Finally, concrete based structures are heavier and thus harder to tow on site. Towing being as explained in section 2.7 the favourite method of installation.
Let's precise that Hybrid concepts are emerging trying to get advantage of both solutions.

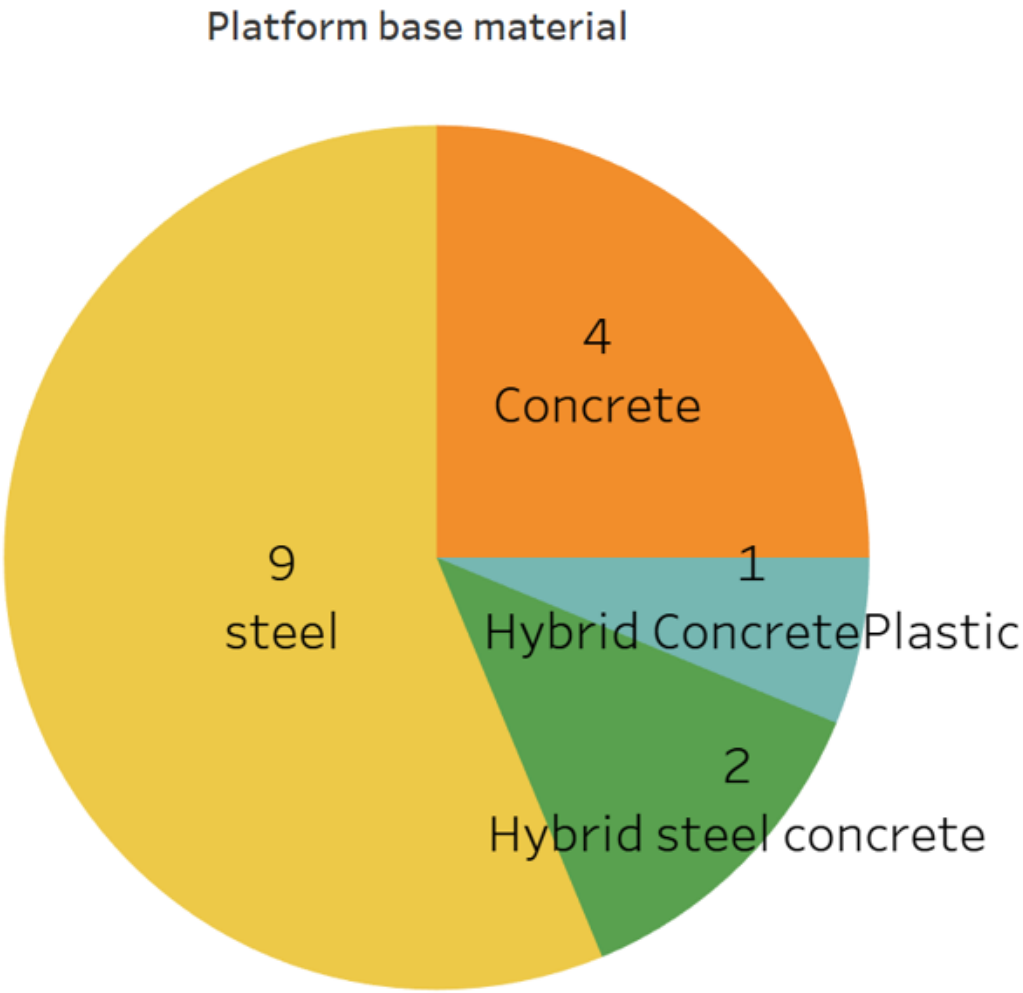

Figure 2.18: Division of counted floating concepts based on base material used

Out of the 19 concepts studied, 10 are already linked with existing projects counted in section 1.4, and can be thus regarded as the more one. This 10 projects are listed and

ranked on the following graph 2.19 according on the expected (or effective) released year of the first . The colour used for the dots represents the current state of development of the concepts: Green for a commercial farm, blue for a commercial-scale pilot and red for a low scale pilot. NOTE: The Naval Steel SS is announced for the french project of Groix and Belle-île (cf [9]) expected by the end of 2023. Yet, very few information are available on the technology and the project is currently facing technological and economical issue that could lead to its abandon. This particular concept will thus not be further analysed eventough appearing on graph 2.19 as one the more advanced one.
On this graph, the 4 concepts (Damping pool by Ideol, TLP by SBM offshore, Spar by Equinor and windfloat by PrinciplePower) presented above appear as the main examples of each types. In particular, PrinciplePower already announced a global pipeline of 300 MW that will complete their 75 MW already installed, figures that are expected to heavily rise regarding the place taken by the company in the field.
Though, other concepts are worth of interest and could answer and optimise some of the issues presented on graph 2.16. These will be presented later on after the physical explanation in subsection 2.3.4

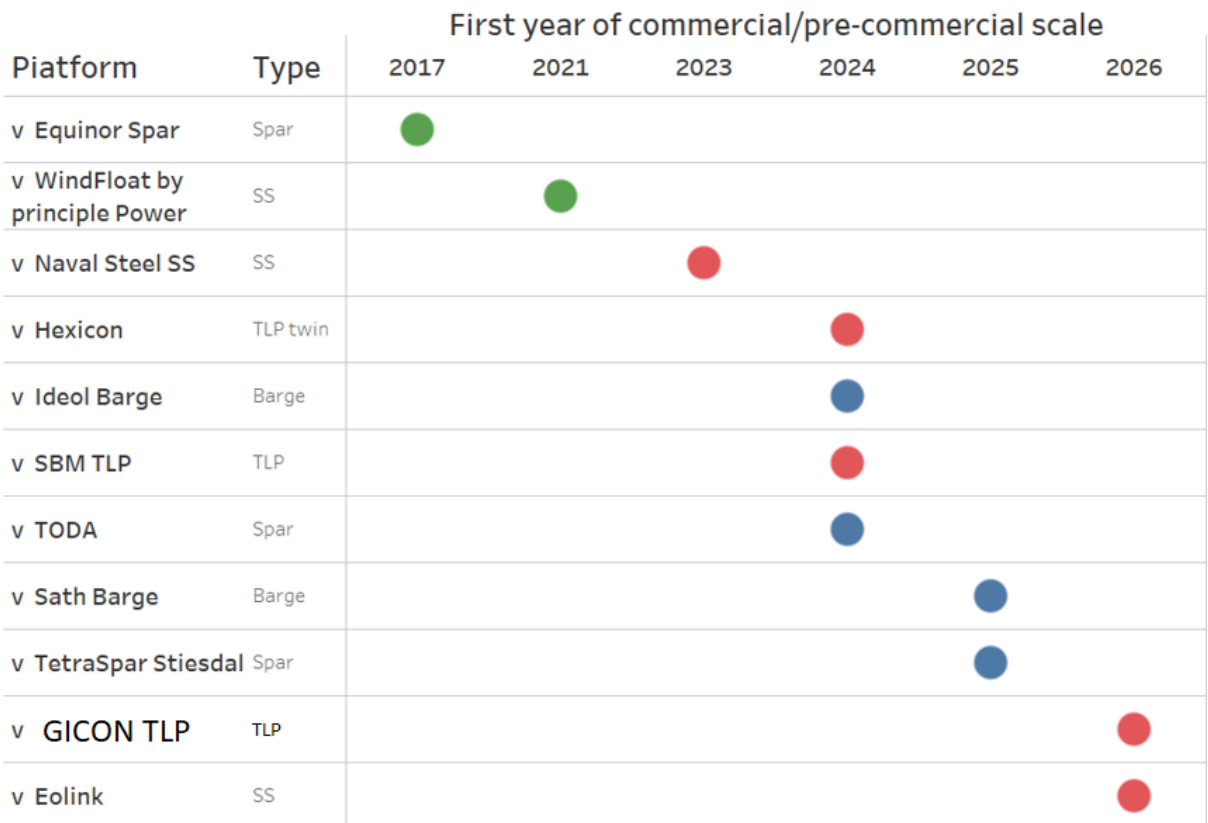

Figure 2.19: Year of first commercial scale project of mapped platforms concepts.

To conclude this general overview, here after is reported a chronological timeline on figure 2.20of floating platforms development milestones, that are is of course linked to the development of the whole FOW field.

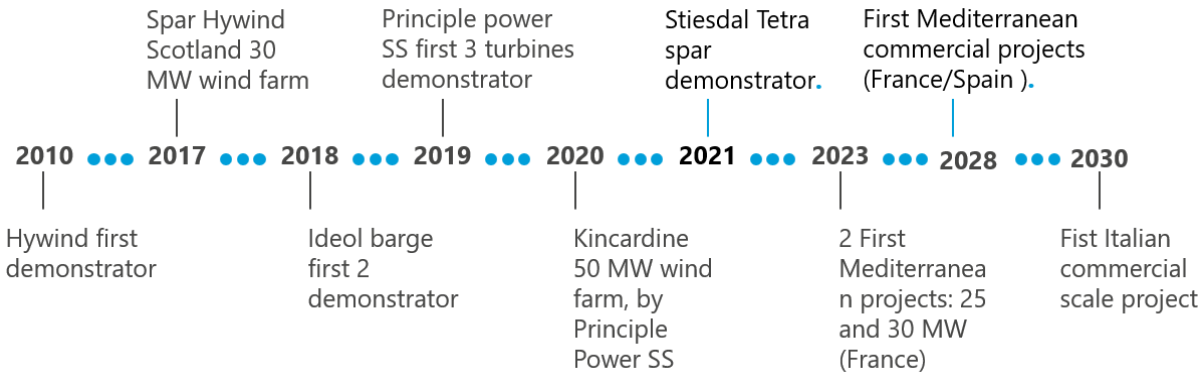

Figure 2.20: Main floating platforms field development milestones

2.3.2. Physical model

In this subsection, the behaviour of each type of structure will be physically analysed to highlight on which principles their buoyancy performances rely and how they cope with the external solicitation while in operation. The main idea of this work is to predict the future dimensional trends of the floaters when used for ever bigger turbines as predicted in section 2.2. Indeed, the few size and cost data now available concerns pilots of wind turbine until 5 MW which are for now way out of competition with fixed-bottom offshore wind as explained in [17]. Yet, [58] explains that use of bigger turbines could enhance intrinsic economies of scale regarding specific costs of wind turbines. The idea is to verify this hypothesis summoning physic-based arguments.

General and basic ideas of typologies under scrutiny will be adopted since the objective is more about identifying general trends that would help actors evaluate the future viability of FOW in a given sector and eventually choose between solutions. Actually, absolute values given must only be regarded as indicative since every concepts will present specificities. Since only the essence of each typology is included in the model, dynamic behaviour that can be heavily impacted by details or additional technologies (active damping etc...) will not be analysed. Indeed, these kind of behaviour can only be performed on very particular designs with few general insights, eventough this kind of study will be required for every single prototype and outputs are interesting and existing in the background of this research [64], [65]. The focus will be made on static condition where platforms are submitted to the worst condition imaginable. Based on this criteria, the forecast of size

evolution with bigger will be made on the maintaining of the performances of the turbine in these worst position and the fewer equations of the static approach will allow to model to have comparable and insightful outputs that will be analysed in subsection 2.3.3.

Let's first identify the forces at stakes in our study case than can first be summarised as on simplified scheme 2.21 as the study of a partially immersed physical corp in water, with wavy and windy conditions. In the static models, 4 actions have thus to be modeled: the two external actions from the waves and the wind, and the two structural ones relatives to gravity and buoyancy. First, let's see how the wave and wind condition defined the external forces applied on a floating platform, independently of the typology.

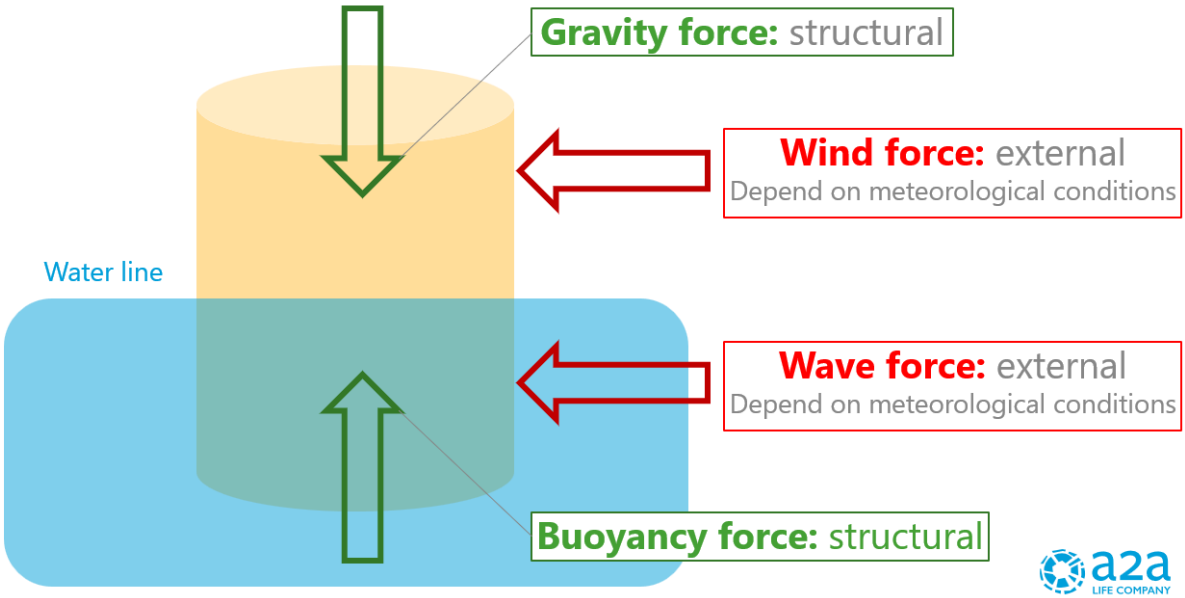

Figure 2.21: Forces taken in consideration in the static model

In some studies, underwater currents actions are also took in consideration as explained in [66]. Yet, these mainly impact large drafts structures as classical spar type and vary a lot from a location to another. Plus, their impact is usually less important than wind and wave actions and will be thus neglect in our work. Yet, for some particular sites this hypothesis could be too strong and project developers should include currents assessment in their early studies.
First, let's see how the wave and wind condition defined the external forces applied on a floating platform, independently of the typology.

2.3.2.1 External forces modelisation

As explained in section 1.2.1, wind flow around blades generate a lift work in a perpendicular direction to the blade line direction (cf [67]). This work generates the torque at rotor axis and allow to generate electricity, these forces are represented in green on figure 2.22. Yet, in its aero-dynamical study of corps in wind stream, [67] also explains that that drag forces are also generated , eventough the pitch angle is generally chosen to decrease the share of these drag forces on rotor. This "damageable" part of wind action on rotor is called thrust force and generates push on the structure instead of torque at the rotor axis. This force is represented in red on figure 2.22.
This thrust force can be expressed as displayed in equation 2.1 according to [67] and [66].

$$F_t = \frac{1}{2}.\rho_{air}.\frac{D_{rot}^2}{4}.C_{drag}.U_{wind}^2 \tag{2.1}$$

ρ_{air} is the air density which can be taken constant at sea level
D_{rot} is the rotor diameter, it evolves with turbine size as explained in section 2.2
C_{drag} is the drag coefficient of the blades that is function of blade profile and angle of attack of the blades [68]: it will be impacted by the pitch angle regulation chosen [3]
U_{wind} is the wind velocity. The one chosen for calculation will be high to represent harsh conditions.

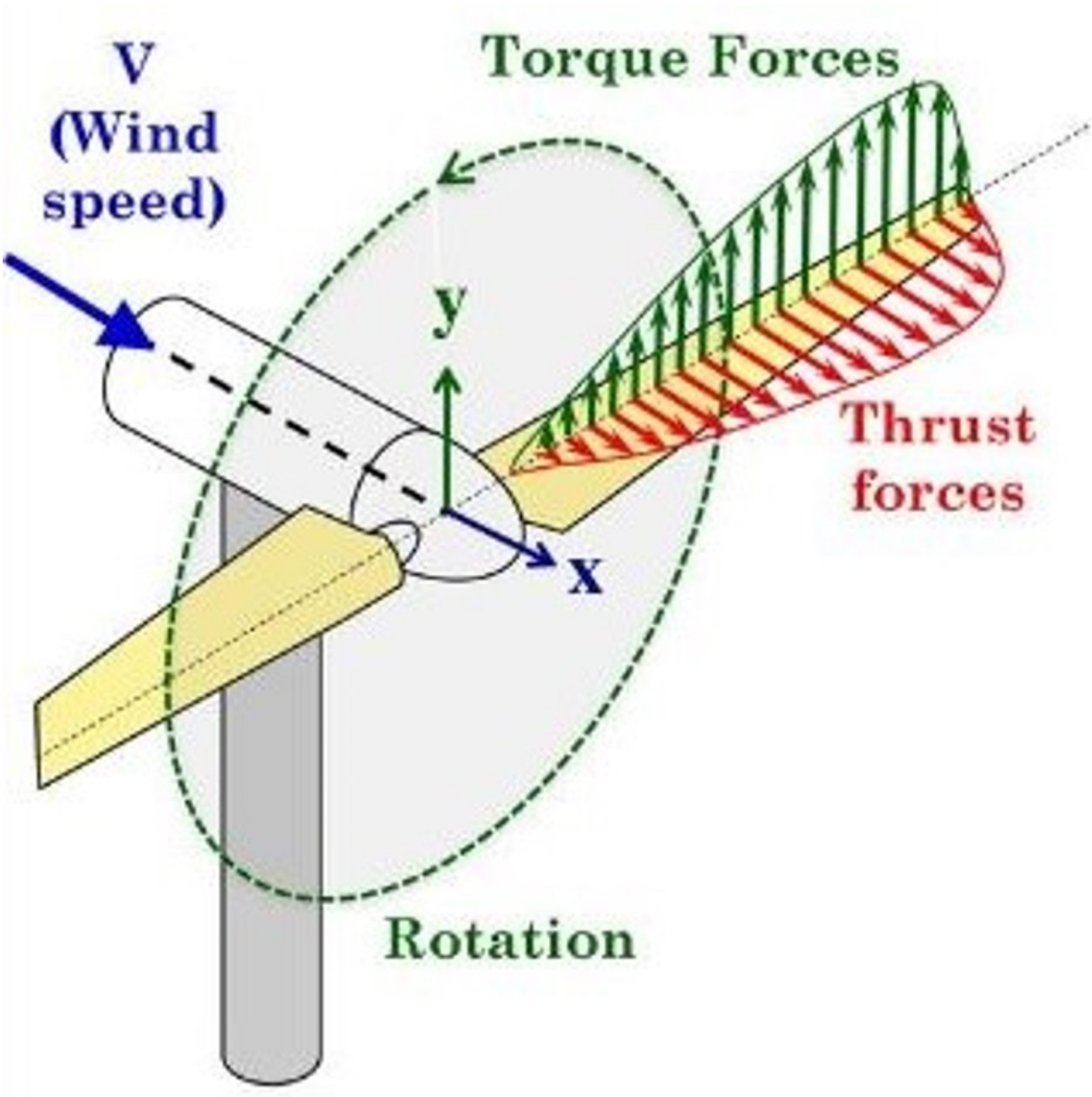

Figure 2.22: Thrust force on rotor

The same phenomenon applies on the tower: in addition to the thrust force on rotor, the wind also apply a load on the whole height of the tower. Eventough the surface facing wind is smaller in that case than the one swept by rotor blades, the tower profile is not optimised for wind flows as the blades ones and the drag effects are thus more important. The wind profile can evolve with height along the tower as display on figure 2.23. Integral calculation is thus used to take account of this particularity. Thus, this drag force on tower can be expressed as displayed in equation 2.2 according to [67] and [66].

$$F_d = \int_0^h \frac{1}{2}.\rho_{air}.D_{tower}(z).C_{drag}.U_{wind}^2.dz \tag{2.2}$$

ρ_{air} is the air density which can be taken constant at sea level
$D_{tower}(z)$ is the tower diameter, it evolves with turbine size as explained in section 2.2. Plus, for a given turbine size, the tower usually has a conic shape and the diameter at the top is thus lower than the one at the base.
C_{drag} is the drag coefficient of the tower that is function of tower profile. The classical value for cylindrical profiles as the tower one is round about 1 according to [69] since the height over diameter ratio of our turbine is about 40. U_{wind} is the wind velocity. The one chosen for calculation will be high to represent harsh conditions.

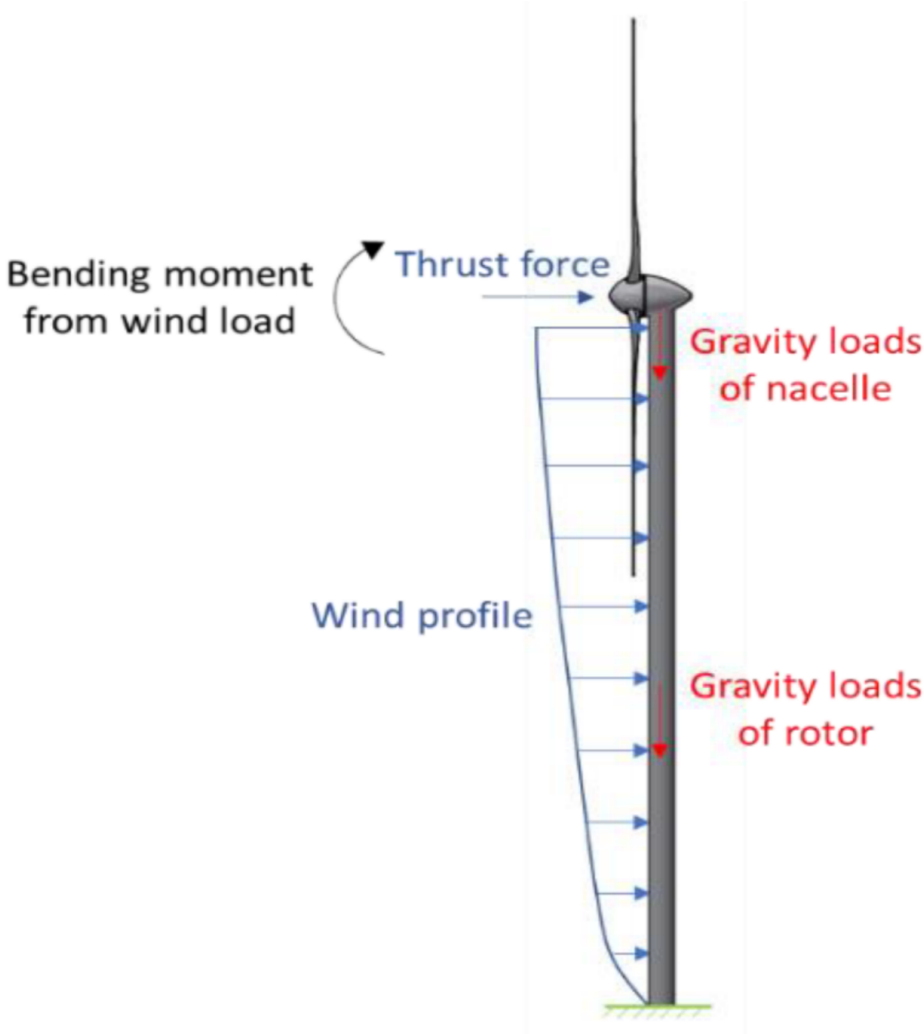

Figure 2.23: Drag force on Tower

The wind actions have been defined, let's do the same for waves. First of all, the waves as the propagation of a mechanical perturbation must be characterised. To do, and since only the macroscopic behaviour of the wave is here under study, the so called linear wave model defined in [70] will be used. In this approach, waves are seen as perfect time-space propagation sinusoidal (as light waves for example) and can thus be defined using only three parameters. The figure 2.24 illustrates the model and the elevation $\nu(x,t)$ of a point, i.e the distance between the undisturbed sea level and the point disturbed by the wave is used to describe wave behaviour via the equation 2.3:

$$\nu(x,t) = \frac{H}{2}.cos(kx - \omega t) \tag{2.3}$$

H is the wave-height in [m]: the vertical distance between a crest and a Trough as shown on figure 2.24.
$\omega = \frac{2\pi}{T} = 2\pi f$ is the time pulsation in [rad/s]. T is the wave period as described on figure 2.24, and f the wave frequency that is the inverse of T.
$k = \frac{2\pi}{\lambda}$ is the time pulsation in [rad/m]. λ is the wave length that is defined in figure 2.24 as the distance between two crests.

The H value depends on meteorological conditions and the T value can be nicely approximated by T = 10 s according to [70]. Then the wavelength is influenced by gravity and sea depth in terms described by equation 2.4:

$$\lambda = \frac{g.T^2}{2\pi}.tanh(\frac{2\pi d}{\lambda}) \tag{2.4}$$

Where $g = 9.81[m/s^2]$ is the Earth acceleration and d is the depth of the seabed at the point concerned.

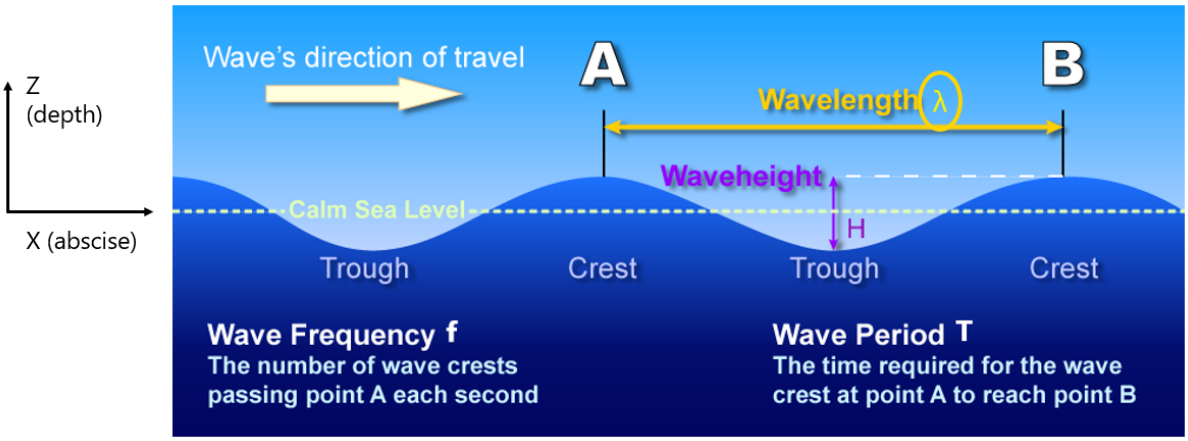

Figure 2.24: Linear wave model explanation

In fluid dynamics the Morison equation is a semi-empirical equation for the inline force on a body in oscillatory flow [71]. The Morison equation is used to estimate the wave loads in the design of oil platforms and other offshore structures and is thus the perfect tool for us to be used in our study.

Yet, since semi-empirical, the morison law can be applied only under hypothesis listed in [71]. Firstly the flow acceleration must be more-or-less uniform at the location of the body. For instance, for a vertical cylinder (that will be our elemental case study of figure 2.26) in surface gravity waves this requires that the diameter of the cylinder is much smaller than the wavelength. If the diameter of the body is not small compared to the wavelength, diffraction effects have to be taken into account. Plus, uni-directional flows must be assumed.

Figure 2.25 delimits the geometrical requirements for the use of the Morison theory. In our study as it will be seen later, the obstacle diameter will remain in a range [3 - 12 m] and the wave height H will tops 10 m at its maximum. Then, the depths under study will remain over 80 meters and thus λ will be around 150 m. The limit value that the rapport $\frac{\lambda}{D}$ has to overcome is five in order to neglect the diffraction effects (cf [72]). Regarding the values of this study, we will always remain in this zone, highlighted in blue in figure 2.25, and the Morison theory for wave loads estimation will be applied.

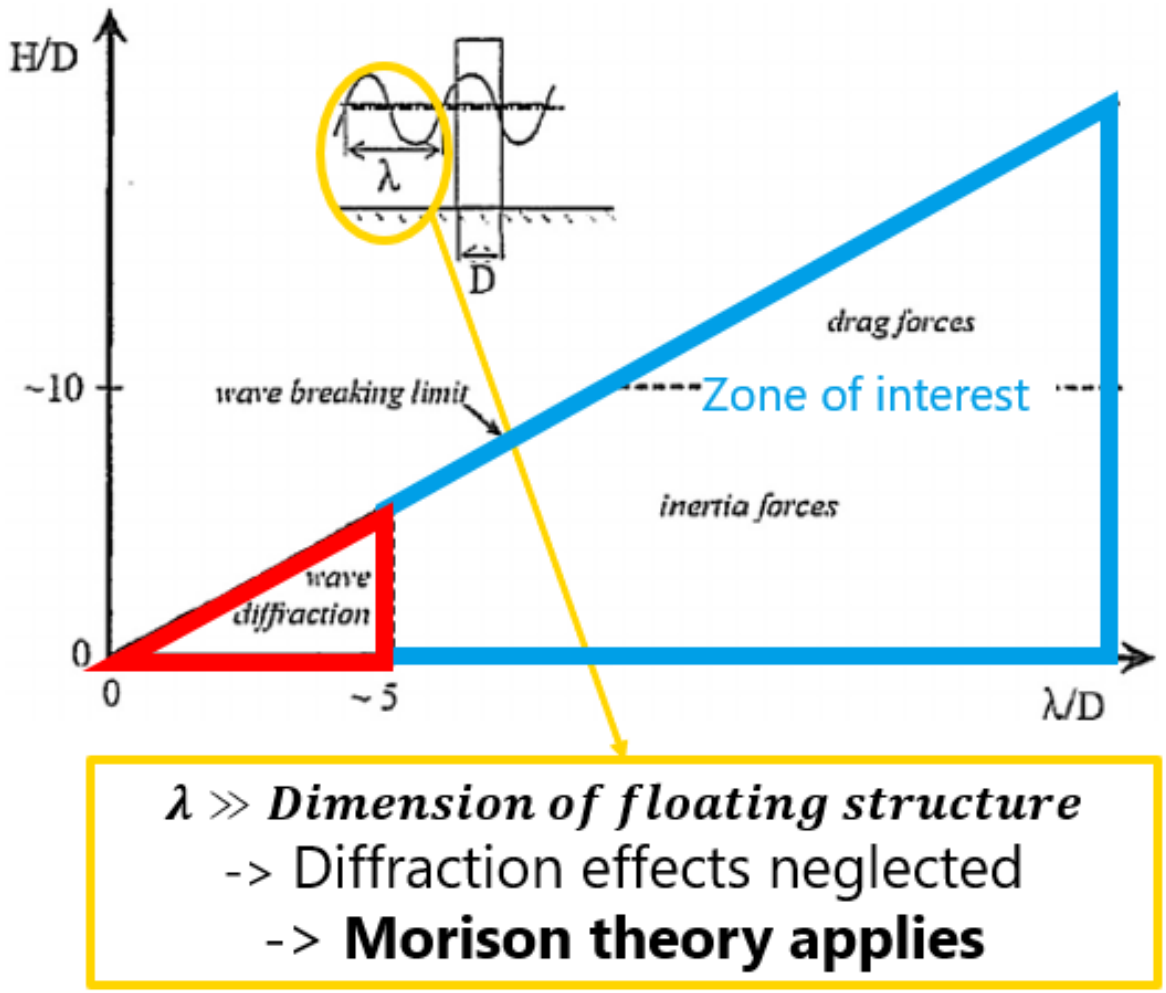

Figure 2.25: Range of Morison's laws application

As previewed from figure 2.25, Morison's forces are distinguished in two components for a fixed body in an oscillatory flow (cf [71],[72]). The Morison equation contains two empirical hydrodynamic coefficients —an inertia coefficient C_m and a drag coefficient C_d — which are determined from experimental data.The scheme 2.26 represents the elemental cylindrical body on which the waves loads will be assessed. Indeed, the result from a single cylinder will be enough to describe the whole structures behaviours in our model. The fluid molecular flow velocity vector $\vec{u}$ is displayed on the scheme with its horizontal and vertical components, respectively u(t) and w(t).

- **Inertia force:** Force in phase with the local flow acceleration and expressed in equation 2.5:

$$\vec{F_I} = \rho_{water} C_m V \dot{\vec{u}} \tag{2.5}$$

V is the volume of the immersed body exposed to wave action.
ρ_{water} is the water density that will be considered as a constant.
$C_m = 1 + C_a$ is the inertia coefficient which take in consideration the effect of the Froude–Krylov force [72] and the and the hydrodynamic mass force via C_a the added mass coefficient.
$\dot{\vec{u}}$ is the vector of the flow acceleration, time derivative of the vector $\vec{u}$ representing the flow velocity.

- **Drag force:** Force proportional to the (signed) square of the instantaneous flow velocity and expressed in equation 2.6:

$$\vec{F_D} = \frac{1}{2}\rho_{water} C_d A \vec{u}.|\vec{u}| \tag{2.6}$$

A is reference area, usually the cross-sectional area of the body perpendicular to the flow direction
ρ_{water} is the water density that will be considered as a constant.
C_d is the drag coefficient which is derive from experimental analysis.

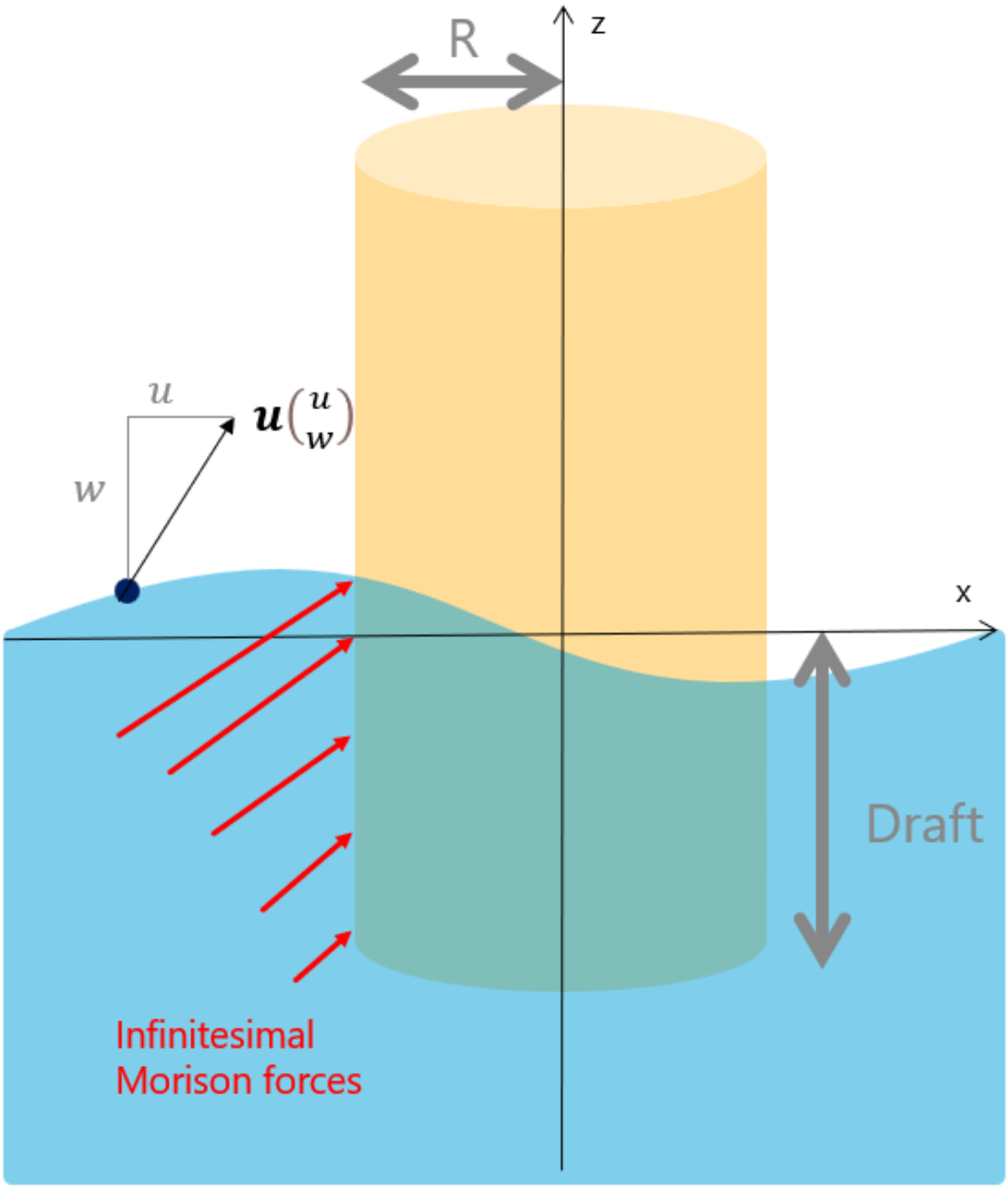

Figure 2.26: Morison laws application framework

To evaluate Morison's forces impacts, the molecular flow velocity vector components must be defined. Their global from is complex since the hydrodynamics influence of the seabed on the mechanical perturbation cannot be taken as linear. Yet, in the related academic courses videos from [12] is explained a more simple framework where these velocities can

be expressed. Indeed in the so called "deep wave configuration", the influence of seabed on wave formation can be neglected and the dependence on the depth d disappears from equations. According to [12] this deep wave model is valid as soon as the wavelength λ defined in equation 2.4 is smaller than half the depth d, i.e. $2\lambda < d$.
This is valid for depth higher than 70 meters, which will cover the calculus of our model since as shown in subsection 2.3.3 our framework lower depth limit is 100 meters. For shallower waters, depth influence should be integrated in the physical model.
In this deep wave configuration, the expression for $\vec{u}$ and its time derivative $\dot{\vec{u}}$ components are extracted from [12] and displayed on the following table of figure 2.27.

Deep wave configuration : No dependance on d (depth)	
$u(z)$	$\frac{\pi H}{T} e^{kz} \cos(kx - \omega t)$
$\dot{u}(z)$	$\frac{2\pi^2 H}{T^2} e^{kz} \sin(kx - \omega t)$
$w(z)$	$\frac{\pi H}{T} e^{kz} \sin(kx - \omega t)$
$\dot{w}(z)$	$-\frac{2\pi^2 H}{T^2} e^{kz} \cos(kx - \omega t)$

Figure 2.27: Deep wave configuration results

From this expression, flow velocities and acceleration components appears as sinusoidal propagation expression traducing the oscillatory behaviour of the water particles with an additional exponential attenuation component depending on the vertical component z. This means than a particle one meter below the surface will have less important

movements than particles on the surface. This dependence in z makes impossible the direct application of general Morison's laws displayed in equation 2.5 and 2.6. Indeed, as shown on scheme 2.26 the cylinder under study is immersed and the water particles responsible of the wave loads will have difference velocities and acceleration according on their z components. As shown on the scheme, infinitesimal Morison forces will thus be considered and their contribution will then be integrally summed along draft of the cylinder to account for the total Morison's loads. The used expression of the 2.5 and 2.6 are thus adapted for our specific elemental cylinder of scheme 2.26 as display in equation 2.7 and 2.8:

$$\vec{F_I} = \int_{-Draft}^{0} \rho_{water} C_m \pi R^2 \dot{\vec{u}} dz \tag{2.7}$$

Since $\pi R^2 dz$ is the infinitesimal volume.

$$\vec{F_I} = \int_{-Draft}^{0} \rho_{water} C_d R \vec{u}.|\vec{u}| dz \tag{2.8}$$

Since Rdz is the elemental reference area.

In our model, in order to be conservative, static Morison forces will be evaluated at their temporal maximum, which means when the sinusoidal part (cf figure 2.27) will be equal to one. Plus, in order to remain conservative and to ease the computation, both drag and inertia Morison forces will be taken at their maximum even tough they are usually not in phase as explain in [71] and display on figure 2.28.

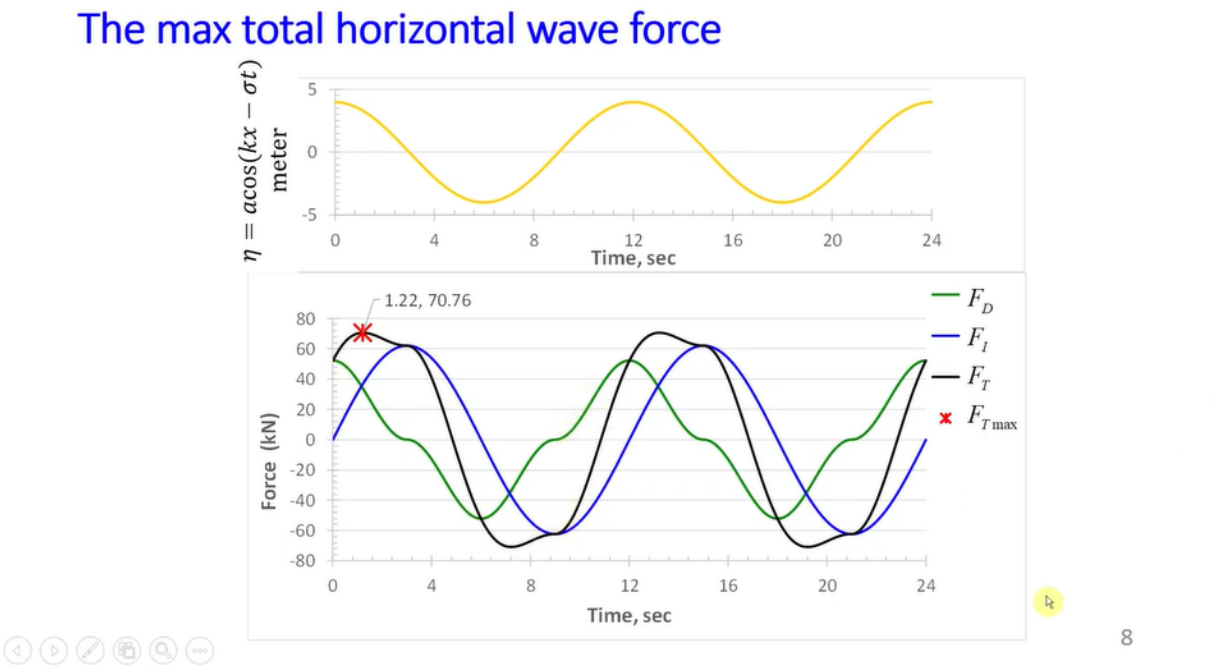

Figure 2.28: Inertia and drag Morison's force time evolution from [12]

2.3.2.2 Buoyancy mechanism

The role of floating substructures is to compensate the external loads presented here above to allow the turbines effectively generate wind power. The first obvious role of the floater is to compensate gravity and prevent the structure sinking. As schematically represented on figure 2.21 the structure has to generate a structural vertical buoyancy reaction when immersed in water to compensate the structural vertical gravity force due to structural weight.

The hydrostatic model built for this study will thus first rely on a direct application of Archimedes push as describe in [73] to our immersed structure. The first main equation of the hydrostatic equilibrium is thus, once the earth acceleration surface is cancelled out from each leg of the equation, the equation 2.9.

This first law will have an important impact on platform sizes, forms and material used in order to balance immersed volume and weight on techno-economic point of view while reaching the desired draft, tremendous characteristic that will heavily rely on this law.

$$M_{tot} = \rho_{water}.V_{Wet} \tag{2.9}$$

Where M_{tot} is the total mass in [kg] of the floater structure plus the turbine.

V_{Wet} is the total volume of the body immersed under water.

Then, the floating substructure has to mitigate the effects of external loads (cf figure 2.21) previously discussed. To do so, it must generate so called "righting moments". Floaters typologies are, as explained in subsection 2.3.1, clustered according on which physical principles are used to provide these righting moments. Three main categories of stabilisation methods exist and can be used by floater concepts, jointly or not. We talk about water plane area stabilisation (or buoyancy stabilisation) which is mainly link to SS and barges; Ballast stabilisation mainly linked to spar concepts and Mooring (or over-buoyancy) stabilisation which are typical of TLP concepts. According on the share of each stabilisation method in the final righting moment, every floating concept can be graphically represented on the stabilisation method pyramid generated in [13] displayed on figure 2.29. This representation is interesting since it can show for example that eventough SS are mainly relying on waterplane area stabilisation, some concepts can "add" ballast stabilisation processes to participate to the righting moment generation.

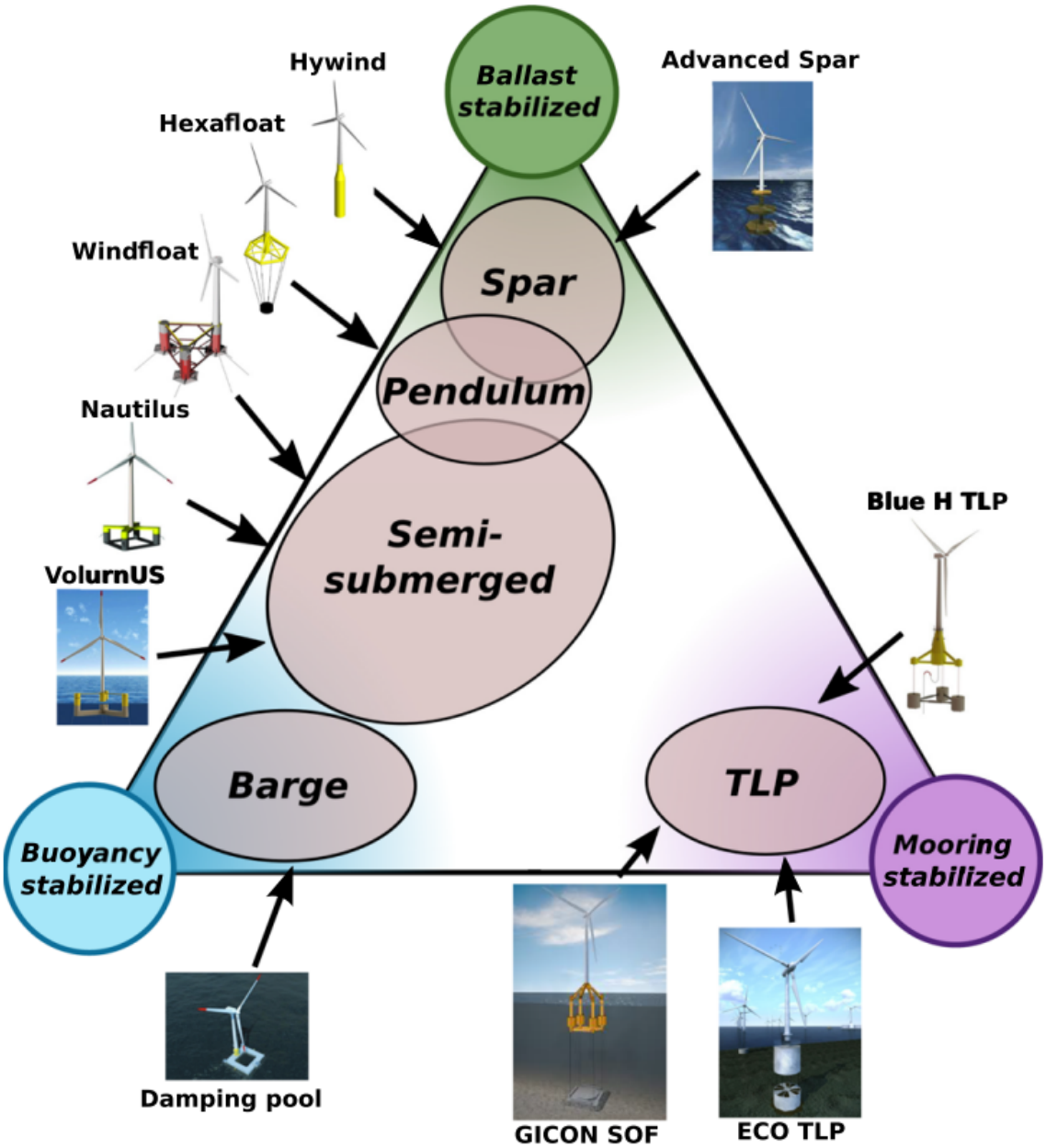

Figure 2.29: Methods of stabilisation of platform types from [13]

To put this hydrostatic stabilisation in equation, the static equality between the external loads forces and the restoring ones must be written. For sake of simplicity, since the beginning of this study, the hydrostatic problem is only studied in two dimensions defined by the (x,z) plan of figure 2.26. In terms of performance, the angular rotating oscillation around the y axis orthogonal to the (x, z) plan will be considered as the main criteria. The two other displacements in a 2D model being translation on horizontal or vertical (surge, can be studied on a dynamical analysis to evaluate fatigue on moorings as in

[65]) axis. The compensation of external loads is thus written via a moment equality (we talk about righting moment) on the orthogonal axis and can thus be written as a single component equation 2.10 and the two forces equilibrium on x and z axis will not be considered. For equation 2.10 written here after, an hypothetical floater using all three stabilisation methods is considered to first remain in a general point of view. The balance of moment is written at the center of the platform where the turbine will be considered to be located, and at sea level. From combination of SS and spar related results [16] and from TLP results from [74] the general restoring equation 2.10 is obtained:

$$\Sigma M_{ext} = \rho_{water}.g.I_y.sin\theta + (F_b.Zcob - F_g.Zcog)sin\theta + d_{pontoon}.F_{tension} \tag{2.10}$$

Where ΣM_{ext} is the sum of external loads bending moments written at the center of the platform at sea level. Lever arms considered will depend on substructure considered and turbine size.
ρ_{water} is the water density that will be considered as a constant.
g is the earth acceleration that will be considered as a constant.
I_y is the second moment of area of the floating structure regarding the y axis. A particular focus will be put on this parameter.
θ is the pitch angle: the tilting angle between the structure at its original position and when it is submitted to external loads, generating a tilt on y axis.
F_b and F_g are respectively the vertical buoyancy force from the water on the immersed part of the structure (Archimedes push) and the vertical gravity force due to structure weight. From equation 2.9, this forces must be equal in static conditions.
$Zcog$ is the center of gravity of the structure, i.e. the point in a body where the gravitational force may be taken to act.
$Zcob$ is the center of buoyancy of the structure, i.e. the center of gravity for the volume of water which a hull displaces and thus the point in an immersed body where the buoyancy forces may be taken to act.
$F_{tension}$ is the force exercised by a mooring on the structure to compensate external loads and to provide over-buoyancy in a TLP configuration.
$d_{pontoon}$ is the horizontal distance between the center of the structure where the restoring equation is written and the attached point of the mooring, usually located at the extremity of the pontoon to increase lever arm.

More than physical formulas, through this formula the effect of each stabilisation methods can be highlighted, and that is the role of figure 2.30 where the part of each method is

highlighted in the restoring moment equation. The water-plane area stabilisation process is highlighted in green and associated with the semi-submersible (SS) platform; the ballasted stabilisation process is highlighted in yellow and associated with the spar platform; the over-buoyancy stabilisation process contribution is highlighted in red and associated with the tension leg platform (TLP). Each principle is further explained later on.

$$\sum M_{ext} = \underbrace{\rho g I_y \sin\theta}_{\text{SS principle}} + \underbrace{(F_b \times Z_{cob} - F_g \times Z_{cog}) \sin\theta}_{\text{Spar principle}} + \underbrace{d * F_{tension}}_{\text{TLP principle}}$$

Figure 2.30: Righting moment equation explanation

First, let's have a glance at the water-plane area stabilisation process at stake for barge and Semi-submersibles concepts mainly. This stability principle is actually well known since used by boats to float and is well describe in the very complete study of Semi-submersibles physics led in [75]. Figure 2.31 represents a floating structure partially immersed that could be a barge concept, a SS one or a simple boat. In the undisturbed configuration (on the left on figure 2.31), the center of gravity is located at the vertical the center of buoyancy which means that that no moment can be created. In the heeled condition (on the right on figure 2.31), the structure has rotated an angle η due to an external disturbance. The center of buoyancy has moved because of the distribution of the displaced volume. Mass of the ship has not changed, and thus the displaced volume is constant since according to equation 2.9 buoyancy and gravity remain equal in intensity. Due to a disturbance, the wet area has changed at the section and the center of buoyancy can be found at the center of the wet area. GZ indicates the distance between the center of gravity and the center of buoyancy, and because of this distance a moment is caused which counteracts the disturbance.

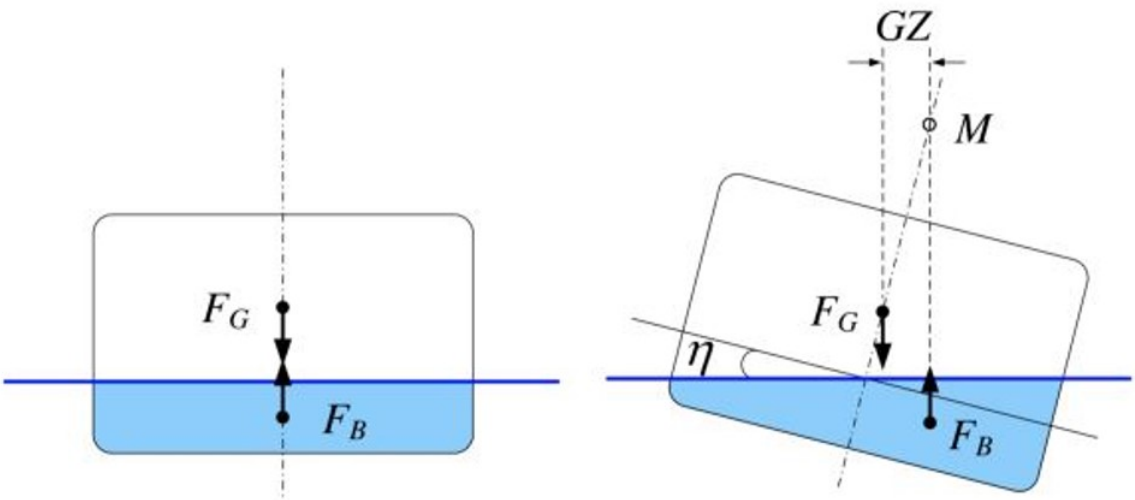

Figure 2.31: Water-plane area stabilisation method explanation

A stable floating structure has a positive value for GZ, meaning that when the structure is inclined due to exciting forces, the center of buoyancy and center of gravity separates such that they create a moment counteracting the inclination of the structure. This moment is equal to the buoyancy force times the distance GZ [75], between the center of gravity and the center of buoyancy. Equation 2.11 shows an expression for the hydrostatic moment, as a function of the tilt angle θ. [75] also gives us the expression of GZ in function of floating structure second moment of area along y axis I_y and volume V, which is inserted in equation 2.11 and helps us re-find the water-plane area contribution of equation 2.10.

$$M_{hydrostatic} = GZ(\theta).F_b = \frac{I_y}{V} sin\theta.\rho_{water} gV = \rho_{water}.g.I_y.sin\theta \tag{2.11}$$

Two interesting insights can be taken out of this equation 2.11.
First, as it will be the case for ballast stabilisation process (cf figure 2.33), the restoring moments is proportional to $sin\theta$. Within the operational framework defined by [76] as a range of [-10°;10°] for tilt angle θ, a quasi-linear approximation can be assumed making the restoring moment proportional to θ: the bigger the disturbance, the bigger the righting moments allowing the structure to be intrinsically stable.
Next, the important characteristic to be techno-economically optimised to provide good stability performances appears to be the second moment of area I_y. From [77], the second moment of area, or second area moment, or quadratic moment of area and also known as the area moment of inertia, is a geometrical property of an area which reflects how its points are distributed with regard to an arbitrary axis. In physics it is thus expressed in $[m^4]$ and equation 2.12 displays its calculation procedure:

$$I_y = \int\int_{Surface} x^2 dxdy \tag{2.12}$$

Results for particular shapes are displayed on table of figure 2.32.

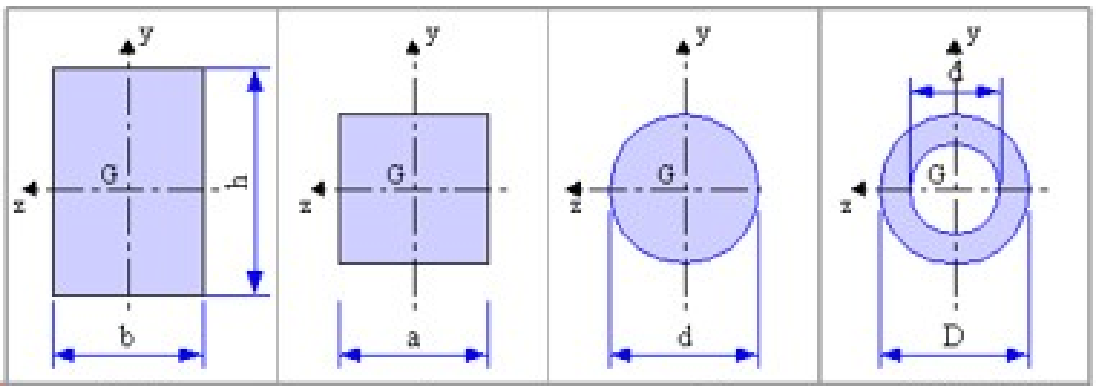

IGz (mm⁴)	$\frac{bh^3}{12}$	$\frac{a^4}{12}$	$\frac{\pi d^4}{64}$	$\frac{\pi (D^4-d^4)}{64}$
I_0 (mm⁴)	$\frac{bh^3+hb^3}{12}$	$\frac{a^4}{6}$	$\frac{\pi d^4}{32}$	$\frac{\pi (D^4-d^4)}{32}$

Figure 2.32: Second moment of area

For floating substructures, it is usually necessary to calculate the second moment of area of a shape with respect to an y' axis different to the centroidal axis of the shape. To do so, the parallel axis theorem is used to derive the second moment of area with respect to the y' axis. The parallel axis theorem states that:

$$I_{y'} = I_y + A.d^2 \tag{2.13}$$

Where A is the area of the surface and d is the perpendicular distance between the y and y' axes.

Physical process behind spar stabilisation is the high distance between the center of buoyancy of the structure near sea water line and the center of gravity of the structure located the further possible above the sea level. In undisturbed position, buoyancy and gravity forces remain aligned with the vertical of the structure and thus no moment is generated. Yet, when external disturbance leads to an angular pitching of the structure as

schematised in figure 2.33 with a pitch angle θ between the vertical axis and the tower axis, this forces are still vertical but are not aligned anymore, generating a non null moment. Writing this moment equation at the same centered point at sea level O (in blue on figure 2.33) as previously, the lever arms of the buoyancy and gravity forces are respectively $Z_{cob}sin\theta$ and $Z_{cog}sin\theta$, where as explained on figure 2.33 Z_{cob} and Z_{cog} are respectively the vertical distance between O and COB and O and COG. Righting moment tends to restore the structure in its original position pushing angle θ towards null value. The righting moment written in O is thus counted positive in trigonometric sense. Since the points of application of the two forces are located on the left of point O, the buoyancy force effect on moment in O will be negative since the upward and the gravity force one will be positive since directing downward.
Since buoyancy and gravity forces are equals in intensity in static conditions from 2.9, the fact that Z_{cob} is made lower Z_{cog} insure a positive righting moment and thus inherent stability, and the ballasted stabilisation contribution is re found and written in equation 2.14

$$M_{hydrostatic} = (F_b.Zcob - F_g.Zcog)sin\theta \tag{2.14}$$

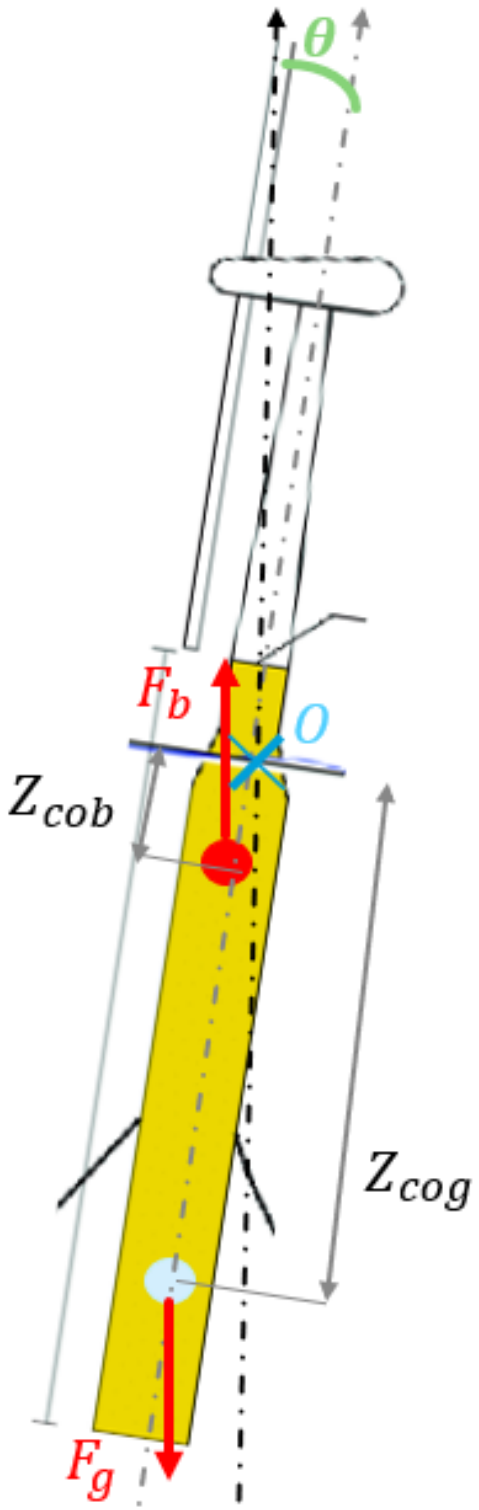

Figure 2.33: Ballasted stabilisation method explanation

The key design parameter here is thus the distance between COB and COG that must be maximised. As explained in [78] where different spar configuration are compared in terms

of static and dynamic performances, many structural variation can influence this parameter. In the end, this stabilisation process appears quite simple and easy to manipulate, explaining why it has been the first ever used.
Real SS and Spar concepts combine both processes eventough only one can be regarded as the main contributor to stability as supposed by pyramidal clustering on figure2.29. Actually, in the case where COG of spar models are located higher than their center of buoyancy, the ballasted stabilisation process can even be detrimental leading to negative restoring moment.

Finally, the mooring stabilisation process behind TLP concepts appears as the most simple one since as schematised on figure 2.34 the tendons, that will be further discussed in subsection 2.4, maintain the structure in position. Theoretically, no pitch angle is allowed with this kind of process and thus the two previous stabilisation methods have no influence on TLP stability that only rely on mooring action. The contribution of mooring stabilisation method in the general restoring equation is obvious and only consist in the multiplication between the tension force of the considered tendons and the levr arms.
In our model, the mooring disposition will be considered symetric and thus will be assumed than half of the mooring (the one on origin side of disturbance) will work to counteract the external loads, while all tendons will constantly assure the over buoyancy for the platform. This over-buoyancy forces balanced between the moorings (and in the end the anchors) actually rules out the buoyancy equation 2.9 that can be adapted as in equation 2.15

$$F_b = \rho_{water} g V_{wet} = F_g + F_{ob} = M_{tot} g + F_{overbuoyancy} \tag{2.15}$$

Yet, as it will be seen later and as explained in [74], various design parameters enter in the optimisation process of a concept. Among us the type of tendons (size, material etc...), their number and their disposition (lever arm size). Even if the stabilisation process is simple, the techno-economic optimisation of the structure is thus far from being trivial. For example, in a webinar associated with [76] the idea of asymmetrical mooring lines around the structure according on current and wave directions is discussed.

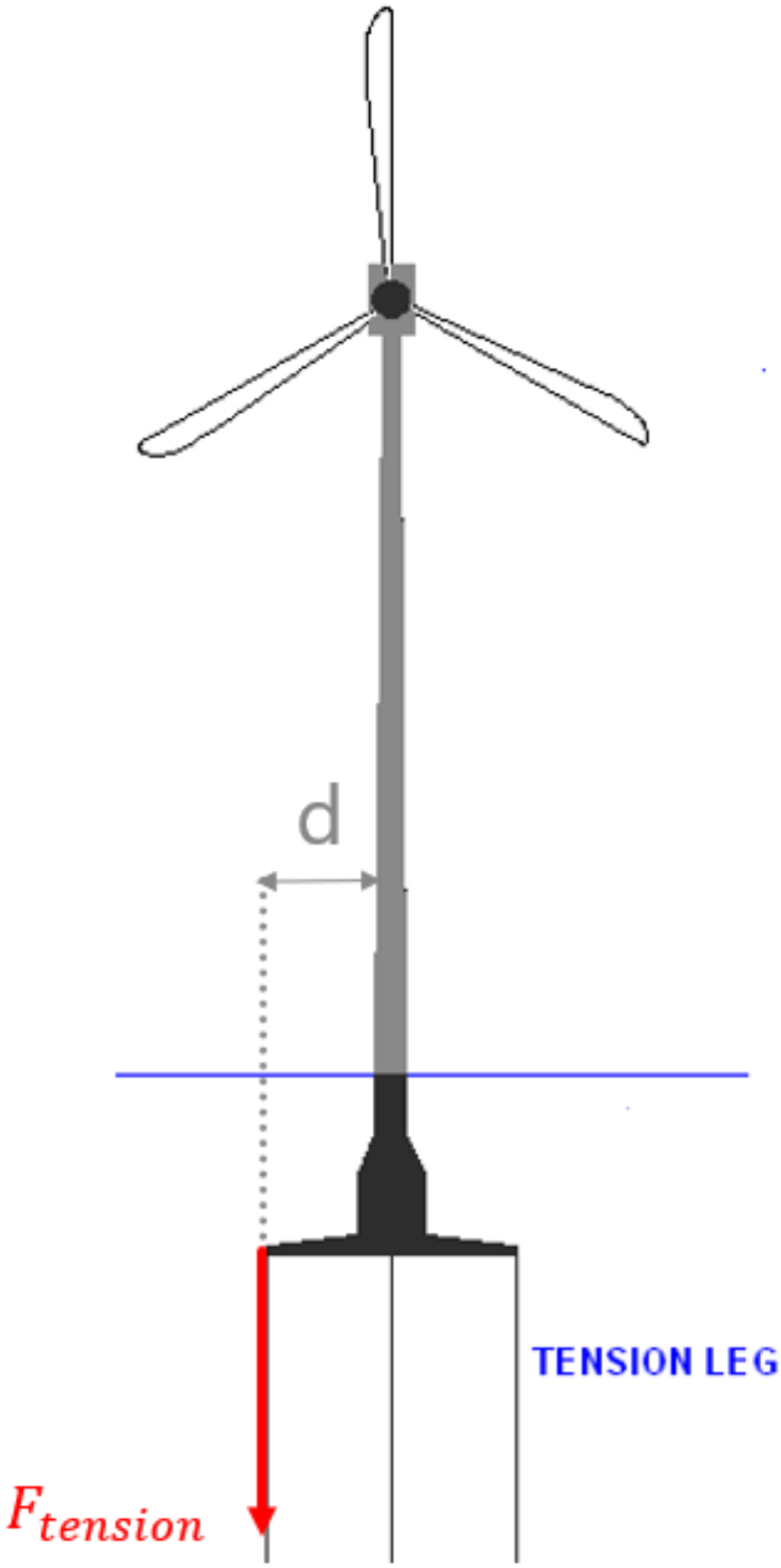

Figure 2.34: TLP stabilisation method explanation

Thus, the platform by itself may not be intrinsically stable when not attached to the

seabed via its moorings and anchors. This particularity can lead to important installation issues and risks that was identified in 2015 at the dawn of the field as a major brake to technology development by Carbon Trust [58].
To resolve this issue, so called "free-floating" tension leg platforms are now developed. As explained in [15] where the design of such a kind of TLP is discussed, these structures can float and remain stable on the sea even when not anchored to seabed, allowing them to be towed from port to site as barge or SS platforms can. This kind of structures usually use water-plane area stabilisation method to ensure free-floating. They can thus be regarded as "small" SS (or barge in a lower extent) that are only designed to support low external loads disturbing them during the installation process before becoming TLP once tendons installed.
As explained in [15], this approach for designing TLPs is gaining momentum and some advanced TLP manufacturers as Gicon or SBM [63] chose it in order to answer the installation issue which used to frighten investors and risk managers. (NOTE: an interview with Gicon representative have been led during the A2A internship that corroborate this direction). In the physical model that will be presented here after, the TLP under scrutiny will thus be a free-floating model which will impact its modelisation and be more representative of what future concepts reaching commercial-scale will look like.

2.3.2.3 Physical model framework, hypothesis and implementation

The physics behind buoyancy and stability of floating platforms under external loads has been describe. Now, let's see how these physical consideration can help us estimate platforms dimensions and costs and furthermore predict their evolution with time and bigger turbines on the market. To do so, every physical laws and hypothesis listed here after have been computed in an Excel program.

First of all, the two general structures under scrutiny will be steel-based semi-submersibles and tension leg platforms. This choice is mainly motivated by insights taken from subsection 2.3.1 both at technological and market trend level. Indeed, Semi-submersibles represent the larger share of existing and more advanced concepts and seem to offer interesting guarantees to investors. Barge concepts, moreover in a static approach, are similar to Semi-submersible and a particular focus on this technological less present on the market was not worth of interest. Next, classical spar concepts complex installation and high drafts reducing their possible depth range make them loose the advance they had in the early 2010's. The choice of Equinor [62] to focus on Semi-submersible structure with the

development of the "wind semi" for their future projects is the symbol of the current SS advantage on spar solution. Unlike spar solutions, TLPs seem to have a promising future, being complementary to the SS in terms of depth range (cf section 2.4) and offering potential material savings.
Then, steel based concepts are considered, following the market general trend exposed in subsection 2.3.1. The lower structural mass, higher modularity and better industrialisation possibilities are the main steel advantages on concrete.
The idea here is to study general typologies to extract cost and dimension trends, not to focus on particular existing concepts. That is why possible active damping system for SS or innovative mooring system for TLP will only be discuss later and not inserted in the model. Of course, the choice of steel SS and TLP is made to follow what would be the main trends of the sector, not to say that other solutions are not viable. Actually, as it as already be said, one solution does not fit all and each project developer will have to lead pre-analysis to identify the best solution for each project.

As it will be seen in the model outputs, more than supporting turbine weight, floaters sizing will mainly depend on external loads compensation. Besides, every single sites will have particular wave and wind conditions that will have to be assessed (wind roses, 50 year return wave height and wind gust, storm historical etc.., good example of such kind of analysis are available in reports disclosed by [54]), but this can not be done in the general analysis led here. Yet, to take this reality in consideration, two types types of external conditions have been assumed: one tough one called "oceanic condition" representative of the main zones of development of the FOW sector, and will mainly defined by North Sea conditions. Another one, softer, is set to represents "Mediterranean condition" where external loads are expected to be a little less important.
As previously explained in order to remain conservative and for sake of simplicity external are supposed unidirectional, in phase, and maximum forces (worse conditions) are considered. Regarding the loads modelisation previsouly described only two parameter are required to model the intensity of these disturbances: a reference wind speed $u[m/s]$ and a reference wave height $H[m]$. Every other parameters will be considered constant and only these two will differ from the oceanic model to the Mediterranean one. Let's assess them for each conditions.
Let's start with wind. The idea here is to model the structure behaviour in harsh condition but still in operation. Thus, the cut out wind speed should not be overcame. Looking on [24] wind speed values evolution for Mediterranean on one hand and ocean or north sea on the other hand. To be representative on these conditions, the reference value for wind speed in the model, that will be thus inserted in the thrust equation 2.1 and the

tower drag one 2.2 will be:

- $u_{ocean} = 25m/s$ for the so called "Oceanic loads"
- $u_{med} = 20m/s$ for the so called "Mediterranean loads"

Then wave linear model parameters parameters has to be assessed. As said previously, and explained in [70] the wave time period value can be accurately estimated to T = 10 s both for oceanic and Mediterranean model.
The wavelength λ is defined by equation 2.4 and remain more or less constant for deep water configuration we hypothesise to be in.
Thus, the main influence on loads will derive from the wave height H. [14] provides an wide analysis of historical maximum wave-height in the Atlantic in the world from which is extracted the insightful map of figure 2.35. This parameter is thus far from being uniform at world level but clear differences can still be pointed out between ocean/north sea and the Mediterranean which appear much more flat.

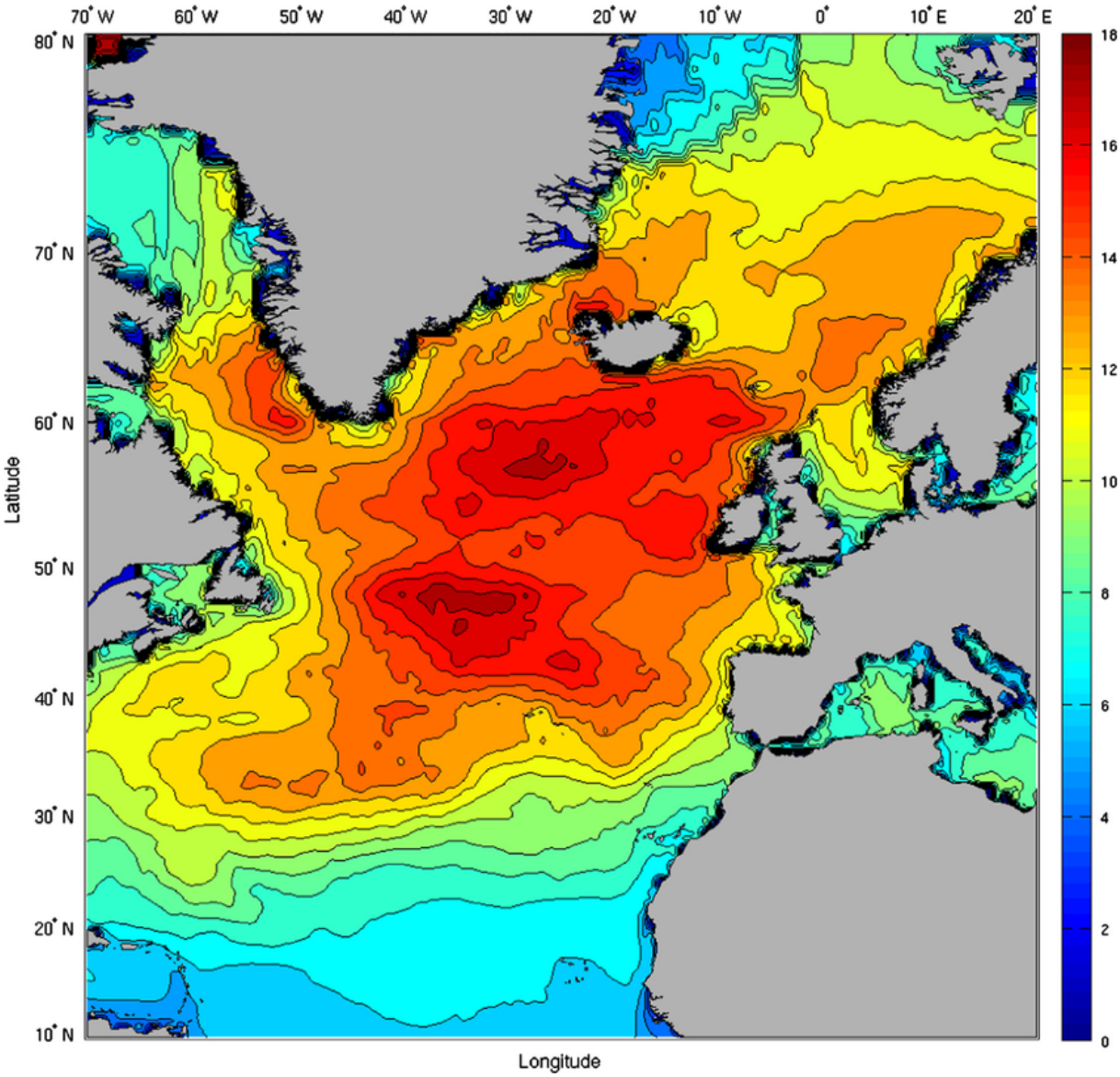

Figure 2.35: Map showing the 100-yr return levels for the North Atlantic Ocean and North Sea from [14]

A particular zoom on the Mediterranean sea is offered by figure 2.36, showing that this wave height parameter is also volatile with time and seasons.

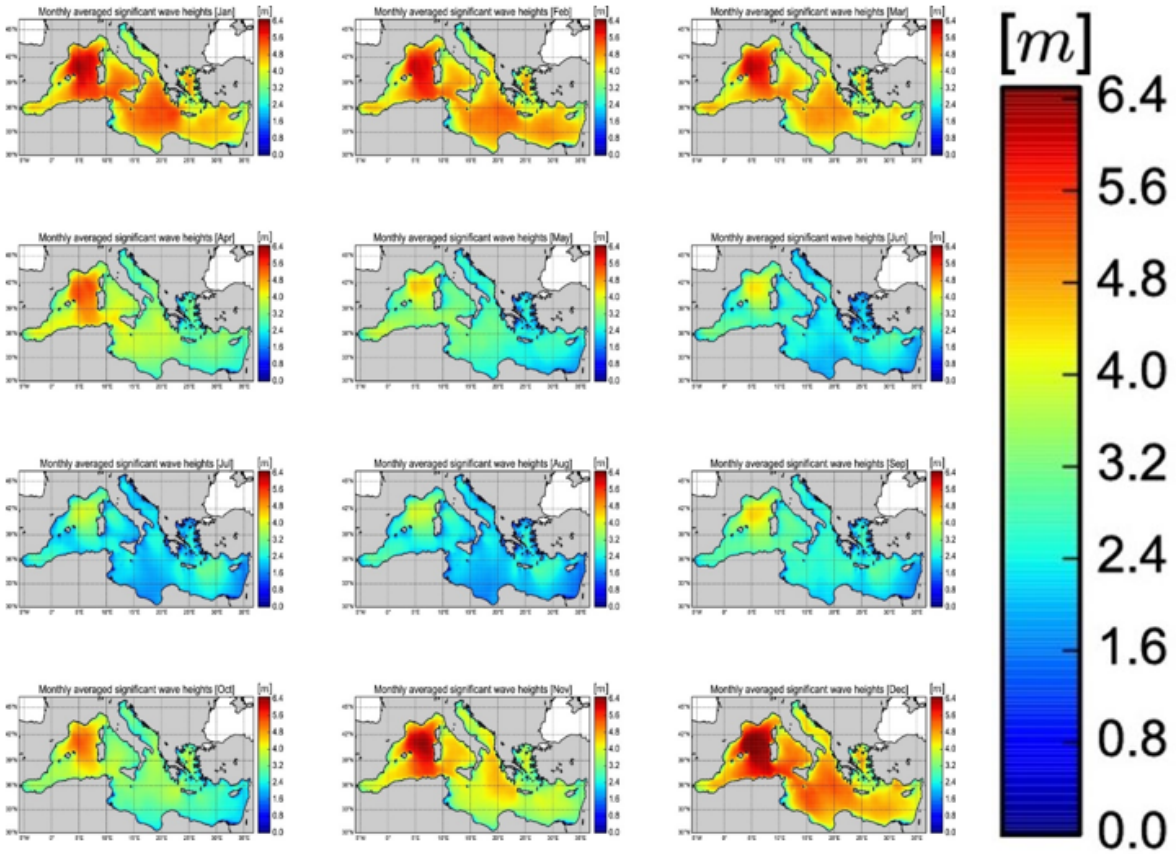

Figure 2.36: Seasonal wave height in Mediterranean

In the end, always in the scope of remaining conservative and displaying harsh conditions, the representative values of wave height in the model will be:

- $H_{ocean} = 10m$ for the so called "Oceanic loads"
- $H_{med} = 6m$ for the so called "Mediterranean loads"

Mediterranean loads end up being softer that so called "oceanic" ones. Eventough it has a concrete background as explained here above, each site will have their particular features and could not be exactly describe by one of these two models. Yet, this distinction can be seen as a sensitivity analysis to give an hint to the reader of how external conditions can affect sizing of the substructures and in the end the final cost of a project. (Note: this distinction between Mediterranean and oceanic condition have been partly motivated by a discussion with platform manufacturers Stiesdal [21] who raised with A2A this idea of special smaller design for Mediterranean projects).

The restoring equation 2.10 is a moment equilibrium. The lever arm of each external forces has to be defined.

- Point of application of thrust force is assumed to be at rotor COG (center of gravity), located at the nacelle. The force is assumed to be along x axis (perfectly horizontal), the lever arm is thus the distance between the nacelle and the point O at sea level, i.e. the tower height. It will be call $Z_{nacelle}$.
- Point of application of tower drag force is assumed to be at tower COG. This point is located below the middle of the tower since the tower is assumed to have a conical shape (base diameter higher than top diameter) describe by its tangent value in table 2.2. The lever arm is the distance between the tower COG and point O where the restoring equation is written. It will be call $Z_{COG-tower}$ and will be defined for each turbine thanks to diameter of the base and the conic angle value assumed in table 2.2.
- For Morison's forces, it will be assume that wave action is concentrated on the column that ensure the buoyancy both for SS and TLP concepts under study since as explained previously in subsection 2.3.1, and as seen in figures 2.40, 2.39, 2.42 and 2.41 these columns represents the main surface of exchange between the sea and the floaters, generating the higher Morison's forces. Plus, since located at the extremities of the platforms, the moment generated are even more important die to higher lever arms.
  For TLP and SS, since draft are relatively low and water plane quite big (in comparison with Spar concepts for example), the bigger moments generated in O will be by far the one generated by the vertical components of the Morison's forces. Horizontal components contribution will be neglected. Thus, the lever arm is the distance between the center of the columns (where the force is applied) and the point O. This distance will be call d_c and is highlighted for SS and TLP in figure 2.40, 2.39 and 2.42.

One objective of the model is to predict the evolution of floater dimension and cost when bigger turbines will enter the market as anticipated in section 2.2. Weight, size of shape of considered turbines have already been discussed in this section via tables 2.1 and 2.2. Yet, additional dimensional parameters were required for the computation of the model such as mean diameter for computation of equation 2.2 or tower COG height for the lever arm of this force. Plus, the computation of the global COG of the whole structure required these parameters in addition to the specific weight of each part of the turbine previously hypothesised as 50 ton/MW for the nacelle; 7.5 ton/MW for the rotor and 42.5 ton/MW

for the tower.

These dimension are characteristic of generic turbines and can slightly change from one turbine to another. For the majority of the turbines considered, they have not been released yet and thus this dimension have been predicted based on existing turbines. To be more precise, basic dimension are the one the 5 MW NREL turbine described in their fourth phase of their large FOW development project [79].

Next, the dimensions of bigger turbines to come have been predicted based on physical laws to evaluate dimensions evolution with turbine power. First, from equation 1.1 we have $D_{rot} \alpha P^{0.5}$ (Note: the symbol α represents the proportionality). Then, since the turbine height H_{tower} is proportional to the rotor diameter, we have $H_{tower} \alpha P^{0.5}$. Then, we know that the specific weight, and thus volume, remains constant. Thus the volume V is proportional to the power. $V \alpha H_{tower}.e.D_{tower}$, and we will assume that e the thickness remains constant with size. We thus have $H_{tower}.D_{tower} \alpha P$. Combining everything, we get $D_{tower} \alpha P^{0.5}$.

Based on 5 MW turbine dimensions and the previous proportionality laws, every dimensions can be assessed, and the results are displayed via a table on figure 2.37.

	Power (MW)	Turbine Weight (ton)	Nacelle Height (m)	Rotor Diam (m)	Mean Tower Diam (m)	COG Height (m)
2020	5	500	94	126	4,6	72,5
2025	10	1000	138	184	6,6	106
2030	15	1500	172,5	230	8	132
2035	20	2000	187,5	250	9	144
2040	35	3500	248	330	12	190

Figure 2.37: Turbines dimensions of interest for physical model computation

Let's gather every hypothesis formulated in the model:

- Hydro-static conditions: no dynamic behaviours analysed.
- Linear wave model adopted, and deep-wave configuration valid.
- Harsh situation condition (external loads) and every load in the same direction.
- The many physical coefficient extract from the literature (drag coefficient, wave frequency, earth acceleration, air and water density, steel density etc...) are regarded as constant and does not change with conditions or turbine size.
- Buoyancy of the structures and interaction with waves are only considered at the columns level.
- Floaters structures are assumed to be 100% made of steel.
- For sake of simplicity, the the thickness of the structures (both turbine tower and floater) will not evolve with turbine size.
- the bigger turbine on the market is assumed to be automatically used as soon as available. Based on forecast displayed in section 2.2, ambitious hypothesis are made and 15 MW turbine are used for 2030 projects, 20 MW turbines for 2035 and huge 35 MW ones for projects released in 2040. This last hypothesis seem strong but it allow to have a wide range of turbine size to assess potential economies of scale.
- To remain general, the only stabilisation method used by SS will be the waterplane area one, eventough some concepts also have a ballast and mooring contribution in the stabilisation process.
- For sake of simplicity and since it did not affect the final results, the integration over tower height in tower drag force equation 2.2 is replaced my mean values of diameter computed respecting the characteristics of table 2.2.
- The influence of wind shear development leading to higher wind velocities at higher heights is not taken in consideration in the sizing of the turbine: the u value remain the same for every turbines. Nonetheless, it will be taken in consideration later in the production assessment of a wind farm.

Here are listed in table 2.3 values of every other physical coefficient assumed non dependant on external conditions and turbine size used in the model.

Coefficient	Value	Dimension	Note
θ_{target}	5	°	Maximum pitch angle admissible [76]
ρ_{air}	1.225	kg/m^3	Classical value
ρ_{water}	1000	kg/m^3	Classical value
$C_{drag-rotor}$	0.03	-	*
$C_{drag-tower}$	1	-	Classical and conservative value [69]
f_{wave}	0.1	Hz	inverse of time period previously described
Depth	200	m	Classic FOW project, > 75 m (deep wave configuration)
$C_{Morison-inertia}$	2	-	Classical value ([72], [12])
$C_{Morison-drag}$	1.3	-	Classical value ([72], [12])
g_{earth}	9.81	m/s^2	Classical value
$Thickness_{structure}$	0.06	m	Dimensions from NREL 5MW turbine [79]

Table 2.3: Value of physical coefficient adopted

* The value here, 0.03, is lower than the one for optimum performance operation, i.e. the zone of a wind tribune power curve (cf figure 1.5) where the Power output is lower or equal to the rated power output. On figure 2.38, the optimal position of the blade in the air flow is represented in yellow. Indeed, as explained in subsection 1.2.1, the blade pitch is regulated for wind speeds higher than rated ones in order to reduced lift of the blade and reducing the torque produced to maintain power constant while wind speed keeps going up. In this zone of the power curve where we will be located in our model since harsh wind conditions are assumed, two pitch regulations strategies exist as described in [80] and displayed on figure 2.38:

- **Pitch-to-stall regulation:** The pitch angle is increased beyond its optimal value until the drag coefficient skyrockets (cf [67]) and the blade evolves in a clear obstacle to the stream flow. The advantage of this control mechanism is its intrinsic stable equilibrium regarding gusts and wind fluctuations. This characteristic has made this strategy widely used onshore.

- **Pitch-to-feather regulation:** The pitch angle is decreased to low values and the blade is almost parallel to the flow, decreasing drastically both the lift and drag coefficient (cf [67]). Eventough this method shows a lesser gust adaptability, it decreases the structural loads due to thrust force on rotor described 2.1. For FOW where the stability of the structure is tremendous, and since offshore winds are less intermittent than onshore ones, this Pitch-to-feather regulation is assumed to be

use in our model.

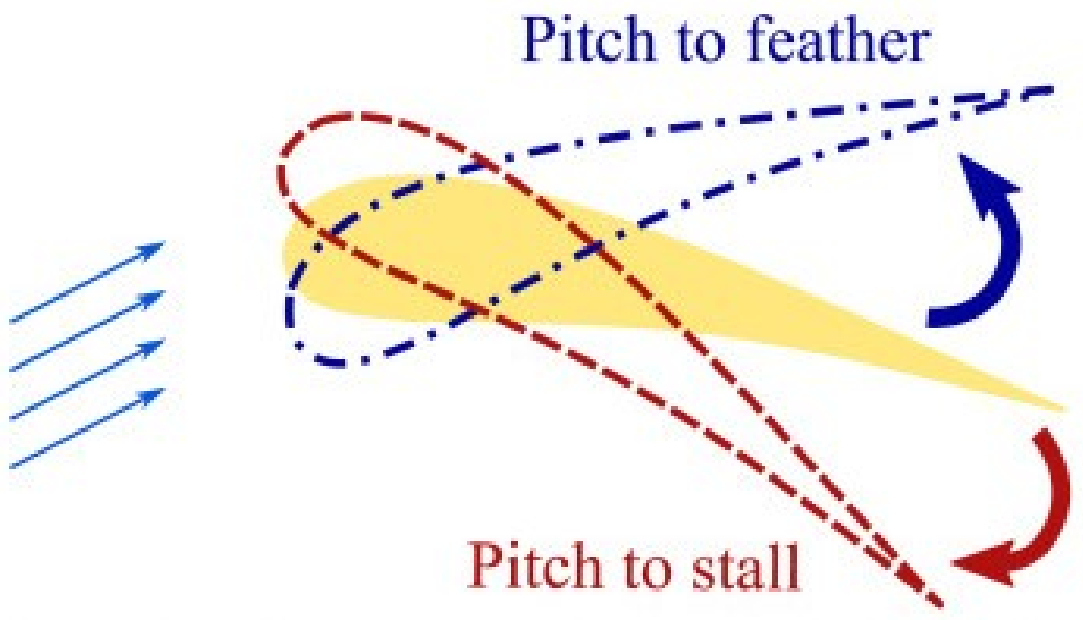

Figure 2.38: Pitch to feather VS Pitch to stall regulation for wind speed higher than rated one

Let's now assess how the model is actually computed on on which parameter the simple optimisation process works, starting with the Semi-submersible case. The exact same operation are distinctly led for Mediterranean and oceanic conditions.
The target of the manual optimisation process is the pitch angle θ that must remain equal at its maximum value since the worst external situation are assumed. For every turbine size, the external loads moments is calculated at point O. The dimensions of the floaters are thus calculated manually in order to ensure that the two equations of our hydrostatic model 2.9 and 2.11 remains valid. As showed in table 2.3, the value of *theta* will be 5°, its maximum admissible value in operation according to standards sets by DNV and transcribed in [76]. The prior computation to deal with these equations thus concerns the second moment of area of our SS platform regarding the y axis.
The Semi-submersible considered, for sake of representativeness, is a basic 3 column V-shaped platform with the turbine at the center for which the whole interaction with water will be concentrated at column level. This semi submersible is described in the two following pictures 2.39 for an upfront perspective and 2.40 for a lateral picture extracted from [16]. Regarding this V-shape profile, it will be assume that, regarding the direction of the external loads, only one column will be submitted to the maximum Morison forces. The scheme from upfront is particularly useful for second moment area along y axis

calculation.
Using results for circular shapes from figure 2.32 coupled to the parallel theorem described in equation 2.13, the second moment of area along y axis for our SS platform is:

$$I_y = \frac{3\pi R^2}{2}.(\frac{R^2}{4} + d_c^2) \tag{2.16}$$

The two main dimensional parameter impacting the restoring capacity of the turbine are thus d_c and R and are highlighted on figures 2.39 and 2.40.

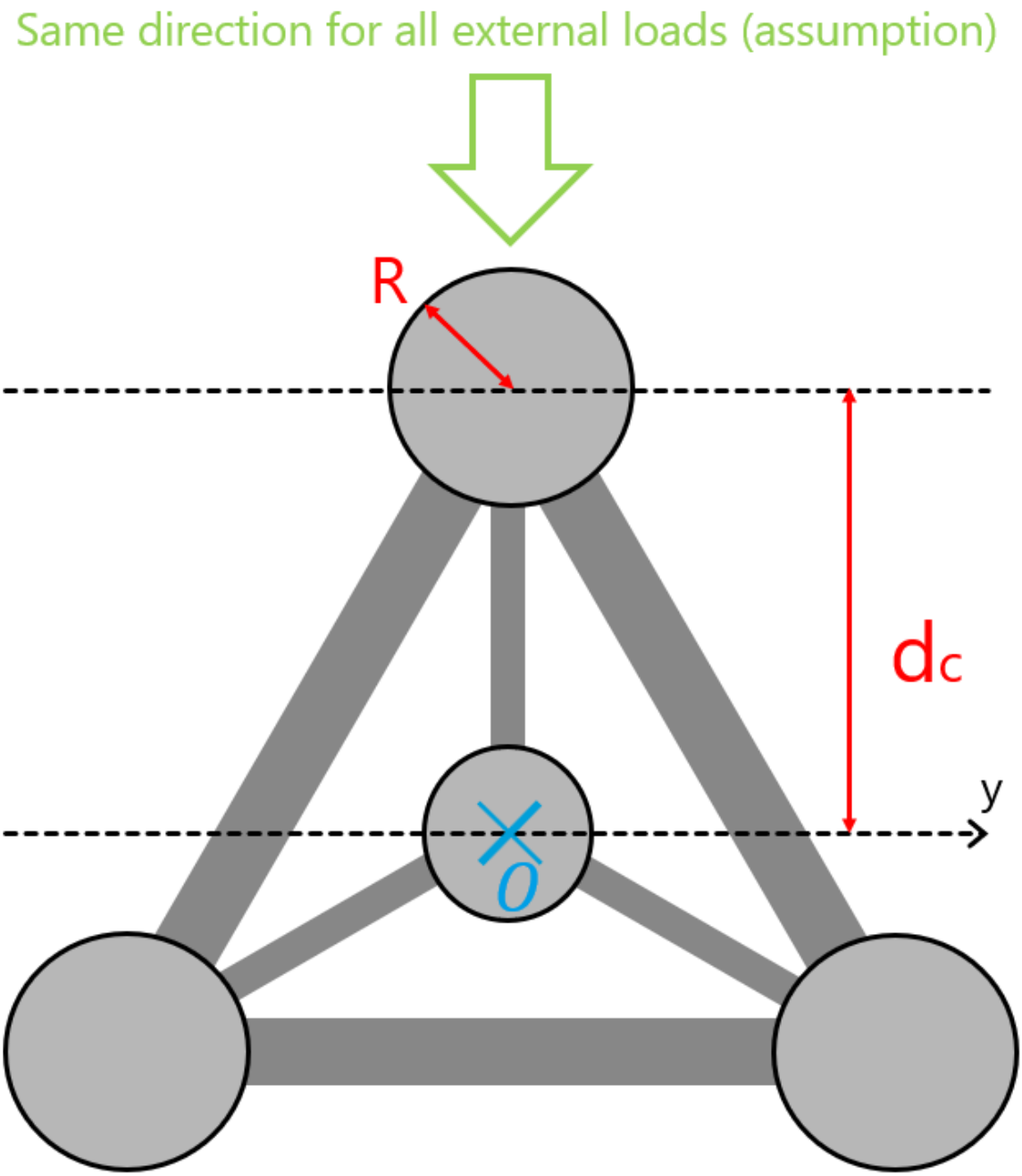

Figure 2.39: Classical V-shape 3 column Semi-submersible upfront view

In [16] a similar analysis (but for fixed turbine) has been led on a semi-submersible and 5 design parameters where pointed out, among which the two already cited. The three others, displayed on figure 2.40, are the draft d, the the height over water f_b and h_b the height of water in the ballast (passive ballast system assumed). In [16], it has been chosen to not modify d and f_b and to work only with d_c and R as optimisation parameters. The same choice will be make in our study, motivated by the fact that, as seen in equation

2.12 only these two parameters impact the static restoring moment. Plus, with turbine size increase, to preserve the whole behaviour of the structure (also on a dynamic side that is not studied here but remain relevant), the scale up of every dimension must be executed accordingly, as explained in [81]. Thus, if draft value enters in consideration, bigger turbines would lead to higher drafts, which could lead to towing and port-side operation issues as explained in [58]. The value for d and f_b will thus remain constant equal to the baseline model of this work: the NREL SS prototype for a 5MW turbine. Thus, once moored and ballasted (in operation), we will get: $f_b = 12$ m and d = 20 m.
Given that draft value, the water height in the ballast h_b will be adjusted in order to satisfy the buoyancy equilibrium equation 2.9.
Then come the core of the work: the determination for each turbine size of the sufficient values of R and d_c to meet the objective on pitch angle. Starting from initial values based on the NREL SS prototype for a 5MW turbine, these dimensional parameters are adapted for each turbine to guarantee stability. Plus, two additional condition are added to take in consideration practical concepts. First the height of water in the column h_b must remain lower than the draft value d. Then the un-ballasted draft, i.e. the draft during towing and port operation, must remain lower than 5 meters to not threaten the assembling operation onshore.
Yet, even adding these two conditions, we only have one equation driving the process while working with two parameters: some freedom in choice still remain. In order to choose values, the driving idea is to remain coherent with initial design and try to maintain its global shape while scaling up, inspired in this way by the work performed in [81].

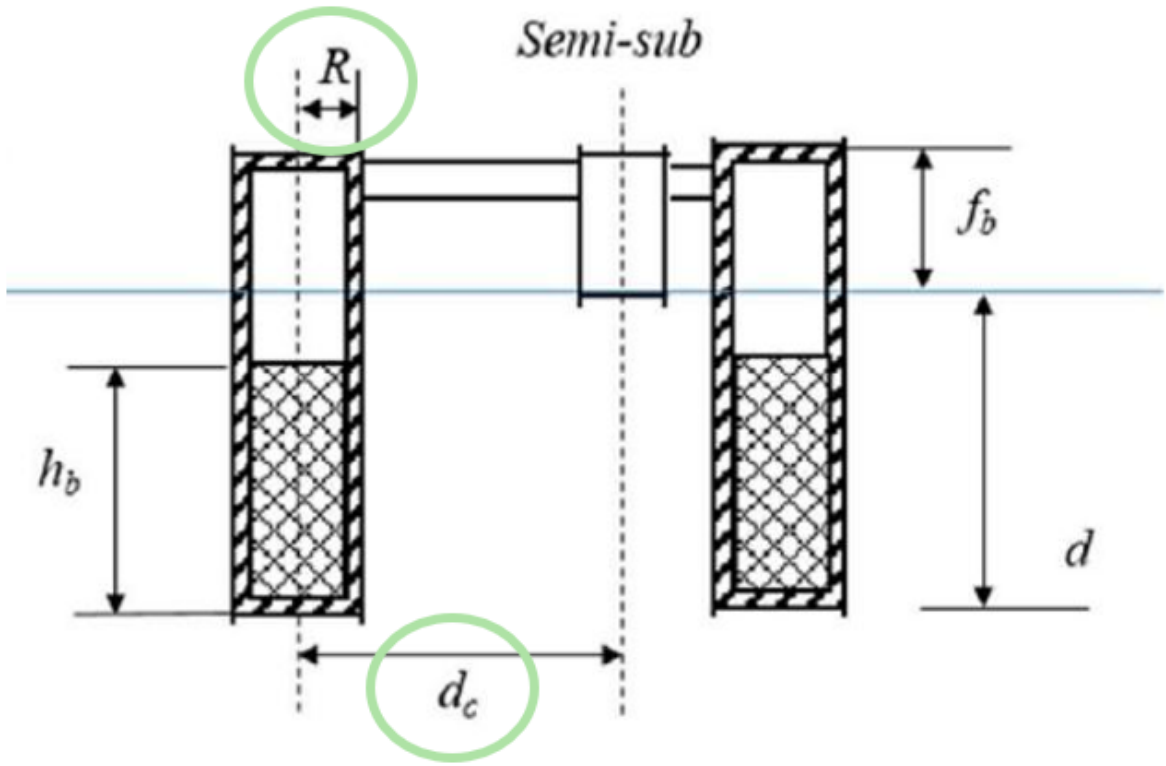

Figure 2.40: Classical V-shape 3 column Semi-submersible lateral view

Similar process is then led for the free-floating TLP. As previously explain, the restoring process of a TLP relies on moorings and over-buoyancy. An important part of this sizing will thus be led in the subsection dedicated to moorings 2.4. In this platform part, the dimensional sizing will be led to ensure free-floating behaviour, making the process equal to the one previously described since in this non moored condition, the TLP is nothing but a "small" SS.

The base of the process is the 10 MW free-floating design from [15] displayed in 3D in figure 2.41 and from an upfront 2D side in 2.42. The dimension of the structure are displayed on the figures on the 2.42 the 2 main design parameters R and d_c are highlighted. For these platforms, four columns are used. In the same idea as previously, it will be assumed that only two columns are submitted to the Morison's forces.

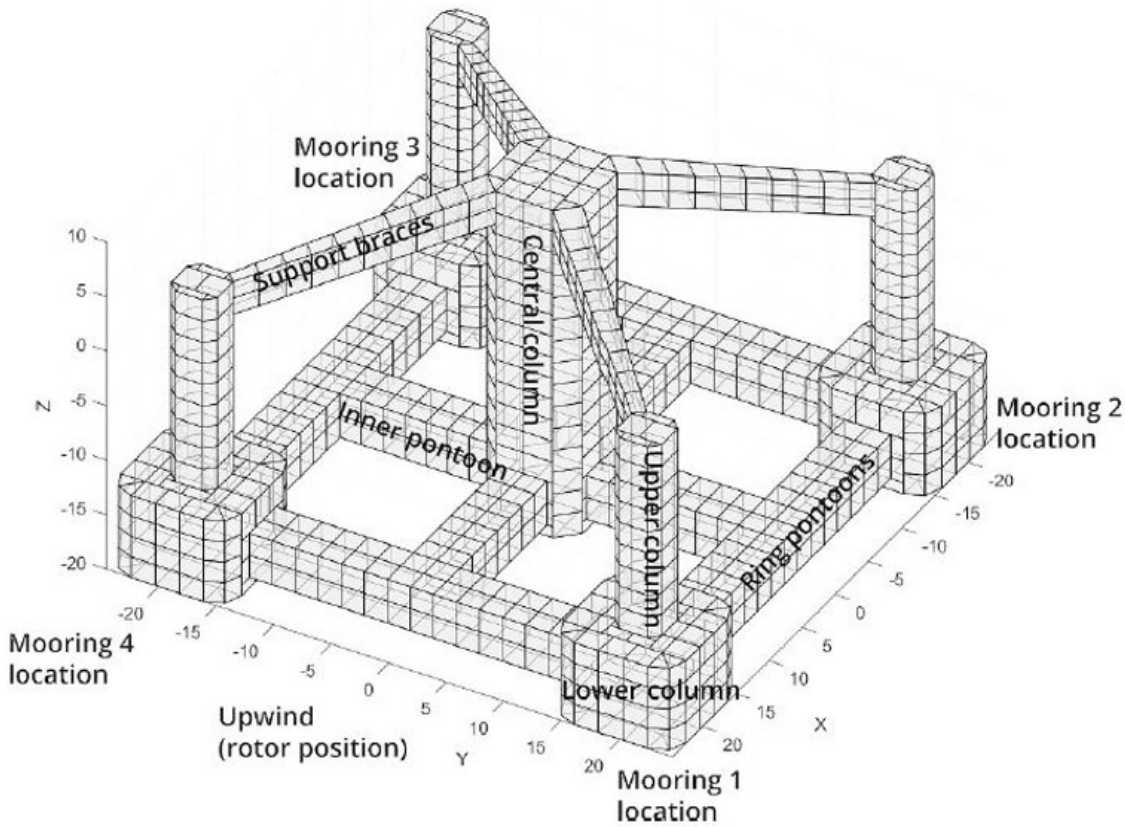

Figure 2.41: Free-floating 10 MW size TLP 3D view with dimensions in operation from [15]

As previously, the height of the structure and its draft in operation is assumed to remain constant with turbine size. The total Height of the structure is thus fixed at H = 30 m (cf 3D scheme on figure 2.41). In operation, the draft of the structure will be fixed at 20 m from tendons. In free-floating operations, the towing operations criteria will be as previously a draft inferior to 5 meters. As previously the whole structure is model with volume and weight (steel density and structure thickness are the same as for SS) but the external loads correspond to towing situation, thus softer than the harsh one in operation. Using results for circular shapes from figure 2.32 coupled to the parallel theorem described in equation 2.13, the second moment of area along y axis for our tension leg platform is:

$$I_y = \pi R^2.(R^2 + 4d_c^2) \tag{2.17}$$

In order to determine the external condition to work with the opposite reasoning has been led: starting from restoring capacity of the oceanic 10 MW model described in [15], the maximum external condition admissible to maintain the 5° degree criteria for θ was:

- H_{ocean} = 6.66 m for free-floating towing operation.
- u_{ocean} = 15 m/s for free-floating towing operation. (wind + towing velocity)

The same condition was kept for performing the same work as previously for SS for turbines size until 35 MW.
Then, for Mediterranean condition, the same consideration has been made for softer condition :

- H_{med} = 4 m for free-floating towing operation.
- u_{med} = 11 m/s for free-floating towing operation. (wind + towing velocity)

These considerations allow us to predict the evolution of the turbine dimensions, knowing than higher value of d_c will increase restoring moments while moored and in operation according to equation 2.10.

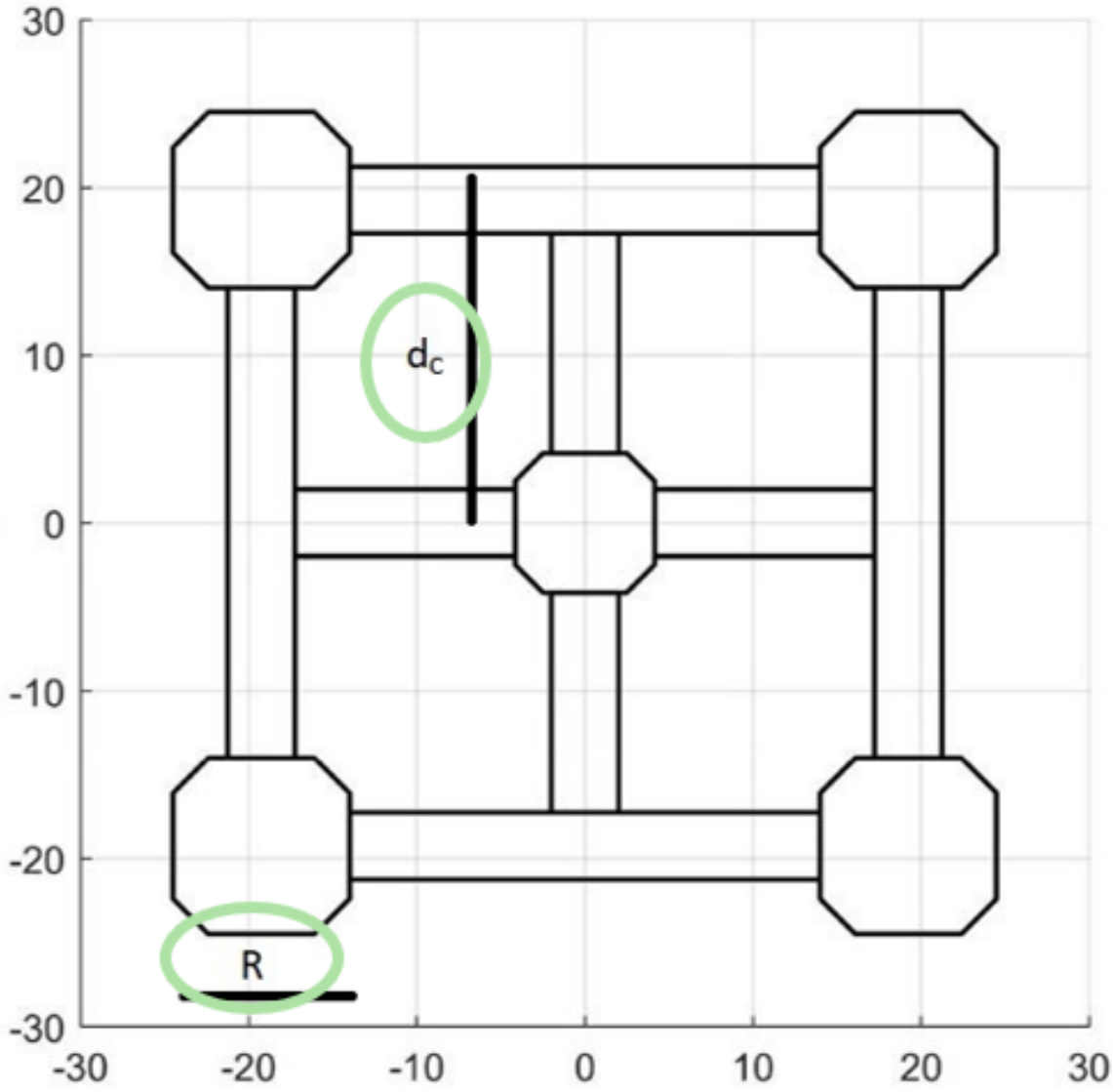

Figure 2.42: Free-floating 10 MW size TLP 2D upfront view from [15]

The computation of the static physical model in excel is summarised through a block diagram in figure 2.43. In Particular, this diagram displayed here after shows the difference between the constants, the input parameters, the outputs and the elements entering in the optimisation process.

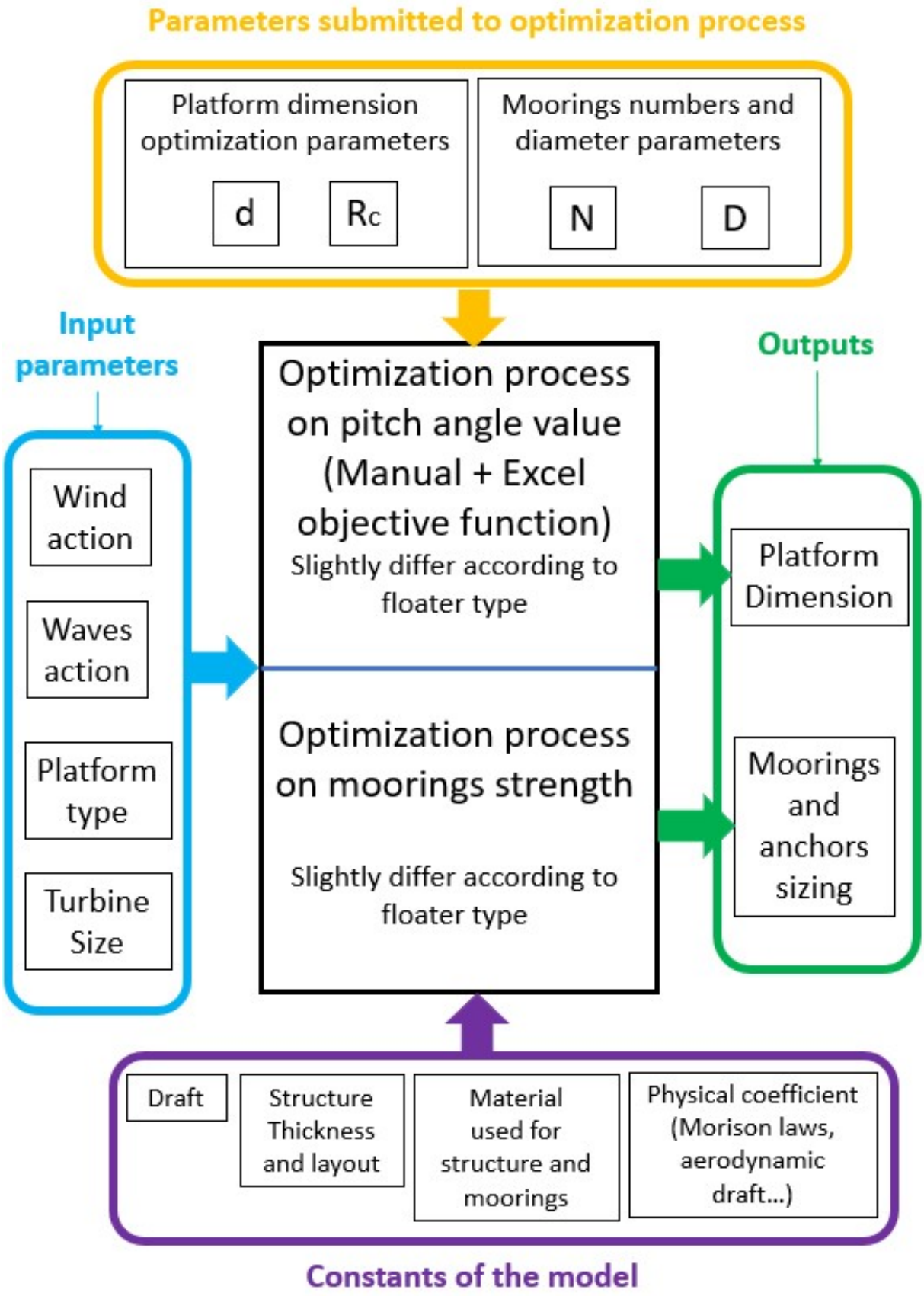

Figure 2.43: Inputs and outputs of the computed static model

The dimension of the structures, and thus the total volume, will be get as an output of the physical model previously described. We assumed that these structures was integrally made out of steel. Thus the integrity of the material related cost is linked to steel price. More generally, since steel also represents a big amount of turbine material demand, the price of steel has a huge impact of a FOW project and project developers will have to lead precise pre-studies and sensitivity analysis to assess the exact price of the projects regarding the steel price volatility.
The evolution of steel price over the last years have been led by BNEF with result displayed on figure 2.44. While specific steel price was low in the early 2020, it then skyrocketed in consequence to pandemic related crisis and a decrease is now witnessed. To remain conservative, the hypothesis made on steel price will be in the hiher range:

$$Steel - price = SC_{steel} = 1200\$/ton \tag{2.18}$$

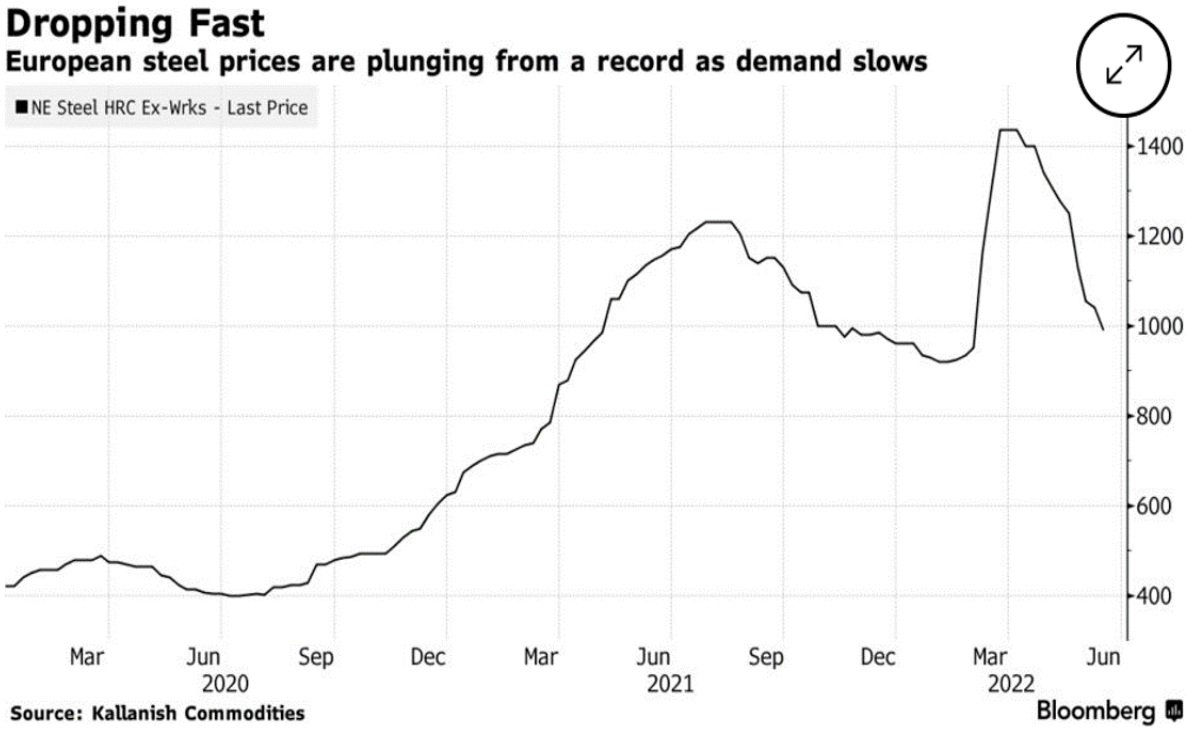

Figure 2.44: Steel price evolution from BNEF

Yet, a structure cost cannot be reduced to its material demand. Manufacturing, supply and assembling cost must be taken in consideration as well. A precise version of such a kind of cost evaluation would be very complex and would integrate many notion out of the scope of this work. Indeed, many parameters such as precise design of platform,

suppliers availability, supply chain complexity, workforce required, economic condition of a given country etc... would have to be taken in consideration. In order to remain concise a simpler tool, historically in naval industry, will be introduced: MCF (Manufacturing complexity factors).
These factors introduced in [16] and allow us to get from toget from the material related cost to its final cost according to equation 2.19:

$$Final - Cost = \frac{V}{P}.SC_{steel}.(1 + MCF) \tag{2.19}$$

Where the final cost is the specific cost of the floater reported to power in [$/MW], V is the volume of the whole steel structure and SC_{steel} is the specific cost of steel in [$/MW].

Weight gives an indication on material related cost (steel in this case). But other important cost drivers are yet to be considered to properly evaluate the cost of a floater, such as supply chain, assembling, manufacturing, dry rocks lease etc... Suitability of the design for mass production is also taken in consideration. These cost depends on the structure complexity and can be considered proportional to the material quantity in a first approach (even if further economies of scale could be expected): the more still you need, the more transport fee you will pay, the more dock space you will need, the more welding and assembling operation will last etc...
All this to model that simpler design will lead to cheaper solution: a fixed bottom monopile which is nothing more than a cylindrical steel tower will end up cheaper than a Semi-submersible floater eventough the same quantity of steel.
In [16], the elaboration of different typologies of floating platforms have been assessed thanks to surveys led on meany experts and industrial players. The results are displayed in table reported on figure 2.45.

Average values of manufacturing complexity factors (gathered from experts).

Floating support structures		Fixed monopile	Spar buoy		Barge		Semi-sub trifloater	
	Structural material	Steel	Steel	Concrete	Steel	Concrete	Steel	Concrete
MCFs	Average	1	1.31	1.54	1.66	1.64	1.81	1.99
	Standard deviation	0	0.28	0.34	0.44	0.25	0.43	0.53

Figure 2.45: Manufacturing complexity factor for different platform typologies and material from [16]

From this table, it is adopted that the MCF for a steel SS platform in 2021 is 1,81. Re-

garding the similitude between SS platforms and free-floating TLPs, the same complexity in manufacturing can be assumed. Yet, as previously explained, tension leg platforms generally have a lower TRL than SS concepts which means that it will benefit later from the decrease in manufacturing cost due to market grow.

Indeed, nowadays, design are not optimised for manufacture efficiency and market is too small to enhance sufficient economies of scale on supply chain side. Yet, improvements in design and market increase are expected in the years to come. A decreasing trend is this expected for MCFs. BloombergNef assumed in [17] that material cost will represent half of the final price by 2035, without further evolution after this. Starting from our 2021 value, this correspond to a 4% yearly learning rate. The MCF evolution forecast for a steel SS is represented on graph from figure 2.46.A similar trend is assumed but with a 5 years delay for TLP.

Independently of material saving due to bigger turbines, floater cost is expected to decrease in the years to come.

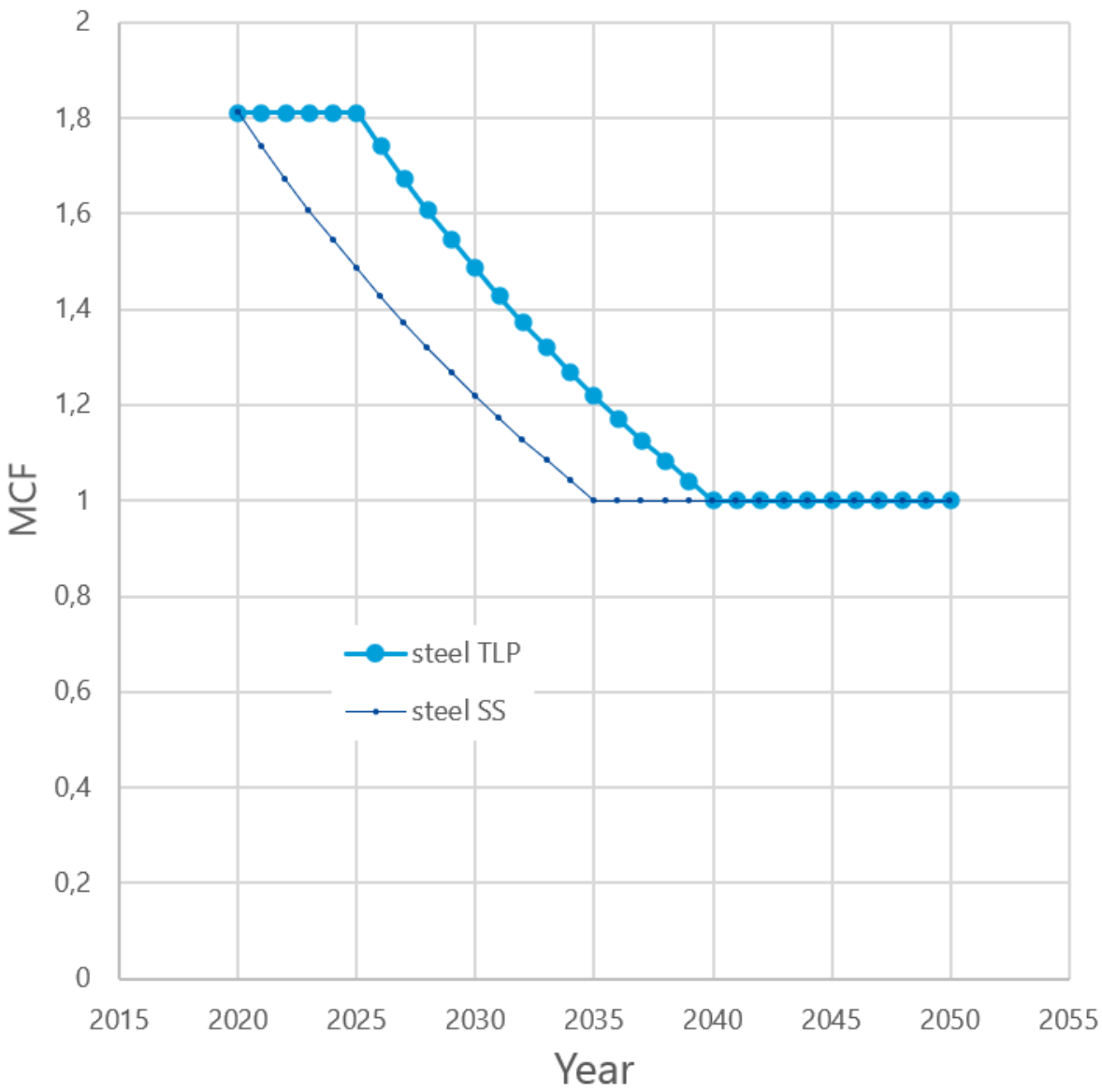

Figure 2.46: Manufacturing complexity factor used in cost model from 2020 to 2050

2.3.3. Model outputs analysis

Once the physics explained, the model computation process described and hypothesis listed, the output of the model can be analysed. The following graph will allow us understand the evolution in terms of dimension, weight, cost and external loads of TLP and SS. Plus, the influence of external condition will be highlighted by the distinction between Mediterranean (softer) and oceanic condition. In the end, specific costs of tension leg platforms and semi-submersible (without moorings and anchors) will be compared.

2.3.3.1 Semi-submersibles

Let's begin with model outputs for Semi-submersible platforms.
Beginning with oceanic conditions, figures 2.47 and 2.48 represent external loads moments from wind and waves respectively in an absolute and specific (per MW) manner. It is observed than wave loads are one order of magnitude more important than wind ones for small turbines and as expected bigger turbines come with bigger absolute external loads. Yet the specific wave moment [MNm/MW] strongly decreases with turbine power while the wind related one slowly increases (cf figure 2.48). Since the wave load is by far dominant in these oceanic condition, the sum of the two specific contributions also follow a decreasing path.
External loads are thus "less than proportional" to turbine size, which announces potential economies of scale already.

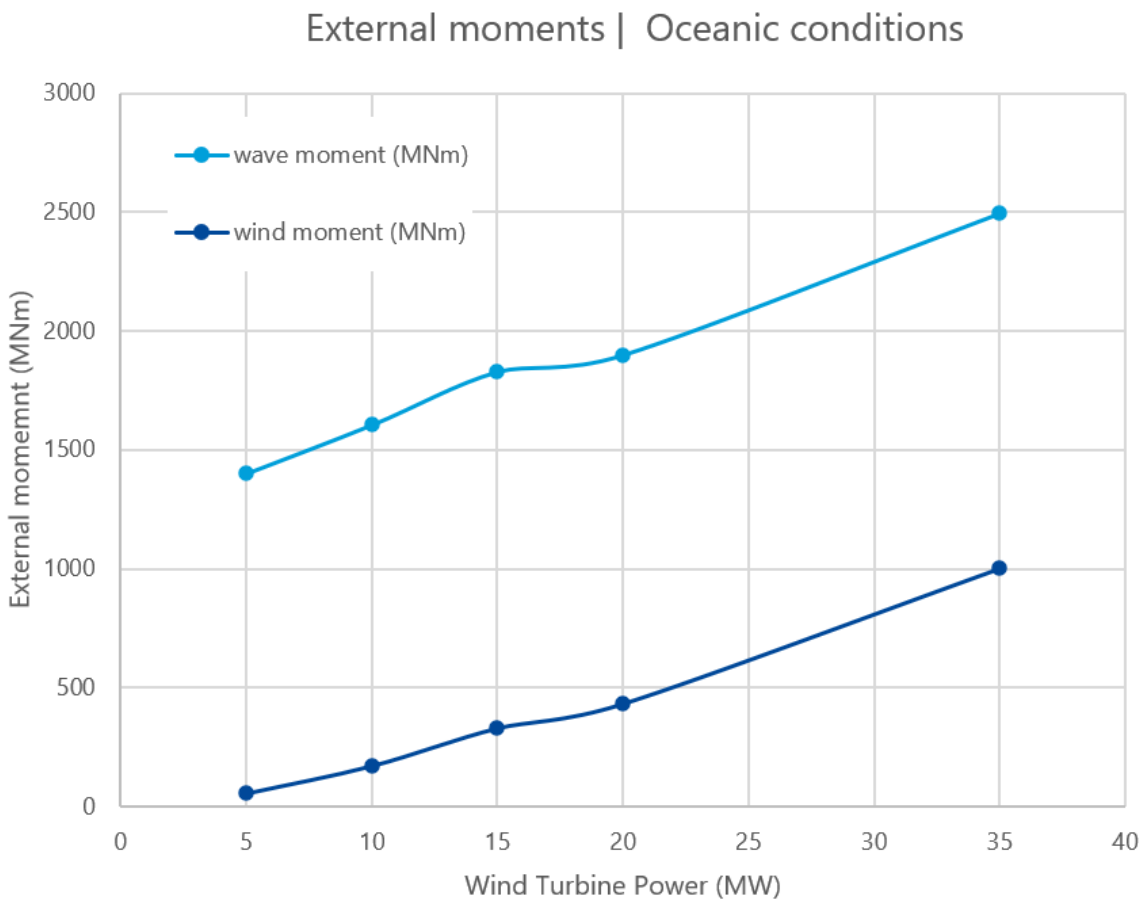

Figure 2.47: External moments Oceanic conditions for SS

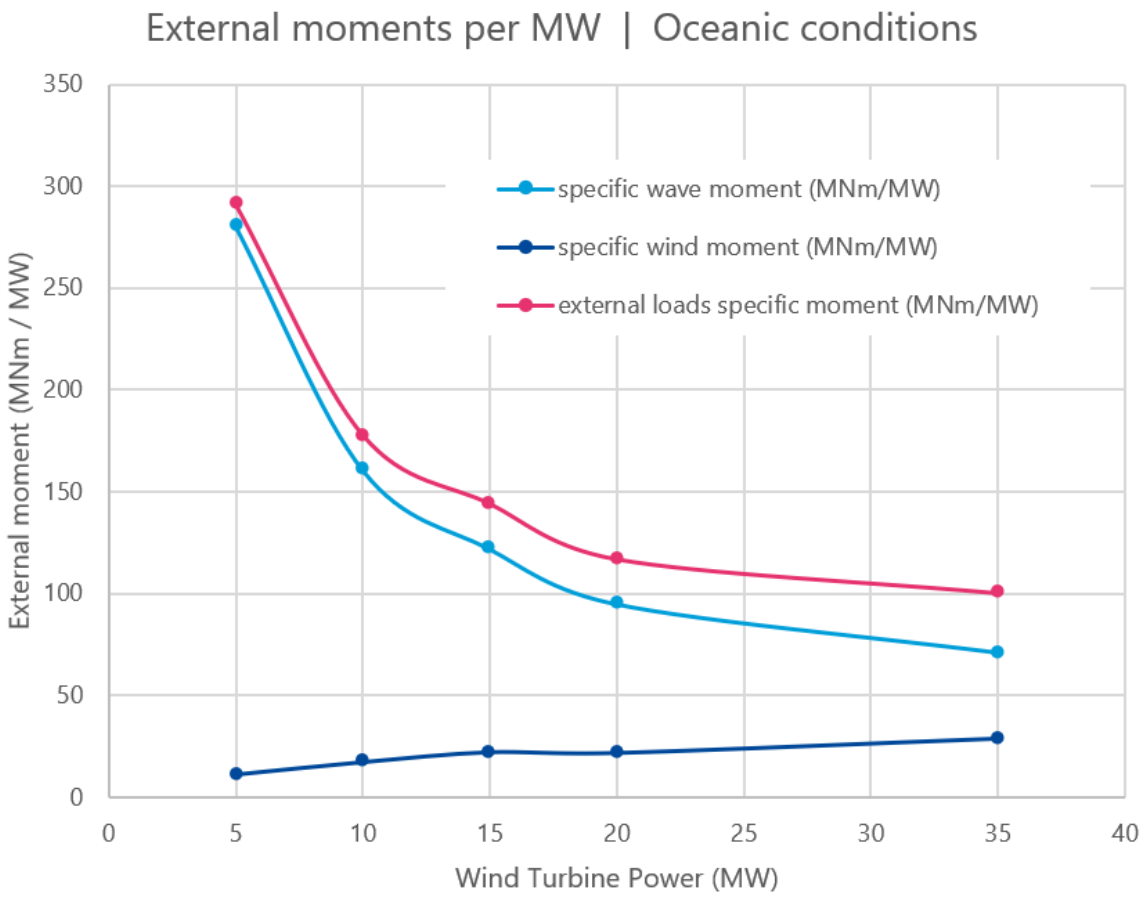

Figure 2.48: Specific External moments per power Oceanic conditions for SS

The same two graphs have been generated for Mediterranean conditions on figures 2.49 and 2.50. Unlike oceanic ones, In Mediterranean conditions wave and wind actions are comparable. The total external load remain almost proportional to the turbine power (in pink on specific external moment graph from 2.50). Specific loads per power actually have opposite trends, such that wind contribution overpass wave one for huge turbines. In Mediterranean condition, specific wave moment still has a decreasing trend with power but this decreasing effect is compensated by the wind behaviour that, unlike for Oceanic conditions, is far from being negligible and even overpass wave contribution for huge turbines (bigger than 20 MW).

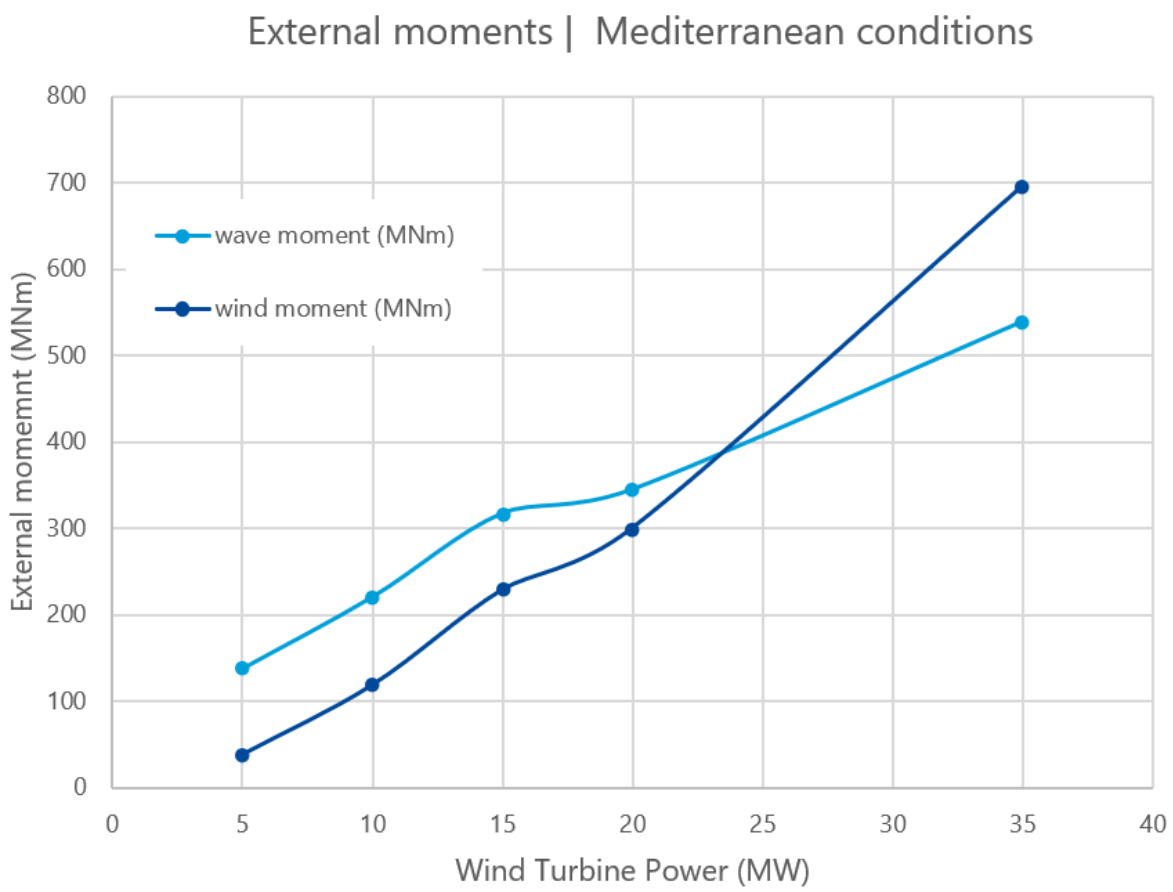

Figure 2.49: External moments Mediterranean conditions for SS

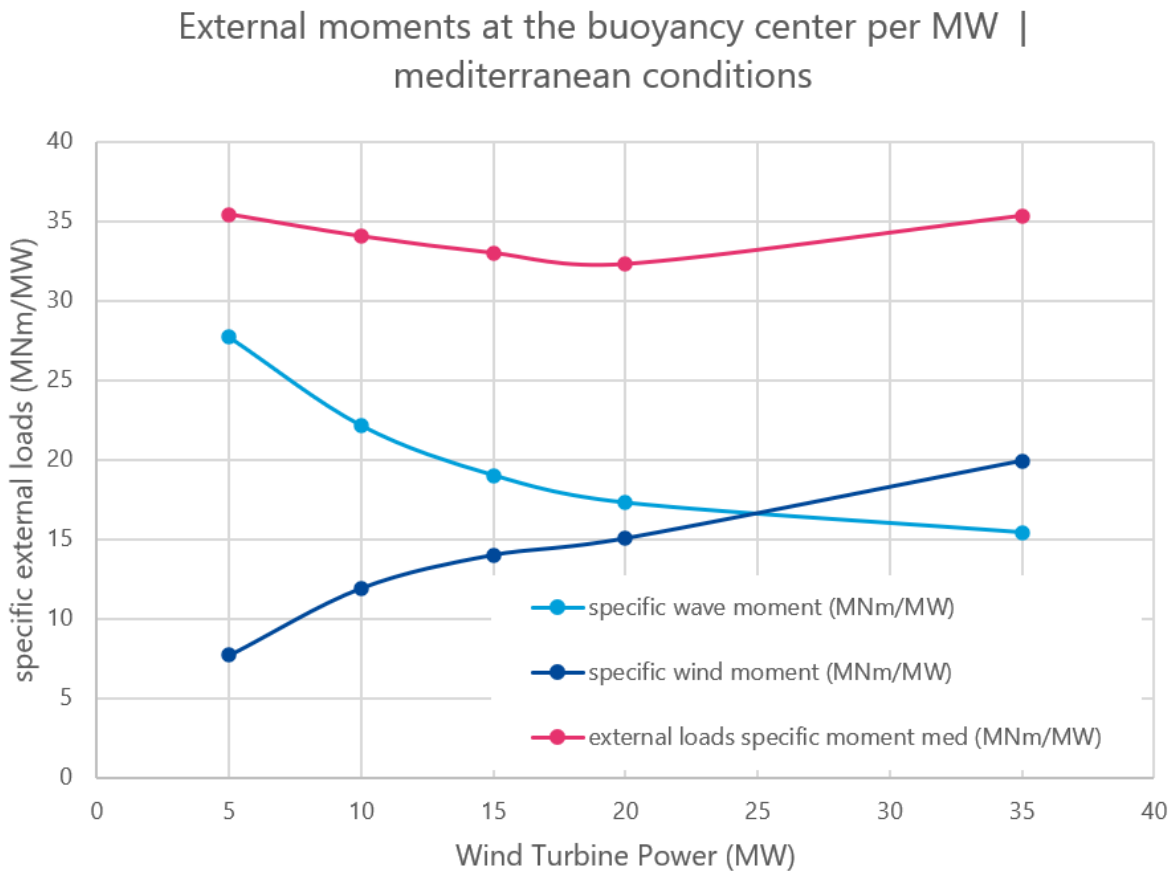

Figure 2.50: Specific External moments per power Mediterranean conditions for SS

Graph on figure 2.51 allows us to easily compare the specific total external loads moments on the floater. It is obtained that loads in Mediterranean conditions are an order of magnitude lower than the one in oceanic condition for small size turbines. Yet, the important decrease with turbine power for oceanic conditions makes the difference between Mediterranean and oceanic conditions way smaller for bigger turbines.
The disadvantage of harsher conditions is thus expected to be ever less important for big turbines.

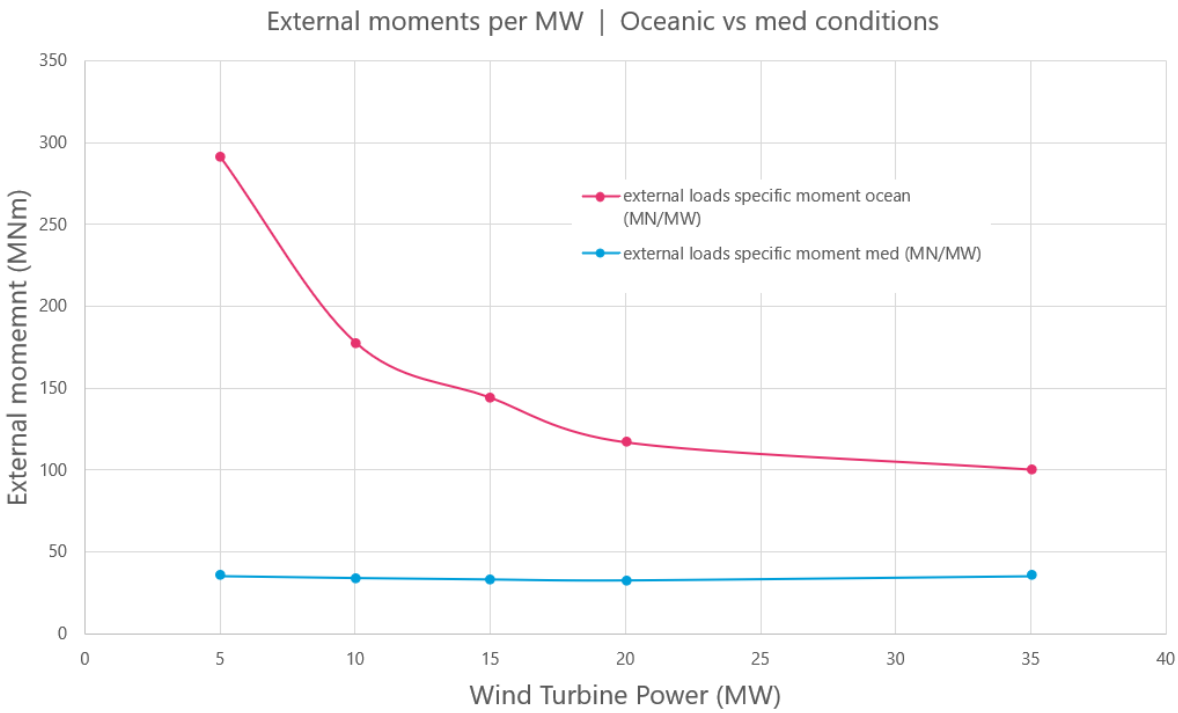

Figure 2.51: Specific External moments per power Mediterranean VS Oceanic conditions for SS

Let's now focus on dimensions of the floater, and more particularly the two dimensional parameters of interest R and d_c.
The specific column radius per Power R/P chart is displayed on figure 2.52. A decreasing trend both for Mediterranean and oceanic condition, meaning the evolution of column radius is way slower than the evolution of turbine power. The difference between Mediterranean and ocean tend to decrease with bigger turbines, as we could anticipate from loads assessment.

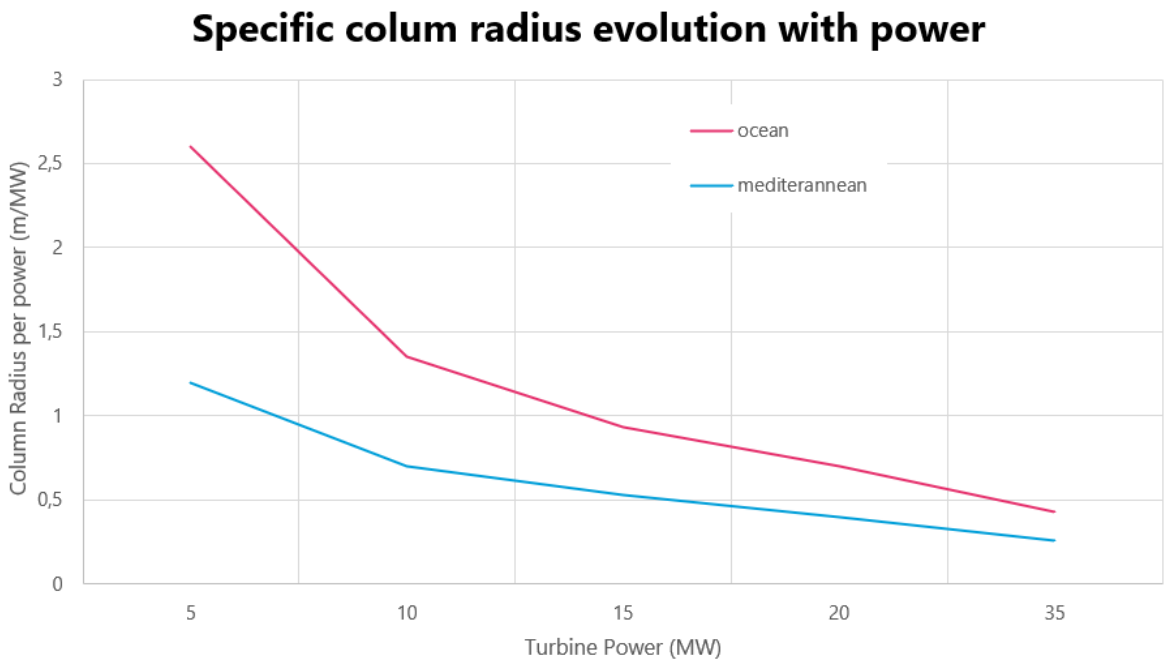

Figure 2.52: Specific column radius R evolution with power for SS

The specific column distance to center per Power d_c/P chart is displayed on figure 2.53.A similar trend is observable, with still a sharper decrease for oceanic conditions.
Dimensions do not have to follow turbine size evolution, which is coherent with the expression of V-shape 3 column SS second moment of area expressed in equation 2.16 where the dimensional parameters where at exponent 2. Since the restoring moment (proportional to I_y from equation 2.11) has to equal the external loads moments, the fact that specific external moments decrease in oceanic conditions while remaining constant in Mediterranean ones explains that the dimensional decrease are sharper for oceanic conditions.

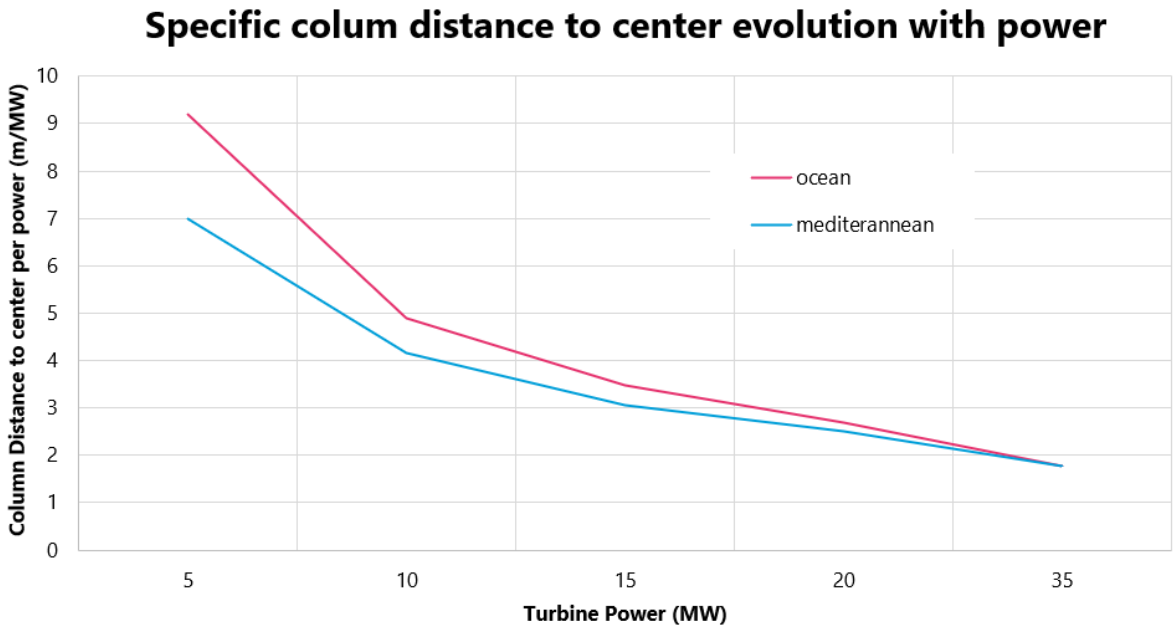

Figure 2.53: Specific column distance to center d_c evolution with power for SS

Dimension evolution will have direct impact on volume, and thus directly on weight since only one material is assumed to be use (steel). Graph on specific weight [ton/MW] evolution of SS both for oceanic and med conditions is displayed on figure 2.54. In addition to two outputs from our physical model, a other forecast made from BNEF in [17] has been add for sake of comparison. As expected, drastic reduction in specific weight are witnessed both for Mediterranean and oceanic conditions, Mediterranean advantage decreasing with bigger machines. The BNEF forecast is quite similar to ours which tend to validate our work. Yet, higher values are found for big turbines. This little gap can be explained by the nature of this forecast: BNEF predictions have extrapolated from industrial results gathered for projects until 10MW, and are actually not based on physical laws.

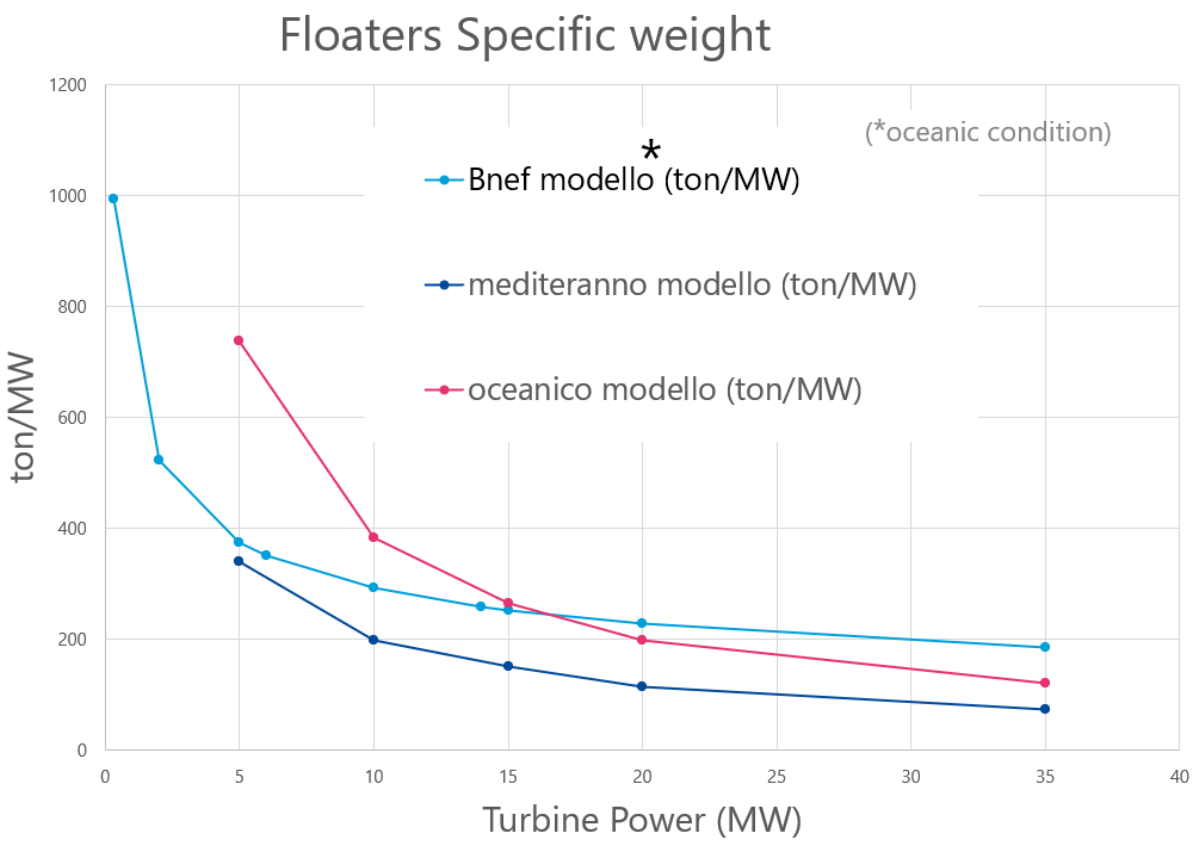

Figure 2.54: Semi submersible specific weight evolution

Based on equation 2.19, the transition from specific weight to specific cost is fast. The specific cost evolution of SS platforms in both conditions is displayed on figure 2.55. As expected from previous insights, both configuration enhance important economies of scale. Easier condition in Mediterranean enhance lighter and thus cheaper structures. Yet, the cost difference between oceanic and Mediterranean condition decrease as well as power increase.

The main insight from this Semi-submersible analysis is here: floaters, the most critical component of FOW projects, benefit from very interesting economies of scale and the introduction of bigger offshore turbines on the market will thus help the market becoming really competitive.

For example, between a 2020 5MW SS pilot as the one described by NREL (cf [79]) and a 2040 (or 2050) 35 MW commercial scale SS in oceanic conditions, the platform specific price is set to drop from 2.5 \$M/MW to 0.35 \$M/MW. As already explained, these values are indicative and are heavily dependant on the various hypothesis of the model. The general trends are in this sense more insightful.

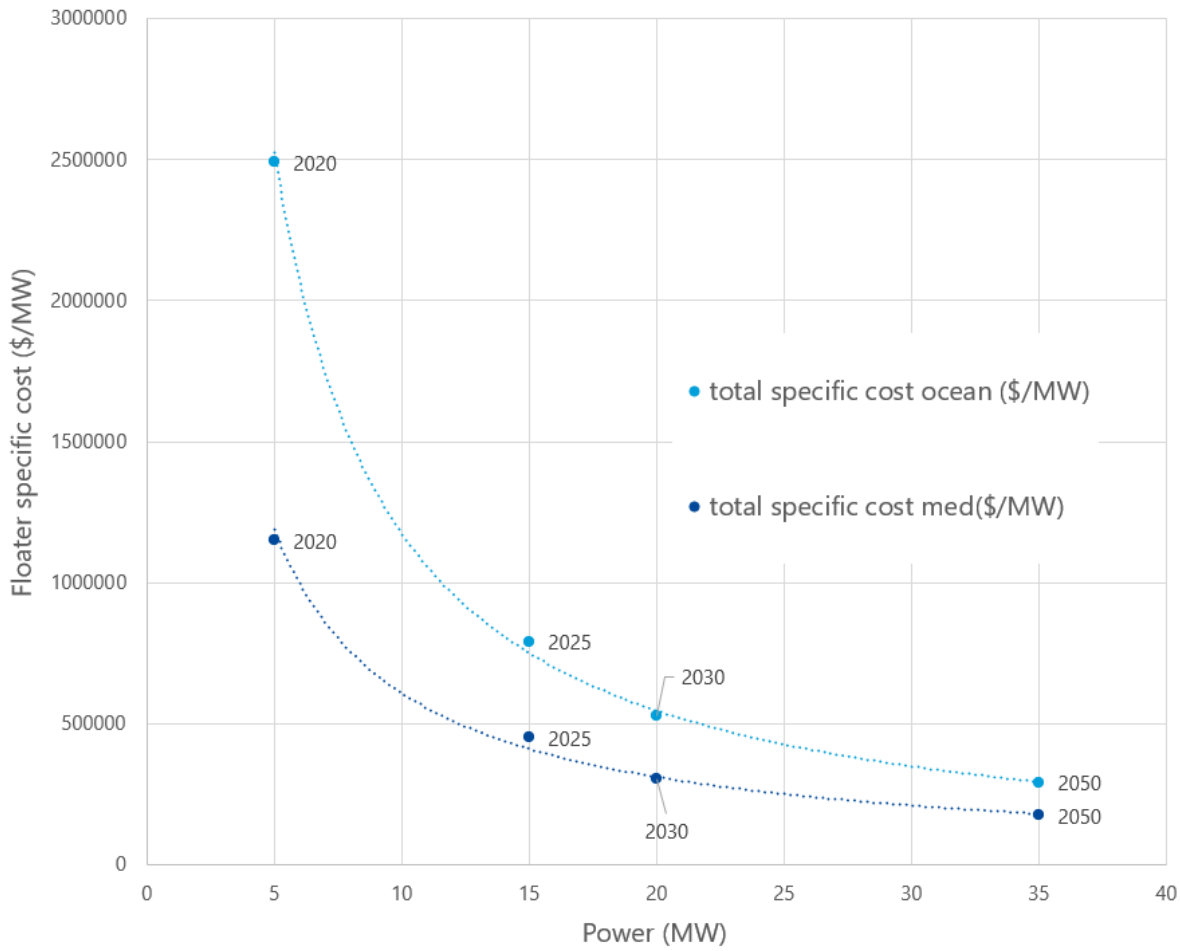

Figure 2.55: Semi submersible specific cost evolution

2.3.3.2 Tension-leg platforms

Let's now analysis similar outputs for tension leg platforms.

Beginning with oceanic conditions, figure 2.56 represents specific external loads moments from wind and waves as well as their sum. It is observed than, unlike for SS, wave loads are the same order of magnitude. Actually the specific wave moment [MNm/MW] slowly decreases with turbine power while the wind related one slowly increases, overvaluing wave contribution for turbines bigger than 15 MW (cf figure 2.48). Since the wind increase is a little faster than the wave decrease, the sum of the two specific contributions also follow a really smooth increasing path.

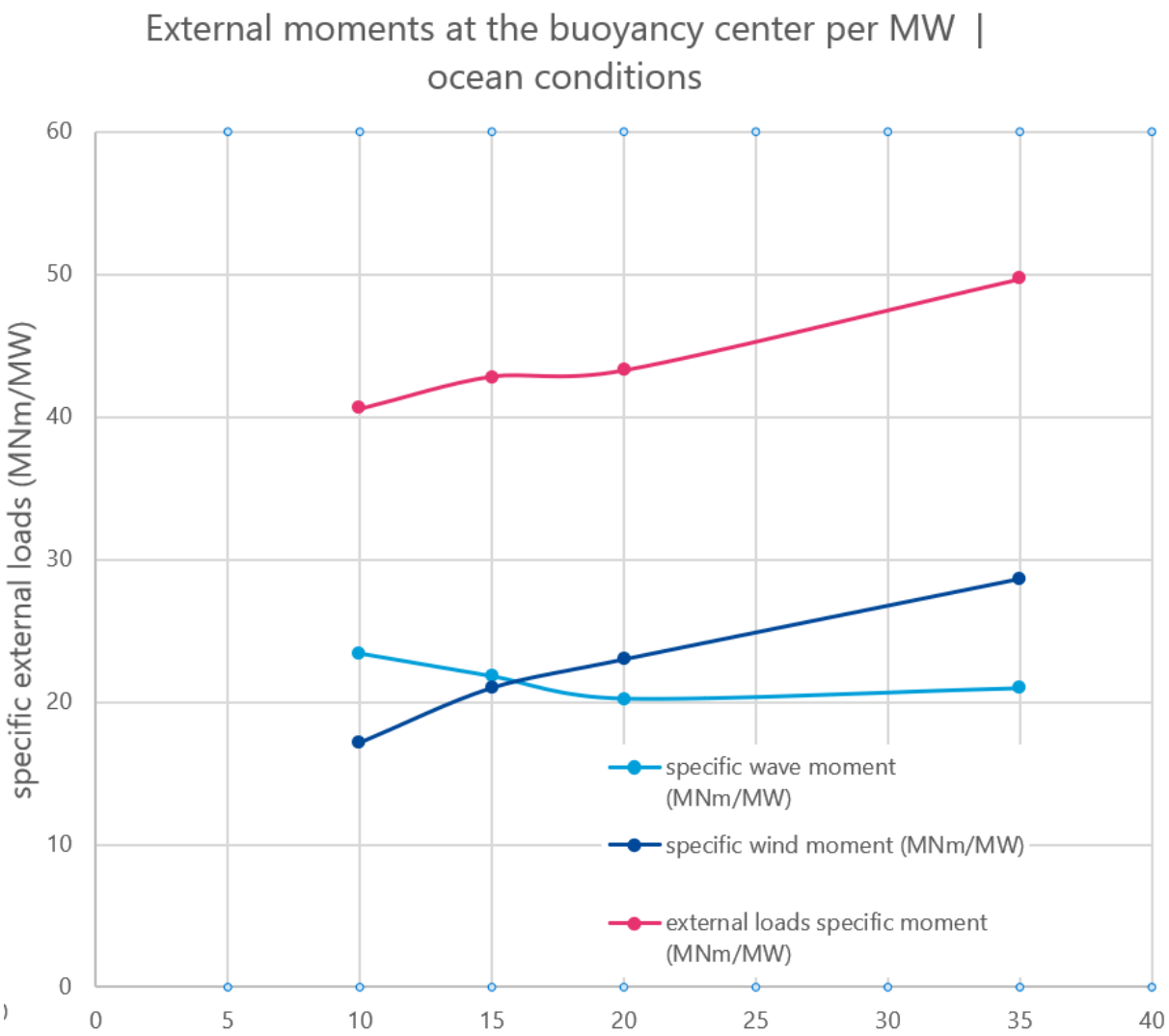

Figure 2.56: External moments Oceanic conditions for TLP

Switching up to med conditions, figure 2.57 represents specific external loads moments from wind and waves as well as their sum. As it was the case for SS, softer Mediterranean conditions logically lead to smaller external moments and wind loads gain importance in the total contribution remaining higher than wave ones for every turbine size. The same trend as on figure 2.56 are then observed: slowly decreasing wave contribution compensated by increasing wind contribution leading to a general light increase of the specific external moments with turbine size, as for oceanic condition. Eventough economies of scale are still possible, this increasing trend for specific external moments already allow us to think that TLP would benefit less from economies of scale than SS.

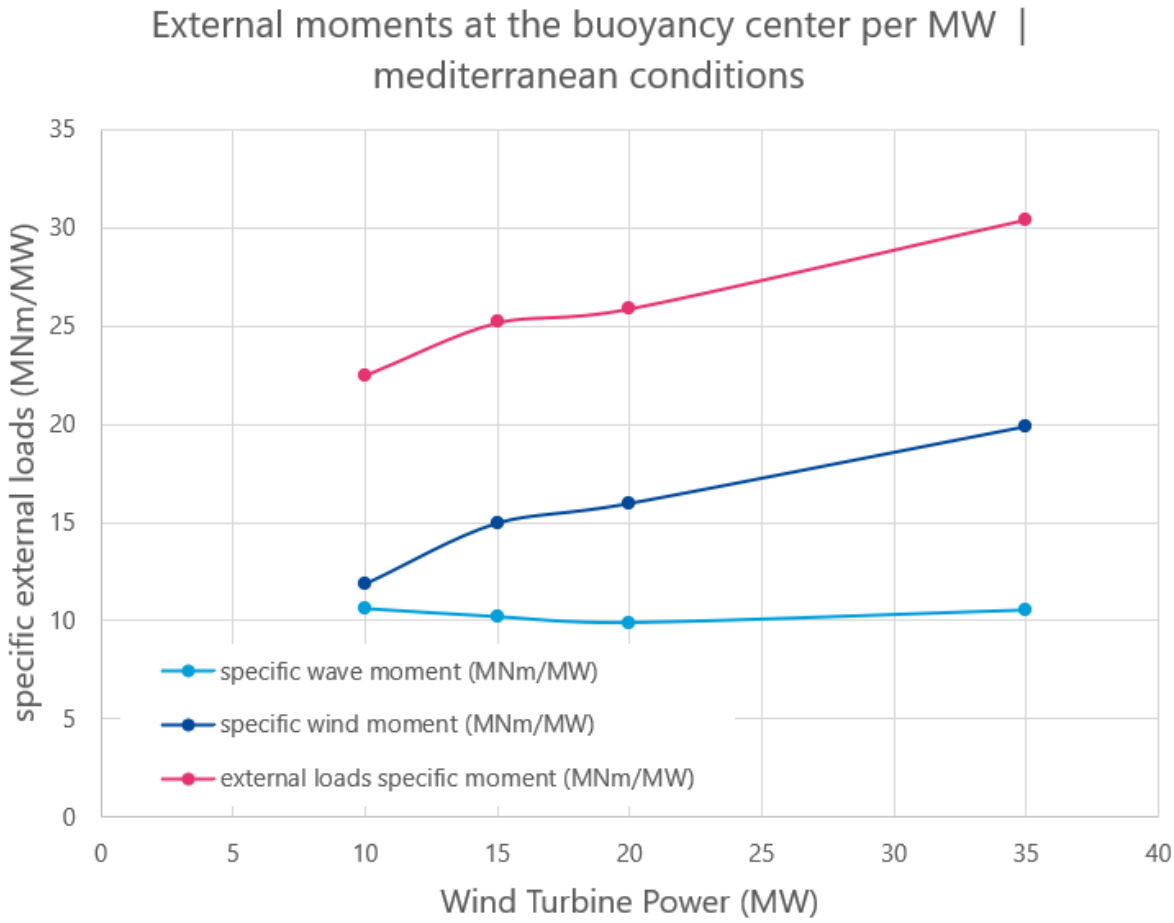

Figure 2.57: Specific External moments per power Mediterranean conditions for TLP

Graph on figure 2.58 allows us to compare the evolution of specific external moments for TLP between the two conditions and as it was explained with the two previous graph similar behaviours are witnessed: the two curves are almost parallel, with a slight increase with turbine size and off course higher values for oceanic conditions.
Eventough economies of scale are still possible, this increasing trend for specific external moments already allow us to think that TLP would benefit less from economies of scale than SS.

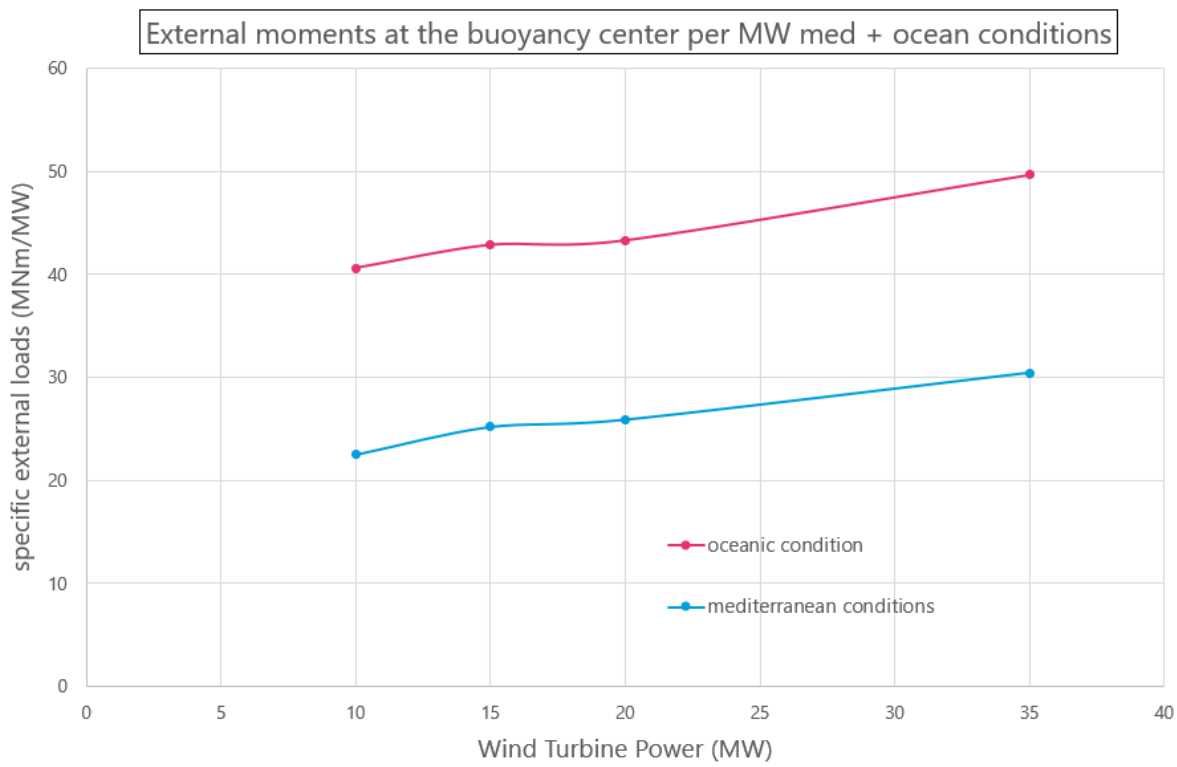

Figure 2.58: Specific External moments per power Mediterranean VS Oceanic conditions for TLP

The dimensional considerations on the two parameters of interest are gathered on the two graphs displayed on figure 2.59. Since these dimensional parameters have been sized on free-floating configuration, they logically follow similar trend to the one of the SS described before.

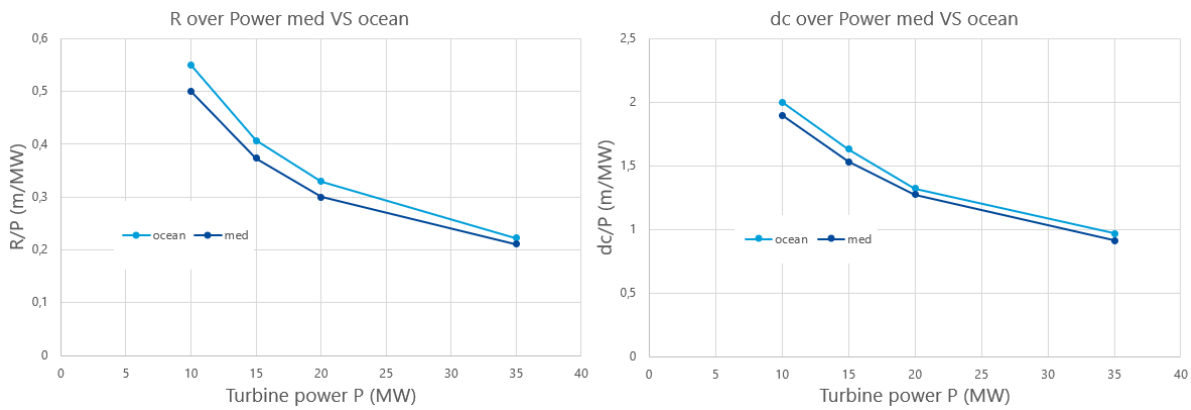

Figure 2.59: Specific dimensions R/P and d_c/P evolution with power for TLP

Once in operation, the restoring moment is ensured by moorings for TLP as explained in

subsection 2.3.2. Moorings cables will thus be submitted to restoring forces to balance the external moments previously displayed, but also to provide the over-buoyancy required for stability. Graph of specific cables loads [MN/MW] for oceanic and Mediterranean conditions are respectively displayed here after on figures 2.60 and 2.61.
Eventough as expected oceanic specific cables' loads are higher than med ones, the curves observed are very similar: following the same trends and with an equivalent gap between the the restoring and over-buoyancy contributions.
For both conditions, over-buoyancy loads are the main mooring loads. Specific over-buoyancy loads decrease with turbine power while specific cables restoring loads remain more or less stable. (NOTE: Over-buoyancy loads will be homogeneously balanced between cables unlike restoring loads that only concern half of the moorings as explained in section 2.4).
The augmentation of d_c allows specific restoring loads to remain more or less constant, and even decrease a bit, eventough the specific external moments tend to increase with turbine size.
These considerations on mooring loads will be tremendous in the second part of the TLP sizing led in the mooring section 2.4.

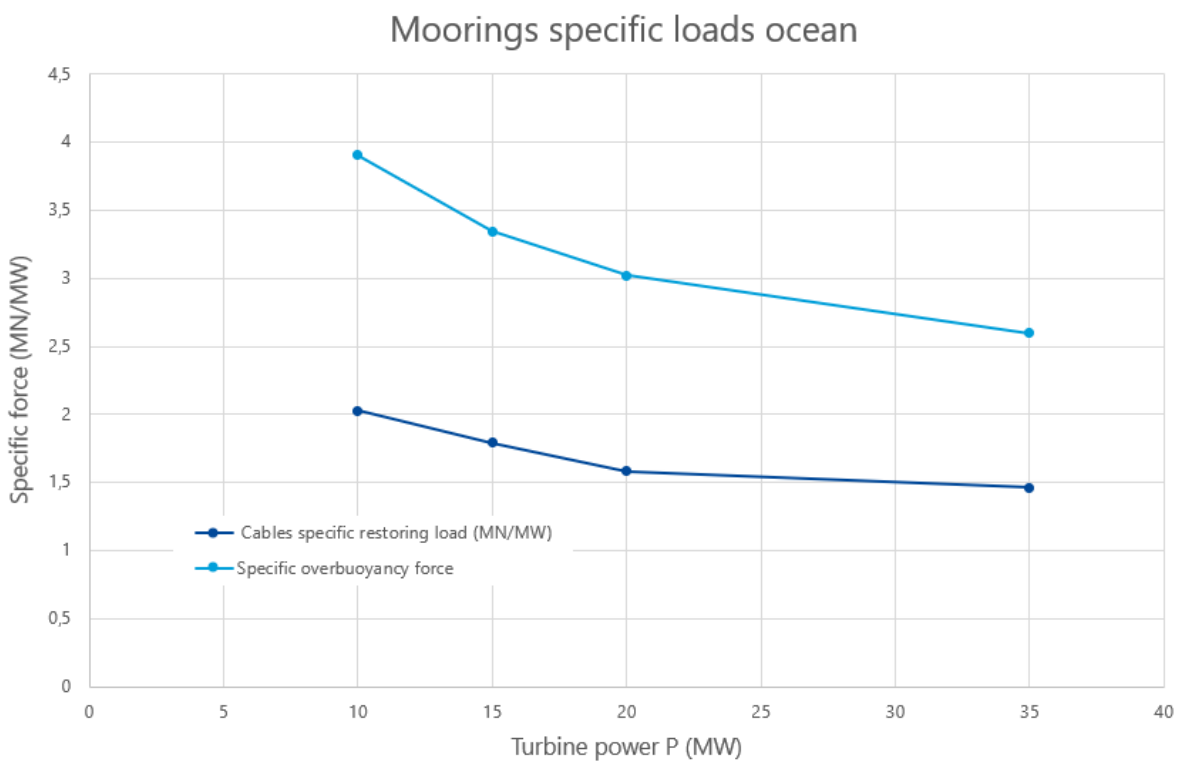

Figure 2.60: Specific loads on moorings in oceanic condition

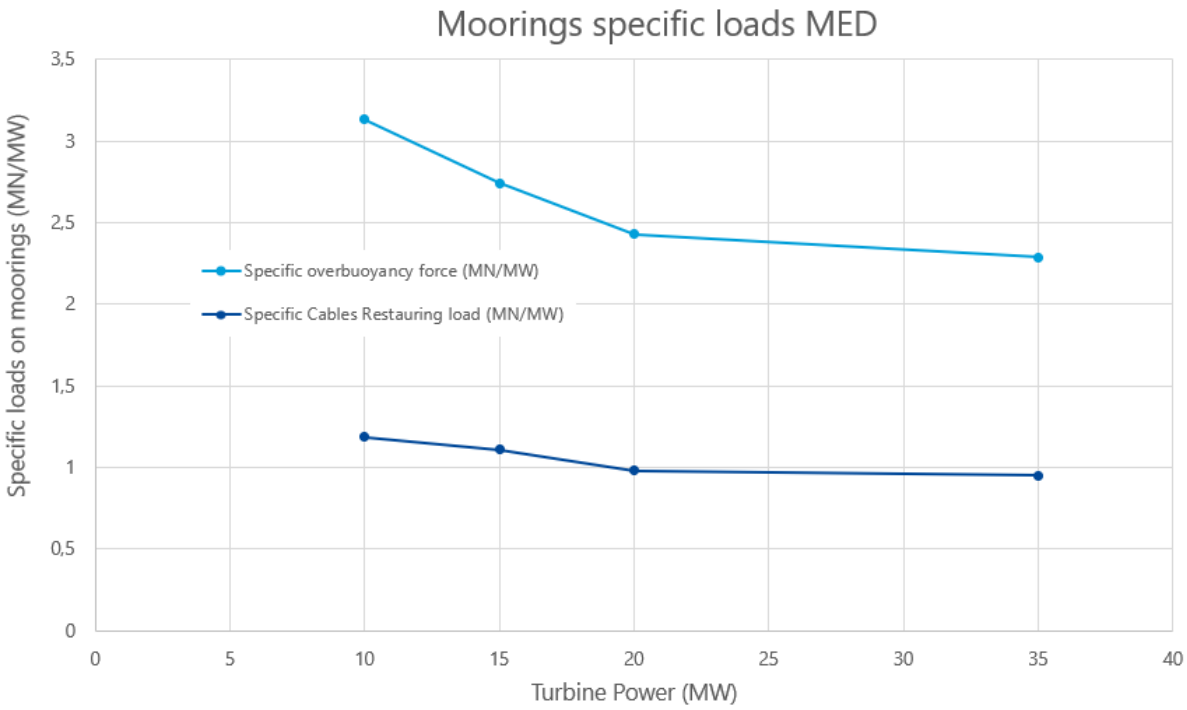

Figure 2.61: Specific loads on moorings in Mediterranean condition

Skipping the weight analysis to directly arrive to the specific cost one, figure 2.62 displays the specific cost evolution of a TLP with turbine size in both conditions. From this graph we get that both configuration enhance important economies of scale. It is Logical since the dimensional design is made at reduced meteorological loads for free floating when the TLP will behave as a SS. Low differences between Mediterranean and oceanic conditions is explained by the soft conditions of the free-floating computation. The very identical dimensions for the two configurations observable on figure 2.59 was a hint toward this conclusion.

The expected lower economies of scale due to increasing specific external moments with turbine size are set to be more visible on mooring design since restoring moments design will be performed in harsh operation conditions.

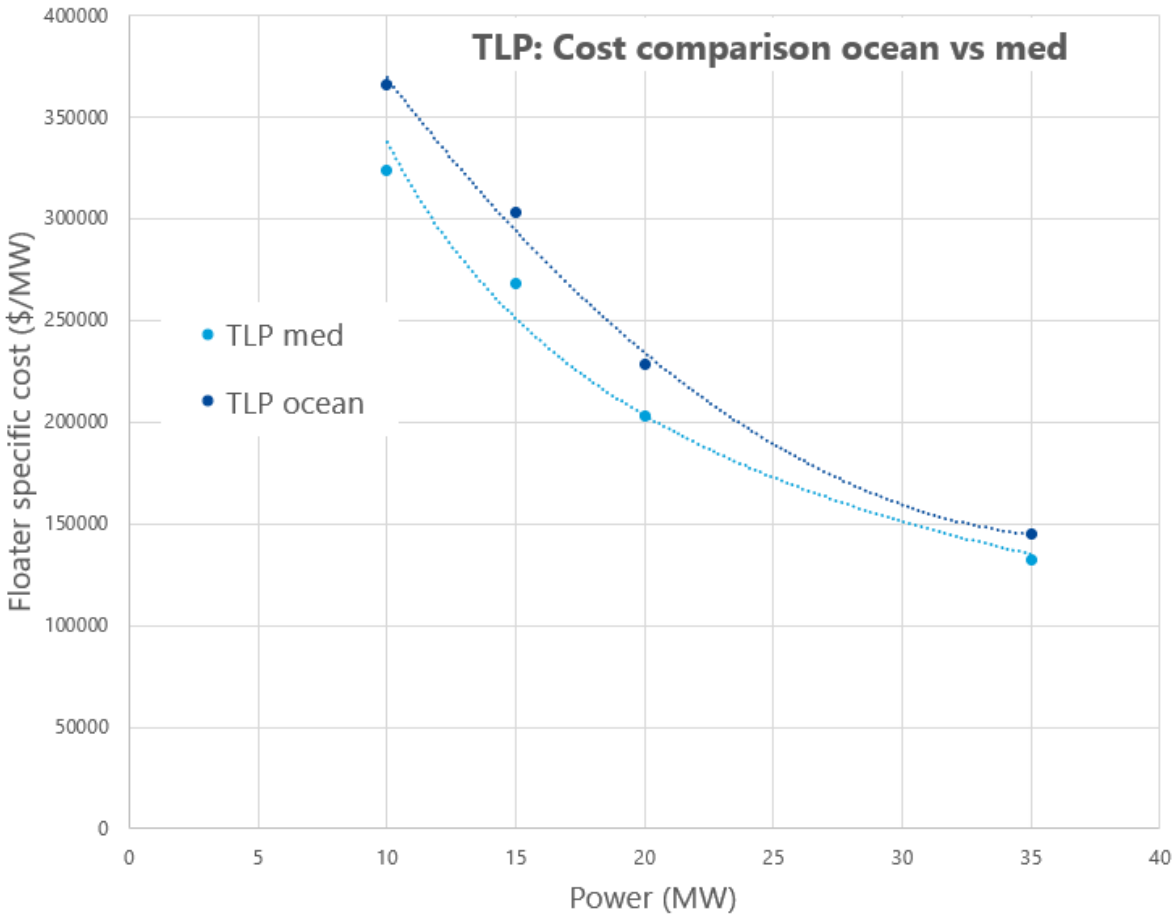

Figure 2.62: TLP specific cost evolution

2.3.3.3 Semi-submersibles VS Tension-leg platforms

Both platform typologies have been studies through the outputs of the model, and can be now compared. The data display here after is the same as the one previously used in 2.3.3.1 and 2.3.3.2 but rearranged in order to ease the comparison between typologies.

First, specific weight of structures is compared and display on figure 2.63 with oceanic condition on the left and med conditions on the right. The main i sight is that as expected TLP offers lighter platforms for every turbine size and every condition.
Yet, it is confirmed that the comparative advantage in terms of specific weight decreases with turbine size. Knowing that TLP concepts are currently facing delays in development compared to SS and that their entry on market could be with already existing big turbines, this insight is important to take out.

Then, since as previously explained TLP are less impacted by conditions, the the comparative advantage of TLP regarding SS in terms of specific weight will be more important in harsher, i.e. oceanic, conditions. Project developers could thus, from this unique point of view, obtain less incentives in using TLP over SS than oceanic project developers.

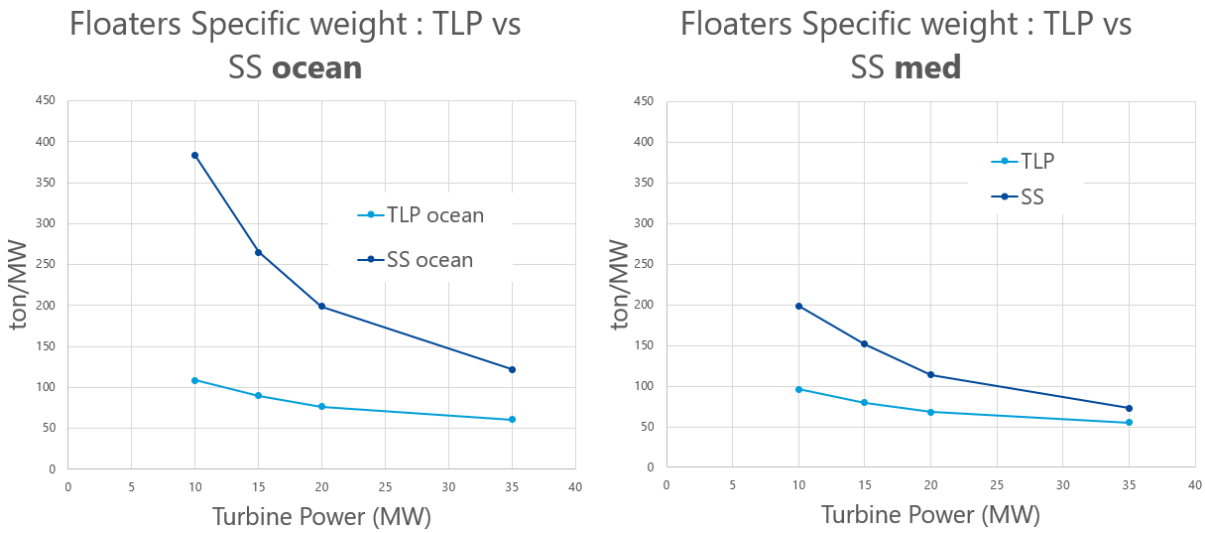

Figure 2.63: Specific weight comparison SS vs TLP

As previously explained weight and cost are intrinsically linked in our model and thus the specific cost comparison trend between SS and TLP, displayed for oceanic condition in figure 2.64 and for med conditions in figure 2.65, are similar to the ones observed on specific weight graphs from figure 2.63.

Thus, eventough the advance in terms of MCFs favours SS concepts over TLP ones in terms of cost, TLPs end up cheaper than SSs in both conditions, with a bigger gap between the two for oceanic conditions.

The economies of scale offered by SS for big turbines are nonetheless way more important that the one offered by TLPs. This fact is very insightful since as previously explained, the trends are maybe more worth than absolute values in this study.

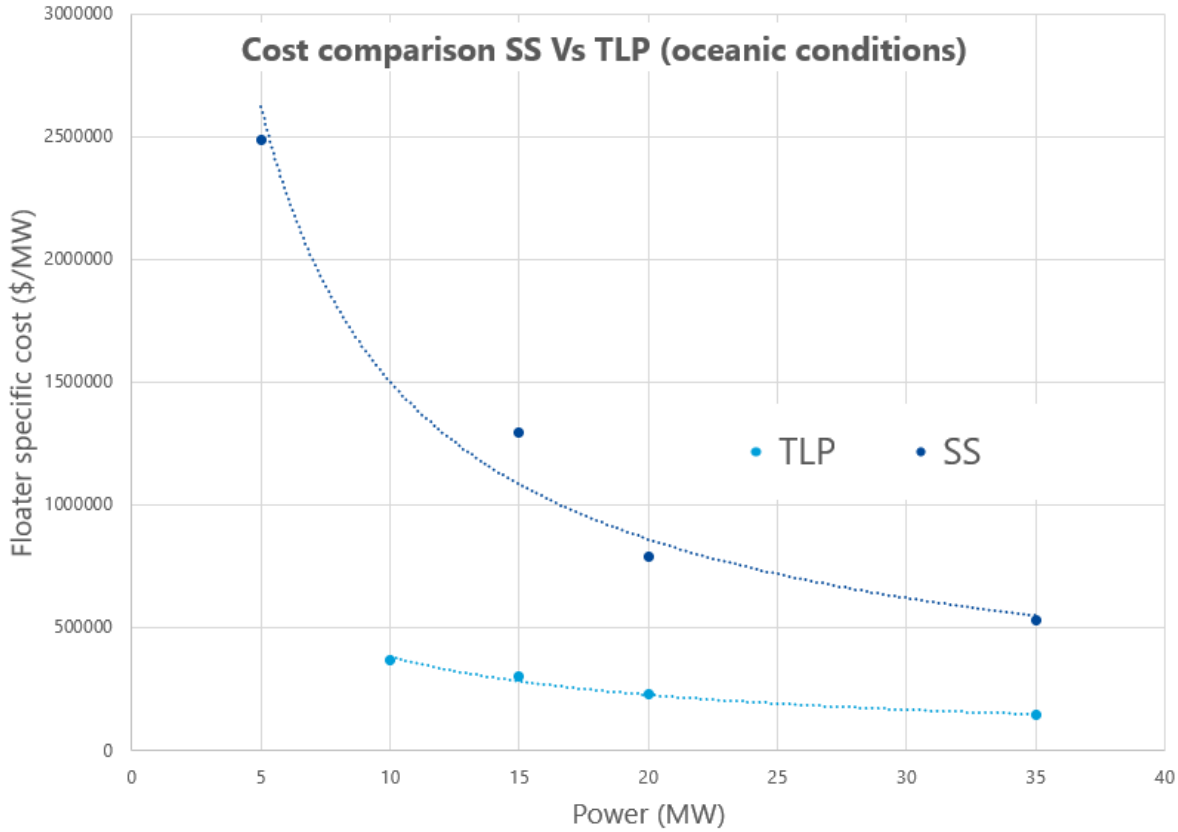

Figure 2.64: Specific cost comparison SS vs TLP for Oceanic condition

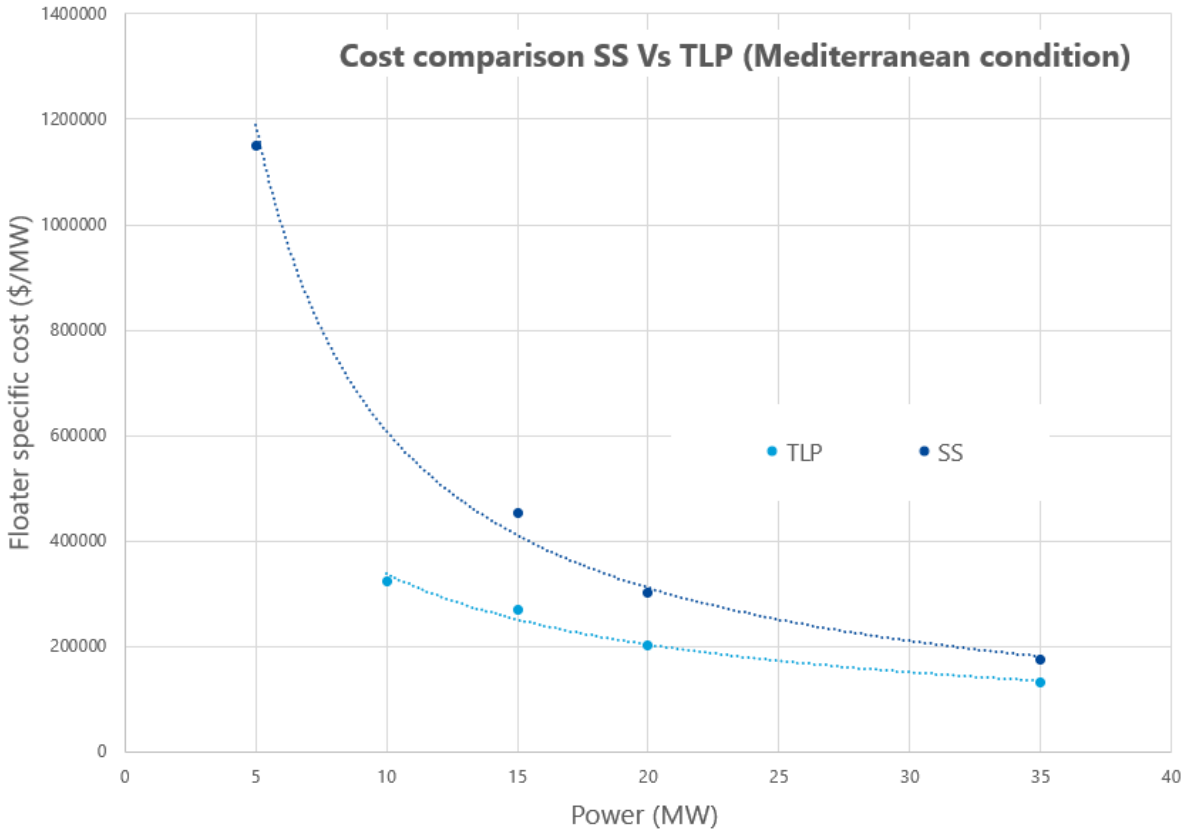

Figure 2.65: Specific cost comparison SS vs TLP for Mediterranean condition

In the end, this work on platforms highlighted the tremendous economies of scale enhanced by the introduction of ever bigger turbines for this critical component of FOW projects. Then, the very interesting potentiality of TLP solutions in terms of cost saving, already mentioned in the technology presentation of subsection 2.3.1, have been confirmed.
In order to complete the cost comparison work between the floater typologies, mooring cost as well as installation costs will be assessed in section 2.4 and 2.7 respectively.

2.3.4. Floaters future and innovative concepts

To close this focus on floaters, let's have a brief glance at innovative floaters concepts that aim to overcome some limit or push further some characteristics of (mainly) semi-submersibles previously described. These floaters concepts have been identified in the market overlook led in subsection 2.3.1.

Stiesdal, a company with which A2A had some exchanges with as already mentioned

earlier, is a FOW project developer and platform manufacturer who developed an holistic concept for offshore turbines substructures : the tetra concept [21]. The Tetra concept can be implemented in a range of floating variants and even in a bottom-fixed variant. It is set to offer competitive advantages over existing foundation concepts, with leaner manufacturing, faster installation, and lower material costs.
The first epitome of this concept installed nowadays is a Tetra-spar pilot displayed on figure 2.66. This solution, technically described in [82], benefits from the modularity and industrialisation friendly features of the Tetra concept while disrupting the ballast stabilisation process and offering a solution to the big draft issue that tend to force risky and complex offshore installation.
Yet, now Stiesdal are pushing in the SS direction since it is considered that for the next decade projects will be concentrated in shallow waters where the so called Tetra sub solution is more suited (cf [21].

Figure 2.66: 3.6 MW Tetra-spar pilot launched in 2021 in Norway

The main idea behind this concept is to push the modularity possibility offered by steel use (this steel characteristic motivated our choice to focus on steel-based floaters in our model) to its paroxysm in order to foster economies of scale, supply chain cost saving and ease installation and assembling. The offshore structure thus end up as a puzzle

where constructors only have to gather simple and standardised steel pieces to created the floater most suited to their project. This assembling process is schematised on figure 2.67 here after.

Figure 2.67: Modularity of Stiesdal design for an onshore assembly

[83]

Next, various new concepts choose a similar disruptive approach that could enhance cost saving for FOW projects : integrated structures. The concept is to integrate the turbine to the floater design in order to optimize the global design, aimin at a better strengths balance and a material optimisation as well as better equilibrium properties. These concepts are promising as explained in [29] and could heavily impact the FOW market if important cost saving were witnessed since the current market segmentation between turbine and platforms manufacturers would melt.
The two main represetants of this integrated structure field are Eolink (France) [83] and X1-wind (Spain) [84]. Eventough these concepts are not at commercial scale step yet, low scale demonstrators are currently under tests. These pilots, heavily sustained by Europe and big groups as EDP for X1-wind or Acciona for Eolink are displayed on figure 2.68 for the Eolink pilot and 2.69 for X1-wind.

Figure 2.68: Eolink small scale pilot in France

Figure 2.69: X1 wind small scale pilot in Canaries (Spain)

Finally, the last concept is good occasion to mention a typology of platform left out of the discussion in this work: shared platforms. The idea of shared platforms concepts, already discussed in the very complete guide made by Carbon Trust in 2015 [58], is to

install more than one (usually two) turbine on a same platform in order to save material and even according to some sources to increase the farm yield by reducing wake effects and improving the structure platforms. For now, the sector has been few invested by industrial actors but remain a potential way for the future of FOW.
The clear leaders of shared platform sectors are the project developers and platform manufacturers Hexicon with their TwinWind concept [85] displayed on figure 2.70. A 6 MW pilot is currently in construction in Norway and is set to demonstrate the theoretical economies on specific cost of platform and moorings offered by the solution. The twindWind solution thus has a High TRL: POC complete and commercial projects in Celtic sea announced by 2026. Plus, the dynamism of the constructor is also corroborate by a huge MOU with Shell for GW-size projects in South-Korea.

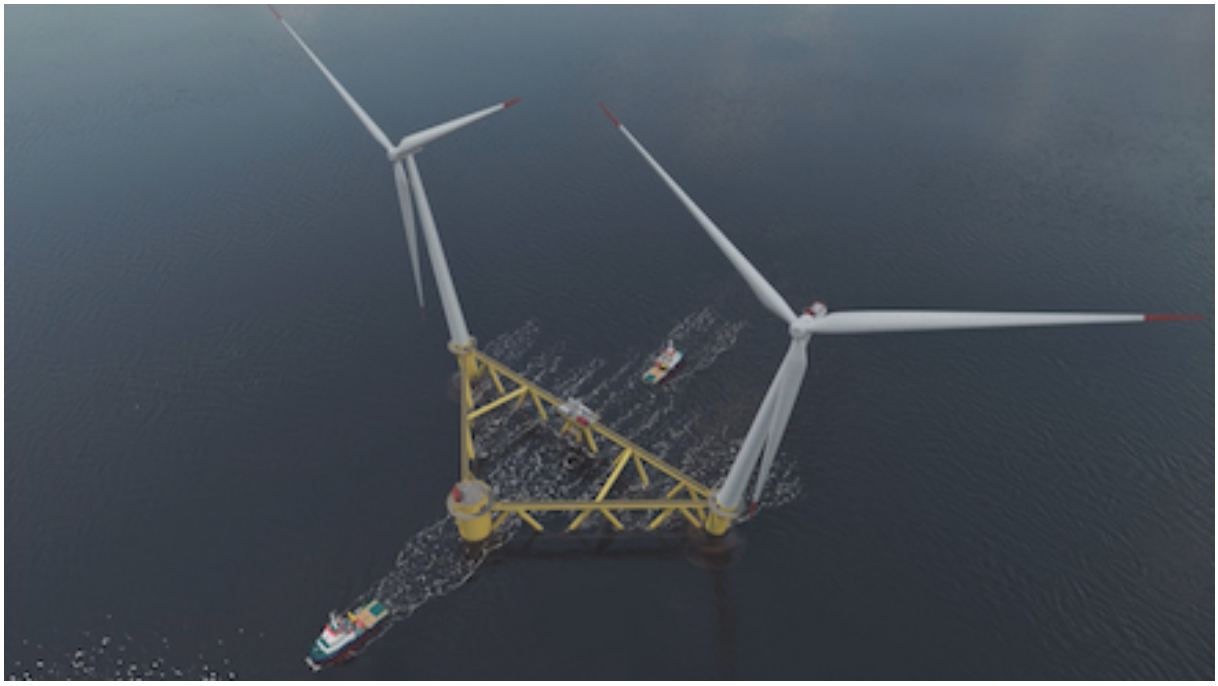

Figure 2.70: Twin wind concept from Hexicon

2.4. Focus on moorings and anchors

2.4.1. General overview

Alongside floaters, moorings and anchors are a key and characteristic feature of FOW projects. A FOW turbine's mooring system provides the mechanical connection between the floating substructure and the seabed. The oil&gas industry has a proven track record in the application of mooring systems for floating offshore energy infrastructure, and the

initial mooring solutions deployed in FOW have been based on those designs [59]. Nevertheless, the knowledge about mooring technologies for FOW application lacks industrial feedback and techno-economic consensus, which constitutes even more of an issue knowing the importance of these devices to insure safety and integrity of a project. Indeed it has been identified that the standards used in the oil&gas sector for mooring system design and inspection do not fully meet the requirements of FOW farm developers. Plus, moorings and anchors have a environmental impact on underwater ecosystem that must be assess and taken in consideration also in term of potential Nimby related consequences. FOW mooring systems are thus the subject of ongoing research and development work and further innovation is required for FOW to become commercially competitive alongside bottom-fixed wind [59].

Various mooring technologies exist which are more or less suited to floater typology or a given depth. BNEF in [17] counts four different mooring technologies that are schematised on figure 2.71. According to BNEF, these moorings are very important cost driver that can represent until 10% of the global cost of FOW project. The so called Semi-taut design is nothing but an hybrid combination of two others technologies and shared application, eventough very interesting and promising, will be let out of discussion since not being at maturity yet. The two main configuration of interest will thus be catenary and taut systems.

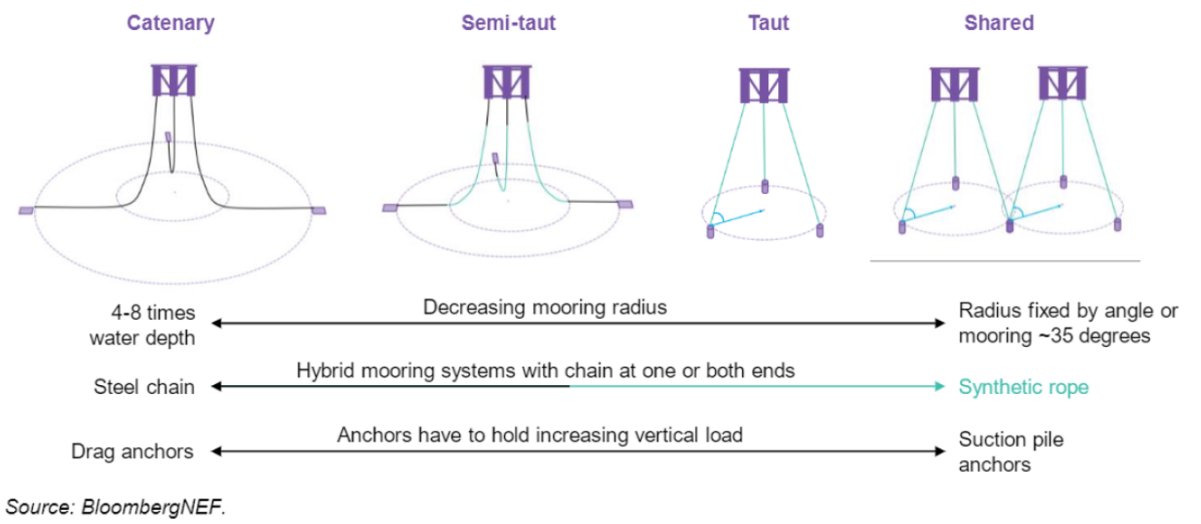

Figure 2.71: Different mooring system for floating platforms from [17]

A catenary mooring system is currently the most common mooring system in shallow

waters since used for every pre-commercial scale FOW farms counted in 1.4. Through gravity the catenaries, between the floating unit and the seabed, will show the typical shape of a free hanging line. The catenaries are hanging horizontally at the seabed. Consequently the catenary lengths have to be larger than the water depth and even a further horizontal distance of chain distance will be required to link the anchors to the actual seabed contact point. The total footprint radius will thus be very important, between 4 and 8 times the depth of the site. A catenary system are the one usually used for Spar, barge and semi-submersibles platforms and the main role of this mooring is thus to use their weight and anchors to prevent derivation. From the static point of view, the restoring action of the chains can be neglect. The main interest of this chain is at dynamical side.
Then, in a taut leg mooring system, mooring lines remain straight since pre-tensioned and arrive under an angel at the seabed and directly link the anchors. Typically the angle between the line and the seabed is between 30 and 40 degrees. The mooring radius is thus way smaller than for catenary solution. The anchor points in a taut leg mooring system have to be capable of withstanding horizontal and vertical forces. In a taut leg mooring, both maintain in position and restoring forces are generated by mooring line that are thus submitted to bigger forces. They are thus more predisposed to suffer from fatigue. This mooring technology is at the base of TLP solutions which are mooring stabilised. Various materials can be used, with different pros and cons.

The depth has of course an impact on many aspect of a mooring solution. Catenary and taut moorings have physical particularities that make them more or less suited to different depth. Indeed, in shallow waters (until 300 meters), complex hydrodynamics phenomenon (cf [59]) necessitate larger mooring systems and less that can withstand the additional fatigue loading, and TLP systems are thus currently considered to be more suited for greater depth. Plus, great depth allows to ease the tension process and improve dynamic behaviour of taut moorings as explained in the very complete book [86] where the best typology fr depth range are discussed.
Nonetheless, catenary system are neither perfectly suited for every depth range. Indeed, as explained in [18] and [59], for depth higher than 500 meters a chain catenary solution begins to become really heavy, costly and with a huge footprint which can be damageable. To limit these detrimental phenomenon, solution with a wire section between the two chain made extremities exist and are indicated for depth higher than 300 m.
These considerations are summed-up on figure 2.72 where for each depth range the possible

solutions - with the most indicated one in bold text - are displayed. These consideration are global considerations that can (and must) be reassessed for every project. For example a site with important submarines currents or fish activity can make a choice prevails over another. This complex consideration - among others such as seabed type analysis etc - are let out of the scope of this study on general CAPEX evolution with size and depth.

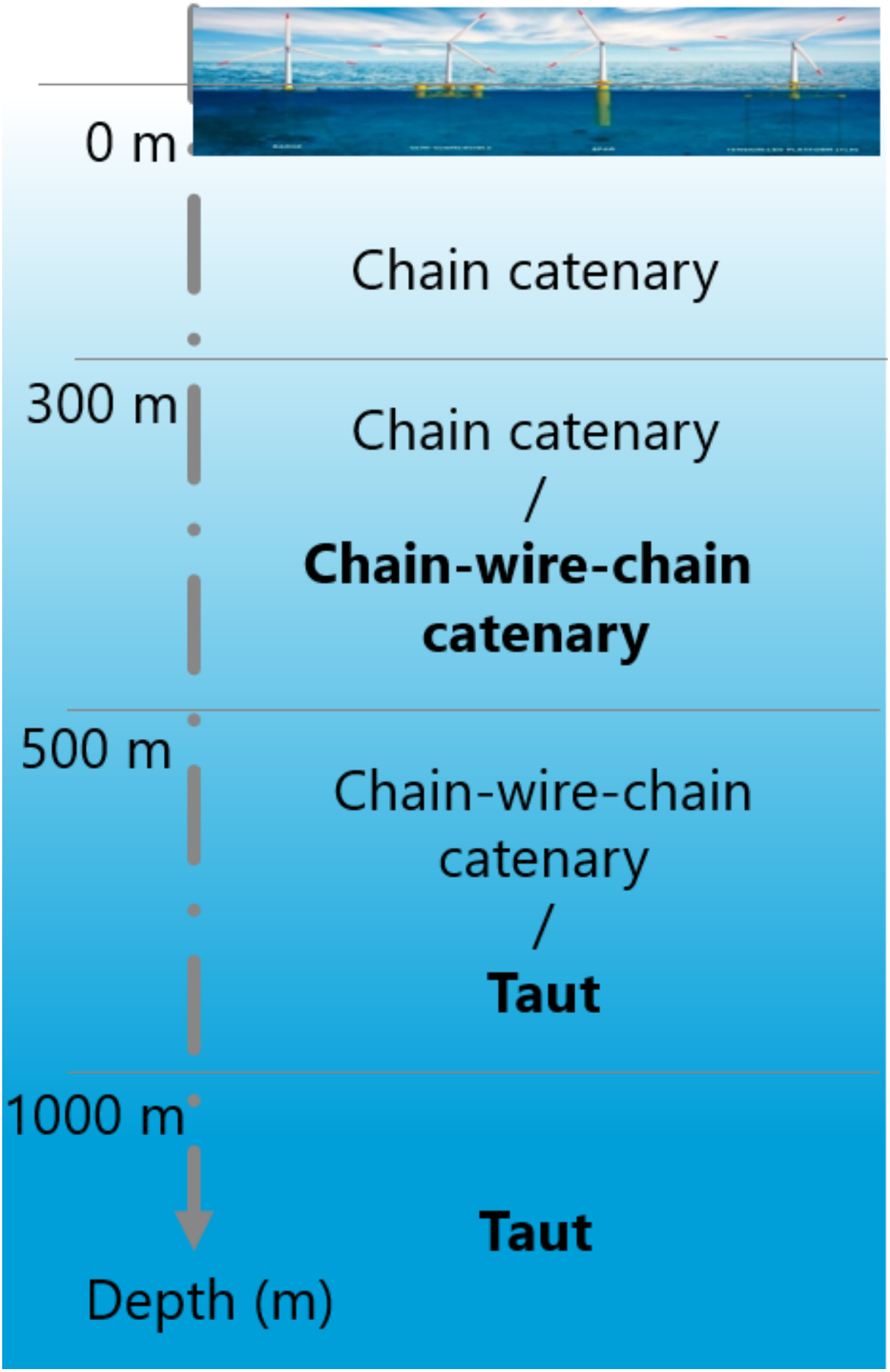

Figure 2.72: Most suited solution evolution with depth

In the end different parameters impact the mooring typology choice. First, the platform type (a TLP platform is design for taut mooring, while semi sub are currently exclusively using catenary configuration). Then Depth taut configuration require sufficient depth for tension requirements, while chain catenary may suffer weight related issues for high depths. Cost of course as it will assessed in the physical based cost model that will be extended to mooring analysis. The installation processes can also governs developers choice as well as Seabed footprint which is deeply linked to environmental and social impact of a project.

External loads and site characteristics will impact the share of moorings and anchors in the global cost of a FOW project. Keeping up with the physical model already computed for floaters section 2.3, the same kind of forecast and sensitivity analysis will be lead for semi-submersibles (catenary mooring) and TLPs (taut mooring). The framework of our physical model developed in subsection 2.3.2 will remain equal and moorings (and anchors) analysis will be performed and integrated in the cost model.
This mooring related extension of the physical model will be described for the SS and the TLP respectively in subsections 2.4.2 and 2.4.3. The outputs of this model will be presented in subsection 2.4.4. For each mooring system, 3 parameters will impact the specific cost $[/MW]$ of the moorings: turbine size and external conditions (med or oceanic as previously), but also the depth that will range from 100 meters to 1000 meters. This depth range is representative of the majority of the upcoming wind farms since deeper sites are currently not considered for economic and installation related issues while for depth significantly lower than 100 meters fixed-bottom solution are expected to keep leading the way over the next decade.

2.4.2. Catenary moorings

The majority of mature concepts counted, both SS and TLP, use distributed mooring lines points located at the extremities of the platforms. Plus as explained by Flotation energy in its early-planning scoping document for the GreenVolt project in England [87], the most plebiscite solution for SS solution are distributed catenary with usually one, sometimes two, mooring point per column.
For us 3 column V shaped SS used in our model (cf figure 2.39), we will thus assume 3 catenary chains equally distributed between the three columns. For each catenary line, the mooring arrangement will be a classical free hanging configuration as schematised on figure 2.73 here after. On this scheme, the main design parameter of the mooring arrangement are defined: the depth h, the total mooring length L, the hanging mooring length L_s between the floater and the seabed, the mooring angle Φ, the total mooring

radius X and the free hanging mooring radius x. Some geometrical equation link the parameter, since it his directly obtained that $tan(\Phi) = \frac{x}{h}$ and

$$L = L_s + (X - x)tan(\Phi) \tag{2.20}$$

In [18], complex physical based equation driving the sizing of this mooring arrangement are described. These equation take in consideration site parameters to optimise the catenary behaviour regarding fatigue, corrosion, hydrodynamic etc... From our general point of view, these complex consideration remain out of the scope of the study and will thus be simplified by an assumption considered acceptable in [18]: the mooring angle Φ is fixed at 35° as displayed in red on figure 2.73. Plus, the free hanging chain length L_s is approximated by $L_s = \frac{h}{cos(\Phi)}$.

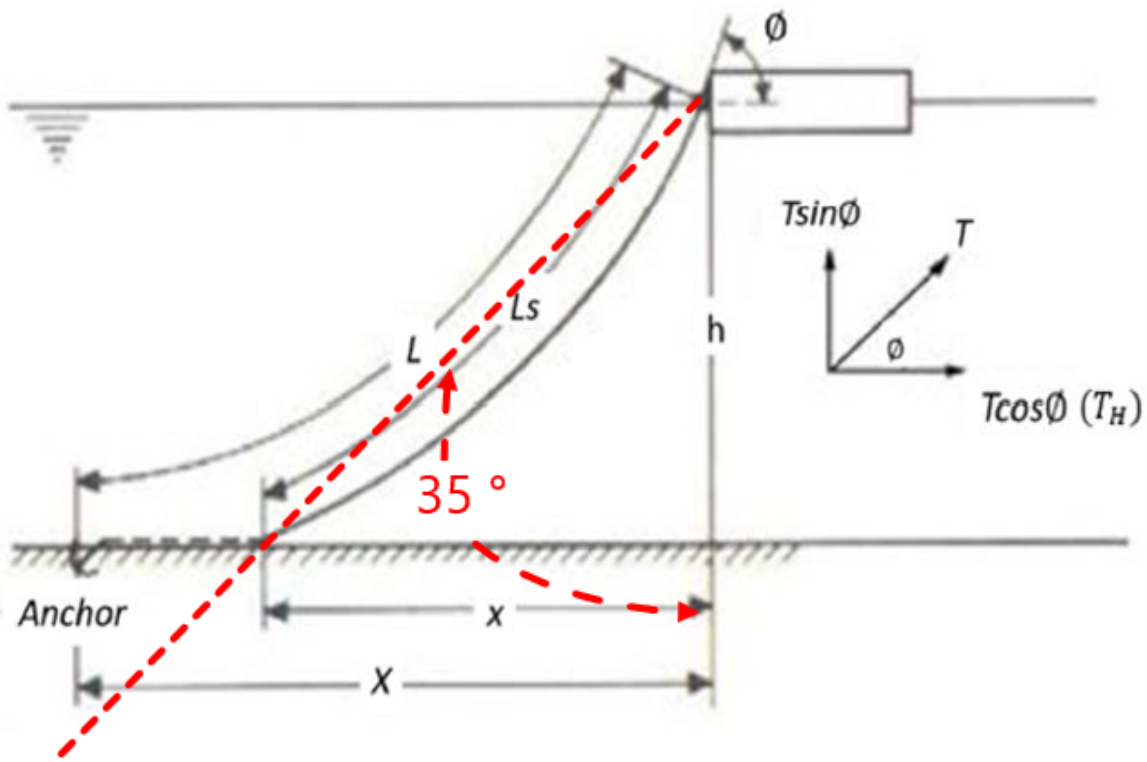

Figure 2.73: Catenary Mooring arrangement from

The cost of the mooring line will of course be proportional to the total length L. A further equation is then required. As previously, an assumption will be made on empirical industrial data, here obtained from [86]. Indeed, in this book, the mooring radius of many offshore projects have been gathered on a graph displayed on figure 2.74. This graph shows a decreasing trend of the Radius over depth ratio with water depth. On

the graph, two zones can be identified: for low water depth (under 1000 feet on the graph, i.e. 305 meters) high value with sharp decreasing trends and for greater depths smaller values with an almost constant trend. This difference is explained by the wider utilisation of taut moorings at greater depth as explained previously. Plus, at shallow depth, the hydrodynamics effects already mentioned here before force the use of more resilient mooring configuration leading to bigger radius.
From this graph, we will adopt a conservative value of 4 for the radius over depth ration $\frac{X}{h} = 4$ of catenary moorings for depth in range [200 m ; 1000 m]. To take in consideration the unwanted hydrodynamics effects in shallow water, this value will be taken as $\frac{X}{h} = 8$ for depth lower than 200m, and particularly for depth of 100 meters in our model.

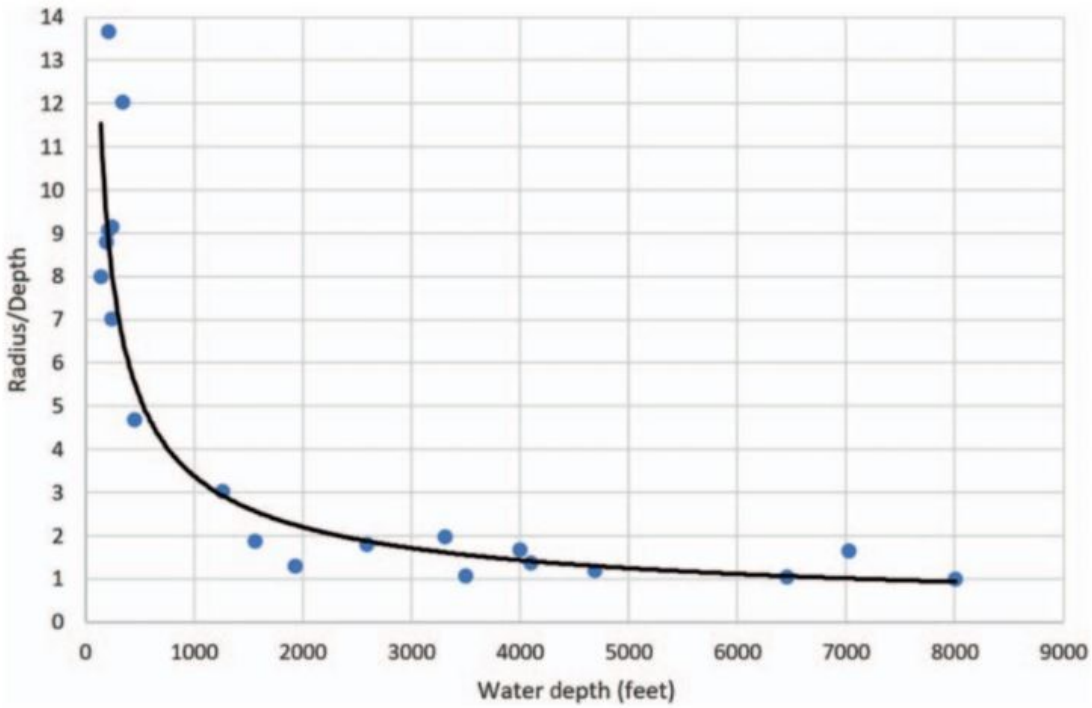

Figure 2.74: Anchoring Radius R over depth evolution with depth, industrial data from Oil&Gas sector gathered in [4]

It will be assumed that catenary chain costs will be directly to their total weight W_{chain} in [ton]. This weight will of course depend on the length obtained from equation 2.20, on the number of moorings lines fixed to 3 in our model and on the size of the chain. The size of the chain will depend on the loads it has to support. As explained earlier, it is assumed in our static model that moorings do not participate to restoring forces but are here to prevent translation of the turbine. As previously, it is assumed that wind and wave loads push in the same direction (cf figure 2.39) and that only the chain linked to the

column facing this external loads will compensated it. Thus as it was computed in [66] for catenary moorings of spar buoy solution, the equation giving the catenary mooring dragging force is the static equilibrium of forces on our structure written on the horizontal x axis, display on equation 2.21:

$$F_{drag-catenary} = F_t + F_d + f_{I-Morison} + F_{D-Morison} \tag{2.21}$$

The thrust and drag force on tower from wind are the same components as the one used before. For the Morison's forces, horizontal and non vertical components are considered here. Since it is assume that maximum value of both are considered here, of sake of simplicity it will be assumed that vertical and horizontal components are equals in value. For each turbine size, the model already built this furnish the force the chain will have to undergo in the worst operational conditions. A chain able to support this force must thus be found for each turbine size and condition. Let's precise that, as usually in this kind of project, a security factor SF=2 will be introduced in the calculation.
The bigger the chain diameter, the greater the force it will undergo. In [18] where a similar analysis for mooring sizing of a semi-submersible has been led, a table linking the nominal diameter of a chain with its unit Weight in [ton/m] and its Break load in [kN] (i.e. the maximum axial load the chain can undergo) is displayed. Since in [18] the study is performed on a small turbine size and that six chains are used, the chain dimensions displayed was not big enough for our analysis. Yet, from these data a wider table has been extrapolated and is displayed alongside a chain scheme on figure 2.75.
For every turbine size and condition (oceanic or Mediterranean), a chain size size is thus assessed based on the Breaking load, and then the correspondent unit weight is computed. The total weight of the mooring [ton] line is then obtained multiplying the unit weight [ton/m] with the mooring line length L obtained from equation 2.20.

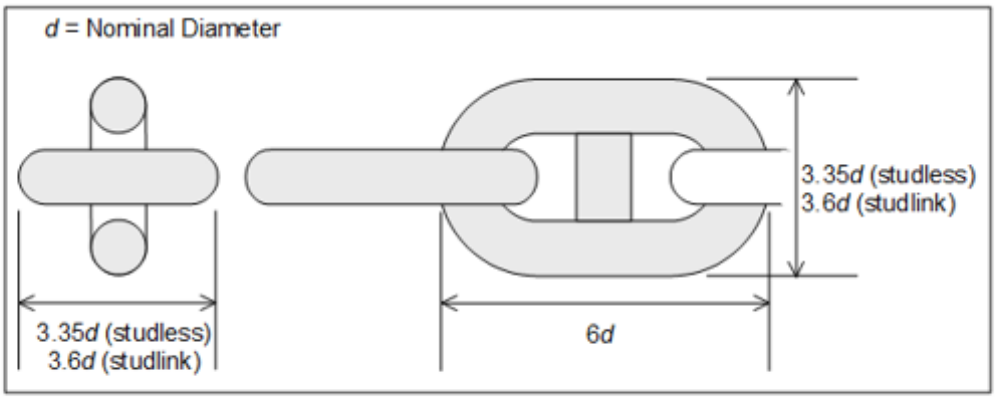

Chain characteristics		
Nominal diameter (m)	Break Load (kN)	Unit Weight (ton/m)
0,095	9.001	0,18
0,115	12.610	0,26
0,135	16.579	0,36
0,155	20.308	0,45
0,175	24.097	0,54
0,195	27.886	0,63
0,215	31.675	0,73
0,235	35.463	0,82
0,255	39.252	0,91
0,275	43.041	1,00
0,295	46.830	1,09

Figure 2.75: Catenary chain characteristics extrapolated from data gathered in [18]

To complete the cost model, a value for chain cost per weight [USD/ton] is required. Few interesting data have been found on this issue, since the cost of catenary line is usually given per length in [USD/m]. Yet, here it has be chosen to work per weight to take in consideration both the length of chain and its size to represent the cost evolution with turbine size. In the end, the cost evaluation have been based on a very important document for our cost assessment: the forecast made by BNEF on future cost of FOW [17]. In thus study, they present a benchmark project of a 15 MW floating turbine in oceanic

condition moored with catenary lines at a depth of 200 meters. In order to match our mooring cost with the one from BNEF, we end up using per weight chain cost of 1800 USD/ton. In the previous section, the cost of steel assumed was 1200 USD/ton. We end up with a chain cost 50% higher than raw steel cost. Since chains are integrally made of steel and relatively simple to manufacture, this value seems totally acceptable. The specific cost of our catenary chain used for every depth, turbine size and condition will be $C_{chain} = 1800$ USD/ton.
The final cost of the catenary mooring has thus be assessed and the results from the model will be presented and discussed in subsection 2.4.4.

Let's now have a quick word on anchors. The type of anchor more suited for a FOW project will depend on the mooring technology as well as the seabed conditions. A range of anchor types have either been deployed or are being considered for deployment at early FOW pilot farms and demonstrators (cf [59]). For catenary moorings , the most common anchor type used is the so called drag embedment anchor, some of which are represented on the deck of an anchor handling vessel on figure 2.76.

Figure 2.76: Drag embedment anchors

These anchors technology appears as the less complex one and actually corresponds to what come in mind while talking about anchors since the principle is the same as the one use for ships. Its design comprises a shank and fluke configuration that is set, when deployed from a vessel and dragged along the seabed, to penetrate the soil. The positioning of the fluke is such that, once embedded, the anchor has a high horizontal holding

capacity and is thus perfectly able to maintain the end of the catenary chained lying on Seabed. No complex installation is required and only gravity and friction are at stake here. Plus, the large mooring radius of the catenary configuration makes the part of the chain lying on seabed participating to the drag anchoring effect. The exact sizing of this type of anchor is thus complex and project leaders usually remain very conservative since the cost of this anchors is really negligible compared to catenary lines. In our study, the anchoring cost for catenary line will be neglected.

2.4.3. Taut Moorings

A similar discussion will now be led for taut moorings, that will be integrated to the physical model of a tension leg platform initiated in subsection 2.3.2. As already explained there, TLP are mooring stabilised and thus moorings and anchors are really critical components of TLP design.
As for catenary configuration, distributed mooring points will be adopted. Yet, it is common to multiply the number of mooring lines per mooring lines for two reasons. First, the technological development of wires or ropes dedicated to TLP floaters is still at its dawn and technological solution able to undergo on its own restoring forces are not mature enough. Designers must also be careful to select mooring lines with the appropriate level of elasticity for the local environmental conditions to ensure that the system will not be overloaded by the site's wave characteristics This sector R&D has thus been widely invested by industrial actors, as for example the company dynamical ropes [88] which develops state of the art mooring ropes solution. Then, the multiplication of mooring lines per point is due to redundancy necessity. Indeed, a potential failure of a single mooring line for a TLP platform would be dramatic and could lead to to the sinking of the platform, while in the case of a SS the platform is set to remain stable even in case of chain failure.

Many mooring are thus considered in our model, symmetrically attached between the four columns, the same 4 columns free floating TLP being under scrutiny here (cf figure 2.41. At least 12 moorings considered, which means at least 3 per columns. In our model, for greatest external loads and biggest turbines (35 MW turbine in oceanic conditions), 20 moorings lines will be used. The sizing of the moorings will be made on the restoring and over-buoyancy loads on moorings as displayed in output of the models on figures 2.60 and 2.61 in the physical model subsection 2.3.2. The dragging forces required for maintaining the structure in position are here neglected in comparison with these restoring and over-buoyancy forces.

The arrangement of a taut mooring is less complex to describe that catenary one. Indeed, as described on figure 2.77, we only have a tensed line linking the mooring point on the floating platform to the anchor at seabed level. The mooring angle Φ usually vary between 0° and 45° as explained in [86] and will influence the mooring length. As highlighted in red on figure 2.77, this angle will be assumed to be equal to 35° in our model, which is a representative value of general FOW projects. Re-using the notations from catenary arrangement (cf figure 2.73), the length of the mooring line will depend on depth as described by equation 2.22:

$$L = \frac{h}{cos(\Phi)} \tag{2.22}$$

The cost of the mooring will of course be proportional to its length and thus directly proportional to the depth.

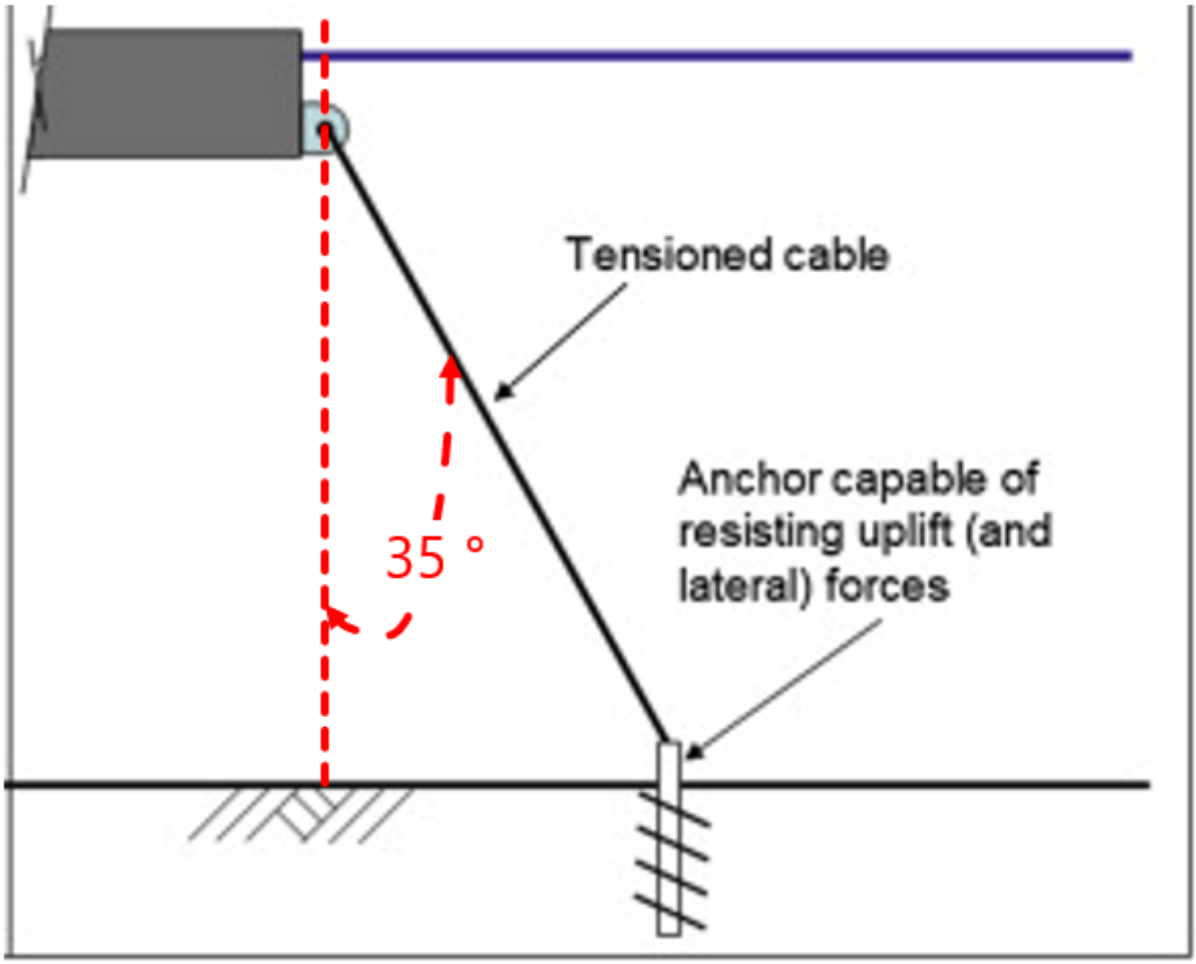

Figure 2.77: Taut Mooring arrangement

It will be assumed as previously that the total cost of the mooring line will depend on its total weight to account for both its length and its size, the latter being representative its ability to undergo higher loads. The length dependence on depth having been previously assessed, the link between load undergone and linear weight [kg/m] must be found for taut moorings.

This characteristic will heavily depend on the material used for the moorings. In the Oil&Gas sector as well as for first TLP pilots disclosed, steel wire ropes were usually used for taut moorings configuration. Like chains, wire rope mooring lines are also fabricated from steel, though they provide advantages over chain in terms of both weight and elasticity properties which make them suited to taut configuration, whilst offering the same breaking point. However, wire ropes are more susceptible to corrosion and damage, and usually need to be coated with a synthetic lining in order to improve their durability which increase their cost (cf [59]). By comparison, synthetic rope offers a more novel mooring line material option. It is regarded by developers as a promising technology that could enable future FOW cost reductions, but with further qualification and development required in order for it to reach full maturity for FOW applications. Synthetic material options include nylon, polyester and high-modulus polyethylene (HMPE), with each displaying varying material properties. Advantages are expected in terms of weight and fatigue performance, as well as reduced material and installation vessel requirements. Synthetic rope is considered to be well suited to taut configurations and less cost sensitive to depth than steel, hence it could be a preferred mooring material for TLP substructures and deeper water FOW farms. Additionally, it may offer potential benefits for very shallow sites where the hydrodynamic conditions require a mooring system with less stiff material properties.

Synthetic ropes thus seem to lead the way for future FOW projects, even if hybrid technology (steel + synthetic) could also be interesting in the future according to [89]. Between synthetic materials possibilities, polyester ropes will be used based on interesting corrosion and cost characteristics described in [89].

Once this choice is made, the sizing of the moorings regarding the restoring and overbuoyancy forces can be done. To do so, the characteristics of the specific "MoorLine Polyester Parallel laid, polyester sub-ropes encased in a polyester jacket with an integrated particle filter system" ropes proposed in The Bridon-Beckaert catalogue (synthetic ropes manufacturers, cf [19]) have been used as based. Indeed, the synthetic ropes manufacturers provides a table with a large spectrum of ropes diameter and their associated unit weight W_{taut} [kg/m] and Maximum Breaking Strength (MBS, the maximum load the rope can undergo without failure) [MN]. This table is displayed on figure 2.78.

Based on this table, for every turbine size and in both external conditions, restoring and

over buoyancy loads are computed and reported to a single mooring and the diameter of this mooring is chosen based on the MBS criteria. A safety factor of 3 is introduced, higher than the catenary case since mooring failure are more critical for TLP solutions. When turbine size rises, and do do cable loads, bigger diameters are chosen. Once the maximum value of diameters offered by Bridon-Bekeart is exceeded, 4 moorings lines (one per column) are added and the loads can be thus more widely balanced and lower diameters can be chosen. Of course, the final mooring cost will be proportional to the number of moorings $N_{moorings}$.

Only the specific cost per weight of the synthetic ropes is thus needed to close the cost model of the taut moorings. Since as previously explained synthetic moorings are new technologies few industrial data are available on cost. Yet, the rope supplier Huyuanrope certified by DNV [90] sells Polyester ropes with similar characteristics at costs varying in a range of [1 USD/kg ; 4 USD/kg]. Then, if we apply the same reasoning as previously for catenary moorings, in order to match our mooring cost with the one from BNEF benchamrk of 15 MW floating turbine in oceanic conditions[17], we end up using per weight synthetic rope cost of 3.6 USD/kg. This value is in accord with the previous range get from industrail supplier, it will be adopted as our synthetic rope specific per weight cost $C_{rope} = 3600$ USD/ton.

The total cost of the moorings is thus given by equation 2.23

$$C_{taut-moorings}[USD] = N_{moorings}.L.W_{taut}.C_{rope} \tag{2.23}$$

Diam (mm)	Linear weight (kg/m)	MBS (MN)
138	12,2	4,9
149	14,3	5,9
160	16,4	6,9
169	18,4	7,8
178	20,4	8,8
187	22,5	9,8
195	24,4	10,8
203	26,5	11,8
213	29,4	12,8
219	31,3	13,7
226	33,4	14,7
234	35,6	15,7
240	37,5	16,7
248	39,5	17,7
254	42,5	18,6
260	44,6	19,6
266	46,5	20,6
271	48,5	21,6
277	50,7	22,6
282	52,7	23,5
290	55,8	24,5
295	57,9	25,5
300	59,9	26,5
305	61,9	27,5
310	64	28,4
315	66	29,4

Figure 2.78: Polyester ropes characteristics from Bridon-Bekeart catalogue [19]

Let's now deal with anchors for taut moorings used for a TLP. Unlike catenary moorings used for SS, anchors in taut configuration are key elements of the global design since they participate to the restoring moments of TLPs. Plus it will have to undergo the integrity of cable loads since there is no part of the mooring line lying on seabed participating to anchoring phenomenon. Simple drag embedded anchors previously describe are not design to deal with vertical loads, and does not provide a sufficient level of reliability. Various others technologies can be used, as vertical load anchors or pile driven anchors, but it will be assumed that suction pile Anchors, considered as more reliable, will be used in our model. As explained on figure 2.79, water is pumped out of the pile during the installation process in order to create a vacuum. This pressure difference causes the anchor to become embedded into the seabed. The suction pile offers advantages over the driven pile in that it allows for easier installation and decommissioning, with reduced environmental impacts. Combined to lower footprint on seabed of taut configuration, this tend to reduce at its minimum the TLPs impact on submarine ecosystem while in operation.

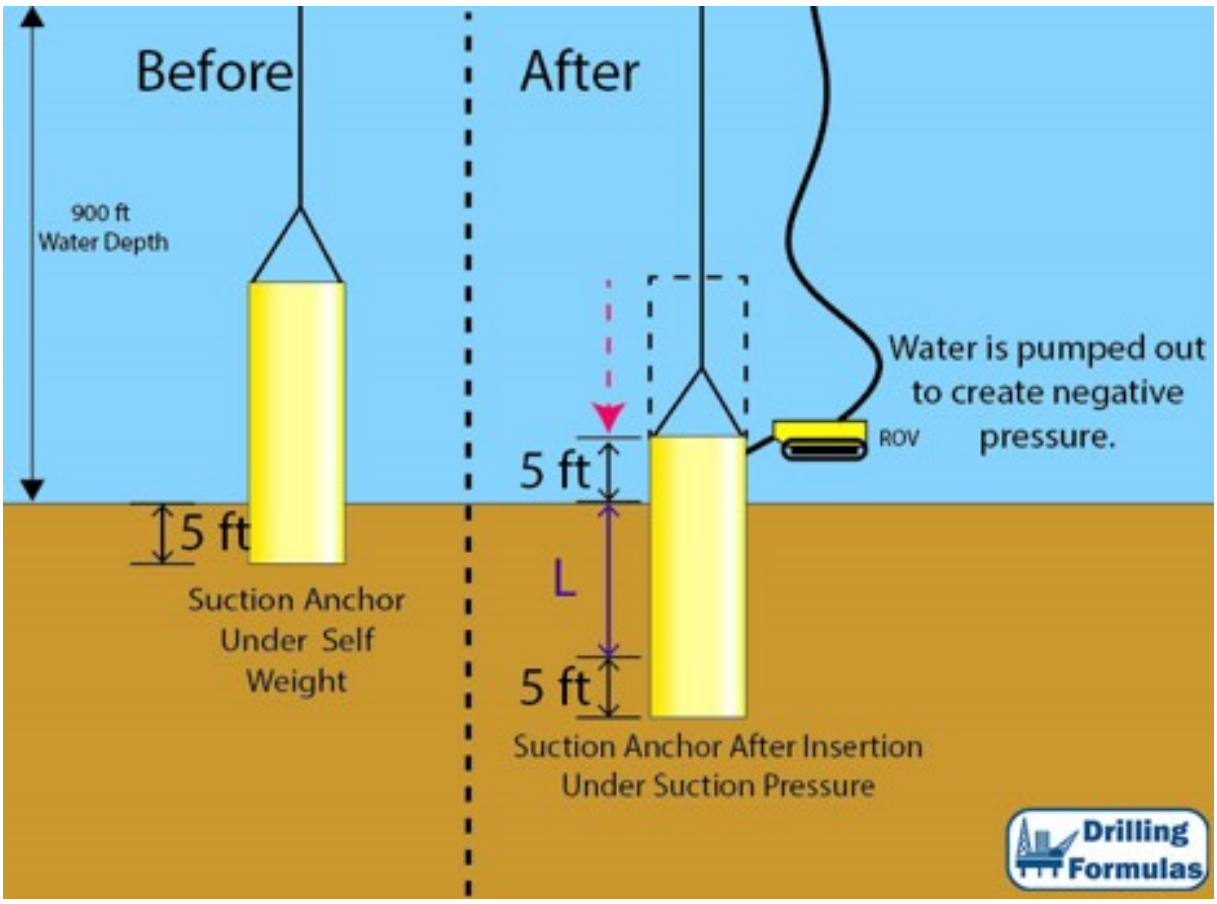

Figure 2.79: Drag suction anchors

Regarding the importance of anchors for taut configuration, and since the technology used are way more complex and heavy than drag embedded anchors, anchors must be considered in cost assessment of a TLP. Actually, the design of anchors require precise and holistic studies from the developers that will be simplify here only to remain coherent with our forecast model. Two hypothesis will drive our cost assessment of anchors:

- First, depth will not influence anchor size and cost. Instead, its cost will be exactly proportional to sum of cables loads computed in physical model.
- Since proportional to one only parameter, one cost value for a given cable load is enough to finish the anchor cost assessment. As previously, this value will be taken out of [7] where a specific anchoring cost of 75000 USD/MW is assumed for a 15 MW taut moored concept in oceanic conditions.

The cost of anchors is thus assessed for every turbine size in both conditions, independently of site depth.

2.4.4. Model outputs for moorings and insights

In a similar approach than the one led in 2.3.2 for platforms, let's analyse the outputs of our cost model for the moorings and anchors of part of SS and TLP concepts. Both for catenary and taut moorings, three parameters influences the price in the following results: the depth, the external conditions and the turbine size.
Firstly, catenary configuration are put under scrutiny and model outputs are displayed on figure 2.80 with the Mediterranean graph on the left and the oceanic one on the right. As expected, catenary specific costs are clearly proportional to depth, with sharper increasing trends for smaller turbines. The cost remains constant between 100m and 200m depth because shallow waters hydrodynamic requires twice bigger mooring radius as explained earlier in subsection 2.4.2. Then, as expected and similarly to the platforms results from subsection 2.3.3, moorings specific cost are higher in oceanic conditions since bigger chains are required to undergo the greater external loads. Finally, clear economies of scale due to introduction of bigger turbines are witnessed in both cases, with a even bigger gap between specific cost when depth increases.

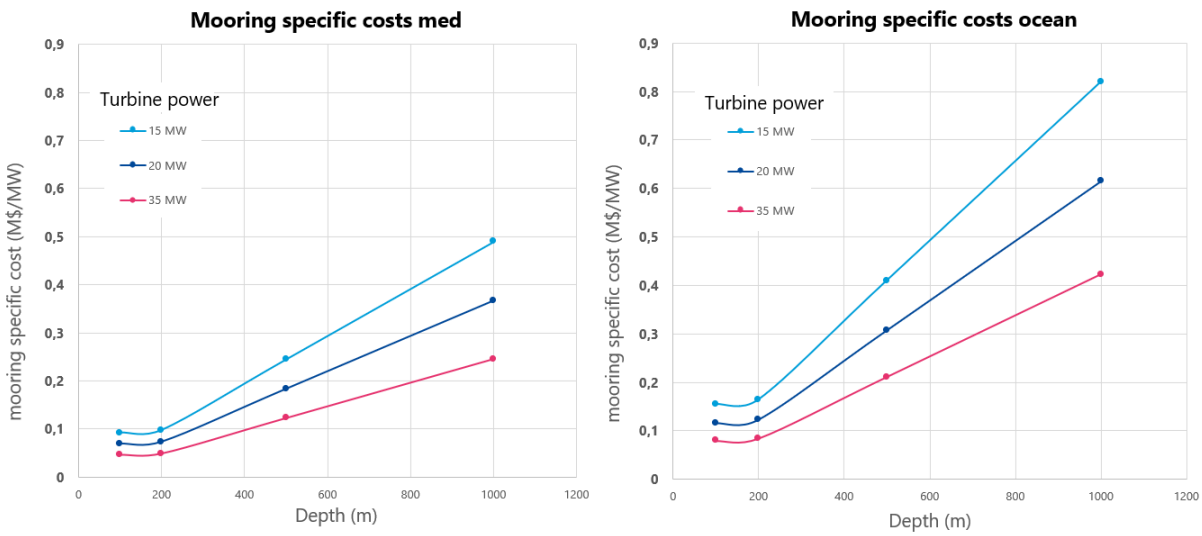

Figure 2.80: Catenary mooring specific cost evolution with depth

As explained earlier, in subsection 2.4.2, anchors costs are neglect in catenary configuration. However this is not the case for taut configuration where suction anchors cost are more important. The cost model outputs for these anchors are displayed on figure 2.81 with turbine size in abscissa axis since as explained in subsection 2.4.3 it is assumed that depth has no influence on anchors cost. As always, specific costs costs are lower for Mediterranean conditions and economies of scale are witnessed with use of bigger turbine.

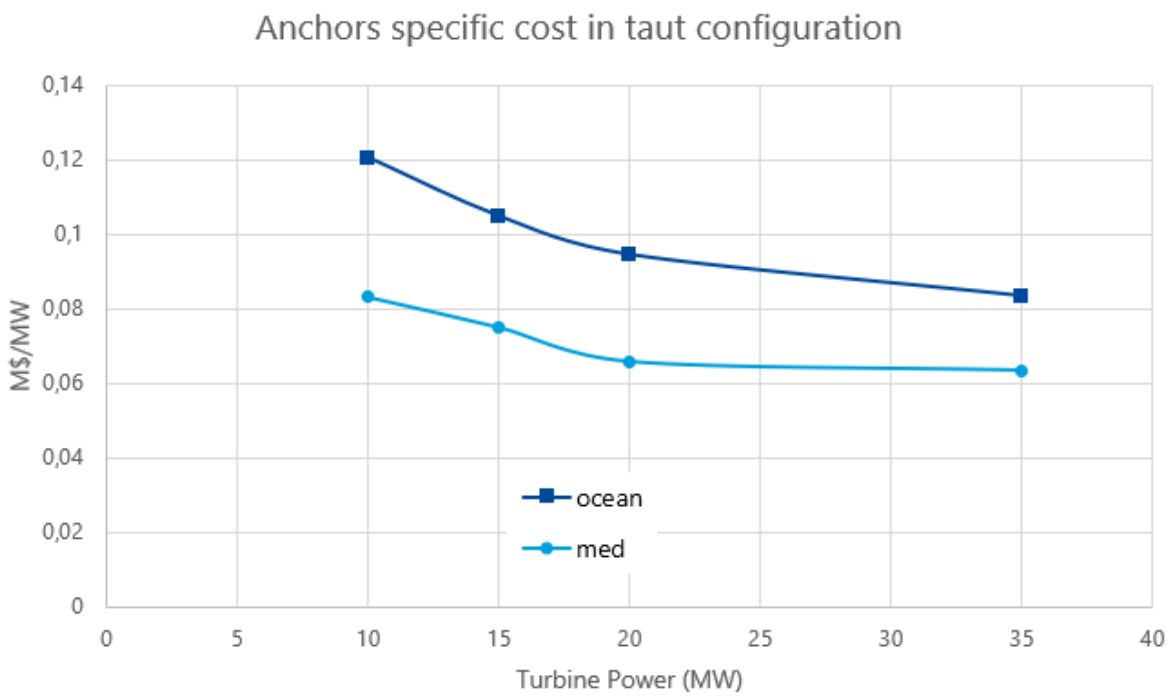

Figure 2.81: Anchors specific cost evolution with turbine size

These anchoring costs are included in the TLP related results, i.e; taut moorings plus suction anchors. Results displayed on figure 2.82 with Mediterranean graph on the left and oceanic one on the right are conform to expectations. Indeed, linear increase with depth are found and higher costs for oceanic conditions for the same reasons as for catenary outputs. Unlike catenary results, no huge economies of scale are witnessed and the increasing trends are more or less similar for every turbine size. The linear functions witnessed on the specific cost per depth graphs are characteristics of the anchor + mooring configuration: anchoring cost is the constant that does not evolve with depth while linear price of the rope are driving the increasing trends.

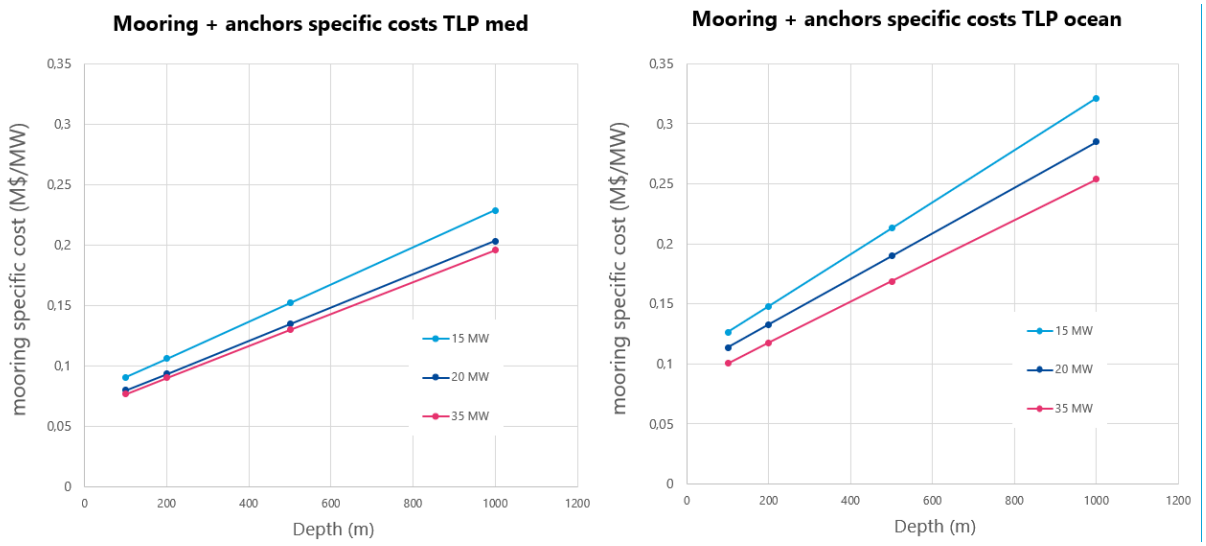

Figure 2.82: Taut mooring specific cost evolution with depth

The behaviours of taut and catenary moorings were thus similar with higher economies of scale and sharper increasing trends with depth for catenary solutions. The sensibility to economies of scale for SS solution (considered in catenary study) were also witnessed in subsection 2.3.3 on platform side. Then, the sharp increase with depth tends to corroborate the idea summarised on figure 2.72 explaining that chain catenary configuration were not cost effective for deep waters sites. The outputs of the cost model for both mooring configuration were thus conform to expectations, let's now compare these two solutions. The results of the cost model are displayed for oceanic and Mediterranean conditions respectively on figure 2.83 and figure 2.84 with catenary graph on the left and taut one on the right.

The main insights from these comparison are common to both conditions: First, at small depth, specific costs are similar between taut configurations and catenary ones. For big turbines, since as already pointed out catenary configuration benefits from higher

economies of scale than taut ones, catenary solution even end out a little cheaper for a 200 meters depth project. Yet, as expected, chain catenary specific cost is way more sensitive to depth than taut one. For depth about 500 meters, taut configuration appears more cost effective, while for even deeper waters (until 1000 meters) a chain catenary configuration seems out of question, even benefiting from economies of scale for bigger turbines.

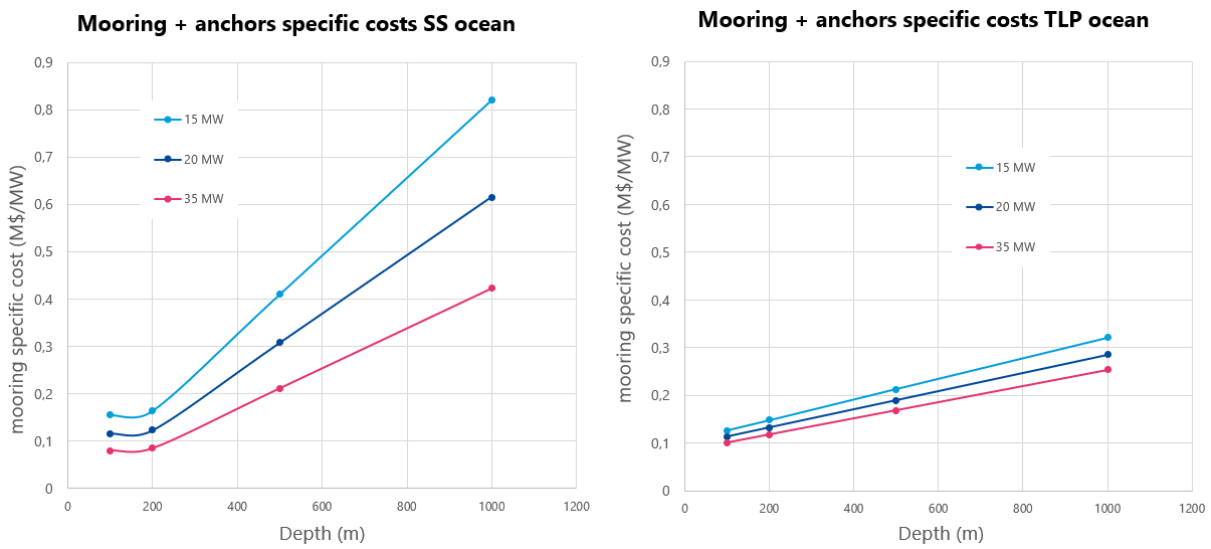

Figure 2.83: Comparison total specific cost of taut VS catenary solutions for oceanic conditions

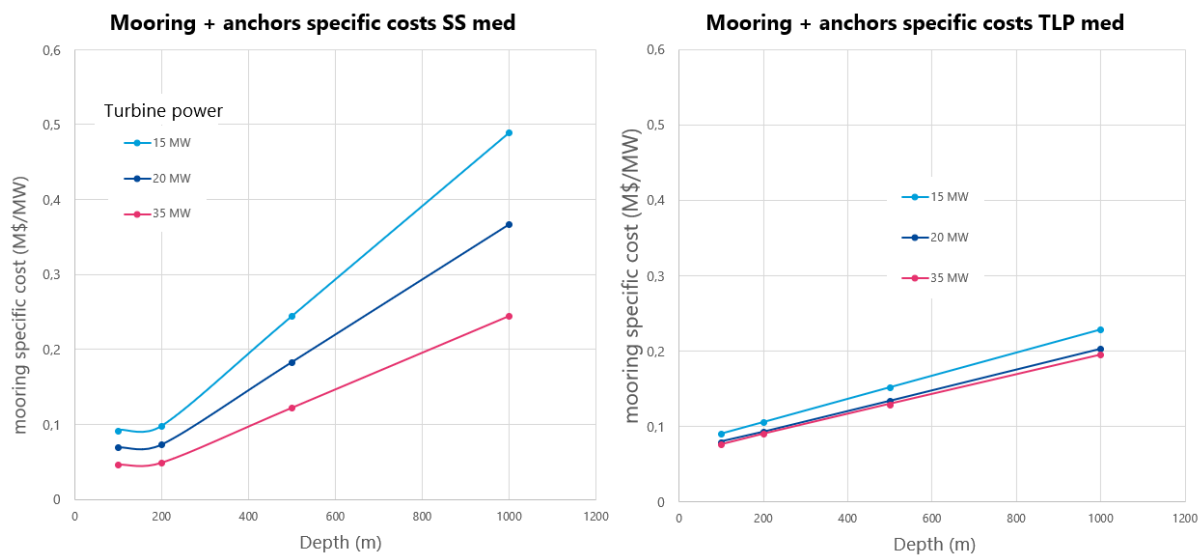

Figure 2.84: Comparison total specific cost of taut VS catenary solutions for med conditions

The main insight from this cost model outputs analysis is thus that taut configuration clearly overpass catenary ones for deep waters. This corroborates the indicated range of application summarised on figure 2.72. Adding this potential cost saving in terms of mooring to the ones linked to platforms highlighted in subsection 2.3.3, TLPs platforms appears as the most cost effective solution for deep water sites (this will be confirmed later on in 2.8 when every other cost drivers, notably the installation one, will be assessed).
Besides, at it will be seen in chapter 3, the Mediterranean features deeper seabeds than ocean and north sea near the shore. Heading back a little to our problematic on Mediterranean potentialities of FOW, the main insight from the cost model on platforms, moorings and anchors TLP could appear as the most cost effective for the Mediterranean case. This question will be further discussed later on yet, at this point of the study, a first summary of the advantages and issues to overcome of the new-coming TLP technology and how it could change the Mediterranean paradigm are summarised in the two following figures: figure 2.85 where main pros and cons are detailed and figure 2.86 where failure condition is schematised, due to seismic activity or seabed deterioration for example.

Why TLP appear as the solution for mediterranean	What are the brakes to its development
Deeper Mediterranean seabed	Lower TRL
Smaller and thus cheaper platform	Smaller Mediterranean market: follow the ocean trends which feature lower depths
Zero tilt during operation	**Fatigue and corrosion issue on cables is more critical:** redundancy and O&M required
Free-floating design allowing towing to site	Anchors issue: more complex anchors are required + bigger dependance on **seabed instability**

Figure 2.85: Summary of TLP pros and cons

The main drawbacks related to TLP concepts are thus linked to more complex installation and moreover higher risks linked to potential critical moorings or anchors failure. These risks illustrated on figure 2.86 coupled to the one linked to corrosion can lead to insurance over costs and more maintenance activities, that could be reflected on LCOE calculation as it will be seen on LCOE. The lack of industrial feedbacks on the real importance of the risks could frighten investors and slow down the TLP development, already less developed than SS solutions.

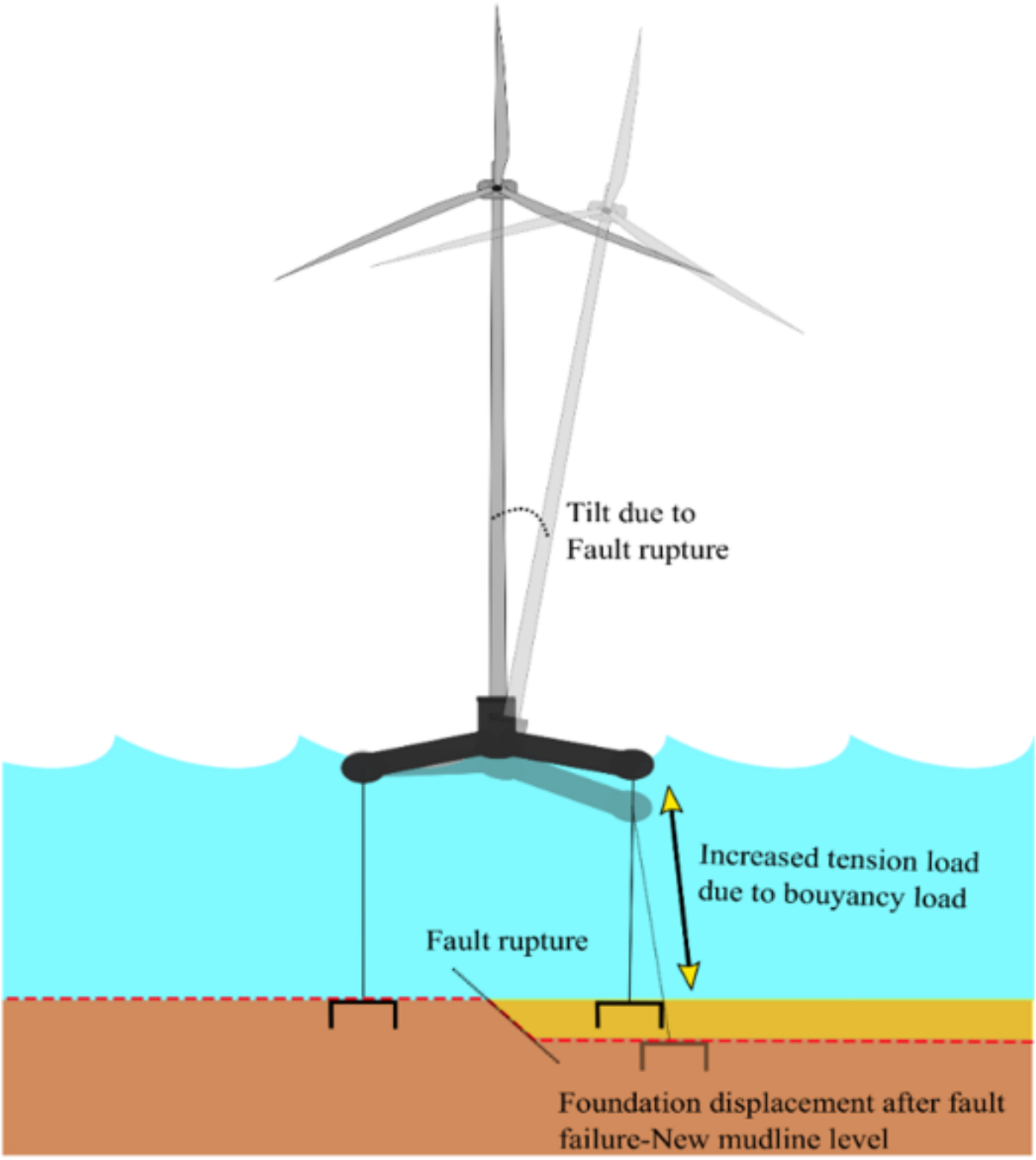

Figure 2.86: TLP failure configuration

2.4.5. Future development and innovative concepts

To close this discussion on moorings and anchors, let's have a glance at some innovative concepts that could help deal with intrinsic issues of solutions described here above. The three floaters concepts presented here after have been identified in the platform market overview of subsection from subsection 2.3.1, two have which (Gicon and Gazelle) have

been in contact with A2A to share information and assess potential future collaborations.

First, Gicon can be seen as one of the main TLP developers alongside SBM offshore. The R&D project started in 2009 and includes renowned partners such as TU Bergakademie Freiberg (Freiberg Technical University and Mining Academy), Rostock University and Fraunhofer IWES. Thanks to the continuous improvements based on results from research like extensive wind and wave tank tests, the GICON-SOF is ready to prove its capacities in a full scale multi-megawatt prototype [91]. A pre-commercial scale pilot is expected to be launched in the months to come in Germany (expected in the late 2023/early 2024). If the floater structure of course presents specific features, with a particular accent made on modularity and simple design of the platform, it remains close to what have been studies in the model with 4 column structures mooring stabilised. The main innovation is related to the use of gravity anchors coupled with a more simple installation process integrated to the structure, as described on figure 2.87. Gravity anchors rely on weight and seabed friction to provide a holding force. Developers may be more likely to select gravity anchors for taut configurations where the emphasis is on resistance to vertical loading [59]. Gravity anchors require hard seabed conditions, and their weight may present handling challenges and increase the cost of installation and decommissioning but still represents an interesting alternative to suction anchors.

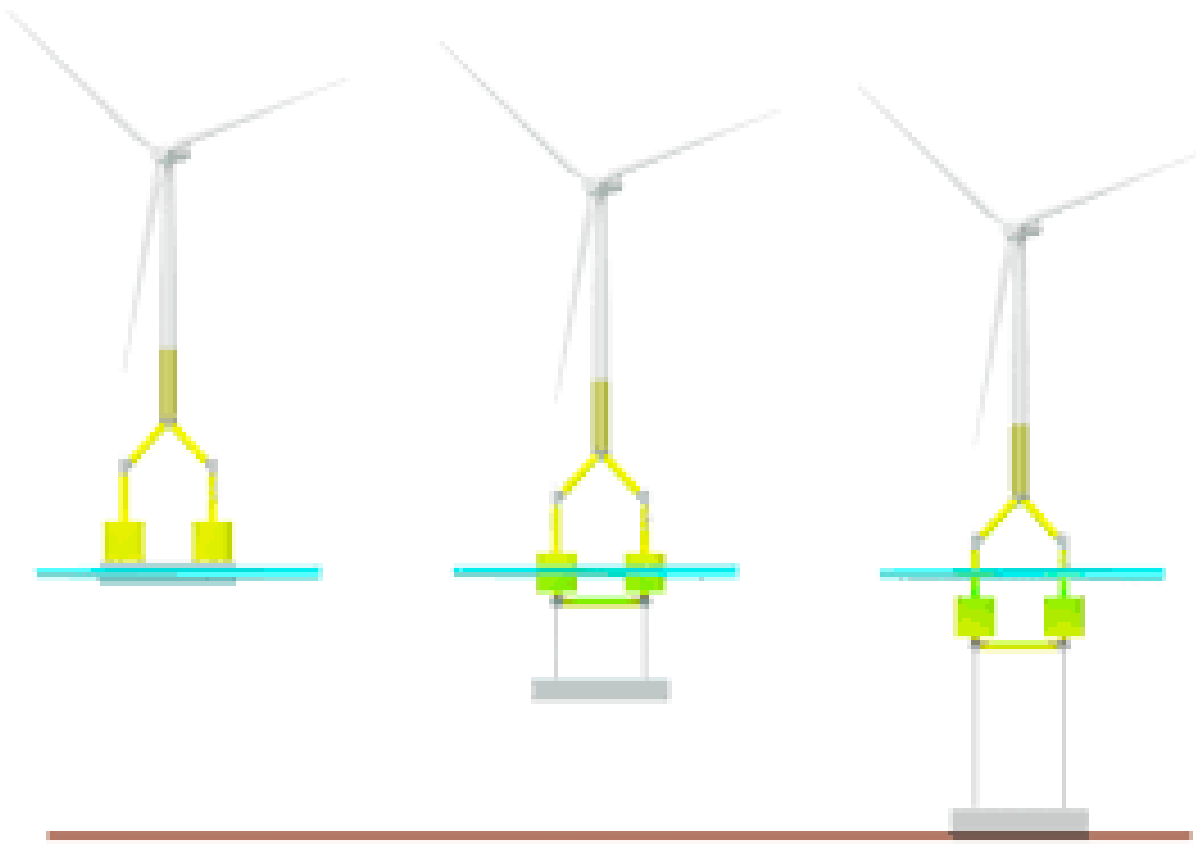

Figure 2.87: GICON TLP concept with gravity anchor

Then, Gazelle concepts is a way more disruptive concept, with thus a lower TRL, but presenting really interesting solution to the main TLP issue of risk and relying on qualified and experienced decision board [92]. As explained of figure 2.88, unique design responds to waves through the action of a central counterweight connected to tripodal arms anchored to the seabed. The geometry is such that the platform can move horizontally and vertically to minimise tilting. This mooring design has obtained DNV seal of approval and is set to decrease the moorings loads by at least 50%. Plus elasticity of moorings are less solicited which tends to decrease fatigue phenomenon.

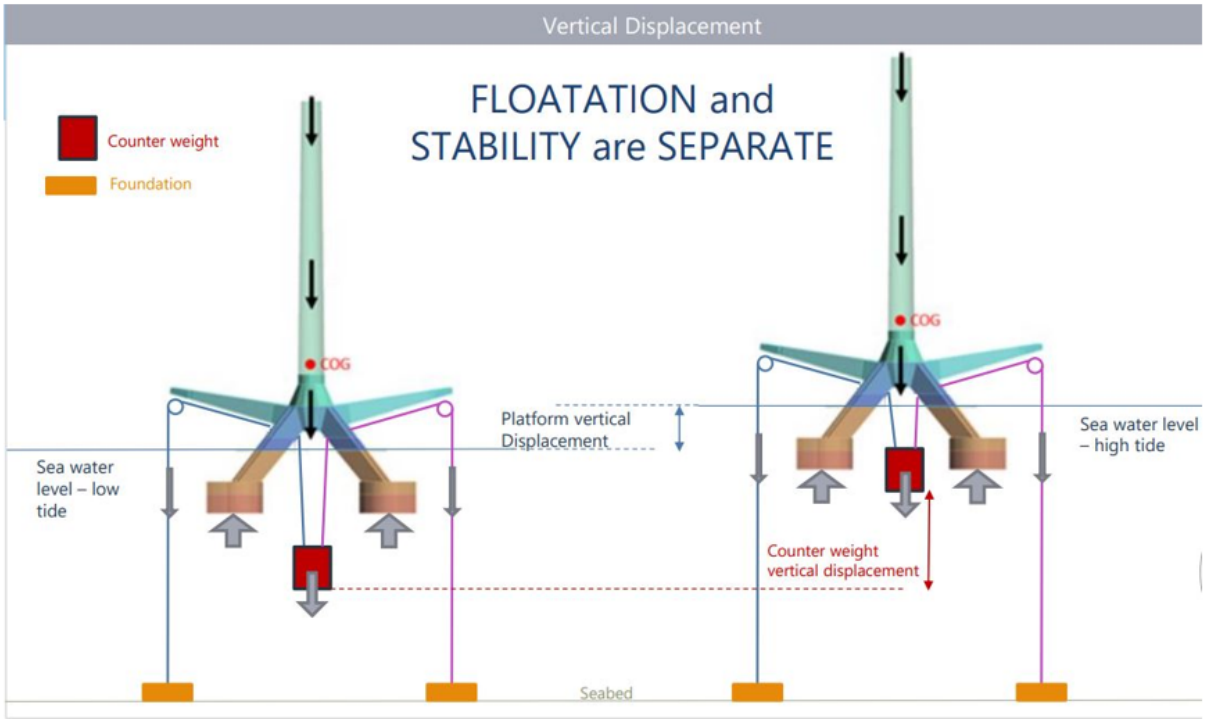

Figure 2.88: Gazelle TLP concept with counterweight mooring concept

Finally, the Sath design developed by Saitec [93] is a disruptive concrete based barge design represented on figure 2.89. In the mooring discussion, the main interesting feature relies in the single point mooring technology located at the front of the platform. The use of single point mooring solutions might offer future cost advantages and enable quicker substructure installation, as well as potential disconnection and re-connection for maintenance, for platforms that utilise catenary configurations. Single point systems include a buoy or "turret" that connect all of a FOW turbine's mooring lines to a single component, around which the FOW substructure is able to yaw passively into the wind. This natural yaw alignment with wind is also interesting since it can substitute the yaw systems included in turbines nacelle. Despite a proven track record in oil and gas, FOW single point mooring systems remain an early-stage technology, with spread mooring systems very much the more commercially advanced option [59].

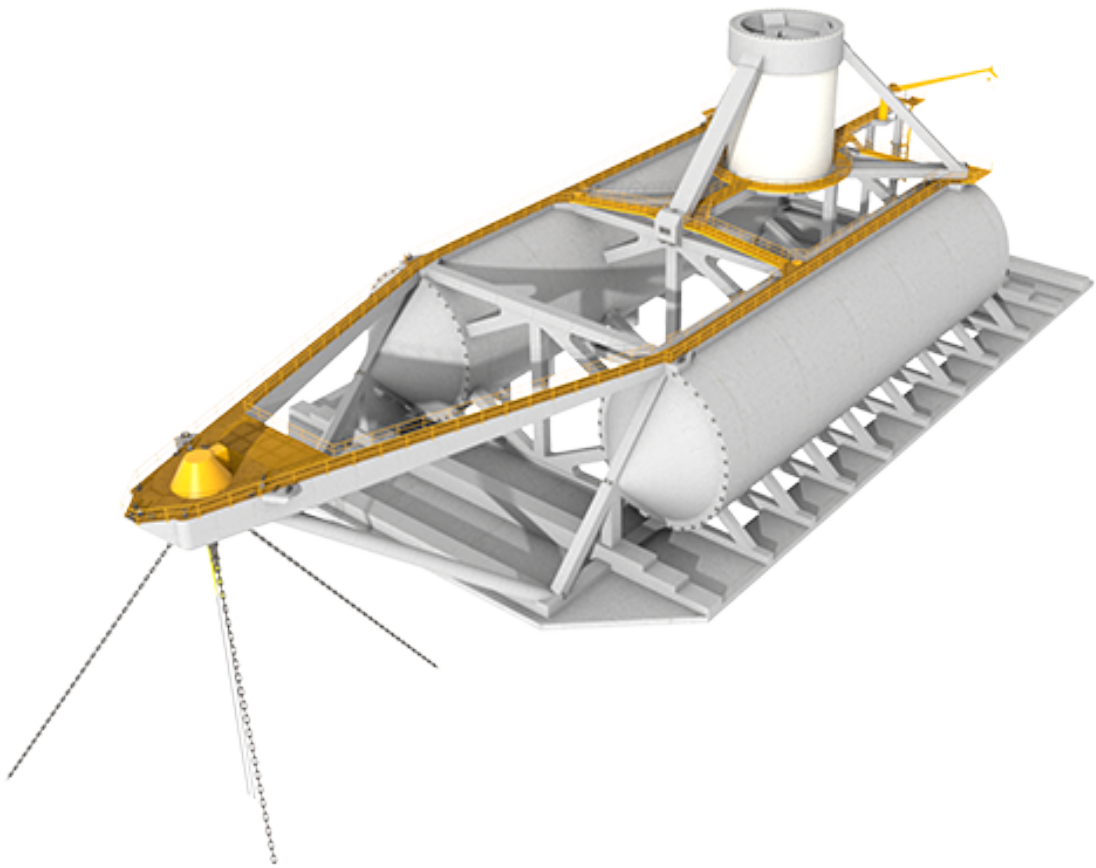

Figure 2.89: Saitec Barge concept with single point mooring system

2.5. Focus on connection to grid

From the technical documentation disclosed by developers describing FOW projects throughout the world and more particularly in Italy - projects counted in section 1.4 - a typical commercial scale offshore wind farm will include an offshore substation that houses the wind farm's major high voltage power electronics. The turbines in the array are connected to the substation via their inner-array cables (cf section 2.6) so that the inner-array voltage (33kV-110kV) can be transformed to a higher voltage (130kV-330kV) in order to minimise power losses during export to shore [59]. The general layout of a floating offshore wind dram is described on figure 2.90.

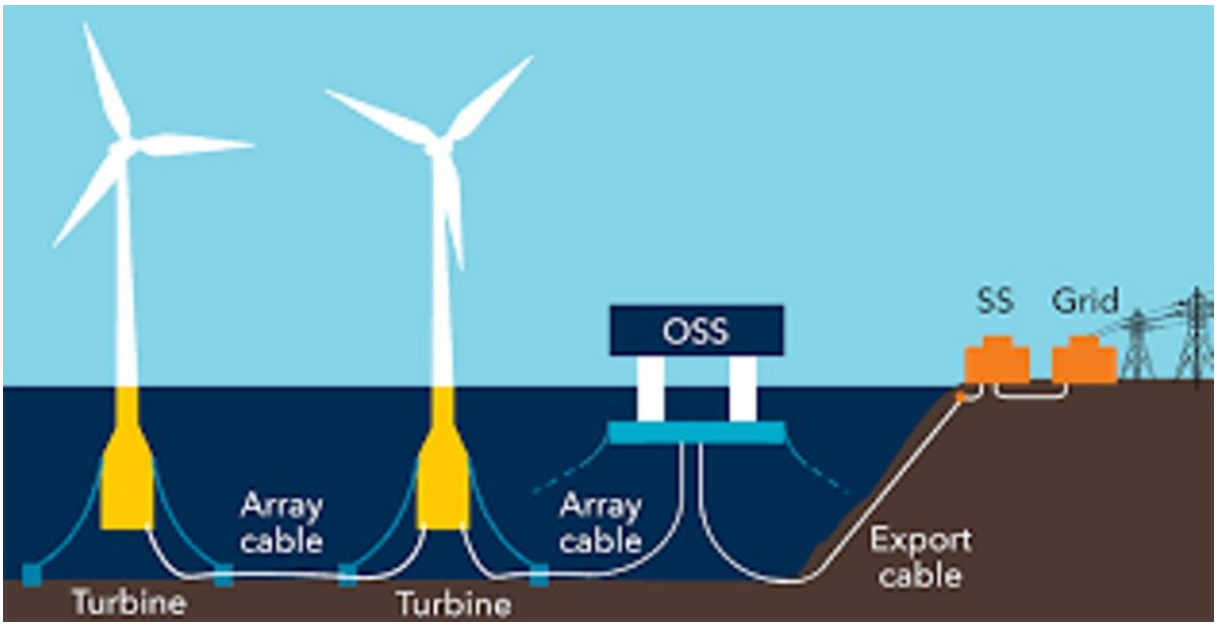

Figure 2.90: General floating offshore farm layout

In this section, cost related to export cable and OSS (offshore sub-station) will be assessed. Let's begin with offshore export cables.

2.5.1. Export cables

The issue of offshore connection the onshore grid is equal for fixed-bottom and floating offshore wind projects, more mature technologies and industrial feedbacks are thus available. Large offshore wind farms that are more than 10 km from shore are usually attached to an offshore substation that is then connected to an onshore substation via an export cable.Two main technologies of offshore connections: alternating current (AC) systems that transport electricity directly through AC cables; and direct current (DC) systems where the current is converted from AC to DC in converter stations and back to AC in the onshore substation before the electricity is supplied to a grid [5]. As shown in [17], HVDC cables have a lower linear cost than HVAC ones, and that is why they are heavily used for long offshore connections as for example the SACOI that links Corsica island with Italian mainland thanks to offshore cables longer than 100 kilometres. Yet, the use of HVDC requires bigger and more complex offshore substation since conversion from AC to DC and then from DC to AC requires more electronics devices as explained in [94]. The use of HVDC thus requires an expensive absolute investment that can be amortised with cable length in regard with HVAC technologies. This matter of fact makes HVAC more suitable for projects nearest from shore as described on figure 2.91 where range of

specific cost [$/kW] per distance to shore are given for HVAC in green and HVDC in blue. From this graph extracted from a cost study led by IEA, it appears that HVAC would be the preferable option for distance from offshore until 100 kilometres in terms of CAPEX. Very few FOW projects are set to be located this far from shore in the years to come, thus HVAC appears to be the best solution.

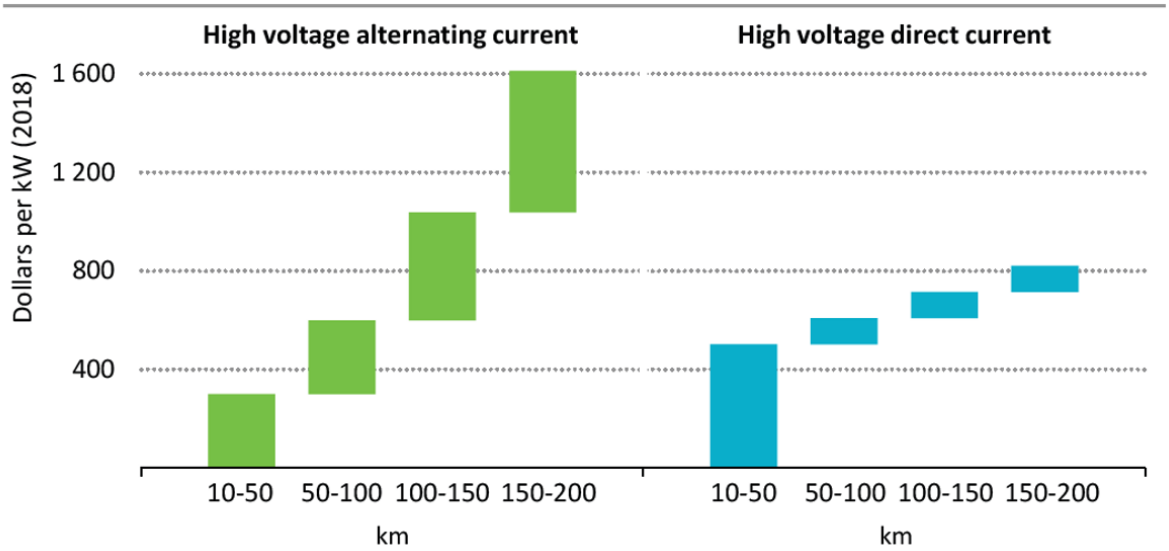

Figure 2.91: HVDC and HVAC connection technologies, from [5]

An other argument in favour of HVAC technology concerns the weight of offshore substation. Indeed, since more complex and requiring more electronic power devices, HVDC DC to AC conversion substation are way more heavy than substation required for HVAC technologies as proven by figure 2.92. This graph generated by BNEF clustered the weight of existing offshore substation of existing projects and it appears that HVDC substation can end up until three times heavier than substation used for HVAC connection. This weight issue becomes tremendous in the FOW sector since, as it will be explained in next subsection 2.5.2, no mature floating substructures concepts for OSS are available, and the heavier the OSS the harder it will be to provide satisfying solutions.

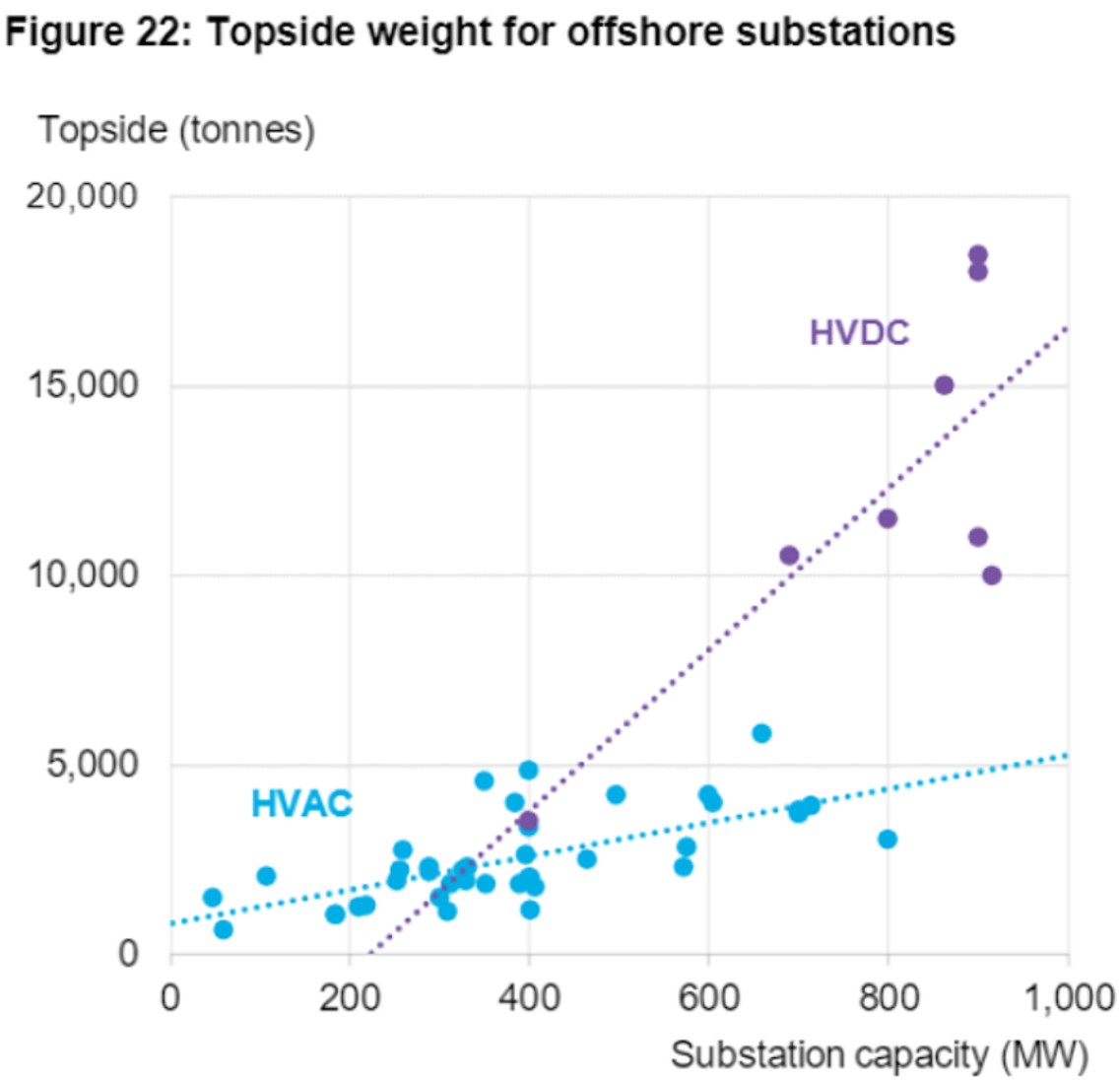

Figure 2.92: HVDC and HVAC OSS weight, from [17]

To end the comparison between the two technologies, let's have a look on transmission energy losses. The use of high voltage transmission technologies, that however lead to additional capital investment for an OSS, is motivated by the reduction of transmission losses. [94] leads an holistic study of these transmission losses for FOW projects and are thus also making a comparison between HVAC and HVDC. The losses depend on many phenomenon (level of maintenance of the cables, isolation with seabed, number and size of cables for a given rated power etc...) but the two main loss drivers are the cable length and the power flowing in the cables. General trends of influence of these two parameters on power losses are displayed on figure 2.93, where power losses are displayed, for both technologies, per percentage of rated power flowing in the cables on the left and per cables

length on the right. The main insights from this study are that for cable length smaller than 80 kilometres HVAC power losses are smaller than HVDC ones and then that HVAC has better performances in part-load operation. These two considerations confirms that HVAC appears as the best solution for FOW projects since distance from shore will rarely exceed 60 kilometres and then Win0d-farms work a certain amount of the time in part load operation (when winds are lower that rated wind velocity).
NOTE: these values of power losses will be computed in the next chapter for the calculation of LCOE of various projects.

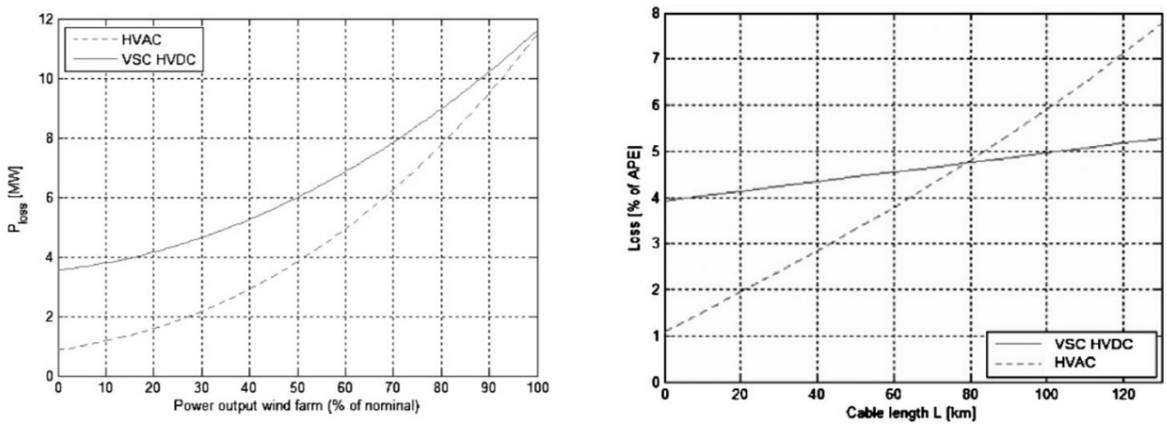

Figure 2.93: Transmission losses for HVDC and HVAC technologies

HVAC technology will thus be used in our model since most representative and most suited for FOW projects. The cost of HVAC export cables must now be assessed. Of course, as explained in [94] the cost of export cables will depend on their size (i.e. the power flows they can undergo), their numbers and finally their length. As already precised, more industrial data is available for export cable and thus the cost assessment of export cables will be directly based on industrial data clustered by BNEF in [17] and whose results are presented in a table on figure 2.94.

Technology	Voltage	Max distance (km)	Capacity rating (MW)	Cost for static cable ($m/km)
HVAC	132kV	250	200	1.2
	220kV	200	400	1.7
	400kV	70	800	2.3
HVDC	132kV	N/A	200	0.9
	220kV	N/A	400	1.3
	400kV	N/A	800	1.7

Figure 2.94: General characteristics of export cables based on industrial survey led by BNEF, extracted from [17]

A final choice must be made to close the export cable cost assessment: the rating of the HVAC cable used. Indeed, for a given output power output different choices can be made: either use one single cable sized for total rater or multiple smaller cables where power flows would be distributed in between. Many parameters enters in consideration in order to make this decision. First, cost consideration tends to favours the single cable option since as shown on table here above doubling the capacity rating does not double the price. The installation of one single cable is also expected to be easier. Yet, the same table also rises the maximum distance issue, that is link with complex electrical phase balanced phenomenon, and that favours the multiple cables solution. Then, redundancy necessity of the export cables is another argument in favour of the multiple cables solution: fish activity and corrosion can damaged cables and maintenance can be required, shuttering the whole production in case of single cable solution. Then other site related consideration, as the voltage of the onshore grid for example, can enter in consideration for this choice.

No clear technological truth thus existed on the number of cables to use and it is up to developers to make the best techno-economic compromise for every particular project. For our CAPEX evaluation model, our choice will be based on a review of existing and planned projects.

First, let's mention, Offshore Renewable Energy Catapult, an entity initiated by CrownEstate Scotland set to foster offshore wind power energy development in the UK by easing the share of information between industrial players, legislators and field experts. This entity is playing a leading role in stimulating innovation in offshore wind and his contribution is resumed in a wide "guide to offshore wind-farms" [23] redacted by the independent consulting cabinet BVG associates based on data shared by many industrial players involved

in fixed bottom offshore wind from various fields such as DEME Group, GE Renewable Energy, Fugro, Generating Better, Innogy, JDR Cable Systems, MHI Vestas Offshore Wind, Natural Power (Fred. Olsen), Oldbaum Services, Ørsted, Senvion, Siemens Gamesa Renewable Energy, Siemens Power Transmission and Distribution, SNC-Lavalin - Atkins, Vattenfall. The guide to an offshore wind [23] is thus very complete and share detailed and well-argued cost values for every cost drivers of a fixed-bottom offshore project. Thus, every time cost drivers of floating projects are common to fixed bottom offshore wind, this guide will appear insightful. This is the case for export cable where the problematic is exactly the same for fixed bottom and floating projects. It is clearly stated in the guide that for the numerous British projects "The industry standard for projects is now 220kV for HVAC export cables" [23].
Then, in France as previously seen projects operating, under construction or planned are heavily documented (cf [9]). In this domestic market which adopts a centralised development strategy the TSO RTE [39] is in charge of the offshore connection. For every commercial scale projects (over 400 MW), RTE will use 2 to 4 220 kV HVAC cables, going in the same way as Catapult guide.

The type of connection adopted in our CAPEX model will thus be multiple 220 kV HVAC cables. The numbers of cable (at least two for redundancy) used will depend on the farm nominal power. In [94] the nominal current of a 220 kV HVAC cable is $I = 1055$ [A]. The nominal power P_{cable} flowing through the cable, since tri-phased cables are used, is thus : $P_{cable} = \sqrt{3}V.I = \sqrt{3}.220[kV].1055[A] = 402[MW]$. This value is by the way coherent with the one extracted from BNEF table displayed on figure 2.94.
As it will be further described in CAPEX model global computational description in section 2.8 projects under scrutiny will be rated at 450 MW, 960 MW and 2100 MW. These projects will thus feature for offshore connection respectively 2 HVAC 220kV cables, 3 HVAC 220kV cables and 6 HVAC 220kV cables. NOTE: for the 450 MW project, the cumulative cables capacity will widely exceed the wind-farm rated output power. This could lead to CAPEX over costs, yet this will be in a way compensated in the final LCOE calculation since as shown on figure 2.93 cables will always work in part load conditions and will thus suffer less energy losses.

2.5.2. Offshore substation

Floating substations remain a low TRL concept (cf [59]) that is the focus of ongoing research projects, however it is believed that the substructure typologies being considered for FOW turbine applications could be successfully adapted for floating substations.

Currently, the low scale of existing pre-commercial floating wind-farms have no use of OSS and thus the only cost data available are issued from fixed-bottom offshore wind field. It will besides be assumed that OSS costs are equals for fixed-bottom and floating projects. BNEF gathered data of offshore substation cost per nominal power in the UK, and displayed the results on a graph reported on figure 2.95. Based on this graph as well as industrial data from [23] the specific cost value for OSS in our CAPEX estimation model will be $C_{OSS} = 0.2\$M/MW$.

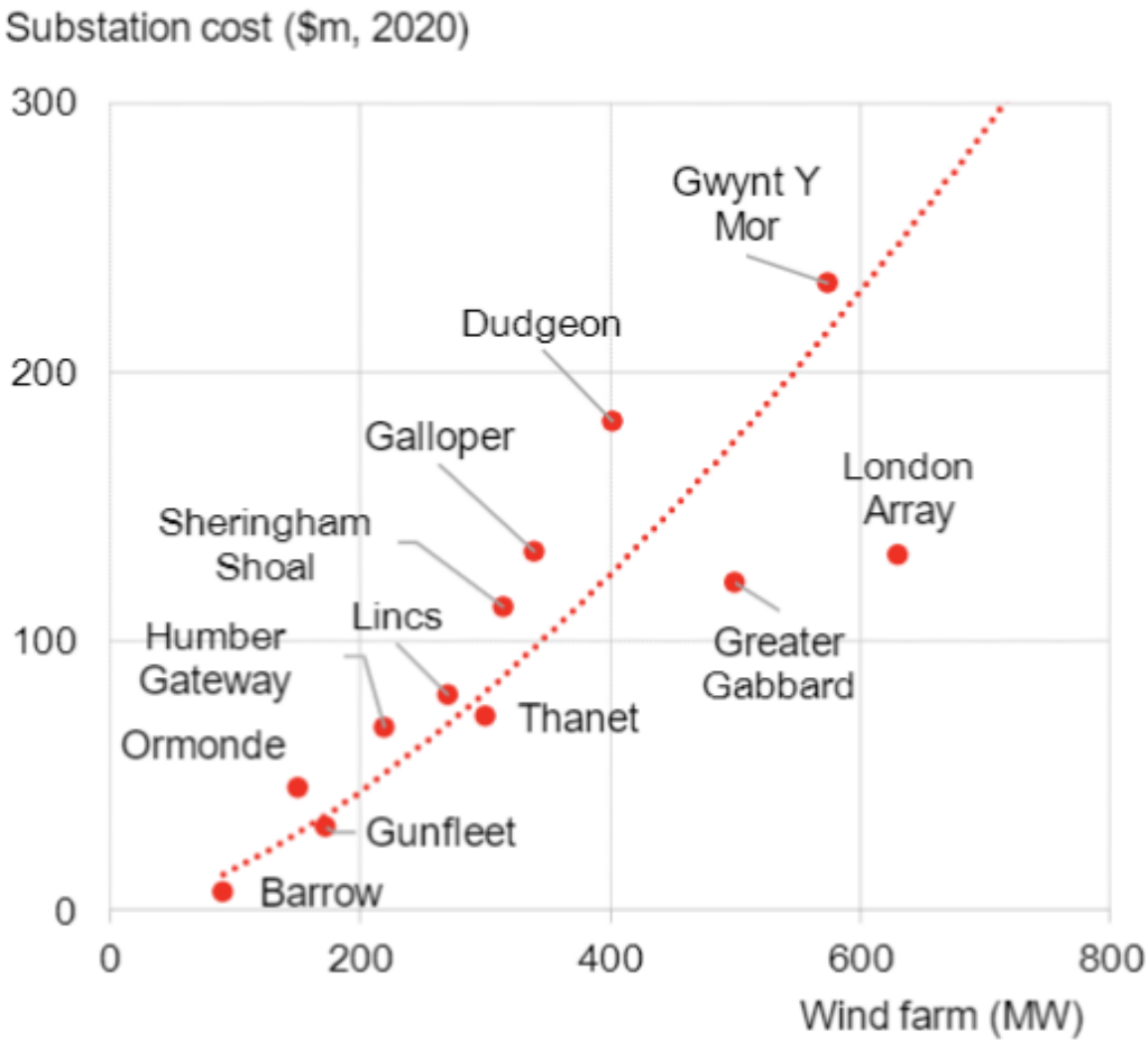

Figure 2.95: Bottom fixed offshore substation cost per nominal power in the UK, from [17]

If the OSS by itself can be assumed similar to one of kind used for fixed bottom project, this is not the case for the substructure. As previously explained, there is currently no mature concept of OSS floaters. This is due to the important weight of OSS : about

3000 tones for a 500 MW farm, i.e. 30 times heavier than a 10 MW turbine for which floaters are designed. Plus, the power electronic devices in the OSS are not set to undergo acceleration and tilting which could increase the failure rate. According to the depth of the side, huge fixed bottom substructure or even submarine OSS can be imagined, but could not be thought as general solution to the problem.
Important R&D is at stake to solve this issue. By now, Fukushima Kizuna demonstrator substation in Japan, displayed on figure 2.96, is the only operating floating OSS pilot. Installed in 2013, the prototype OSS was deployed to step the output voltage from the project's prototype floating turbine from 22kV up to 66kV for export to shore. Installed on a spar platform concept, the substation's transformer system was subjected to vibration and inclination testing prior to deployment to establish its suitability for floating applications. The project has demonstrated that a substation's high voltage power electronics can, in principle, operate successfully while undergoing accelerations due to floating platform motions [59]. However, further testing and qualification is required in order to scale up this technology from output voltages of 66kV to 250kV, and the economic case is yet to be proven in practice.

Figure 2.96: Fukushima floating OSS pilot, 2015, Japan

Classic floaters concepts designed for carrying turbines studied in floater section 2.3 could

then be adapted to OSS. That is the idea of the Damping-pool barge floating OSS concept developed by Ideol [61]. Based on BW Ideol's patented and shallow-draft Damping Pool concept, this floating offshore substation is engineered to operate in the world most extreme environments and to offer maximum modularity.

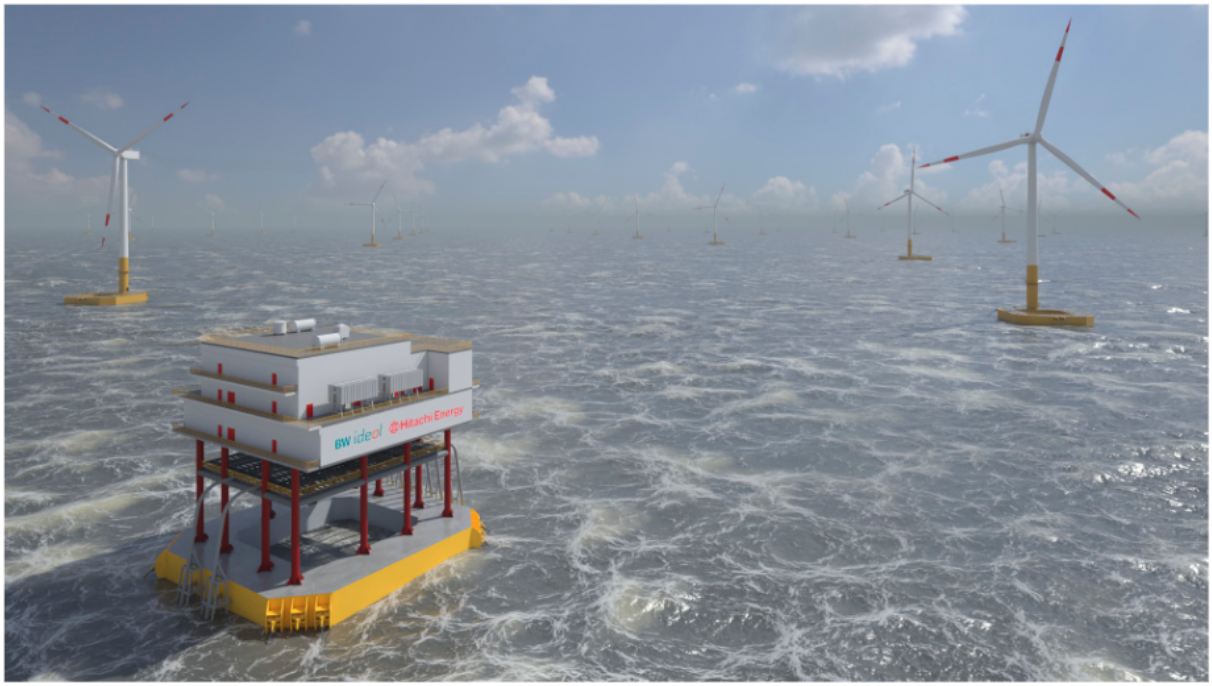

Figure 2.97: BW Ideol damping pool floating OSS concept

This issue is set to be solved in the years to come, even if cost optimisation of the solution is not reached from the outset. In our cost model, to take account of this cost drivers, hypothetical huge floaters have been assessed starting from the bigger platforms modelled in our work: 35 MW SS for offshore turbine. The floater price of the 450 MW rated OSS will be thus twice the price of 35 MW SS floater, the one of the 960 MW rated OSS will be thus 4 times the price of 35 MW SS floater, and the one 2100 MW rated OSS will be thus 8 times the price of 35 MW SS floater.
Actually, as it will be seen in the CAPEX summary in section 2.8, even if the floaters cost are huge, once reported to the nominal power of the wind farm, the specific cost of the OSS floater [USD/MW] is not that important.

2.6. Focus on inner-array cabling

A major component of a wind farm's electrical infrastructure is the inner-array cabling that provides the electrical connection between each of the turbines and the offshore

substation. Groups of turbines can be connected to the OSS either in strings or loops, as determined during the array optimisation design phase. As explained in [95], In an offshore wind farm (OWF), the turbines are connected to a transformer by cable routes that cannot cross each other. Finding the minimum cost array cable layout thus amounts to a vehicle routing problem with the additional constraints that the routes must be embedded in the plane. Plus, constraints links to the size of rotor, redundancy, losses from the inner cables and string capacity (cf figure 2.99) enter in consideration.
Inspired from the optimum path described in [95], the layout of inner-array route used in our model will follow the template described on figure 2.98. In this configuration, the OSS is located at the front of the wind farm to minimise the export cable length, and then a symmetry axis is generated between the left and the right part of the wind farm, with similar same number of strings on both size, and with same number of turbine on both size. The total route (plan distance) of cables will thus depends on the number of strings $N_{strings}$, the number of turbine per strings $N_{Turbines_{per_{string}}}$ and the distance d between two consecutive turbines. This distance d is assumed to be the same in both direction on the plane and is an empirical value depending on rotor diameter in order to minimise the wake losses (cf chapter 3). From [5], we get that the classical value for d is $d = 8 * D_{rotor}$. The route length of the inner cable array is thus defined by equation 2.24:

$$L_{route} = N_{strings} * (N_{Turbines_{per_{string}}} - 1) * d + \frac{N_{string} * (N_{string} - 1) * d}{4} \tag{2.24}$$

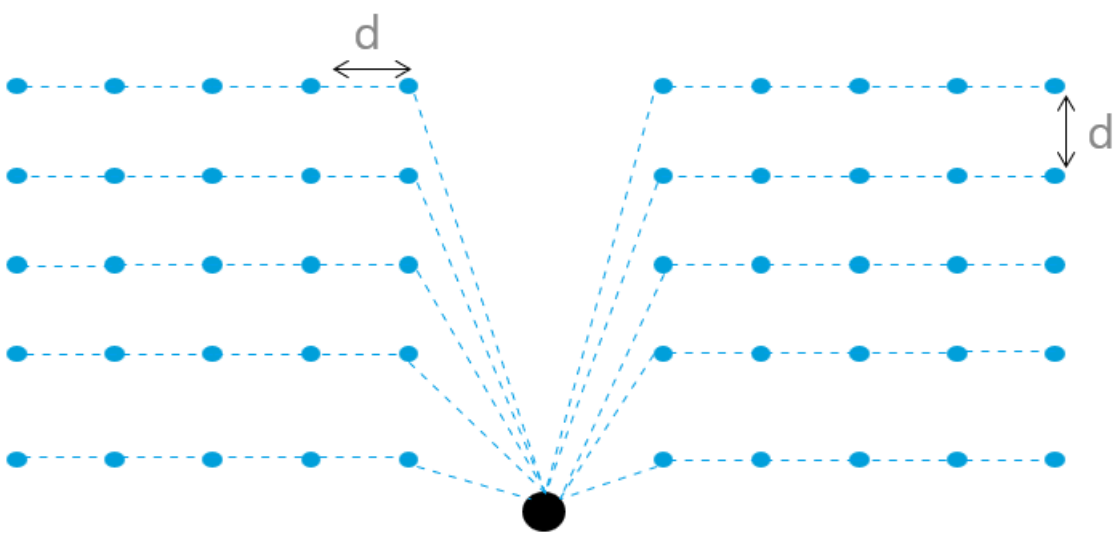

Figure 2.98: Layout of the general electrical array considered

The maximum number of turbine sharing the same cable depends on the cable capacity and turbine power. First, inner array cables used for offshore projects were rated at 33 kV, for a power capacity of about 40 MW according to [17]. While bigger turbines used were lower than 8 MW, a 33 kV rated cable could thus allow at least five turbines to be connected in string. According to the fixed-bottom guide from Catapult [23], array cables are now typically rated at 66kV since after first generation of offshore wind farms typically using 33kV, the high voltage has been a major focus of technical development because they enable more capacity to be connected on a single string, reducing the length of cable required and reducing the number of switch-gear bays needed on the substation. BNEF generated an insightful graph displayed here on figure 2.99. BNEF assume, and these assumptions will be used for our model, that 33 kV cables are rated for 40 MW, 66 kV for 80 MW and 110 kV for 120 MW.
In our model, projects using 15 MW and 20MW turbines will have inner arrays rated at 66 kV, allowing respectively 5 and 4 turbines per string. For future projects using even bigger 35 MW turbines, it will be assume that 110 kV or even 132 kV (cf [76]) rated inner array will be used in order to allow 5 turbines per row.

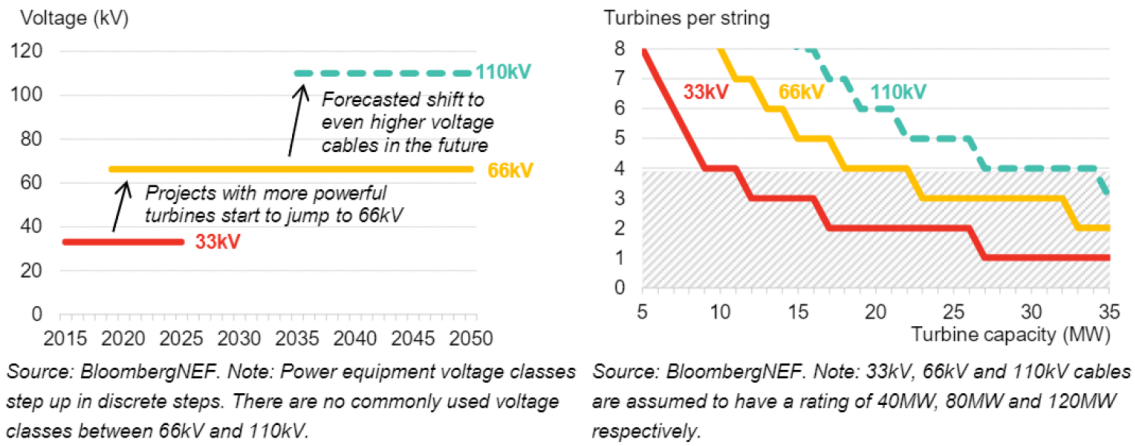

Figure 2.99: Number of turbine per strings depending on cable size, from [17]

The following consideration were based on general considerations for offshore projects. Yet, as explained in [59], ue to the inherent motions of floating substructures, FOW farms require so called "dynamic inner-array cables" that are mechanically designed to withstand the additional bending moments due to platform movements that they will be subject to through a project's lifecycle . Dynamic cabling is only required between the substructure and the seabed, and static cabling can be used for the sections of the inner-array cables that run along the seabed.
The design of these dynamical cables is thus more complex as widely explained in a

dedicated report from Corewind [76] on current R&D at stake in this field. The sector has actually not reached maturation yet and bigger dynamic cables imaginable recently reached 66 kV. It is expected that assume 110kV cables will be available for projects after 2035 (even before actually). For now, the vast majority of counted commercial scale projects in our market analysis (cf section 1.4) are set to use 66 kV rated cables. For example, the integrity of the 18 Italian projects discussed in domestic market subsection 1.4.4 are set to use 66 kV rated inner electrical array.
A typical dynamic cable layout is displayed on figure 2.100 with some of its components. Indeed, in addition to inner technologies in terms of material for inner and outer core as well as external armour that is a critical component for fatigue [59], dynamic cables use come with external components such as Bend Stiffener to connect to the floating platforms, a transition joint to link the static cables, protection sleeves to prevent at corrosion at seabed and Buoyancy module to maintain a desired profile.

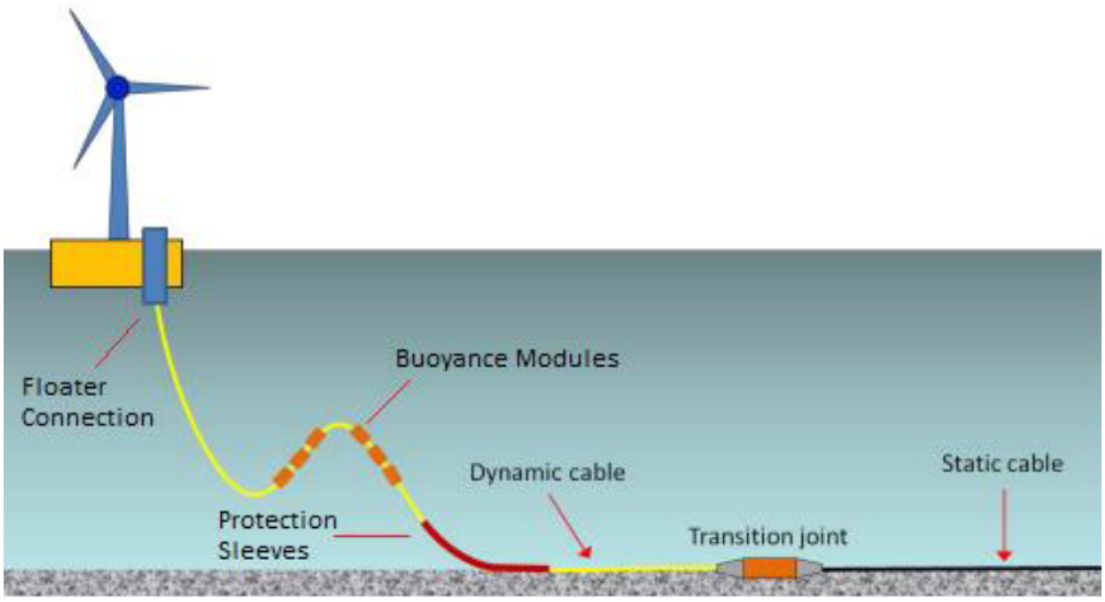

Figure 2.100: Components of dynamic cable system

A dynamical cable will thus have to undergo movement, forces and acceleration making them more sensible to fatigue and failure that static cables. In order to minimise these detrimental phenomenon, the vertical profile a dynamical cable must be adjusted. This optimisation process is based on complex hydro-dynamical out of the scope of this work, but [96] developed an hybrid MATLAB-OrcaFlex tool that considers fatigue life, performance in extreme weather events and economic evaluation criteria to deal with this issue. Based on this hydrostatic optimisation, a general design rule for lazy wave cables can be deduced and the typical profile obtained is obtained on figure 2.101. This profile

is obtained and maintain in position thanks to buoyancy modules represented on figure 2.100.

This techno-economically profiled will be assumed in our model, and thus the length of a dynamical cable between the floating platform and the transition with static cable will be $L_{dyn} = 2.8 * h$ where as previously h is the seabed depth. As explained on figure in [96], in this optimum profile, the vertical horizontal path covered by the dynamic cable will be $2h$, two times the depth. Between two turbines, we will have a section dynamic, then an horizontal static section on seabed, and then another dynamic section to link the other floating turbine. Let's take a concrete example: for 15 MW turbines and with a depth $h = 200m$. The dynamic section will have a length of $2 * 2.8 * h = 1120[m]$. 15 MW turbine have rotor size of 230 meters. The distance between two turbines is thus $d = 8*230 = 1840[m]$. The static section will thus have a length of $1840-2*2h = 1040[m]$. These type of computation are integrated in the model for the whole plan path described on figure 2.98 and thus the global static and dynamic cable length will be assessed.

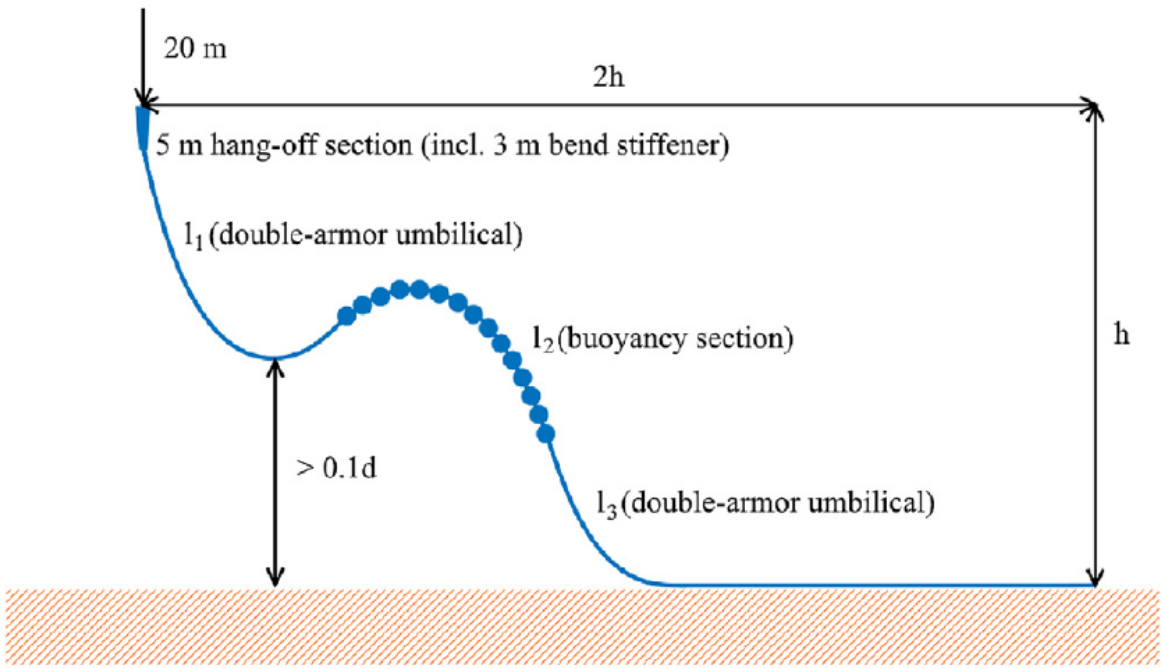

Figure 2.101: Optimised vertical profile of a dynamical

For really deep sites, it could happen that the dynamic path section obtained from the optimum profile described in [96] would end up longer than the distance between turbine d. In this case, to be more cost effective, so called W-shape profiles connection as schematised on figure 2.102. In this case, no static cable is used and the dynamic cables both are respecting the optimised profile and float between two waters. The depth of connection is

thus fixed by the distance between the turbine d. Indeed, since according on figure 2.101 the horizontal path must be 2 times the depth h, we get that $h_{connection} = \frac{d}{4}$. The total dynamic cable length between the turbine is thus $L_{dyn} = 2 * 2.8 * h_{connection} = 1.4 * d = 1.4 * 8 * D_{rotor}$.
Let's precise that the scientific and industrial knowledge related to the dynamic cables behaviour towards fatigue is less mature.

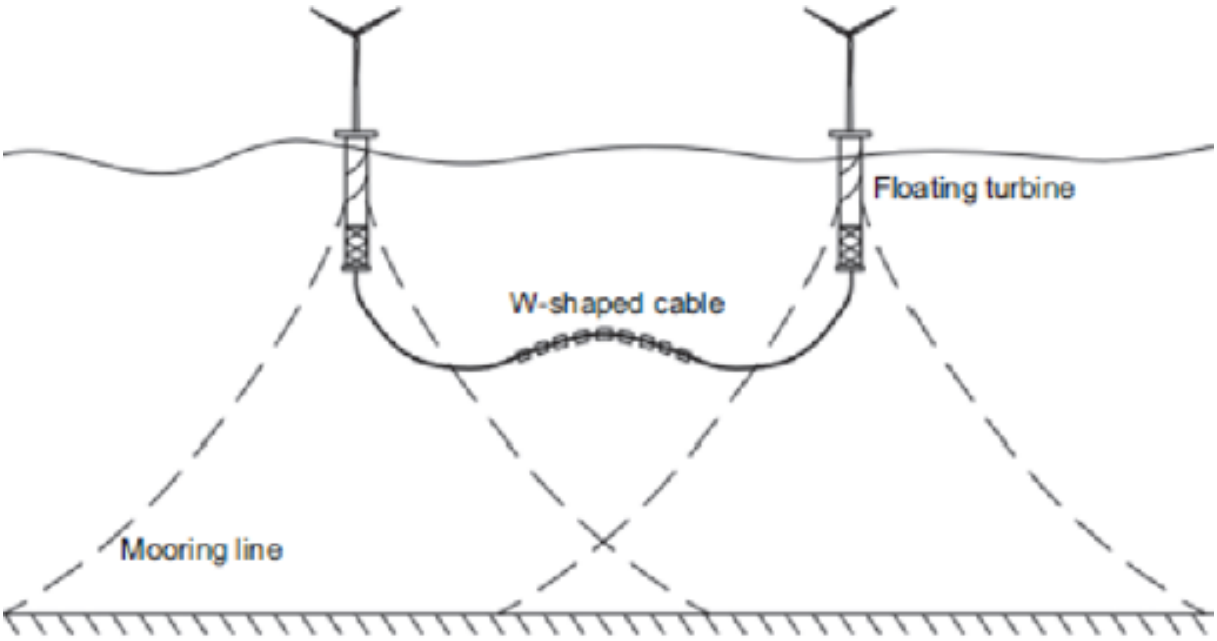

Figure 2.102: W shaped profile for dynamic cables

To close the inner-array cost assessment, linear cost of both static and dynamic cables are required. For static cables, the technology is very mature and has a wide industrial record. Based on this experience, cost of static cable evolution with their rated capacity is well known and in their dedicated report Corewind disclosed a precise cost function of static cables with apparent power S [MVA] flowing through the array cables which parameter c1, c2 and c3 are described for each rated voltage on a table on figure 2.103. For our model, the rows of this table interesting are the 66 kV and 132 kV and are thus highlighted in blue on the table. The linear cost of static cables is thus given by equation 2.25:

$$C_{static} = c_1 + c_2^{c_3 \cdot S} [k\$/km] \tag{2.25}$$

For dynamic cables, these industrial feedbacks are not existent and such precise cost function cannot be easily created. Yet, based on BNEF assumption described in [17],

the cost of dynamic cable will be assumed to be 60% higher than static ones. This over cost is motivated by the technology involved as well as additional accessories required as described earlier. Thus, The linear cost of dynamic cables is thus given by equation 2.26:

$$C_{static} = 1.6 * c_1 + c_2^{c_3 \cdot S} [k\$/km] \tag{2.26}$$

Equations 2.25 and 2.26 will allow us integrate inner array cost assessment in our model even taking in consideration actual power flow within the cables.

Voltage (kV)		Cost Coefficient			Range	Units	Year
Rated	Max	c1	c2	c3	(MVA)		
6.6	7.2	67.63	8.24	0.44	[2.9, 7.5]	k€/km	-
11	12	49.37	16.32	0.22	[4.8, 12.5]	k€/km	-
22	24	−1.27	50.66	0.07	[9.5, 27.2]	k€/km	-
33	36	−35.29	80.17	0.04	[17.0, 44.0]	k€/km	-
66	72.5	−57.35	105.20	0.02	[34.3, 94.3]	k€/km	-
132	145	−1337.00	1125.00	3.5×10^{-3}	[121.1, 188.6]	k€/km	-
MV	ns	0.5–2.0	0	0	ns	k£/m	2015
22	ns	0.284×10^6	0.583×10^6	6.15×10^{-2}	[10, 45]	SEK/km	2003
33	ns	0.411×10^6	0.596×10^6	4.1×10^{-2}	[15, 67.5]	SEK/km	2003
66	ns	0.688×10^6	0.625×10^6	2.05×10^{-2}	[35, 135]	SEK/km	2003
132	ns	1.971×10^6	0.209×10^6	1.66×10^{-2}	[100, 230]	SEK/km	2003
220	ns	3.181×10^6	0.11×10^6	1.16×10^{-2}	[290, 385]	SEK/km	2003
MV	ns	300–800	0	0	ns	€/m	ns
HV	ns	1000–2000	0	0	ns	€/m	ns
132	ns	7.471	39.28	1.40×10^{-2}	[150, 189] *	£/m	2008
220	ns	−1044	963.4	1.91×10^{-3}	[250, 315] *	£/m	2008
33	ns	100–200	0	0	ns	€/m	2012
132	ns	200–600	0	0	ns	€/m	2012

Figure 2.103: Static cables costs from [20]

The outputs of our cost model for specific CAPEX of array cables are displayed through a graph visible on figure 2.104 of specific cost [$M/MW] of the inner array (dynamic + static cables) in function of the depth and for every turbine size considered. As expected, array cables cost clearly increase with depth. Yet this increase is non linear because of the cost-effective use of W-shaped configuration for higher depths. Then, unlike what have previously been witnessed for moorings and floating platforms, no clear economies of scale are generated with the use of bigger turbines, and the evolution witnessed are actually hard to analyse. This is the results of opposite phenomenon at stake in the price evolution of array cables with bigger turbines. Indeed three phenomenons leads to opposite results and their share in the final result hard complex to anticipate:

- Bigger turbines leads to higher spacing between turbines which leads to higher cost.
- Bigger turbines leads to less turbines per row or bigger cables leads higher cost.
- Bigger turbines leads less turbines per MW leads lower specific cost.

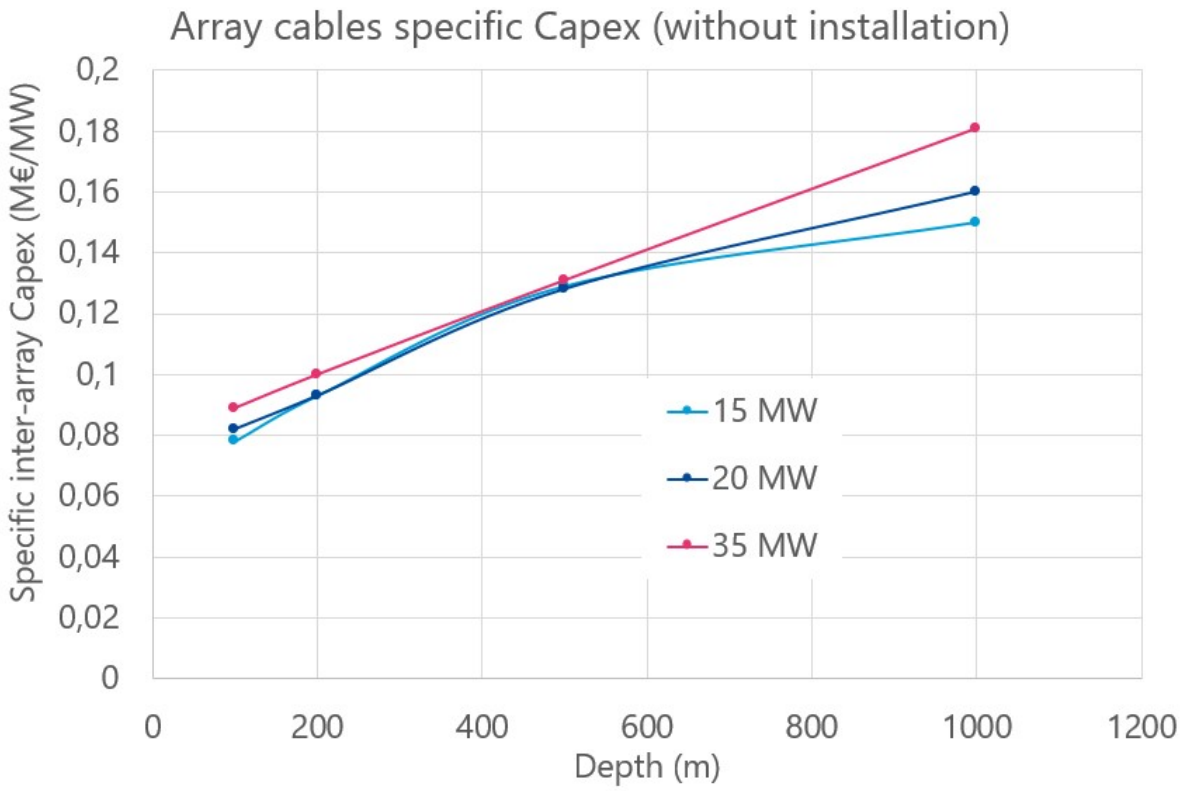

Figure 2.104: Cost model outputs for inner array

2.7. Focus on installation

Finally, installation cost of the previously detailed components will be assessed in this section. At the exception of export and inner-array cables, the installation processes for these FOW components are not common to fixed bottom offshore projects and thus clear reliable industrial feedbacks are lacking. In this section conservative hypothesis will thus be made, all the more so as these installation cost can be very volatile according on the domestic market, the concept use and the site characteristics (depth, seabed composition, distance from shore etc...).

The hypothesis will mainly be inspired from similar work from [17] and [57] as well as from [23] for installation processes common to fixed-bottom offshore projects.

2.7.1. Turbine installation

One clear advantage of floating offshore wind over fixed-bottom offshore is the possibility to assemble the structure at port before being towed to site. This cancel the need for offshore crane operation that are complex, risky and expensive. Instead, only onshore crane is required, with standard lifting capacity (50 ton/MW for the nacelle), thus it is assumed $N_{crane} = 1$. From time-lapse videos of assembling of various projects as for example the stiesdal tetra assembly displayed on figure 2.105, it is get that $Days_{turbine} = 2$ days of crane use are required for the installation of one turbine on the floater. BNEF make the same assumption in [17], and furthermore assumed a value of a crane day rate of $DR_{crane} = 100000 USD/day$. From other researches this value appears conservative and will be thus adopted in our model. The specific cost of the turbine installation for a turbine of power P [MW] is then obtained following equation 2.27:

$$INST_{turbine} = N_{crane}.\frac{Days_{turbine}.DR_{crane}}{P}[USD/MW] \tag{2.27}$$

No learning rate is assumed for these installation processes since the operation are actually similar to onshore turbine installation and thus well known.

Figure 2.105: Turbine onshore assembling for tetra concept by Stiesdal [21]

NOTE: In this simple cost model the size of the turbine has no incidence on the day rate of the crane, leading to important economies of scale. Actually, since cranes designed for port operations can usually easily deal with turbine components weight, this assumption make sense. In the case special crane infrastructures were used only for the FOW project, crane size exactly suited to turbine dimensions could be taught.

2.7.2. Platform installation

Another field that could win in precision with industrial feedback. Plus, this is maybe the installation process that could lead to wider price range since parameters as type of floaters (heavier structures are slower to tow), meteorological condition, domestic market day rates and moreover distance between port and site can strongly affects the specific cost of platform installation. The first ever demonstration of towing to site floaters was performed for the WindFloat demonstration (cf [22]) in Portugal as displayed on figure 2.106. In this case, two full days were required for two multipurpose tug vessels for platforms to bring it to site and come back to shore. Similar time duration were assumed in [57] and [6]. Keeping in mind that is value is conservative and may change in particular cases where the site is near or very far from port, it will thus be assumed that $Days_{towing} = 2$.
Then, as explained in [58] and witnessed in [22] case, two tugboats of sufficient capacity are required. Yet, as explained in [58], a third tugboat could be required for bigger platforms or for harsher conditions. To remain conservative, it will be assumed that $N_{tugboats} = 3$. Then, as explained in Carbon trust report [58], vessels required, in addition to the big towing capacity, must be able to transport and operate technicians and material to attach the platforms to the mooring. We talk about "Multi purpose tug vessel", and their day rates, a little higher than classical tugboats, is assumed in [17] to be $DR_{tugboats} = 40000 USD/day$.
The specific cost of the SS installation for a turbine of power P [MW] is then obtained following equation 2.28:

$$INST_{platform} = N_{tugboats}.\frac{Days_{towing}.DR_{tugboats}}{P}[USD/MW] \tag{2.28}$$

No learning rate is assumed for these installation processes since the operation are actually limited by the tugboat speeds more than a real complexity where an important optimisation margin would exist.

Figure 2.106: Towing of pre-assembled floating structure on site, from [22]

As explained in sections 2.3 and 2.4, TLP solutions offer potential advantages over SS ones. Yet these advantage comes with more complex and time-consuming installation. Since now scale projects of FOW TLP have been installed yet, these complexities are hard to quantify: for example, the multiplication of moorings lines and the need to provide over-buoyancy would for sure increase the time spent of mooring connection to the platform. In order to take account of this reality described earlier, and based on the order of magnitude of cost differences disclosed in [57], it will be simply assumed that the installation specific cost of tension leg platforms will be two times more expensive than SS ones.

2.7.3. Moorings and anchors installation

As explained in [58], mooring and anchors installation requires dedicated vessels equipped but trucks specially designed for chain, wires or ropes. The depth of the site can have little influence on the time spent at sea, as well as the numbers of moorings per floater, yet, as explained in [97], one AHTS vessel will need about 5 days to install the anchors and moorings of one floating turbine: $N_{AHTS} = 1$ and $Days_{AHTS} = 5$. Then the day rate of an AHTS can be very volatile since eventough not very complex devices, relatively few model are in circulation except in specific part of the world as North Sea where Oil&gas offshore operations are intensive. In the end, the BNEF assumption made in [7] appeared conservative enough and it will be assumed that $DR_{AHTS} = 50000USD/day$.

The specific cost of the catenary mooring installation for a floating turbine of power P [MW] is then obtained following equation 2.29:

$$INST_{moorings} = N_{AHTS}.\frac{Days_{AHTS}.DR_{AHTS}}{P}[USD/MW] \tag{2.29}$$

No learning rate is assumed for these installation processes since these kind of operation has a strong record track from the oil&gas sector has explained in [58] and are already more or less optimised. [97]

Figure 2.107: Anchor Handling Tug Supply (AHTS) vessels

As explained in sections 2.3 and 2.4, TLP solutions offer potential advantages over SS ones. Yet these advantage comes with more complex and time-consuming installation. Since now scale projects of FOW TLP have been installed yet, these complexities are hard to quantify: for example, the multiplication of moorings lines and the need to perform underwater operations as drilling or water pumping for suction anchors will require more assets and more time. In order to take account of this reality described earlier, and based on the order of magnitude of cost differences disclosed in [57], it will be simply assumed that the installation specific cost of tension leg platforms will be three times more expensive than SS ones.

2.7.4. Export and inner array cables installation

Similar processes are at stake for export cables and static inner array cables installation, only size of the cables differs. As expected, the installation cost will be proportional to the length of cables to install. These operations are common to fixed-bottom projects and are thus widely described in [23]. The vessel used for this installation is called a cable laying vessel, with a carousel attached to it to store and deploy the cables as rep-

resented on figure 2.108. Catapult explains us in its report that the seabed type impacts the technology of cable burial : Use of trenching ROV, use of cable plough use of vertical injectors and jetting sled and even cable pull-in can be used singularly or conjointly to bury efficiently the cables [23]. The assumption of day rate for cable laying vessel coupled with the desired cable handling and trenching assets are thus based on fixed-bottom industrial data from [23] and it is obtained that $DR_{export-cable} = 170000USD/day$ and $DR_{array-cable} = 150000USD/day$ for export cables and inner array cables respectively. The higher day rate for export cables is due to the bigger cables diameters that thus require bigger carousels and trenching assets.

Then, the length covered by the vessels must be assessed to close the cost model. Always based on fixed-bottom data from [23], it will be assumed that the velocity of installation the vessel for expert cable will be $V_{export-cable} = 0.4km/day =$ and $V_{array-cable} = 0.25km/day =$ for export cables and inner array cables respectively. The slower installation rate for inner arrays is due to the non linear path as well as more connections required during the process.

The specific cost of the array cables and export cables installation for a floating wind farm of nominal power P [MW] are then obtained respectively from equation 2.30 and 2.31:

$$INST_{export-cables} = L_{export}.\frac{V_{export-cable}.DR_{export-cable}}{P}[USD/MW] \tag{2.30}$$

$$INST_{array-cables} = L_{static-cables}.\frac{V_{array-cable}.DR_{array-cable}}{P}[USD/MW] \tag{2.31}$$

Figure 2.108: Cable Laying Vessel

Finally, the installation of dynamic cables is not common to fixed-bottom offshore wind. A linear installation cost is assumed by BNEF in [17]. It will thus be assumed that $C_{dynamic-cables} = 360000$[\$/km].
The specific cost of the dynamic array cables installation for a floating wind farm of nominal power P [MW] is thus obtained from equation 2.32:

$$INST_{dynamic-cables} = L_{dynamic-cables}.\frac{C_{dynamic-cables}}{P}[USD/MW] \tag{2.32}$$

2.8. CAPEX summary and cost breakdown of FOW projects

Every main cost drivers listed on figure 2.1 have been deeply assessed in the previous sections. The goal of this last part is thus to close the CAPEX discussion by aggregating the results of the cost model for each cost driver and present it in a manner to highlight the balance between each cost driver - we will talk about cost breakdown - and getting insight about the cost evolution with years and every others site related parameters previously described (depth, distance from shore, meteorological conditions etc...).
First, let's explain how the cost model for each cost drivers have been computed together and how the results will be presented.

2.8.1. CAPEX model explanation and summary

As previously explained, BVG associates, via the entity Catapult Offshore renewable energy, has disclosed an holistic, augmented and industrial based LCOE cost breakdown assessment of fixed-bottom offshore projects [23]. The main part of the LCOE breakdown, whose output is displayed here after on figure 2.109, is the CAPEX analysis from which some of our cost assumption have been extracted of. To make sure to not forget any cost driver, this complete CAPEX breakdown have taken as a base for ours and adapted to our cost model assumption made for floating field. Some of the very precise distinction made in [23] will be in our case gathered under a same cost module: for example the turbine part will constitute only one module in our model, while BVG chose to distinct the nacelle part, the tower part etc... Then, the main clusters of cost modules will not be exactly the same as the one for BVG (highlighted by same colours group on figure 2.109) but will instead follow the cost driver distinction described on figure 2.1 at the beginning of this chapter. This breakdown from catapult have thus been mainly used as database of cost drivers in order to not neglect any part of the global cost breakdown of an offshore wind project.

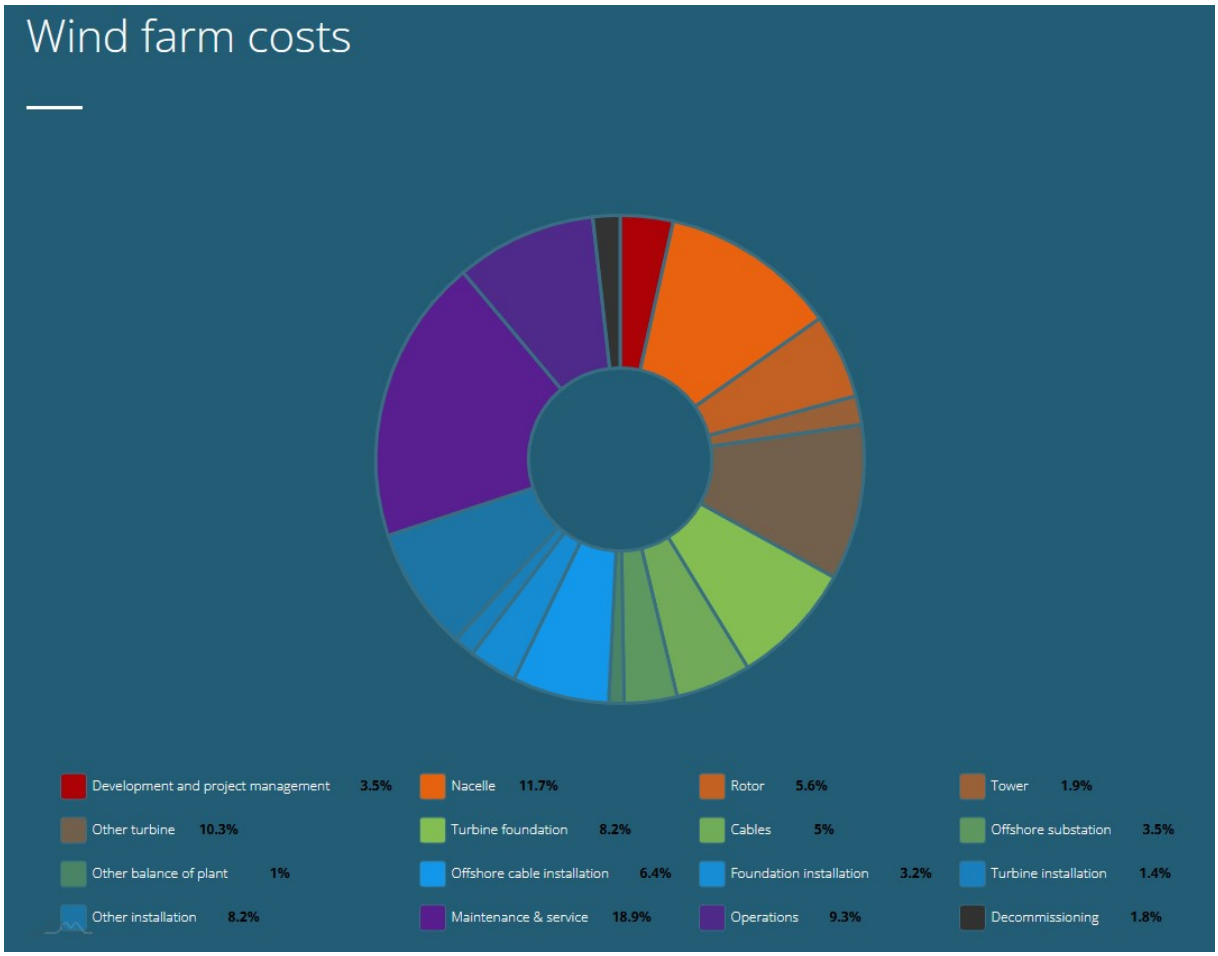

Figure 2.109: Fixed Bottom LCOE breakdown from [23]

In the end, 17 cost modules have been considered in our CAPEX model, clustered in 7 main cost categories as explained here after:

- **Turbine:** Cost model described in section 2.2. Will be represented in orange.
- **Connection to Grid:** Will be represented in green.
  - Offshore export cable: Cost model described in section 2.5.
  - Offshore export cable installation: Cost model described in section 2.7. Let's note that the installation of export cables are in the connection to grid section and not in the installation section. This choice has been made to cluster every connection to grid related cost for the case where the TSO would take in charge the connection cost.
  - Offshore substation (OSS): Cost model described in section 2.5.

  - Offshore substation (OSS) floating substructure: Cost model described in section 2.5.
  - Onshore substation: Non covered by our previous cost assessment discussions. Assumed to be equal to cost for fixed-bottom project. Taken from Catapult fixed-bottom offshore farm guide [23].
  - Onshore substation installation and facilities construction: Non covered by our previous cost abasement discussions. Assumed to be equal to cost for fixed-bottom project. Taken from Catapult fixed-bottom offshore farm guide [23].

- **Floater:** Cost model described in section 2.3. Will be represented in dark blue.
- **Moorings and anchors:** Cost model described in section 2.4. Will be represented in light blue.
- **Inner-array cables:** Cost model described in section 2.6. Will be represented in yellow.
- **Installation:** Will be represented in purple.
  - Offshore logistic: Offshore logistics covers marine coordination, sea-based support and weather forecasting and met-ocean data. It will taken from [23]. In order to take in consideration the more complex offshore operation for TLP installation, this offshore logistic cost (relatively low) will be multiply by two for TLP.
  - Floating foundations installation: Cost model described in section 2.7.
  - Moorings and anchors installation: Cost model described in section 2.7.
  - Turbines Installation: Cost model described in section 2.7.
  - Inner-array cables installation: Cost model described in section 2.7.
- **Other:** Will be represented in grey.
  - Insurance and contingency: Value taken from A2A classical model for development of renewable projects. It will represents 10% of the total CAPEX.
  - Development and project management: Value taken from A2A classical model for development of renewable projects. It will represents 10% of the total CAPEX.

This cost clustering allows us to cover every cost driver and is computed in our model as the table extracted from our CAPEX model for a 2030 project using SS platforms

and featuring 200 meters depth, 50 km distance from shore and Mediterranean conditions shows on figure 2.110.

The output of our model can be represented as a PIE chart highlighting the share of every cost section for different parameters. The pie charts relative to previous example, with the corresponding colours, is displayed on figure 2.111.

2030 floating Capex Breakdown		
Category	Rounded Cost ($/MW)	Percentage
Turbine	864000	28,7%
Connexion to grid	773046,0693	25,7%
Offshore Cable	377777,7778	12,5%
Offshore export cable installation	94444,44444	3,1%
Offshore substation	208100,1984	6,9%
Onshore substation	35700	1,2%
Offshore substaion floater	27273,64866	0,9%
Onshore substation construction	29750	1,0%
Floater	450000	14,9%
Mooring and anchors	97 957,250	3,3%
Cables array	93013,84483	3,1%
Installation	130407	4,3%
offshore logistic	4375	0,1%
Foundation installation	16000	0,5%
Mooring installation	16666,66667	0,6%
TurbineInstallation	13333,33333	0,4%
cables array installation	80032	2,7%
Other	602 106,041	20,0%
insurance, contigency	301 053,021	10,0%
Development and project management	301 053,021	10,0%
Total	3 010 530,205	100,0%

Figure 2.110: Example of CAPEX model breakdown for a 2030 SS project featuring 200 meters depth, 50 km distance from shore and Mediterranean conditions

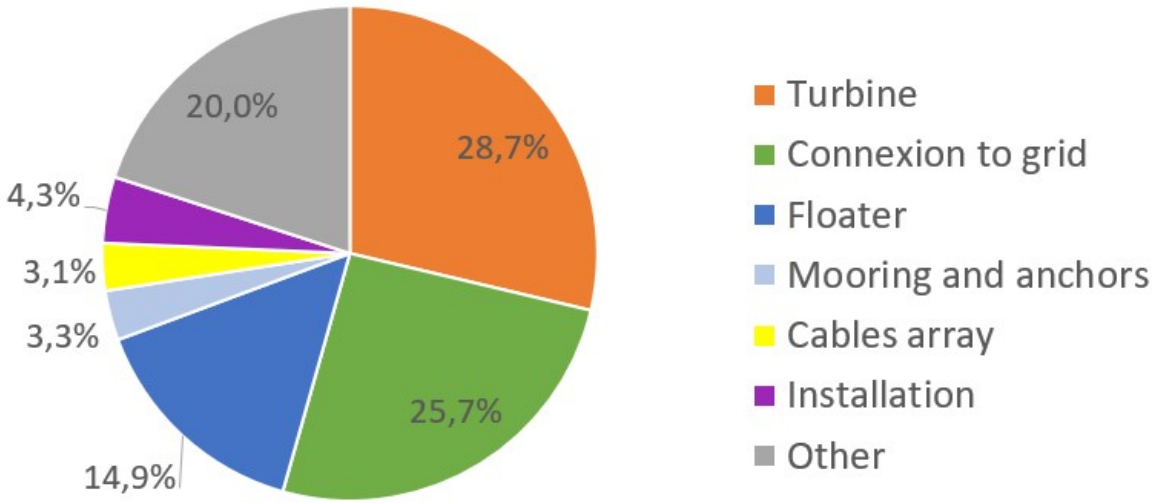

Figure 2.111: Pie-chart representation of CAPEX model breakdown for a 2030 SS project featuring 200 meters depth, 50 km distance from shore and Mediterranean conditions

As previously explained, in our model turbine size and yea of commissioning will be linked assuming that the bigger turbine available will always be used in order to enhance economies of scale (that will be witnessed in 2.8.2). 2030 projects will thus feature 15 MW turbines, 2035 projects 20 MW turbines and 2040 projects 35 MW turbines (this last hypothesis is ambitious since 35 MW turbine could arrive on market after 2040, yet it allow us to demonstrate all the possibilities offered by introduction of big turbines). The year of commissioning does not only impact the turbine size but also the farm total size, that will be assumed ever bigger with year. The farm size and layout characteristics, that will impact the array cable costs, by year are:

- **2030:** 30 turbines rated at 15 MW are considered, for a total farm output of 450 MW. As previously explained, 66kV array rated at 80 MVA cables are considered leading to strings of 5 turbines. The farm layout is thus 6 strings of 5 turbines.
- **2035:** 48 turbines rated at 20 MW are considered, for a total farm output of 960 MW. As previously explained, 66kV array cables rated at 80 MVA are considered leading to strings of 4 turbines. The farm layout is thus 12 strings of 4 turbines.
- **2040:** 60 turbines rated at 35 MW are considered, for a total farm output of 2100 MW. As previously explained, 132kV array cables rated at 175 MVA are considered leading to strings of 5 turbines. The farm layout is thus 12 strings of 5 turbines.

The CAPEX model generated offers to the user four uncorrelated parameters impacting the outputs:

- **Depth:** four discrete values available representative of potential future projects: [100m; 200m; 500m; 1000m]
- **Distance from shore:** Can continuously range from zero to 300 km.
- **Commissioning Year:** 2030, 2035 or 2040 projects. As explained above the turbine parameter is directly linked to the turbine and wind-farm power ones.
- **Floater and meteorological conditions**: Since floater type and meteorological conditions impact the same cost drivers (floaters and moorings related) they have been gather in a same parameter. For sake of simplicity and to not be too redundant regarding the outputs of floaters and moorings cost models discussed in subsections 2.3.3 and 2.4.4 respectively, only 3 possibilities have been integrated in the general CAPEX outputs analysis. First has been introduced the configuration that could be considered as the basic one since most representative of the FOW market and that has been used as a based for the development of our physical model: the Semi submersible platform in oceanic conditions. Then, accordingly to the discussion made in 2.4.4 on the role of TLP in med conditions and in order to fuel the discussion on the FOW potentialities in the Mediterranean at the base of this study and that will be further assessed in chapter three, Mediterranean conditions for both TLP and SS have been introduced as parameters in the model. Thus, the oceanic TLP configuration, already studied through the cost model for floaters as well as mooring and anchors will not be introduced. Two reasons, in addition to the arguments described here above, motivated this choice. First, in the (relatively) shallow waters of the north sea or in seismic zones of the Korean or Japanese sea, TLP in oceanic conditions may not be the most used solutions in oceanic conditions. Then, since this parameter will always influence the same cost driver, the trends for oceanic TLPs can be easily derived from the 3 others ones based on cost outputs from subsections 2.3.3 and 2.4.4. The addition of this fourth possibility would thus add complexity to the graph without bringing many more insights, that would in addition not be reused in chapter 3 where emphasis will be put on projects in the Mediterranean.

The computation of this whole CAPEX model, with the inputs and outputs of the model as well as the direct and indirect impacts of various parameters on the final cost drivers highlighted, is holistically described by the following block diagram of figure 2.112. This block diagram shows how the CAPEX model includes the computation of the static model described in sections 2.3 and 2.4. The analysis of this block diagram must thus be done complementary to the one of figure 2.43.

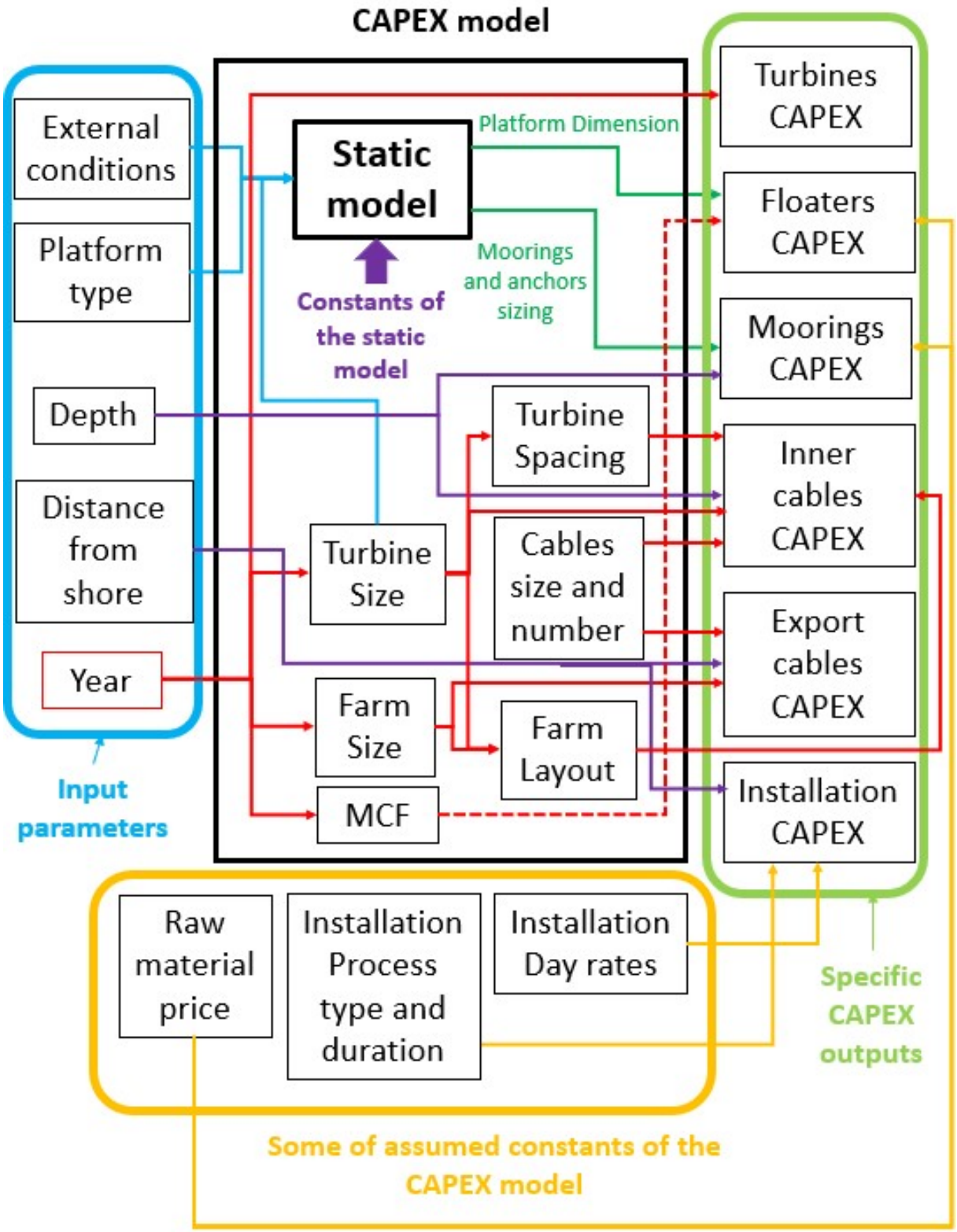

Figure 2.112: Inputs and outputs of the whole CAPEX model

2.8.2. CAPEX model global outputs and FOW cost breakdown

Many combination can be made out the four independent parameters included in the model. The idea here is not to display all of these combination outputs but to get insights on the impact of each on the CAPEX of a FOW project. As previously explained, due to the various hypothesis made in the analysis in order to remain general the trends and the order of magnitude are way more insightful that the exact values obtained. Actually, precise value of CAPEX will have to be assess for every single project by developers.

The first two graphs displayed on figure 2.113 represents the total specific CAPEX [$M/MW] evolution with commissioning year (and thus turbine size) for the three floaters conditions: on the left the depth of the site is taken at 200 meters while on the right it is taken at 1000 meters. In both cases distance to shore is fixed at 50 km and will thus have no influence on trends. on both graphs, and for every floater/meteo configuration, clear economies of scale are witnessed. This is the direct consequence of economies of scale announced for turbine side, floater side, moorings and anchors side and even installation side respectively in sections 2.2, 2.3, 2.4 and 2.7. For example, focusing on a SS catenary in oceanic condition at 200 meters depth, which would consist in according to [7] the most representative benchmark for FOW projects of the decade to come, global specific CAPEX would drop from 3.52 to 2.17 M$/MW between 2030 and 2040 projects, resulting in 38% drop. As explained earlier while focusing on floaters and moorings, the economies of scale on this side present a lesser magnitude for softer meteorological conditions. Anyway, still focusing on SS catenary configuration since most common one at 200 meters depth, in Mediterranean condition specific CAPEX would drop from 3.01 to 1.98 M$/MW between 2030 and 2040 projects. A very interesting 34% drop in CAPEX in thus enhanced by introduction of bigger turbines and global maturation of market for SS catenary design in Mediterranean conditions.

As expected from specific analysis led on moorings and anchors (section 2.4) as well as Inner array cables (section 2.6), higher depth will have a detrimental impact on project CAPEX. For SS catenary solutions, huge gap between 200 meters depth CAPEX and 1000 meters one are obtained by comparing the left and right graph of figure 2.113. Yet, since as explained previously such configuration is not set to be used at such big depths, let's focus for a very important depth of 1000 meters on a Mediterranean TLP solution. In this case, global specific CAPEX would drop from 3.15 to 2.23 M$/MW between 2030 and 2040 projects, resulting in 29% drop. The economies of scale is still very important but yet smaller than the ones witnessed for SS catenary configuration. Plus, the comparison between the two graphs confirms that TLP solutions are as expected less sensitive to depth that SS catenary ones.

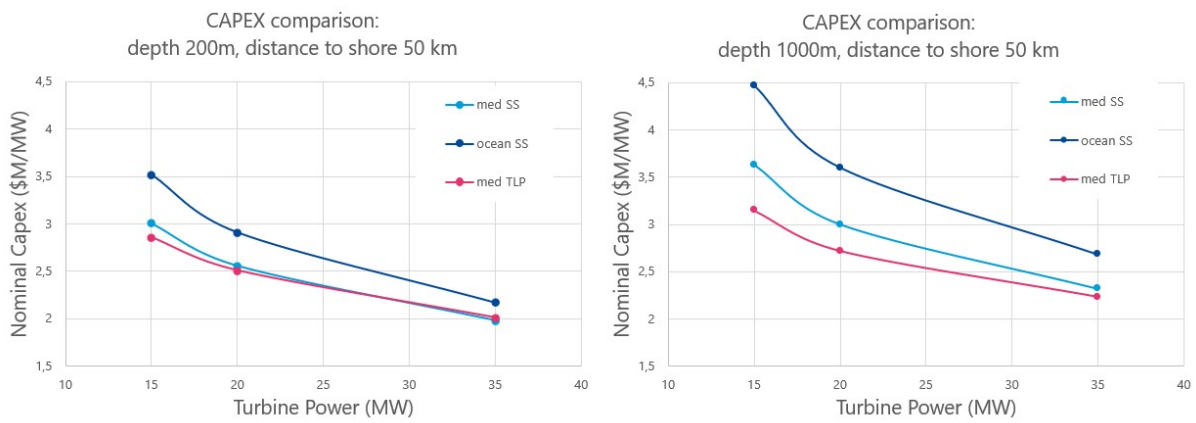

Figure 2.113: CAPEX evolution with turbine power for depth of 200 meters and 1000 meters, at a fix representative distance to shore of 50 km

TLP solutions nowadays are less mature than SS ones as explained in sections 2.3 and 2.4. Yet, the CAPEX model outputs presented here above confirm the potential cost savings offered by TLP solutions. In order to deal with this question, on figure 2.114 is displayed a graph presenting the cost savings offered by TLP solution regarding SS catenary solutions in percent (negative values will mean that TLP solutions are most expensive). As previously, CAPEX estimation have been made assuming a distance to shore of 50 km. With this representation, it's easier to spot in which cases and to what extent TLP are cost effective solutions in comparison with SS catenary ones. Two clear phenomenons are highlighted by this graph: first, TLP solutions offer bigger cost reductions for smaller turbines and then TLP solutions offer ever bigger cost reductions with increasing depth. On graph 2.114 the two indicative common depth range of application of the two technologies as summarised on figure 2.72 have been represented. On cost side, it can be seen that our CAPEX model confirm these results. At high depth TLP solutions are indeed way cheaper than SS ones with more than 12% of total savings in CAPEX for a 15 MW turbine assumed to be used for projects commissioned in 2030. At such depths, catenary SS technologies are whatever out of question even for technological and environmental impact considerations. Yet, even at the "frontier" between the two zones located at 500 meters depth, TLP solutions offer CAPEX reductions of about 8% for 15 MW turbines (2030 projects) and 4.3% for 20 MW turbines (2035 projects). Eventough TLP development is currently lagging behind SS one (as taken in consideration in the model), the cost saving discussed here concern projects that would be disclosed 7 or even 13 years from now, offering time to platform manufacturers to close the technological gap between the two solutions. For the yet to born Mediterranean market that as it will be deeply discussed in chapter 3 features big depths, the TLP solutions could make FOW

competitive and viable for more sites.
For smaller depths (100 or 200 meters) located in the indicative SS depth range (cf picture 2.114), the cost savings offered by TLP solutions are smaller, and even negative for huge 35 MW turbines. In this zone, it is unlikely that this solution will be chosen over SS catenary ones since the low cost savings may not compensate the higher risks and lower investors trust in the technology. SS and TLP thus really appear as complementary solutions that would both have a place in the future development of the FOW market in the Mediterranean.

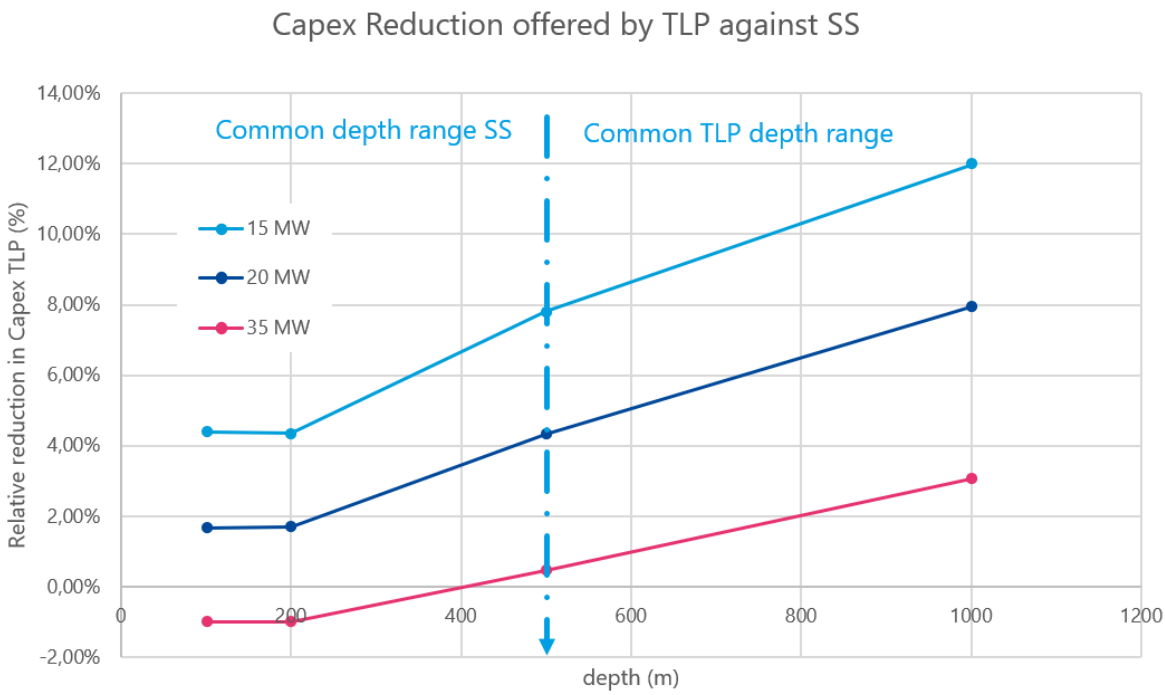

Figure 2.114: CAPEX Reduction offered by TLP over SS (platform + mooring and anchors) against SS in % for Mediterranean conditions

More than the global CAPEX values, the share of each cost driver in the total cost breakdown is interesting to analyse. To support this analysis, cost breakdown pie charts alongside the specific CAPEX value in [$M/MW] are represented for combination of year parameter (2030, 2035 and 2040) and of floater/meteo configuration (Med TLP; Med SS and ocean SS) are displayed on figure 2.115. To compare these cost breakdown one to another, the two other parameters, depth and distance to shore, are maintained fixed for every pie chart respectively at 500 m and 50 km.
Except the grey part corresponding to the "other" module described in 2.8.1 and that is set to always represent 20% of the total CAPEX, the other parts evolve with commissioning year for different floater/meteo configuration.

- The installation part in purple does not evolve much with commissioning year. It globally represents the smaller part of the CAPEX breakdown, eventough the cost related hypothesis made in 2.7 were . Yet, this share is more important in TLP breakdown due to higher installation cost coupled to slightly lower total CAPEX value.
- Inner array cables in yellow represent a small yet non negligible share of the total CAPEX. Since, as explained in section 2.6 inner-array does not benefits from clear economies of scale with the introduction of bigger turbines, its share tends to increase with commissioning year. By 2040, it represents about 6% of Mediterranean projects CAPEX using TLP or SS solutions at the considered depth and distance from shore.
- Platform and moorings in dark and light blue respectively have been heavily discussed in sections 2.3 and 2.4. As expected, the share increases going down on figure 2.115 since at 500 meters depth Med TLP have less expensive floater and moorings than Med SS which have less expensive floater and moorings than ocean SS. Then, thanks to the important economies of scale enhanced in this cost module by introduction of bigger turbines, its share also strongly decreases with commissioning year. This share is thus very sensitive to the two parameters considered: it can be the bigger part (about 33%) of a 2030 oceanic SS project while representing only 11% of 2040 Mediterranean TLP project.
- Turbine share in orange is always a very important of the total CAPEX of a project, ranging between 23% and 31% of the total cost for the projects here considered. However small decrease in specific price are expected from section 2.2, the share of turbines in total CAPEX of a project tends to slowly increase with the commissioning year since the total cost decreases faster.
- Connection to grid share in CAPEX breakdown, here in green, is almost as important as turbines one for distance to shire of 50 km. Since benefiting from no economies of scale with increase of turbines power and since no learning rate is applied for this well known technology, its share is inversely proportional to the total CAPEX value. It represents more than 25% of the total CAPEX for many projects described on figure 2.115.

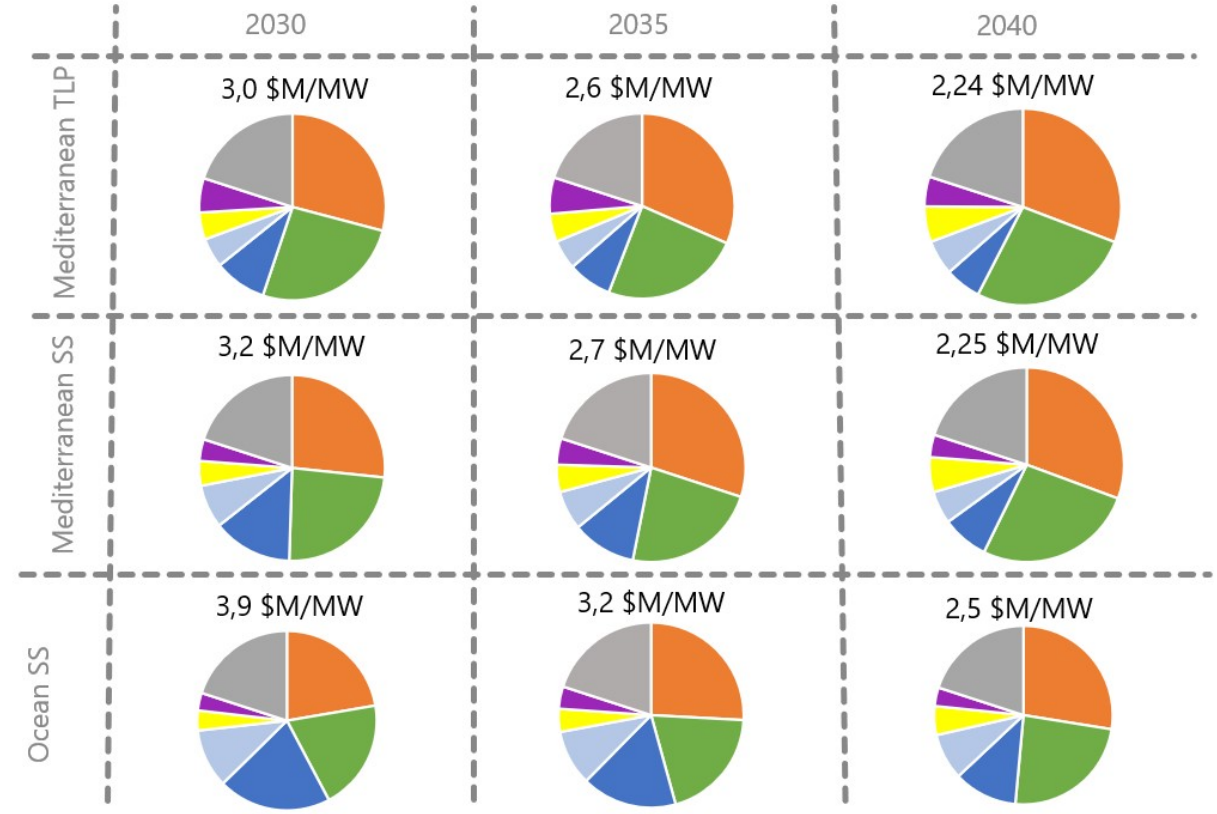

Figure 2.115: CAPEX breakdown evolution with commissioning year and floater used. Depth = 500 m ; Distance to shore = 50 km

For a given commissioning year, once the floater technology as been chosen, the site characteristics will drive the CAPEX of a FOW project. The impact of two main characteristics, i.e. depth and distance to shore, can be assessed thanks to the two graphs - one for a Med SS project on the left, another for a Med TLP project on the right - are displayed on figure 2.116. 2035 Mediterranean projects are considered.

The evolution with depth for the two configurations are very similar to the moorings cost trends displayed in section 2.4 on figure 2.84 for example, with increasing trends in both trends and a cost function less sensitive to depth for TLP (taut moorings) than for SS (catenary moorings). Yet, the difference between the sharpness of the curves is less important than in section 2.4. This is because other cost drivers are impacted by depth: inner array and installation (through the inner array installation process). These two cost drivers are generally less important than moorings in the global CAPEX breakdown of a project but evolve in the same way for SS or TLP, making the curves more similar.

The influence of distance from shore on CAPEX can also be pointed out of this graph : it can be seen that going from 30 km to 100 km can lead to CAPEX increase of about 50%. This behaviour is directly linked to the high share of connection to grid in the

global CAPEX of FOW project described in figure 2.115. Indeed, for distance to shore representative of future FOW projects (between 30km and 100 km), between 50% and 75% of connection to grid related costs will be the sum of export cables cost and their installation cost. These cost modules being directly proportional to distance from shore, and since distance from shore do not impact any other cost driver, the global CAPEX evolves linearly with distance to shore. In the two graphs from figure 2.116, this is materialised by parallel curves going up on the graphs with higher distance from shore (the distance considered are 30 km, 50 km, 70 km and 100 km).

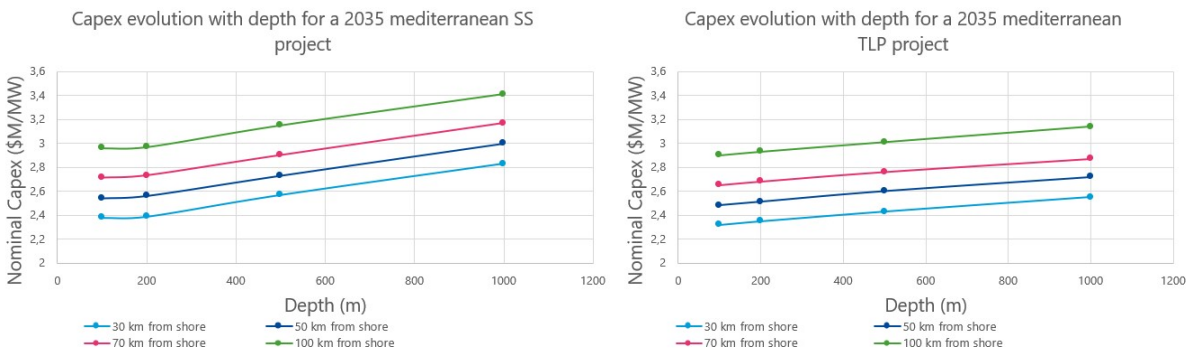

Figure 2.116: CAPEX evolution with depth for SS and TLP projects, 2035 Mediterranean projects are considered

The influence of depth on share of various cost drivers is further assessed thanks to cost breakdown pie charts alongside the specific CAPEX value in [$M/MW] represented for combination of depth parameter (200m, 500m and 1000m) and of floater configuration (Med TLP and Med SS) displayed on figure 2.117. Here, 2030 Mediterranean projects featuring a distance from shore of 50 km are considered.

As previously explained, the total CAPEX increases with depth for both configuration. The trends witnessed are actually similar both for TLP and SS here. Thus the share of cost drivers non dependant on depth, i.e. the turbine share in orange, the connection to grid one in green and the floater one in dark blue are decreasing due to increase of CAPEX. Then, as previously the "other" share in grey remains fixed at 20%. Then, the most interesting shares here are the ones whose cost depend depth : moorings in light blue, inner-array in yellow and installation in purple. The last one is impacted by depth via the array cable installation cost module. The share most sensitive to depth is as expected the moorings ones, continuously rising from 3.3% to 13.5% for Med SS and from 3.2% to 7.3% for Med TLP. The other behaviours are less clear: since less sensitive to depth than moorings ones, installation and inner array costs might increase less fast or faster than total CAPEX with depth. That is why the installation share for Med TLP

drops from 6.4% to 5.9% between 200m and 500m before going up to 7.5% for 1000 m. The behaviour is similar for med SS configuration.

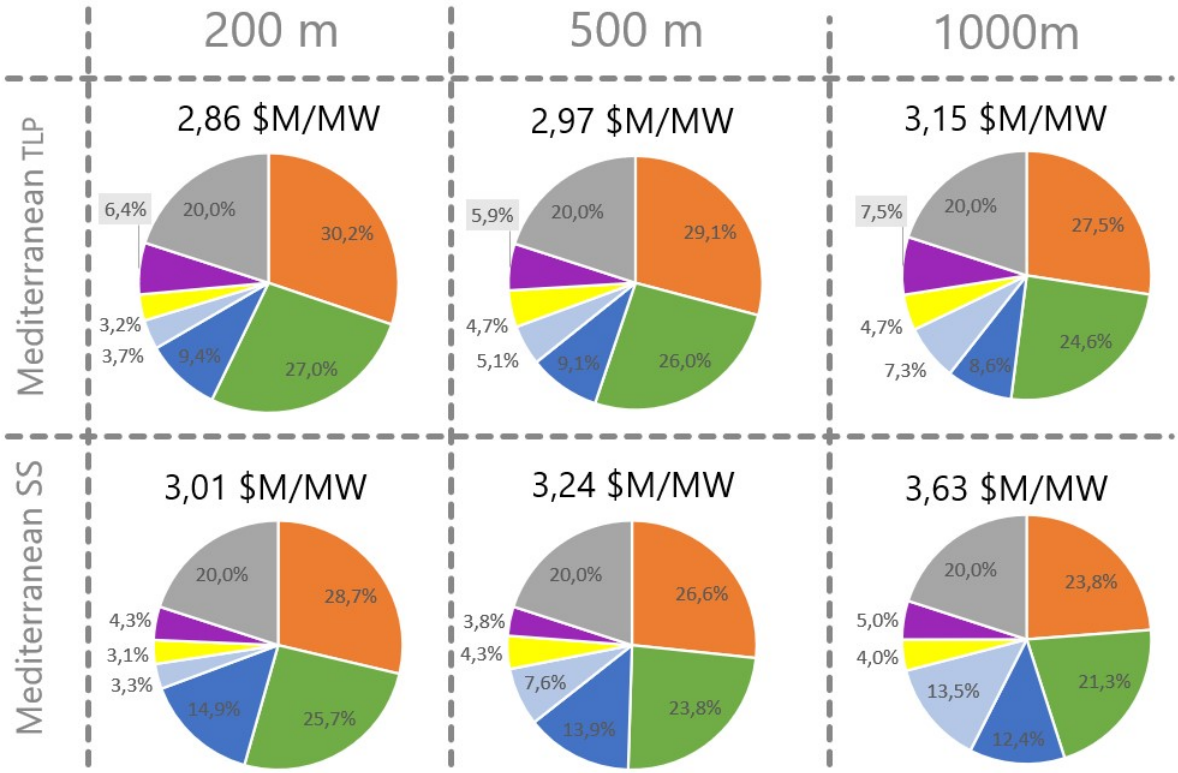

Figure 2.117: CAPEX breakdown evolution with depth and floater used, 2030 Mediterranean projects are considered, and distance from shore is maintained at 50 km

In this chapter, the various cost drivers of FOW projects have been identified and their evolution with floaters types, external loads conditions, depth, distance from shore and commissioning years have been widely discussed and analysed thanks to our CAPEX model. To close this study, this CAPEX model will be used in chapter three to estimate the LCOE of Mediterranean and more specifically Italian projects. In this chapter, a particular emphasis will be put on site features (landscape impact, bathymetry, wind conditions, supply chain) in order to identify the most interesting development zones and discuss the effective potentialities of FOW in the Mediterranean.

3 | Chapter three: Site impact assessment and LCOE estimation

3.1. Site Impact assessment for zones of interest

3.1.1. Identification of sites of interest

A CAPEX model for FOW projects have been created in chapter 2. Now, this cost estimation will be applied to assess the potentiality of FOW in Mediterranean sea and more particularly for the Italian domestic market. The site features of typical Mediterranean projects will thus have to be described and taken in consideration in order to make an holistic representative portrait of the field potentiality in this area. In chapter 2, to remain general, only two typical meteorological conditions were considered in the model. In reality, not all Mediterranean projects will feature the same external conditions and various sites of interest, mainly in Italian seas, will have to be selected to get a complete and representative overview.

As explained in chapter 1, the first parameter to work on to identify potential zones of development for offshore wind projects is obviously the wind resource. As previously explained, a very good tool to assess the wind resource geographical distribution is the Wind Atlas developed by DTU [24]. Figure 3.1 displays the output of the wind atlas for wind speed 100 meters above sea level for the surroundings of Italy. Data presented is the mean of the last 15 years and Italian windiest zones appear to be all around Sardinia, West Sicily, Calabria and Puglie in the south and to a lower extent northern Adriatic sea. Then, out of Italy, a huge potential appears for France in Lion golf in term of wind resource. From french domestic market study performed in subsection 1.4.4, this windy zone is precisely the zone of development of french projects as displayed on figure 1.36, projects that are set to drive the Mediterranean development of FOW.

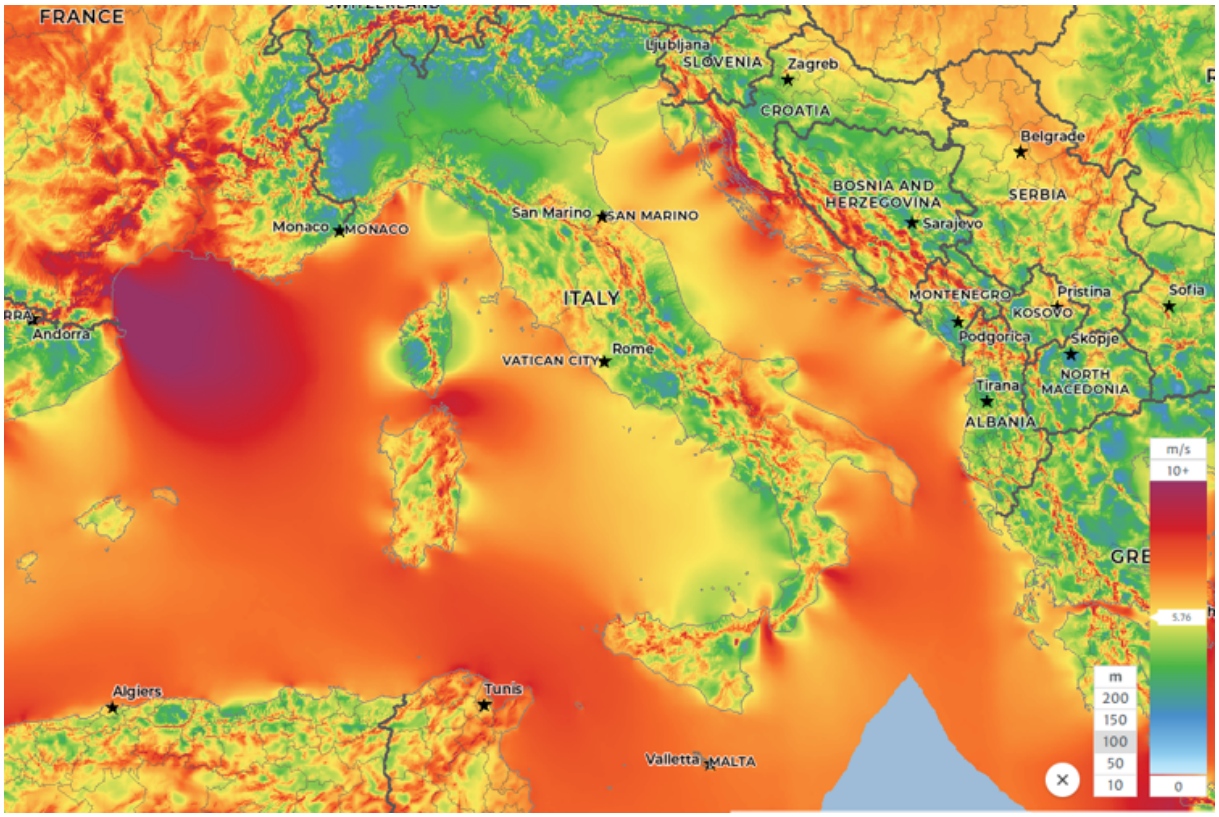

Figure 3.1: Wind resources in the Mediterranean at 100 meters height from [24]

Based on the previous wind potentialities considerations, 12 sites of interest have been identified and will be the base of our site impact assessment to come. Among these 12 sites, represented by points on a European map in figure 3.2, 9 are located in Italy: 4 in Sardinia surroundings (North N, North east NE, South S and South West SW), only one in West Sicily (W Sicily) since wind conditions are more uniform in this zone, 2 in Puglie (Brindisi and Puglie), one in Calabria and finally one in northern part of Adriatic sea (North Adriatic). In addition to these Italian sites, the GDL site is set to represent the highly windy site identified in Golfe du Lion and will thus allow us to assess the potentialities of the current main zone of development of FOW in the Mediterranean. Finally, two non Mediterranean points have been added called Scotwind and Celtic sea on figure 3.2. These two points corresponds to more "classical" sites of development of floating wind in the Europe as explained in market overview performed in 1.4. Scotwind, as its name indicates, is representative of the very interesting conditions of Scotland Northern sea that enhanced the development of the huge Scotwind floating wind pipeline (cf 1.4.4).

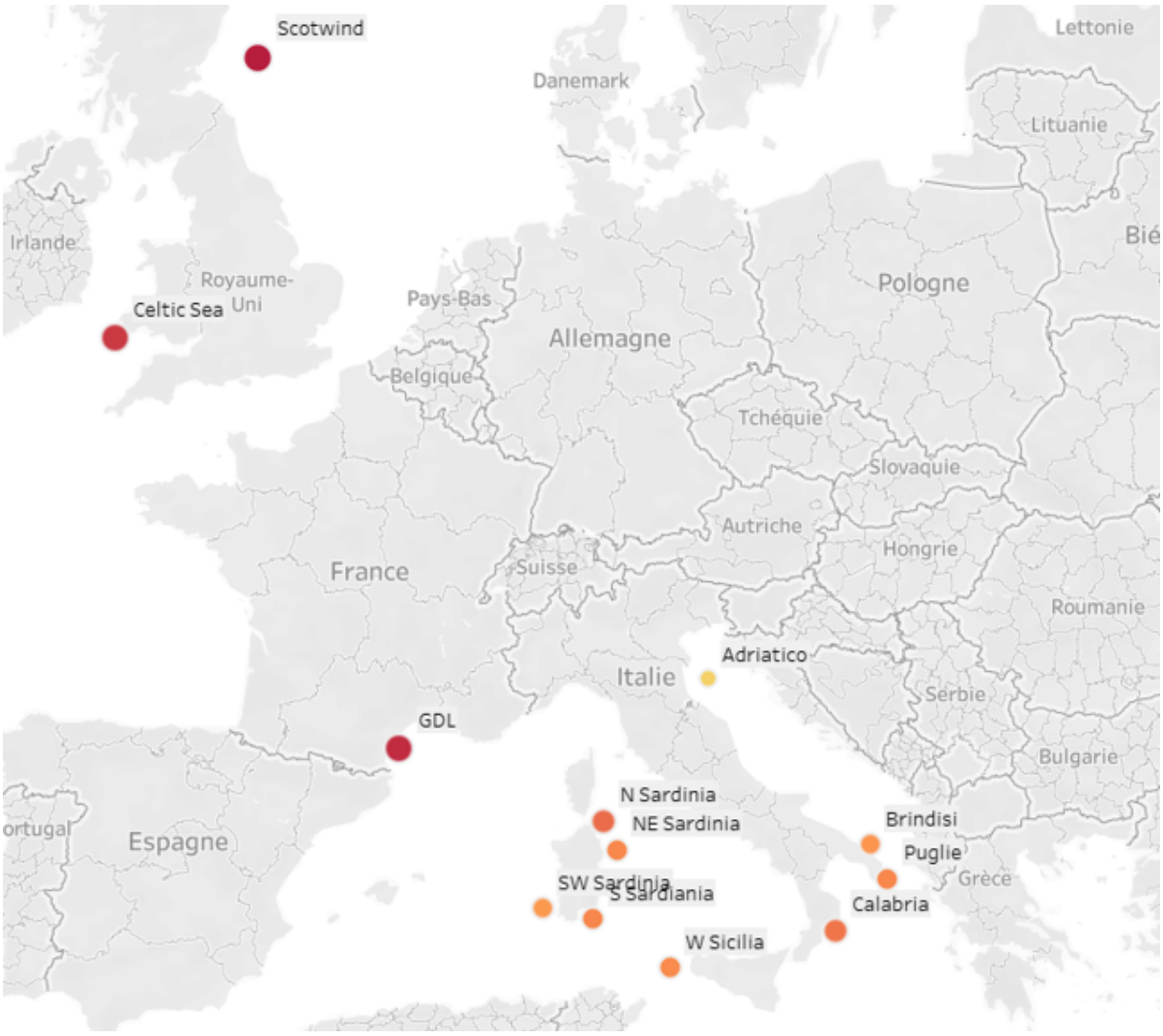

Figure 3.2: Sites of interest

On map of sites of interest chosen in figure 3.2, colours and size of points gave an indication on the energy production potentiality of the site. This assessment is described in subsection 3.6.

3.1.2. Wind resource assessment and equivalent hours estimation

Equivalent hours are an excellent indicator to describe and compare the potential electricity production from wind (and more generally for renewable energy sources) for a given site. For a given turbine with a nominal power P_{nom} [MW] and with a gross annual energy production AEP_{gross} [MWh], the equivalent hours of the site where the turbine produces is $h_{eq} = \frac{AEP_{gross}}{P_{nom}}$. Thus, the equivalent hours represents the actual number of hour at

which the turbine works at its rated power. There are 8760 in a normal year. The closer h_{eq} will be to 8760, the more the site will be interesting in terms of electricity production. Sometimes, the load factor LF [%] is used to represents the ability to produce energy, being strictly linked to the equivalent hours since $LF = 100.\frac{h_{eq}}{8760}[\%]$. The load factor thus represents the percentage of actual power production regarding the maximum production the site could offer in the case the turbine would work at its rated power all of the time. Here, equivalent hours are used as indicators of the wind power potentialities of a given site. Thus, losses due to the farm layout and the operations are not taken in consideration in the calculation of AEP_{gross}: whether or not the farm layout is optimised to minimise wake losses, availability or electrical losses should not enter in consideration for the wind resource assessment of a site. This consideration will nevertheless be taken in consideration in the calculation of the net annual energy production AEP_{net} of a windfarm (cf subsection 3.3.1) that will be used for the calculation of the LCOE.
In section 1.2.1, the physics of wind power generation have been detailed, and power curves were introduced (cf figure 1.5). This power curve are based on equation 1.1 and links the power delivered by a wind turbine in operation to the wind speed at his hub. The power curve is specific to a given turbine model and thus gives us the function of electrical power P delivered by the turbine in function of wind speed u : P(u). Of course, the wind speed varies over time during the year, u and thus by extension P(u) are thus function of time. The gross annual energy production is thus calculated thanks to equation 3.1:

$$AEP_{gross} = \int_{year} P(u(t))dt \tag{3.1}$$

Since we will work with discrete set of data, this results will be approximated by a discrete sum over the year, with data available for a a sample of time periods of same duration called time steps Δt. For every time division i of duration Δt, we will get from the data set the associated wind velocity u_i. The time step must represent an exact divider of a year duration, in a way that $year = N * \Delta t$ N is the number of time steps in the year. The gross annual energy production is thus calculated thanks to equation 3.2:

$$AEP_{gross} = \Sigma_{i=0}^{N} P(u_i).\Delta t \tag{3.2}$$

Here, we actually are approximating a continuous integral by a sum through the so called method of rectangle. Doing so, if the time step duration tends to zero, the approximation will tend to the exact result. This means that in order to obtain precise results, the calculation of the gross AEP requires wind speed data with the smaller time step possible. If as already explained the global Wind Atlas developed by DTU [24] provides reliable

annual mean wind speed value that allowed us to identify windiest zones in subsection 3.1.1, it provides monthly data at is smaller time step. The calculation of the gross annual energy production can thus not be based on a dataset from [24] since monthly mean data are far from describing the real evolution of wind velocity, and thus the real production of a turbine, during a year. Two main arguments explain this: first P(u) is not linear with u (cf equation 1.1) and thus the mean power over a month <P> is different from P(<u>). Then for wind speed over the rated one, the power output is constant equal to P_{nom}.
Another wind dataset is thus required for the estimation of the gross annual energy production. Few open-license datasets are available, and in [98] two of the most-used ones for renewable energy application have been studied and compared to real data from TSO's a posteriori to evaluate which was the most suited. This two data gathering projects are EMHIRES and Renewables ninja. Both projects used meteorological reanalysis data from NASA (MERRA-2 model) and Meteosat-based datasets from CM-SAF (Satellite Application Facility on Climate Monitoring) to generate long-term hourly PV and wind power capacity factor time series [98]. From this comparison it ends up that Ninja datasets provided more realistic results fro wind related projects. Plus, Renewable.Ninja (cf website [25]) features an easy geographical interface displayed on figure 3.3 where zone of interest as well as nacelle height can be easily computed. Then Renewable Ninja provides wind data over a year with a hourly time step, which is way more precise than the monthly time step offered by [24]. The ninja dataset will thus be used for the calculation of the AEP_{gross} of every sites of interest identified in 3.1.1. Entering the precise locations of each site in the Renewable ninja interface, we obtain twelve (one per site of interest) sets of wind-speed data composed of 8760 time slots of one hour coupled to a wind velocity value in [m/s].

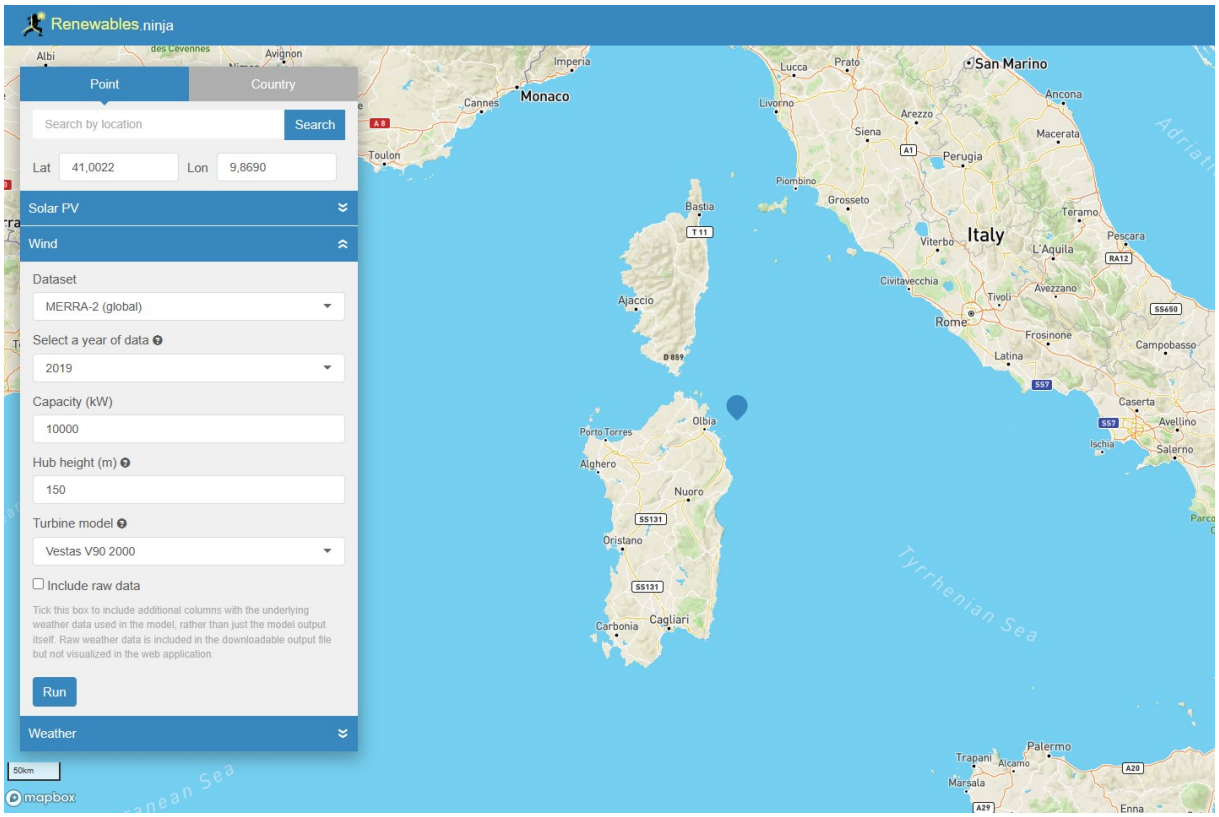

Figure 3.3: Renewable Ninja Interface, from [25]

Yet these data, as explained in [98], are not exactly similar to the real measurements made by TSOs and could be improved. To do so, as it has been done in [99] where open photovoltaic and wind production time series (among which Ninja dataset) for Norwegian locations were evaluated, the strongly reliable from the global wind Atlas [24] will be used. Indeed, unlike Ninja time series that are only given for a year, the mean data disclosed by the wind atlas are the mean of 15 years results. Plus, DTU calculation model implemented in their wind atlas allow to take more geographical features in consideration resulting in more precise spatial meshing: zones are delineated by squares of 3km side while the meshing of Ninja features squares of 30km side. In a nutshell, while ninja time series allow to represents more precisely the time fluctuation of wind speed over a year (with a hourly time step), the yearly mean value disclosed by the wind Atlas is more trustful. The same reasoning has been made in [99], leading to the adjustment of every ninja wind speed values $u_{ninja}(i)$ - and thus for every sites of interest - through the formula 3.3:

$$u_{adjusted}(i) = u_{ninja}(i).\frac{< U_{wind-atlas} >}{< U_{ninja} >} \tag{3.3}$$

Where $< U_{wind-atlas} >$ and $< U_{ninja} >$ are the yearly mean wind velocity of a site ex-

tracted from Global Wind Atlas and from Renewable ninja respectively.
Doing so, the data adjusted will have be coherent with the mean wind speed used for the identification of windiest zone while presenting representative hourly variation over a year. Let's precise that the differences between $< U_{wind-atlas} >$ and $< U_{ninja} >$ ranged from 3% to 16% among the 12 sites, proof of the acceptability of this method since datasets were globally anyway coherent one to another.

We have thus yearly wind speed data time spaced by an hourly step for every site of interest. The function P(u) now have to be assessed. As explained in section 2.3.2, this function id defined by the power curve of the used turbine. These power curves are usually disclosed by turbine manufacturers for turbines in utilisation. To be coherent with our study, power curves from turbines used in offshore projects have been researched. The bigger offshore turbine available for which power curve data were available was the 9.5 MW V164/95000 model from Vestas (cf Vestas website [46]). The power curve and other characteristics of this turbine have disclosed by [100]: the turbine rated at 9.5 MW has a rotor diameter of 164 m and is considered as class IES S. S class being a term specific to offshore turbines and which is analogue to a class 1 as explained in table 1.1. The wind curve data communicated by [100] corresponds to power value for wind speed range between 0 m/s and the cut-out wind speed 25 m/s. Discrete values were given with step of 0.5 m/s : [0 m/s; 0.5 m/s; 1 m/s; 1.5 m/s; .... ; 24.5 m/s; 25 m/s], with a cut-in wind speed of 3.5 m/s and a rated wind speed of 14 m/s. This power function has been introduced in our Excel model and is represented on figure 3.4 alongside the ideal wind power curve computed thanks to wind power equation 1.1 and the rotor diameter of the Vestas V164/95000. A VBA function have coded in order to linearly interpolate a continuous function P(u) from these discrete power curves points and will be use to calculate $P(u_i)$ for every wind speed in the time series of every site and thus calculate the gross AEP thanks to equation 3.2. As shown on figure 3.4, a class 2 power have been extrapolated from the existing class I power curve function. This have been made to model the potential introduction of lower class wind turbines for less windy zone of the Mediterranean. (NOTE: As it has previously been explained, these turbine classes are currently not existent but could be designed on demand in some years to foster the development of FOW in Mediterranean or other zones less windy than North Sea for example). This class 2 power curve have been obtained by contracting the class 1 power curve to make it fit in in a smaller range: the rated wind is assumed to drop from 14 m/s to 12 m/s.

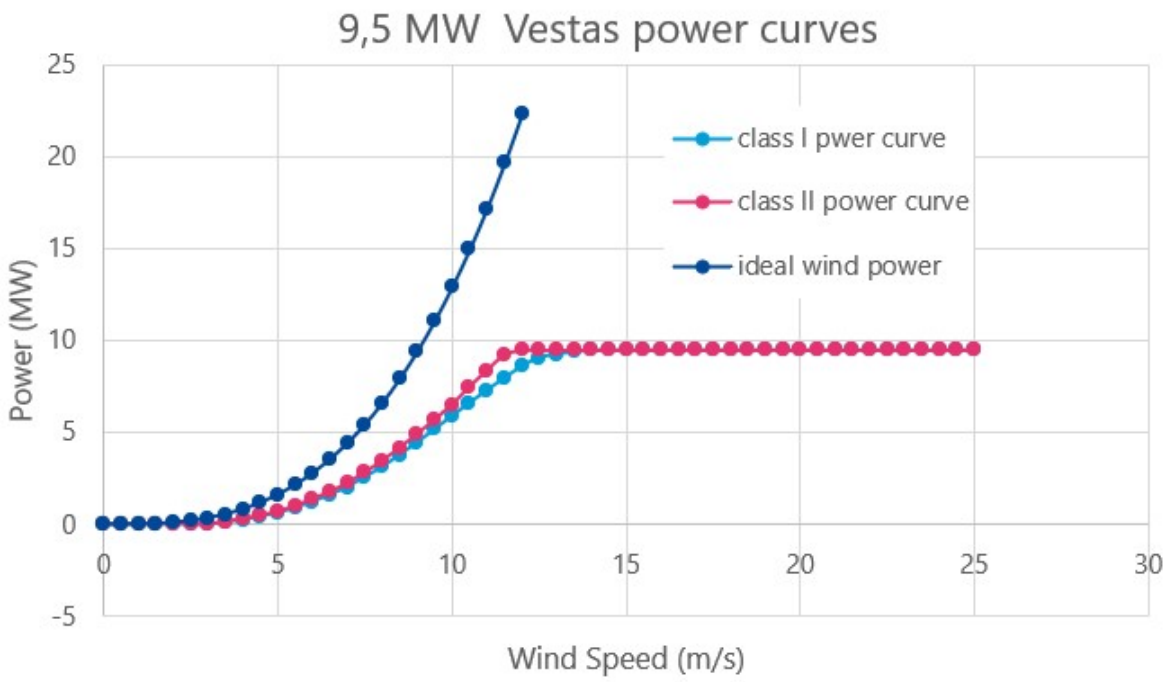

Figure 3.4: Power Curve of a 9.5 MW offshore wind turbine, based on Vestas V164/95000 model

Based on these power curves of a 9.5 MW turbines, power functions for higher rated turbines have been coded in VBA in similar ways to model the impact of the introduction of bigger turbines. The work of forecast performed in chapter 2 for CAPEX evolution with year and bigger turbines will thus be continued in this chapter for the calculation of the LCOE.

For a given wind condition, the use of bigger turbines is not set to drastically modify the equivalent hours of a turbine. Yet, the main impacting parameter here is not the machine rated power but the height of the nacelle that increases with turbine power. The impact of height on wind speed have been discussed in subsection 2.3.2, let's quantify this impact on power production, and thus on equivalent hours, for our site of production. The global wind atlas furnishes wind speed values at 5 different heights: [10m; 50m; 100m; 150m; 200m]. These wind speed mean values have been computed for each height. Then, in 3.3 it is explained that for higher heights were the ground effects were less complex to model, wind Atlas calculation model was using a logarithmic trend to forecast the wind speeds at a height z according to this exact formula: $u_{hub}(z) = u_{ref}\frac{ln(h_{hub}/z}{ln(h_{ref}/z}$. Reference height and wind speed will thus be the values for [10m; 50m; 100m; 150m; 200m]. This logarithmic behaviour has been introduced in our model to estimate the mean wind at the desired height for every turbine size of interest. The link between turbine power and

nacelle height will be made thanks to table 2.1. The results of this process for every sites is available on graphs from picture 3.5 here after.
For every turbine size and associated nacelle height h, the mean wind speed value of adjustment used in equation 3.3 to adjust the Ninja time series will thus depends on h: $< U_{wind-atlas} > (h)$. From 3.5, we get that this effect can lead to non negligible increase in mean wind speed: about 10% increase can be witnessed between "small" turbines with nacelle height topping 100 (5 MW) meters and the huge one to come (35MW) that could reach 250 meters nacelle height (cf table 2.1).

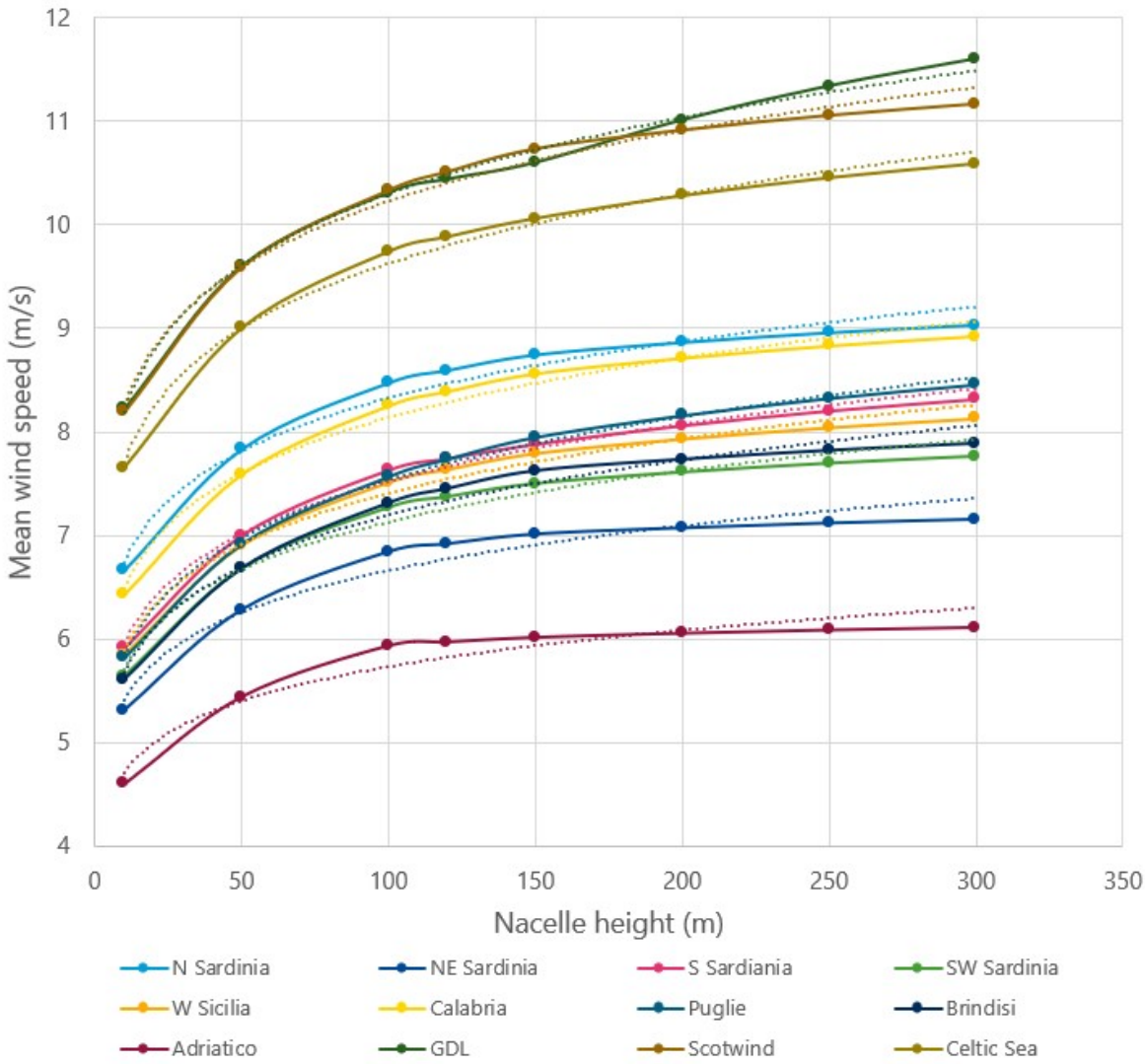

Figure 3.5: Mean wind speed evolution with nacelle height

From picture 3.5 it is obtained that the wind resource for different sites varies. First, there is a gap between Italian locations and the 2 oceanic and GDL locations. As expected, these 3 zones are more windy, and this was actually confirms the process of distinguishing

oceanic condition of softer Mediterranean conditions as seen in Chapter 2. Let's note how good the wind condition in Golfe du Lyon zone actually are, even compared to north Sea conditions known for their excellent predisposition for offshore wind. 2 Italian sites, N Sardinia and Calabria, then appear to be the more windy, with yearly mean wind speed topping 9 m/s for bigger turbines. Then, wind resource distribution for other Italian sites is quite homogeneous with Puglie, S Sardinia, W Sicily, Brindisi and SW Sardinia displaying similar wind conditions. Then, NE Sardinia turns out to be the less windy Sardinian zone considered. Finally, as expected from 3.1, The northern Adriatic zone is the less windy of all.

For every sites of interest, based on equation 3.2 and following the method described here above, the gross annual energy production and thus the equivalent hours have been calculated. The results are presented of figure 3.6 for different turbine sizes in order to take in consideration the height impact previously described. Of course, the equivalent hours results are strongly correlated with mean wind speed results described here above (cf figure 3.5) and the "order" globally remains the same eventough the gaps are increased since as explained by equation 1.1 electricity power produced evolves with the square of wind speed. SW Sardinia and Brindisi sites presents a bigger equivalent hours gap with other Italian sites than mean wind speed results from picture 3.5 might indicate. This could be explained by wind time profile less constant with big variation. Let's precise that sites with bigger equivalent hours estimated by our model are represented by bigger circles and in ref on European map from picture 3.2.

For sake of comparison, the equivalent hours of a typical onshore wind farm in Italy has been added on the graph comparing the equivalent hours of different sites of interest on figure 3.6 through a green bar. The value is 2100 hours and has been taken out from GSE report [101]. It is representative of a good performing project using big turbines. Going offshore could thus unlock very interesting production perspective even in Italy: for more windy sites of our study (Calabria and North Sardinia), between 71% and 86% (according on turbine height) increased in gross annual electric production are modelled here. The advantages of offshore wind regarding onshore wind described in section 1.2 are thus confirmed in Italy. Later with the calculation of the LCOE in section 3.3 it will be discuss to what extent this increase in production counterweights the over cost of FOW regarding onshore wind projects.

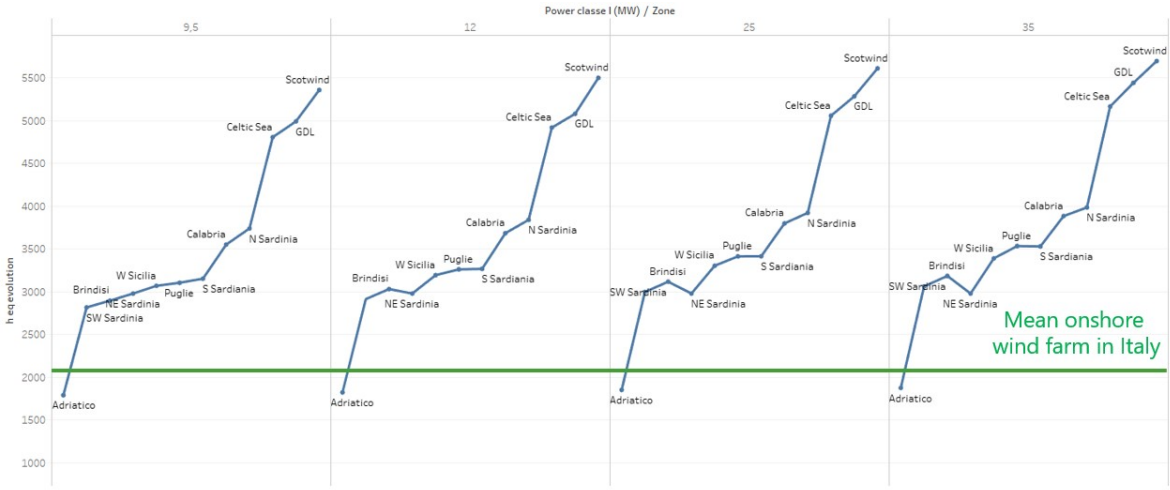

Figure 3.6: Equivalent hours of site of interest for different turbine sizes

3.1.3. Port infrastructures issue

Let's now have a word on supply chain and more precisely port infrastructures that also enters in the equation to evaluate if a site is good or not for the development of floating offshore wind project. The idea here is not to go deeply in the description of port operations (a whole study would be required) but to discuss how the existing or yet to be built port infrastructures can foster or not the development FOW project at a given site. Of course, the closer the site will be from the port were assembling and construction is made the more advantageous it will be from an economical point of view. Indeed, with lower distance comes lower towing time and thus installation cost. Plus, lower time spent in sea lower the constraint on meteorological windows during which towing can be performed. Yet, from a strict technological challenge point of view, long distance can be covered by tugboats as demonstrated by towing route followed by Stiesdal for their Tetra Demonstrator displayed on figure 3.7. For this project, about 400 kilometres have been covered by tugboats to link the Danish assembling port displayed on the left of the left of figure 3.7 to the operating site located in the Norwegian sea.

The insight here is thus that generally the distance from an industrial port will have to be taken in consideration in the global economical assessment of a project but is not likely to be a clear technological barrier to its development.

Figure 3.7: Construction port and towing route for Tetra demonstrator from Stiesdal [21]

The Northern Sea, epicentre of development for offshore wind, has benefited of a long track-record in naval industry as well as Oil&Gas offshore operation to solve the port side issue. Indeed many port infrastructures already existing in these countries (UK, Denmark, Norway, Netherlands etc...) as well as the technological knowledge from industrial players have been naturally re-used and adapted to offshore wind enhancing its development in this zone. The material and assembling related supply chains are then similar and thus near to optimisation already, reducing the technological and financial risk. This inner knowledge is actually a strong asset for offshore wind development in Europe. In brief (many more complex arguments out of the scope of this study complements this note and are gathered in EU report on the implementation of the Marine Strategy Framework Directive [102]), the development of offshore wind allows EU to cope with its green objectives while concentrating their investment in Europe, creating jobs and supporting internal economy. In comparison, the solar industry for example concentrates its manufacture in Asia and thus less European jobs are created by investments made in solar power industry. That is why EU led various incentive policies and support many R&D projects linked to FOW as detailed in [102].

In the Mediterranean, the naval industry is historically less intense and less similar industries have pre-existed before FOW. The port infrastructures as well as the number of ports could thus appear as a potential brake for FOW development in the zone. Let's see

how France, identified in subsection 1.4.4 as the leader of the FOW development in the Mediterranean, is dealing with this problematic. Since as previously explained, France adopts a centralised scheme development strategy, the assembling and port operation were early identified by authorities. It end up with the development of a dedicated industrial cluster dedicated to FOW within the pre-existing naval industrial zone of Fos-Sur-Mer. Located in the northern part of the Golfe du Lyon were french projects, current and futures, will be located, this industrial hub is set to concentrate all the assembling and late supply chain operations related to FOW in the French Mediterranean sea. Doing so, France aimed at controlling and optimising the development of the field and the creation of jobs in the country. The main piece of this industrial clustering strategy is the naval building site of Eiffage Metal [103], a French international farm leader in metal manufacturing and engineering, located in Fos-sur-mer. This site already owned various asset (cranes, storage zones, dry rocks with important drafts) and few modifications thus allow it to be perfectly designed for FOW port-side assembling and manufacturing. In late 2020, the SBM-offshore [63] TLP floaters for Provence Grand-Large pilot project presented in subsection 1.4.4 were manufactured in the site as displayed on figure 3.8.

Figure 3.8: Eiffage Metal building site of Fos-Sur-Mer in France

In the Italian case, a developer led development strategy is at stake and thus no assem-

bling zones have been a priori identified by authorities. Plus, the zone of interest are way widely distributed than for the French case and one port could hardly handle the operations related to every projects located in distant zones. To answer this problematic, an overview of industrial port in Italy have been performed, with the aim of identifying ports or naval building sites in capacity or not of assuming FOW related operations. Out of hundreds on Italian ports, 23 label as "industrial" by naval authorities have been selected and more deeply analysed. These 23 ports have been localised on an Italian map on figure 3.9 The idea here is to use existing facility to gain in efficiency: the construction of dedicated structures could be a possibility in case of future intensification of the sector but is currently out of question.
For each of these 23 ports already performing industrial - i.e. crafting, lifting and assembling - operations, various data were gathered and evaluation criteria were selected. Based on the previous considerations detailed in chapter 2 and corroborated by dedicated chapter in [58], the suitability of a port for floating offshore industry will be assumed to depend on:

- Dry rock size: Enough space for assembling and storage of large pieces of the substructure is required. Plus, for large scale farms, it is desirable that various floating substructures could be assemble at the same time.
- Draft: The draft at dry rock level and along port or naval building site entry must be important enough to allow the free-floating of floating structures fully assembled. This value may differ from one concept to another. But ideal ports must feature draft of at least seven meters deep. This criteria appears as the most critical one since its modification would require complex and costly operations.
- Lifting structures (cranes): The site must feature lifting structure able to deal with the heaviest pieces of the substructure. Actually, this kind of cranes are widely available in industrial and even commercial ports, and can even be rented out from external providers.

Based on these criteria, the 23 Italian ports have been classified in three categories. First, 4 ports out of 23 simply do not meet the requirements and must be taken out of considerations for potential FOW projects. Then, 10 of 23 are currently not matching every needs for FOW development but reasonable investments could be performed to make them enter in the discussion. The amount of this investment from one case to another and will thus be cost-efficient only if a strong development of the FOW field occurs in their zone and if no other near site offers better features. Finally, 9 ports out of 22 have been considered as well suited for FOW projects without any barriers in terms

of facilities and asset. Among these 9, size differ and huge ports as Genoa or Gioia Tauri for example will more easily handle large commercial scale pace than smaller port as the Oristano one in Sardinia. Yet, FOW related operations would easily be performed there. These considerations are summarised on the map of Italian ports displayed on figure 3.9 where green points represents ports perfectly appropriate for FOW operations, orange ones ports that can potentially be suitable after some adaptations, and ports represented by red ones do not meet requirements.
This work is here indicative and developers will obviously have to perform deeper analysis of specific port features to verify that a port potentially suited for FOW development is actually able to assume the port-side operations required.

Figure 3.9: Review of Italian industrial ports and compatibility with FOW port operations

Superposing this map of Italian ports with the map of main zone of interest for future Italian FOW projects (cf figure 3.1.6), it seems that Italian industrial ports network will be able to cover the future FOW projects. If some investment and infrastructural evolution will probably be required to promote the field, this important part of supply chain do not appear as a major brake for the industry development in Italy. Up to the developer to

assess the real cost of this port operation in the final cost of their projects.

3.1.4. Distance from shore and visual impact

Nimby (not in my backyard) phenomenon has already be defined in chapter 1. For offshore wind in general, and more particularly for floating offshore wind, this phenomenon could trigger strong political and social outcries from local communities concerned by a FOW project due to its detrimental impact on landslides. Indeed, the use of numerous big turbines going until 400 meters in maximum height (cf table 2.1) with very large moving parts can potentially drastically modify the sea landscape viewed from the shore. This problematic is even more tremendous when touristic or densely populated sites are considered. This is the case for Italian projects since as seen on map 3.2, the most interesting zones for potential FOW development are located in very touristic areas where a change in sea landscape could denature remarkable sites and negatively impact the important touristic related economies of these zones. Actually, the negative landscape related externalities potentially generated by an offshore project can drastically slow down the commissioning and even stop the project.

The impact of a project on a landslide is hard to quantify since it brings subjective criteria. Yet, it can still be quantitatively studied and its relation with some project parameters can be discussed. Here, the two main parameters selected for the visual impact analysis are the turbine size: bigger turbine will have bigger impact; and distance from shore of the nearest row of turbine of a farm: the further away from shore the farm will be located, the lower the visual impact will be. A relation between turbine power (and thus size), distance from shore must thus be found.

The visual impact of an object from a human eye, in a simple approach, varies linearly with distance: an object displaced at a distance twice bigger will seem twice smaller for a human eye. Yet, in our special case here since we observe objects located at sea level and a sufficient distance, the earth curvature will have an effect and will tend to "hide" objects located far from observer. This effect can not be neglected for distances at stake here (tens of kilometres) and is schematised on picture 3.10 here after.

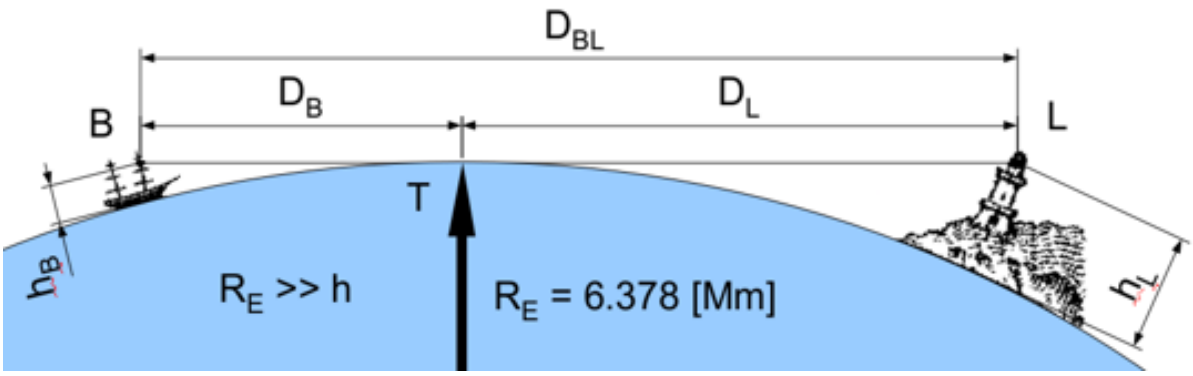

Figure 3.10: Earth curvature effect on visualisation from long distance

Reusing the notations from figure 3.10, point B will be the observer and h_B will be its height. Then Point L will be the nearest turbine from observer point of view, and its height h_L will thus be the maximum height of the diameter, i.e. the nacelle height plus half of rotor diameter, which evolve with turbine size according on table 2.1. The distance $D_{BL} = D_B + D_L$ for which the object located in point L is integrally hidden by earth curvature for an observer located in point B will depend on the heights h_B and h_L (in our case h_L the maximum height of the turbine will be the critical parameter since the observer is assumed to be located at sea level). The earth Radius $R_E = OT$ (O being the center of the earth and T is represented on figure 3.10) measured 6378 kilometres. It is thus at least two order of magnitudes higher as any other distance considered here. In this configuration, the two triangles OBT and OLT appear as rectangle in B and L respectively. Using Pythagorean theorem it is obtained that:

$$OB^2 = BT^2 + OT^2 \tag{3.4}$$

Thus:

$$(R_E + h_B)^2 = D_B^2 + R_E^2 \tag{3.5}$$

And thus developing the quadratic form:

$$D_B = \sqrt{h_B^2 + 2.R_E.h_B} \tag{3.6}$$

The exact same reasoning is made for the point L, and thus the relation between the height hidden by the earth curvature and the distance from shore is given by equation 3.7:

$$D_{BL} = D_B + D_L = \sqrt{h_B^2 + 2.R_E.h_B} + \sqrt{h_L^2 + 2.R_E.h_L} \tag{3.7}$$

Thanks to this equation, we can either determine the distance at which a turbine of a

given height will be hidden or inversely the height hidden by the earth curvature for a given distance. Let's precise that it is here assumed that the observer is located at sea level and, it will be assumed that $h_B = 1.80m$. If the landslide is for example made of high cliff on the cost offering a higher point of view, this will impact the results presented here after. Developers will thus have to lead holistic analysis taking every site specific features in consideration. In picture 3.11 an extract of such a kind of study led for an Italian (located in Calabria more exactly) FOW project, found in scoping documentation disclosed by project leaders of Italian projects in [54], is displayed.

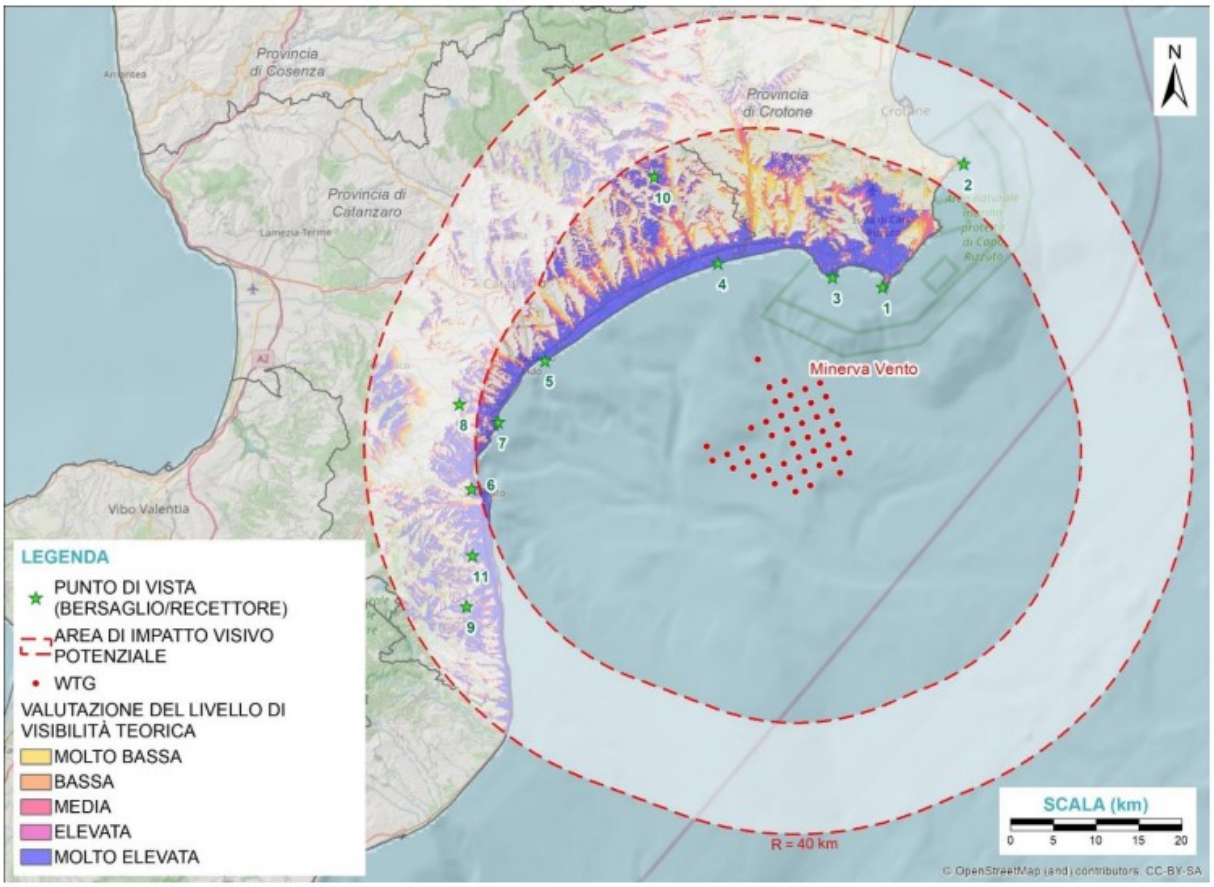

Figure 3.11: Geographical evaluation of the visual impact on landscape of FOW project called Minervia and located in south Italy (Calabria)

For sake of simplicity, our visual impact considerations will be made for an observer located onshore, at sea level. To be socially accepted, it is not mandatory for an offshore wind project to be integrally hidden by earth curvature. For example in France, after long official public discussions with local authorities and citizens, the minimum distance from shore on which agreement has been found for the St-Nazaire project in Britain is 15 km. At this distance, since turbine used there are rated at 6MW, equation 3.7 gives us that

only 8.4 meters are hidden by earth curvature, i.e. 4.4% of a 6MW maximum turbine height. Yet, the visual impact for an observer from shore located at sea level obtained for this distanced is shown on figure3.12 here after:

Figure 3.12: Offshore turbine visual impact example for French project

This visual impact can be considered as acceptable, or at least it has been so in this french case in touristic zone as well. To be integrally hidden by earth curvature, the farm would have been located at 53.5 km from shore, resulting in a 250% increase of the adopted distance, and thus in drastic increase in CAPEX - mainly on connection to grid side as explained in sections 2.5 and 2.8. A wide range of distance potentially acceptable exist and the developers will have to discuss with local entities to determine which one to agree on. A kind of socio-economic compromise will have to be found between developers aiming at reducing distance and thus cost and local authorities and citizens that would prefer to reduce the visual impact at its maximum. In our model, the visual impact obtained in St-Nazaire as represented on figure 3.12 will be considered as our limit acceptable impact, while the best case in term of impact will be model by the distance at which turbines would be integrally hidden. For various turbine sizes (and thus heights), the distance from shore associated with each case will be calculated, defining a domain of possible distance from shore/turbine height. In order to maintain a similar visibility as the one from picture 3.12 for bigger turbines, calculation made using equation 3.7 and maintaining the same angle of vision defined as the report between the turbine height and distance from shore has bee performed. The outputs from this calculation are displayed on figure 3.13. On this graph are represented for every turbine power in dark blue the minimum distance at which the farm must be located to obtain a visual impact similar to the one from picture 3.12 and in light blue the distance from shore at which the farm must be located to obtain a zero visual impact since the farm will be integrally hidden from earth curvature.

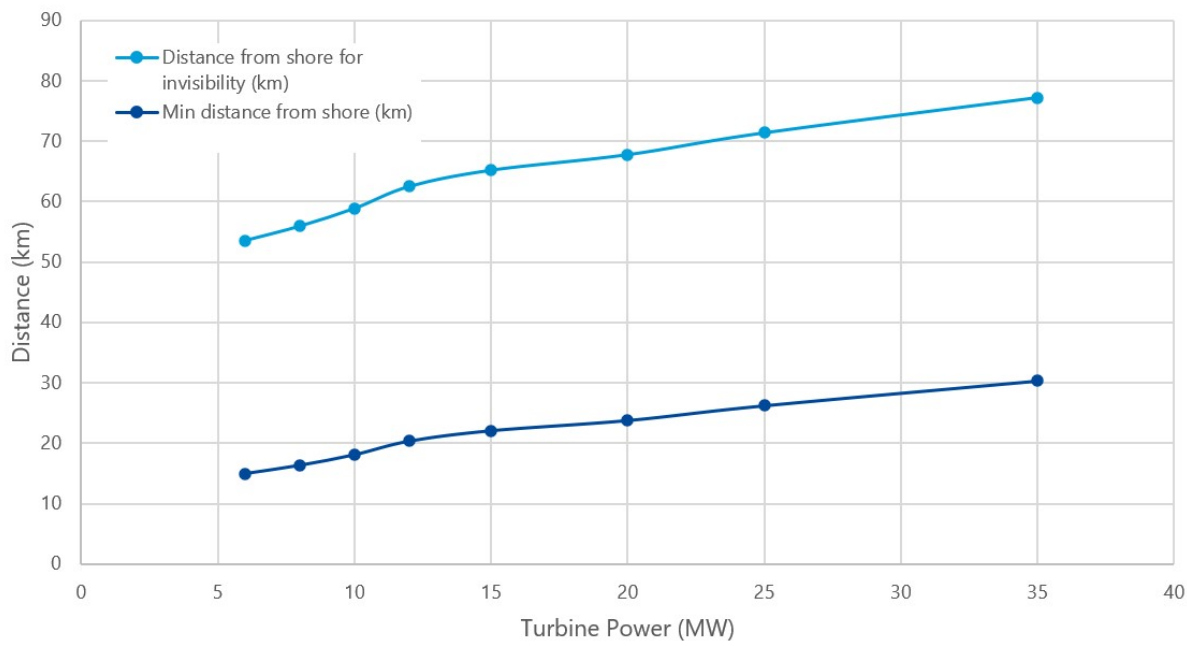

Figure 3.13: Evolution of minimum distance from shore to obtain limited visual impact with turbine size

This graph will help us to quantitatively assess the visual impact of different projects. As previously said, further inquiries will be required for each specific projects and consultations with local authorities will be required early in the planning phase to prevent developers from strong social outcries.

3.1.5. Bathymetry

As explained in chapter two, the site's depth has a tremendous impact on the CAPEX of a FOW project since it will directly influences moorings and inner-array cables costs (cf section 2.4 and 2.6 respectively). Plus, as explained in section 2.4 and summarised by picture 2.72, the site's depth will influence the technological choice for the type of floater used. In chapter 2, emphasis has been put on two technologies : Semi-submersibles (SS) and Tension leg platforms (TLP). It has been seen that SS were clearly more indicated for shallower water (until 200 m deep) while TLP solutions were clearly ahead for deep waters (over 500 m deep). It has also been precised that SS were currently a more mature technologies used for more projects existing or in construction.
In chapter two, Mediterranean and North sea (and Ocean in general) were opposed through their meteorological conditions. Actually, the analysis of Bathymetry map for North Sea and Italian surroundings displayed on picture 3.14 and 3.15 shows that bathymetry as well was a distinctive points between these two zones. Indeed, in the north sea, depth

rarely overpass 100 meters near the shores while it can quickly reach 2000 meters depth in the Mediterranean. It can be noted that the SS, well designed for shallow water, could further benefits from this condition since the FOW sector is very dynamic in this sector.

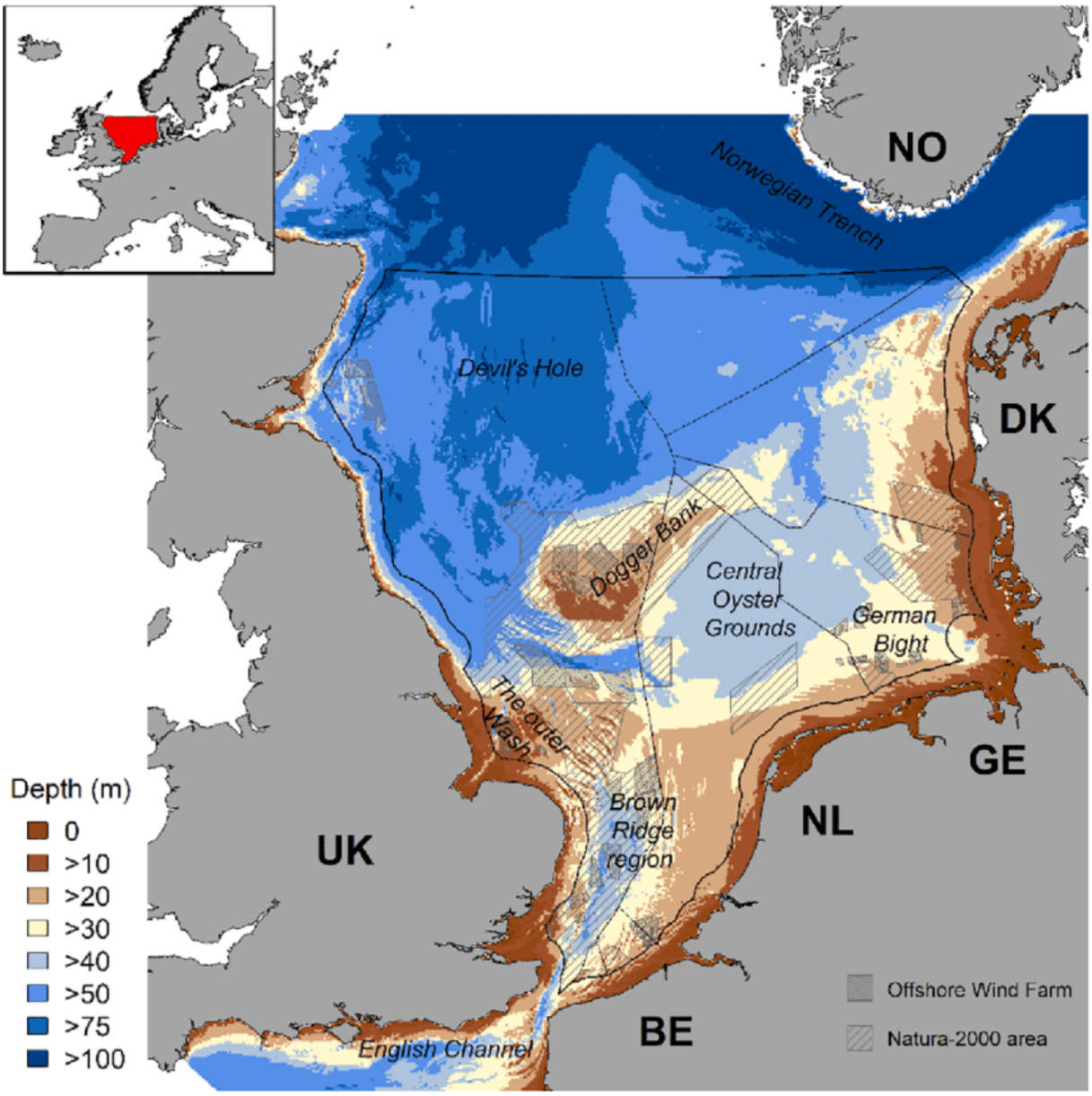

Figure 3.14: North sea bathymetry, from [26]

Let's further analyse the bathymetry of Italy. A very useful tool for this analysis is provided by the Italian ministry of Environment: il Geoportale Nazionale [27]. This tool offers interactive maps of Italy and a bathymetry dedicated layer can be applied, from which picture 3.15 have been extracted. Plus, this tool allow us to precisely measure the distance between points, very useful to assess the distance from shore on an hypothetical

FOW project. The legend of the map distinguishes zones according on their depth range, with pivot depth being [200m; 500m; 1000m and 2000m]. This pivot depths will thus perfectly match the parameter values used for depth in our cost model in Chapter 2. Each site has its particularities seabed depth profile is not uniform all over Italian seas. Yet as previously explained the main insight is way that Mediterranean in the surrounding of italy is deeper than Northern sea and moreover that seabed vertical profile is harsh: we "fall" quickly. Indeed, at the notable exception of the Adriatic and to lower extent of the Sicilian channel at the west of Sicily, at 40 km from the 200 meters depth is already reached.

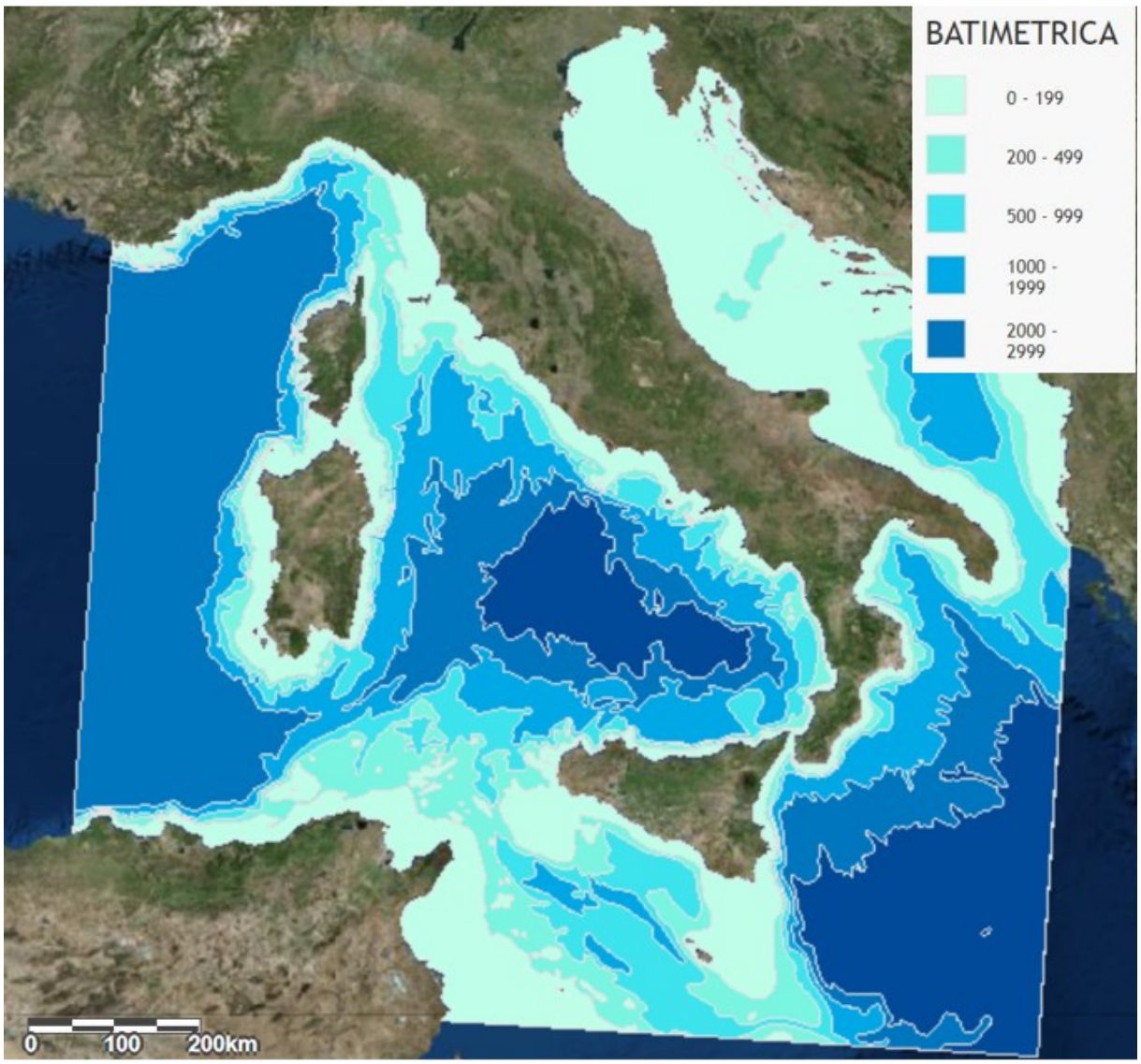

Figure 3.15: Map of the bathymetry of Italian surroundings, from [27]

From this analysis, an important insight to get is the link between depth and distance from

shore. Generally, a more distant project - leading to connection over-costs - will be located in deeper waters leading to moorings and inner array over-costs. The relation between depth and distance from shore will be characteristic of the zone considered for a project. For every zone of interest identified in section 3.1.1, this relation will be quantitatively described by assessing at which distance from shore each depth milestones were achieved : [200m; 500m; 1000m]. The results from this analysis are summarised in table from figure 3.16 here after.

From this table the trend of the vertical profile of seabed for different sites of interest can be interpolated. For example from the table on figure 3.16 we get that for Calabria site, identified in subsection 3.1.2 as one with a big potential in terms of wind resource, the seabed profile "falls" very fast. Indeed, only 16 kilometres from the shore, at a distance at which according to limits from picture 3.13 only small turbines would be socially accepted from a visual impact point of view, the depth is already 500 meters. In order to install bigger turbines, to limit their visual impact in this highly touristic zone, we must go beyond 34 kilometres and thus the "1000 m line". Depth will thus be a major issue of any future project in Calabria. The 1000 m line is achieved even faster for NE Sardinia zone since it is located at only 24.3 km from shore. In the table, some cells are highlighted in green: this is the case when the none visual impact barrier as described in figure 3.13 is reached (at least for small turbines). This mean that in these zones there will be a real possibility, being distant enough from shore, of developing floating project at reasonable depth without impacting much the landscape. For the two zones previously discussed, this green cell is not achieved within 1000 meters depth. For the Adriatic zone, this is the contrary: only shallow waters exist and depth will represent a small issue, fixed bottom offshore wind might even be a possibility, yet regarding the wind resources estimated for this zone (cf figure 3.6), this represent a small interest eventough this interesting depth properties. Then, for the majority of remaining Italian sites of interest, this "low visual impact zone" is achieved for depth of 1000 meters. In particular, for the N Sardinia zone considered as the most windy italian zone in subsection 3.6, the 1000 m line is located at 62 km from shore. In comparison with other Italian sites, N Sardinia seems to emerge as a interesting zone in terms of productivity and bathymetry. That is why it will be chosen as good candidate to further work on in section 3.3. Out of these Italian sites, an other interesting zone emerges in term of bathymetry: W Sicilia (located in Western Sicily on map 3.2). Indeed a plateau exists in the Sicilian channel and the 200 meters line is thus achieved only 58 kilometres from shore, with a smooth decreasing trend. Even with big turbines used, it will thus be possible to implement in this zone project distant enough from to not impact the landscape too much while profiting of drops in CAPEX and complexity of 200 meters deep waters. This zone is besides more suited for the use

of more advanced SS technologies.
Finally, let's have a quick word on GDL bathymetry. It is obtained that in addition to the very interesting wind resources of the site, the zone presents very interesting bathymetry characteristics with a 200 m line located at 85 km from shore according to french equivalent of [27].

	Lat	Long	Linea 200 m	Linea 500 m	Linea 1000 m
Adriatico	44,52	13,02	none	none	none
Calabria	38,69	17	10	16	34
S Sardiania	38,96	9,46	17	32	67
NE Sardinia	40,6	10,21	18	21	24,3
N Sardinia	41,28	9,79	23,5	31,3	62
SW Sardinia	39,24	7,9	24	47	55
Puglie	39,92	18,6	32	38	63
Brindisi	40,74	18,06	39	36	none
W Sicilia	37,78	11,86	58	80	100
GDL	42,94	3,45	85	120	none
Scotwind	56,61	-0,92	85	120	none
Celtic Sea	51,54	-5,36	85	120	none

Figure 3.16: Bathymetry and distance from shore table for 12 zones of interest

Analysing these results from a CAPEX evaluation perspective as developed in chapter two, a main insight would be the important role of TLP solutions for FOW in Italy and in the Mediterranean in general (Spanish projects would face similar depth issues). Indeed, to unlock the full potential of offshore wind in Italy, viable solutions to develop projects without impacting remarkable landscapes at depth (way) higher than 500 meters will have to be develop: as explained in chapter 2 and more precisely in section 2.4, TLP solutions are more indicated than other typologies for these kind of projects. Actually, it can even be hypothesised that development of FOW in Italy and in the Mediterranean and the one of TLP solutions that are a little lagging behind SS ones in terms of TRL will be correlated. Indeed, if the FOW market remains in its first time concentrated in "shallow zones" (until 300 meters) as the North Sea, the Atlantic cost or some zones in Korea the SS may remain the preferable solution and the development gap between TLP and SS solutions might take time to be fill. At small depths where as explained in section 2.8 on

figure 2.114 the CAPEX reduction offered by TLPs are less important, industrial might not take the step toward developing TLP based project which could further slow down the global TLP market. For example, as previously explained in chapter 2, strong industrial feed-backs are still lacking on the installation complexity and the fatigue behaviours of tendons for TLP solutions. That is why the clear need of TLPs solutions for deep waters zones as in the Mediterranean will be beneficial for TLP development since developers will have no other choice that advance in this direction. The SBM pilot project in France (cf subsection 1.4.4) could unlock this development path in the Mediterranean: this is meaningful that the first Mediterranean FOW pilot features TLP substructures.
Globally, the high depth of the Mediterranean could be seen as a brake for FOW development in this sea and more particularly in Italy. Yet, this could actually become an asset since the FOW sector will not suffer a "competition" with the fixed-bottom offshore sector, that as explained in section 1.3 is set to keep leading the way in the offshore sector in the decade to come. Indeed, eventough many floating projects are planned in various countries (cf Scotwind in the UK or ULSAN in Korea, cf 1.4.4), many countries as USA, Germany, Belgium and even UK and France that are FOW pioneers are favouring fixed-bottom solutions for the majority of their offshore projects. In these zones, for techno-economic reasons, a less windy zone where fixed-bottom solutions can be used might be chosen over a more windy zone where only FOW can be considered. Thus, the development of FOW could be a little slow down until a saturation effect appears, FOW covering a way larger potential territory than fixed bottom. In the Mediterranean, Fixed-bottom is almost out of question everywhere, and thus countries and industrial players will have no other choice than developing the floating sector if they want to unlock their offshore wind potential.

3.1.6. Review of Italian projects

To conclude this site impact assessment section, let's further discuss the 18 more advanced (yet still in their planning phase) commercial scale Italian projects presented in section 1.4 and analyse them through the prism of previous site related insights. To do so, a deep analysis of scoping documents transmitted by project leaders to the Italian Environment ministry (available at [54]) have been performed and every 18 projects information on - location, farm power, turbine size, connection to grid type, inner array cables ratings, wind velocity, productivity estimated, floater typology, depth, distance from shore and even early CAPEX estimation for some - have been gathered. Globally, as previously explained in chapter 2, these features in terms of technological choices (inner array rating, turbine size, connection to grid technology etc...) corroborate the hypothesis made in

our CAPEX model of technology. This subsection will be more focused on site impact assessment related data.

The two following map on picture 3.17 and 3.18 are extracted from Tableau software where results from this analysis have been processed and represent the localisation of each project. The first insight to get from these maps is that the projects considered here are globally in adequacy with the site of interest identified in subsection 3.2 (NOTE: the point on the maps are indicative and, for sake of readability, do not represent the exact location of the projects). Then, in terms of wind resource as well as predicted equivalent hours, results were also matching within a reasonable range (never more than a 20% difference in yearly mean wind speed). Though, these wind assessment sometimes present important differences between sites very close one to another (many project expected in west Sicily or south west Sardinia) and are set to be indicative, on site real measurement will sharpen these data while project will go on. Plus, similar wind velocities sometimes lead to very different equivalent hours estimation and few information on the method used to calculate these are disclosed. This information will thus be taken with caution and will not be further discuss. Same thing for CAPEX estimation given that are not supported by strong argumentation and thus hard to get insights from.

Actually, since these projects are all in their early planning stage, the Scoping documents do not have any contractual value on technologies and some modifications can be made in the future. Though, the zone in which project are set to be commissioned theoretically cannot change since the environmental impact assessment realised concern these exact zone. Same for wind farm size since the connection to grid request formulated to TSO depends on a given farm nominal power. The mean depth of the projects, its distance from shore and the size of the farms are thus not expected to be modified, or the project would have to re-initiate a Scoping process. These parameters have thus been analysed and put in perspective with the arguments of previous subsection 3.1.4 and 3.1.5. First, based on the turbine size of the farms, their distance to shore and accordingly to visual zones established in subsection 3.1.4 and summarised in figure 3.13, the potential visual impact on landscapes for an observer located onshore have been estimated. Every 18 projects have been ranked in four categories based on their visual impact and outputs are displayed on picture 3.17. Only two projects were classified as having a null impact on landscape since located at distance where turbines would integrally hidden by earth curvature. These are coloured in green on the map. Then, 8 projects coloured in blue on the map would have a low visual impact. This mean that they would be located between the two barriers lines defined on figure 3.13 but would be closer to the higher lines making the turbine look very small for an observer located on the shore. Then, 3 projects coloured in orange on the map would have a high visual impact. This mean that they would be

located between the two barriers lines defined on figure 3.13 but would be closer to the lower line making the turbines look bigger for an observer located on the shore. Finally, 5 projects coloured in red on the map would have very high visual impact. This mean that they would be located below the lower barrier line defined on figure 3.13 making the turbines look big for an observer located on the shore. Besides, on this map, farm size are also indicated by size of points.

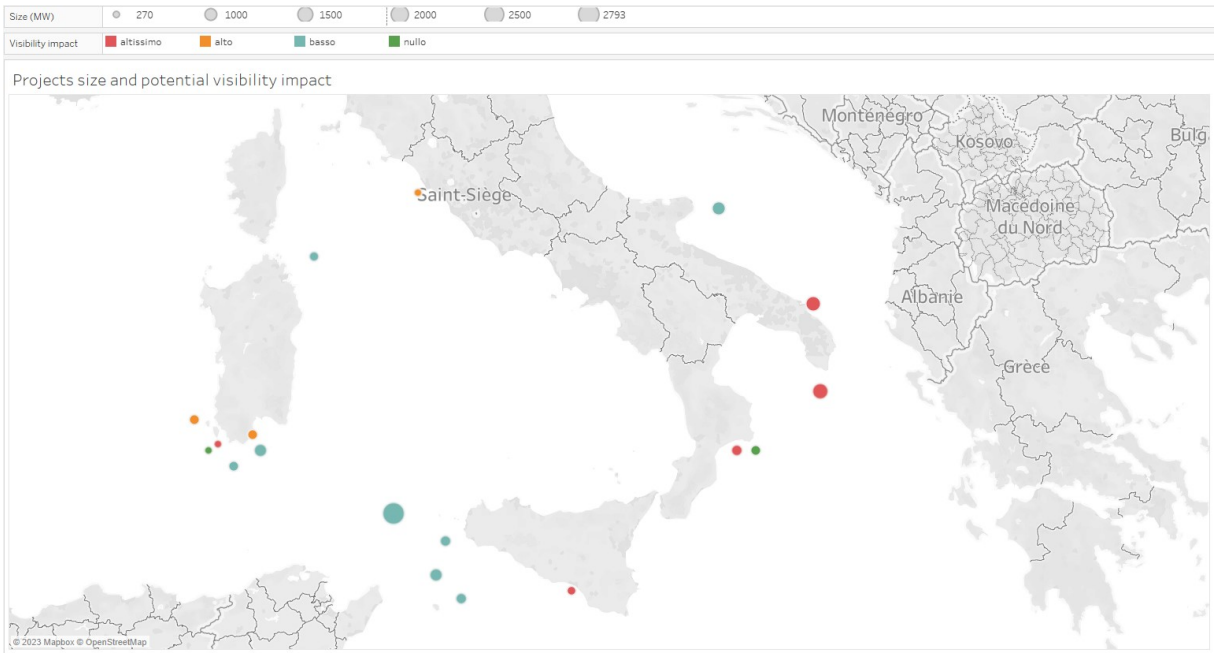

Figure 3.17: Overview of the potential impact on landscape of announced FOW Italian projects

The project with high and moreover very high impact on landscapes will probably face important social outcries and thus major brakes for their development. It is safe to see that long debate with local authorities and citizens will take place and slow down, and even potentially definitely stop the project development as currently described. Indeed, this projects are located on the Sardinian, Sicilian, Calabrian and Pugliese coasts that heavily depend on touristic activities linked to the beauty of their littoral landscapes that would be damaged by these projects. Maybe the developers have neglect this aspect or are prepared to fierce discussions to maintain their future unpopular projects.

Then, the next map displayed on figure 3.18 put in perspective project depth with the potential floater typology used. To do so, for each project forms indicates typology announced, while the colour gradient from green for low depth to red for high depth

represents the mean depth of the projects. A majority of projects, 12 out of 18, are mentioning SS floaters in their scoping documentation, while only two are considering TLP solutions. Three others developers did not mentioned any typology in their scoping documents and a last one is considering multi solution: both TLPs and SS could be used on the site (make sense since this project, as shown on previous map, is very big and will involve many turbines over a large surface where depth can vary). This results could appear in contradiction with the insight from subsection 3.1.5 stating that TLP solution were the best solution to answer the depth issue for many Italian and Mediterranean projects. Yet, let's not forget that in these early planning stage the description of the floater used is only indicative and that the final design phase has yet to begin. Thus, this over-representation of SS solutions is here more representative of the current FOW market where SS technology is, as previously explained, more mature than TLP one. Looking at the couples depth / floater typology evidenced by picture 3.18, it can be seen that SS solutions are considered for projects featuring depth over 1000 m, which is a technological non-sense. Indeed, as explained in section 2.4 at these depths, more than economically cancelled this solution is impossible from physical and practical point of views: footprints would be huge, the weight of the chains would sink the structure etc... Thus, it can legitimately be thought that these projects have no typology already identified and that more TLP solution will be effectively adopted. NOTE: No spar or barge technologies have been considered, which can be seen as validation of our model hypothesis made in chapter 2.

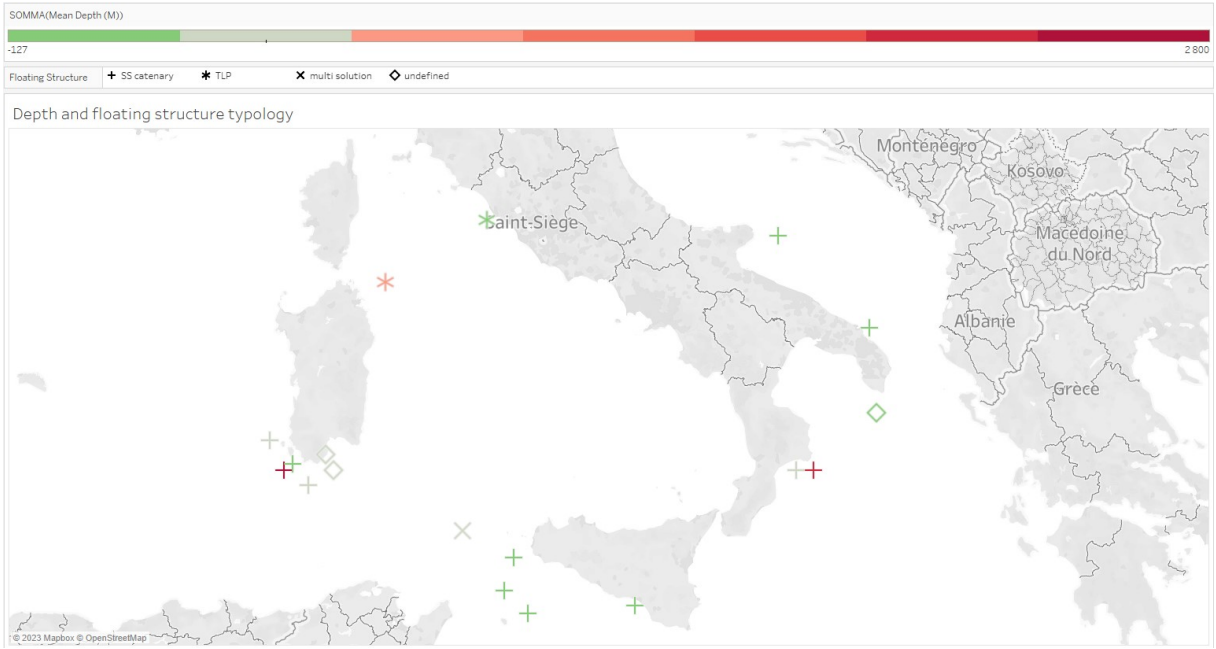

Figure 3.18: Overview of the mean depth and floater technology currently considered for announced FOW Italian projects

From the previous considerations it can be concluded that Italian projects might evolve from their current definitions and might face major challenges through their developments. Yet, their numbers shows the strong interest industrial players have in this sector in Italy and the commissioning of first projects will probably arrive in the early 2030's, letting developers time to terminate the design of their projects and to face social and legal issues that other countries as France or UK already faced before launching their FOW field.

3.2. A Word on Operation and Maintenance (O&M)

The core of this work have been concentrated on CAPEX estimation in chapter 2. To calculate the LCOE of a project, operation and maintenance related expenditures (OPEX) must also be assessed. For renewable power farms, OPEX generally does not represent an important part of the LCOE in comparison with fuel based power plants since the fuel cost enters in this category. In the particular case of offshore wind, this statement is less true since every actions linked to monitoring, maintenance or repairs involve complex offshore operations (helicopters, vessels, submarine rovers may be required). Thus, according to [57] OPEX can represent until 25% of the LCOE of a FOW project. In the Catapult guide for fixed-bottom LCOE assessment, the OPEX share is 28% (cf purple part of the pie chart displayed on figure 2.109). Focusing on data relative to fixed-bottom offshore

wind is interesting since nowadays few data specific to FOW OPEX are available. This is due to the low commercial-scale maturity of the field: Operation and maintenance operations knowledge is feed by industrial experience that nowadays lack in the FOW field as explained by Carbon trust [58]. In this report the strong similarities in O&M between floating and fixed-bottom are detailed. The main difference could be in favour of floating wind: indeed, floating wind offers the ability to tow back the structure in case of major repairs (blades, gearbox etc, yaw mechanism etc...) preventing the operators from performing complex expensive lifting offshore operations involving designed and expensive crane vessels. Though, there is no absolute consensus on whether or not this operation would be economically advantageous since no track records exist. Many more information will be available in the years to come with the democratisation of commercial scale floating project and the share of information between industrial player fostered by entities as Corewind or Catapult supported by the EU. If FOW could thus offer drops in OPEX cost, it could also bring new complexities in regard with fixed-bottom projects. Indeed, as explained in section 2.4 the behaviour of moorings and anchors with fatigue, corrosion and even fish activity is not enough documented. In the particular case of taut moorings used for TLPs, the critical aspects of tendons and suction anchors could lead to additional monitoring operations. Based on these considerations and since the further exploration of FOW specificity would require a wide work out of the scope of this study, OPEX cost model and considerations for FOW will be assumed to be equal to the ones for fixed-bottom offshore wind more documented.

In [28] a very complete overview of strategies, technologies, challenges and future evolution in the offshore wind turbine operations and maintenance sector is presented. It is there explained to what extent Operations and maintenance of offshore wind turbines (OWTs) play an important role in the development of offshore wind farms. Maintenance is a more critical element than operation in the LCOE - as industrial data from Catapult [23] confirms it - given the practical constraints imposed by offshore operations. Indeed, the distance from an offshore wind farm to a port or shore reduces the accessibility and increases the downtime. The ownership or hiring of a maintenance fleet and an increased number of technicians is costly. Moreover, weather conditions have a high impact on offshore maintenance: if a maintenance task must be postponed due to weather issues, a longer waiting period and greater loss of power generation will occur. Even without considering the effects of weather, OWT maintenance costs are higher than that of equivalent tasks onshore due to the specialised equipment required.

The effects of maintenance on the life cycle of an offshore wind farm are highly complex and uncertain. The selection of maintenance strategies influences the overall efficiency, profit margin, safety, and sustainability of offshore wind farms. The following picture

3.19 displays a graph extracted from [28] supporting the explanation between the different maintenance strategy and how tremendous they can be in the life cycle of a farm. On this scheme, the green, red, and yellow colours denote the normally operated OWT, the stopped OWT due to failures, and the stopped wind turbine due to maintenance, respectively. The blue and orange colours stand for the waiting maintenance vessel and the vessel performing tasks, respectively.

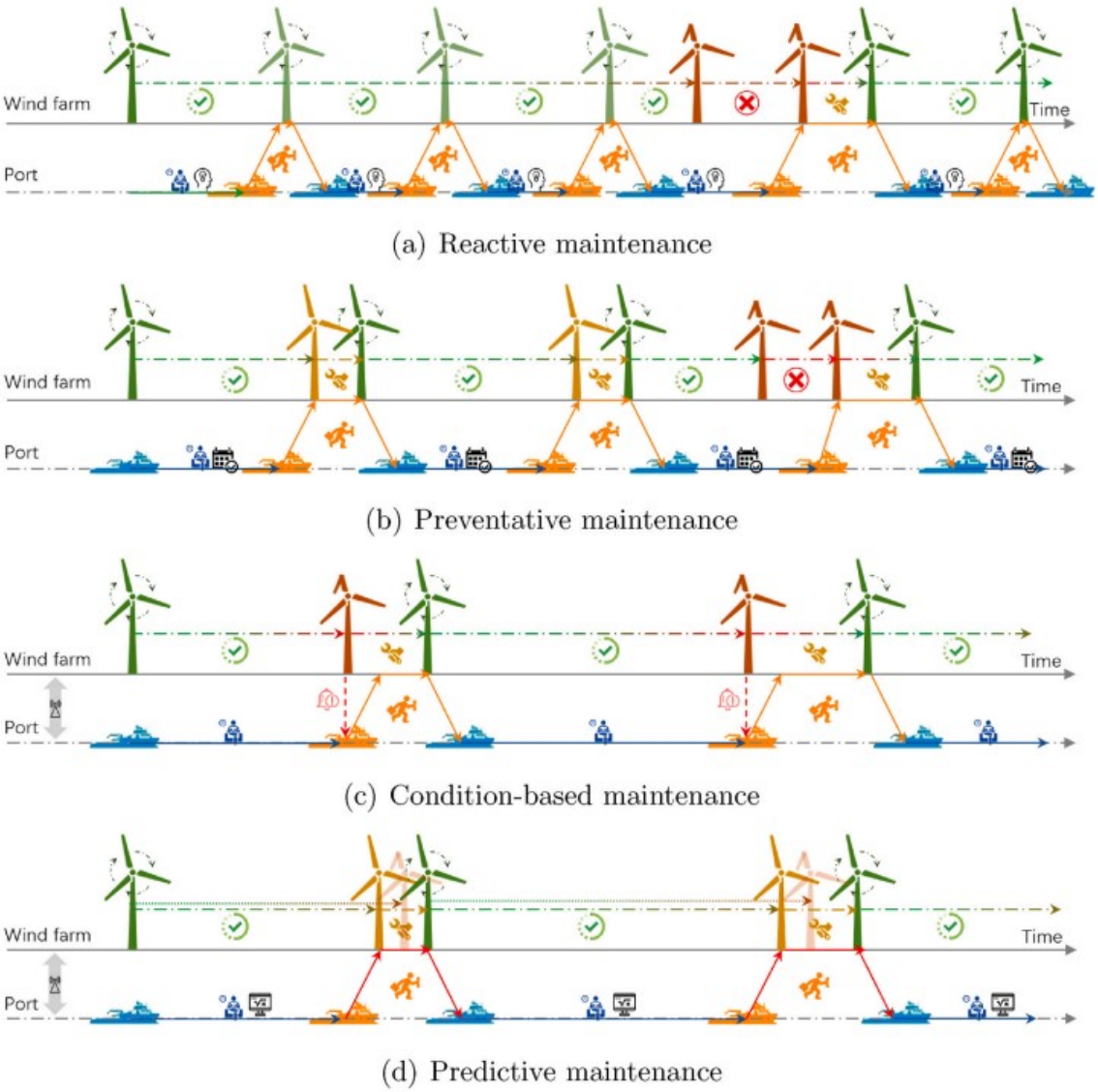

Figure 3.19: Diagrams of different maintenance strategies from [28]

The advantage of pro-active ((b), (c) and (d) on picture 3.19) maintenance strategy ahead of reactive maintenance ((a) on picture 3.19) is one the main insight to get from [28]. Indeed with pro-active maintenance strategies scheduled inspection and replacement is carried out before failure to prevent minor faults from developing into a major failure. Major

failures (only 25% of all failures) contribute to 95% of unavailability. Proactive maintenance is a relatively mature technique, and proactive maintenance strategies nowadays mainly comprise preventive and condition-based maintenance strategies and are adopted by a majority of newest farms improving the availability of the offshore farms. The development of these strategies have been supported by the improvement of sensor equipment allowing to obtain reliable data on meteorological condition, corrosive environment, vibrations in the structure, electrical malfunctions etc... Plus, the researches on going on aging of wind turbines components released insightful laws helping the operators to make the better choices. Finally, a upcoming strategy is on the rise: similar but more advanced proactive maintenance strategy is predictive maintenance. According to sensor measurements, parametric analyses are conducted to determine when maintenance should be performed before a failure occurs. The main idea is to minimise the downtime and maximise the reliability allowing the maintenance events to be conducted when they are indeed necessary. Though the associated equipment cost is higher, the benefits of this strategy include reduced maintenance frequency and time, downtime, and cost of spare parts and supplies [28]. The use of artificial intelligence in this field is particularly promising and and when fully mature and widely adopted OPEX of offshore wind farms could be reduced by half.

Actually, these considerations can be extend to any power plant but are particularly important for offshore wind regarding the complexity of maintenance and the important share it can represent in the LCOE on an offshore wind farm. The offshore power sector is thus set to play a major role in the development and optimisation of this new pro-active and sensor-based maintenance strategies, and R&D as well as commercial scale testing are part of the offshore wind ecosystem.

Alongside maintenance strategies improvements, the evolution of offshore wind maintenance will be supported by the technological improvements and robotising. The epitome of this phenomenon is the ever wider utilisation of drones to monitors wind turbines as illustrated by picture 3.20. These technologies, widely use for onshore wind-turbines has a strong potential for offshore wind since it would replace complex and expensive offshore monitoring and be perfectly complementary to the pro-active maintenance strategies described here above.

Figure 3.20: Drone inspection of wind turbines

These expected evolution previously described previously are set to giving an decreasing trend to OPEX cost in the years to come. Plus, in a similar way to CAPEX evolution with bigger turbines described in chapter 2, the use of bigger turbines will theoretically generate economies of scale for O&M costs, at least from the monitoring side since the monitoring of 1 turbine rated at 20 MW will not be twice as long as the one of 2 turbines rated at 10 MW. Furthermore when the distance between two turbines that can easily top one kilometre is included, the economies of scale are even more expected. In their global offshore outlook of 2019 (still mainly focused on fixed-bottom technologies), IEA took these parameter in considerations while remaining conservative to deliver a forecast of the evolution of OPEX costs in the years to come for offshore wind projects. The results are distinguished according on domestic market considered and a worldly mean is added, as the graph on figure 3.21 shows:

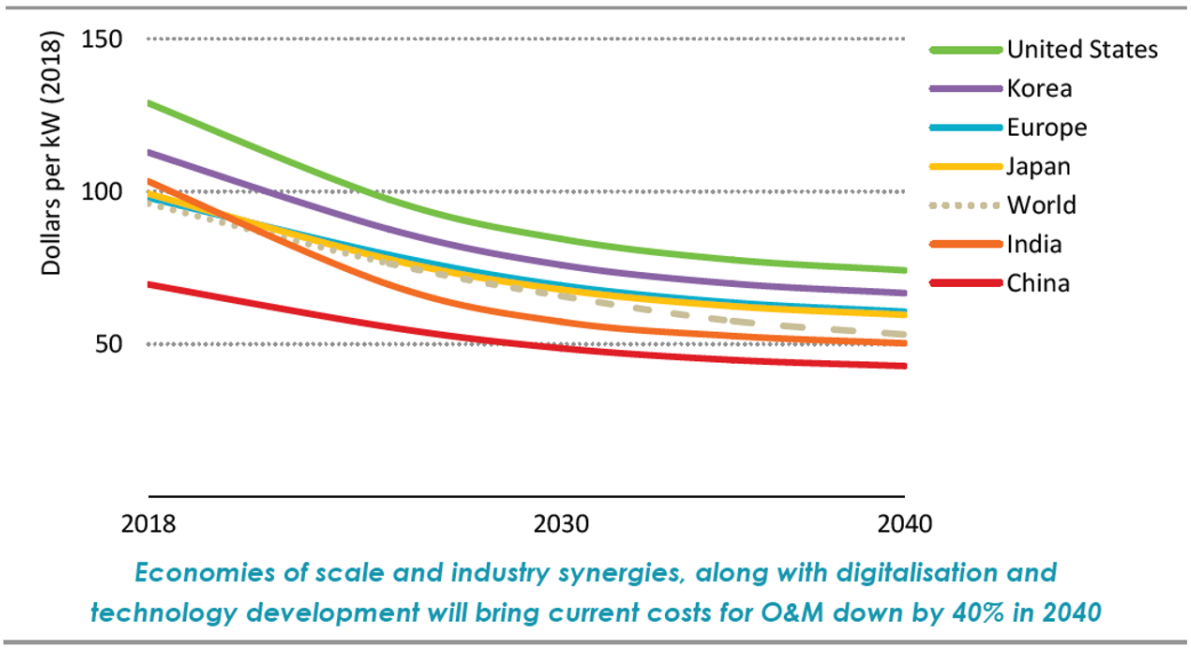

Figure 3.21: Annual O&M costs forecast in the world, from [5]

Based on these results, and considering a little delay regarding fixed-bottom projects to remain conservative, in our LCOE calculation model presented in next section 3.3, the yearly O&M cost values taken for project of different commissioning year will be:

- 80 USD/kW for a 2030 FOW project.
- 60 USD/kW for a 2035 FOW project.
- 50 USD/kW for a 2040 FOW project.

This value would have to be sharpen to suit a given project. The idea in this was to get representative values to insert in our LCOE calculation model and to present some of the main challenges related to O&M offshore wind farms operators will have to deal with.

3.3. LCOE calculation

To conclude this study, the considerations made on site impact assessment in section 3.1 and on OPEX in section 3.2 will be added to the CAPEX model developed in chapter 2 to calculate the levelized cost of energy (LCOE) for benchmark projects whose characteristics will be chosen to be representative of different zones and conditions. As previously explained, the LCOE is used to compare the economical viability of power plants (potentially of diverse type of energy) between them of an energy-generating asset can be thought of as the average total cost of building and operating the asset per unit of total

electricity generated over an assumed lifetime [33]. It could be seen as the price electricity would have to be sell to obtain a NPV (net present value) of the plant equal to zero, meaning the price at which electricity would be sell to obtain at the end of the lifetime a perfect balance between expenses and revenues (the return on investment for investors being comprised in the expenses, via a discount rate parameter). The LCOE evaluate the economical potential of a plant over its whole lifetime, and thus inflation and discount rate mechanism are taken in consideration. In finance, a discount rate is the rate of return used to discount future cash flows back to their present value. This rate is often a company's Weighted Average Cost of Capital (WACC), required rate of return, or the hurdle rate that investors expect to earn relative to the risk of the investment [33]. In our case, this WACC will be assessed in subsection 3.3.2. The calculation of the LCOE is mathematically defined through equation 3.8:

$$LCOE = \frac{\Sigma_{i=-n}^{i=N}(CAPEX_i + OPEX_i)(\frac{1+j}{1+d})^i}{\Sigma_{i=0}^{i=N-1} AEP_{net}(\frac{1+j}{1+d})^i} \tag{3.8}$$

Where N is the lifetime of the wind farm in years.
n represents the years of construction during which CAPEX will be spent.
j is the inflation rate.
d is the discount rate.
AEP_{net} is the net annual electricity production in [MWh]. It is obtained from AEP_{gross} after applying losses as described in subsection 3.3.1.

For various sites of interest identified in section 3.2, various commissioning years and various site features the LCOE of wind-farms will be calculated and discussed in subsection 3.3.3. But first, the elements of equation 3.8 will be defined in subsections 3.3.1 and 3.3.2.

3.3.1. Losses assessment

The objective of this subsection is to go from the gross annual electricity production of a given turbine which only depend on the wind resource of a site the annual net annual electricity production of a farm that is the effective amount of electricity transmitted to the grid by the farm. At the root of these differences, various detrimental phenomenon are at stake at different places of the conversion process. First, before the wind energy is transformed in mechanical energy at blade level, the wind turbines will disturb the wind flux that go through them and this wind flux will have a lower quality when arriving to he other ones: this is the wake phenomenon. Then, before this mechanical energy

can be transformed in electric energy, the availability of the turbine over the year enters in consideration. Indeed, a wind turbine due to maintenance operations or outages, is not working 100% of the time in a year, leading to availability losses. Finally, once this electricity is produced at farm level it still has to be exported to the onshore grid, which lead to transmission losses already discussed in section 2.5. In the end, the the path from gross to net annual energy production is described by equation 3.9:

$$AEP_{net} = \eta_{wake}.\eta_{availability}.\eta_{transmission}.AEP_{gross} \tag{3.9}$$

Where the η_i are coefficient between 0 and 1 representing the loss discussed earlier.
First, let's describe wake losses and find a reasonable value for η_{wake} to be inserted in our model. Wake phenomenon is complex non linear aerodynamics phenomenon which analysis would require a fully dedicated work. A simple definition of wake definition can be found in [104]: wind turbines extract energy from wind and reduce the wind speed behind the rotor and swirl the air flow. For wind turbines working in the same air flow direction, the second turbine would receive a reduced wind speed and would not optimally run because of the incoming wind turbulences caused by the first turbine, as illustrated on figure 3.22. The spreading of the wake is called wake effect and is one of the most important impacts of neighbouring wind turbines that influences the electrical energy production. The maximal power output of the wind farm cannot be reached due to the described effects and should be considered for the design of the entire farm referring to the distances between the wind turbines.
This phenomenon is complex to describe and depend on many parameters as wind characteristics (velocity and turbulence mainly), turbine size, turbine rotational speed, space between turbines, layout of the farm etc... Project leaders will use aerodynamic models to find the optimal arrangement taking in considerations economical, technological, footprints aspects. This phenomenon is responsible of the design criteria chosen in subsection 2.6 for the the distance d between two turbines. In [105], a parametric study of wind turbine wake effects in a hypothetical offshore wind farm with varying turbine separation using a Computational Fluid Dynamics (CFD) model have been led. From these results, we extracted a conservative value for the implementation of wake losses in our model, stated at 10%. Yet, in the years to come, a deeper analysis from specific offshore wind case may lead to a new industrial consensus on the layout of a farm - that as previously explained also impact CAPEX drivers - that could lower this value. In our model, we will thus take $\eta_{wake} = 1 - 10\% = 0.9$

[105]

Figure 3.22: Wake phenomenon

Then comes the issue of downtime, already discussed in O&M section 3.2, during which the turbine cannot produce due to outages of maintenance operation as illustrated on figure 3.23. This thematic was discussed in section 3.2 since the loss of productivity during maintenance can be seen as an maintenance related cost. Few reliable industrial information on this point have been found, thus a classical value of $\eta_{availability} = 0.97$ will be taken in our model for 2030 projects. To model the expected improvements in maintenance strategies described in section 3.2, this value will be increased to $\eta_{availability} = 0.98$ for 2035 projects and $\eta_{availability} = 0.99$ for 2040 projects.

Figure 3.23: Offshore wind turbine maintenance operation

Finally, transmission losses have to be assessed. Already widely discussed in section 2.5, these loss depends on type of cable used, in our case HVAC cables and, once this the cable technology was fixed, on power output and distance of cables as explained in [94]. This dependence on cable length and power output (in percentage of the rated output power of the farm) was described by two graphs displayed in section 2.5 on figure 2.93. These laws have been implemented in the LCOE calculation model making few hypothesis for sake of simplicity. First, instead of computing the transmission loss for every time series point and the related hourly production, the yearly equivalent hours (before application of wake and availability losses to remain conservative) have been used. Then to be easily coded in VBA based on the only graph given in [94], the loss law in function of percentage of rated power has been discretised. This discretisation is made on Load factor LF that is defined as $LF = h_{eq}/8760$ as explained in subsection 3.1.2. Finally, this loss law in function of percentage of rated power is implemented for a 50 km cable length, assumed equal to the distance from shore. Then, the dependence on cable length L will be assumed to be strictly linear, which is acceptable while using HVAC cables where the majority of losses come from cables and not from the OSS [94]. Applying this hypothesis, the computation of the transmission loss law in the model LCOE model can be done for every site of interest and their specific parameters (equivalent hours h and cable length L) using the VBA algorithm displayed on figure 3.24: [94]

LCoE_WindOffShore_new.xlsm - Modulo3 (Code)

(Général) | Powerloss

```
Function Powerloss(h, L)
    LF = h / 8760
    If LF < 0.05 Then
        Loss = 0.33
    ElseIf LF < 0.15 Then
        Loss = 0.43
    ElseIf LF < 0.25 Then
        Loss = 0.57
    ElseIf LF < 0.35 Then
        Loss = 0.73
    ElseIf LF < 0.45 Then
        Loss = 1
    ElseIf LF < 0.55 Then
        Loss = 1.33
    ElseIf LF < 0.65 Then
        Loss = 1.67
    ElseIf LF < 0.75 Then
        Loss = 2.1
    Else: Loss = 2.62
    End If

    Powerloss = L * Loss / 50


End Function
```

Figure 3.24: VBA code implemented in the LCOE calculation to model the transmission losses

In the outputs (cf subsection 3.3.3), the transmission losses ranged in our analysis from 0.47% for a 2030 project in Puglie close from shore to 2.57% for a 2040 Scotwind project more distant from shore. The factor $\eta_{transmission}$ will thus be different for every project considered.

3.3.2. Financial and project life-cycle related hypothesis

The idea now is to use our previous work and notably to couple our CAPEX model developed in chapter 2 to our our site impact related insights discussed in section 3.1 to assess the LCOE of typical future FOW projects, and then analyse these results. The

same framework and hypothesis described in Chapter 2 for CAPEX predictions of future projects will be reused. Thus, for each site of interest selected, the same 3 potential dates of commissioning will be considered: 2030, 2035 and 2040. The farm features considered for these farms will be the same as the one described in chapter 2 (farm rated power output, turbine sizes, layout, cables ratings etc...) and the entry of projects characteristics (depth, floater typology, external conditions, distance from shore) in the CAPEX model will thus provide coherent results.

In terms of site productivity, the net annual electricity production will be calculated as explained in section 3.1 and losses described in subsection 3.3.1 will be applied. As explained in subsection 3.1.2, two turbine classes were considered (cf figure 3.4). Starting from 2035, leaving thus the time for manufacturers to adapt their turbines to softer conditions, "class II" turbines will be used to assess the net AEP of site presenting lower mean wind speed values. In terms of floater technology used, based on considerations widely described earlier in this work, TLP solutions will be used for projects featuring depth higher or equal to 500 meters. SS solutions will be used in the other cases.

The lifetime of the plant in years, named N in LCOE equation 3.8, has an important impact on LCOE estimation. Usually (cf [17], [29], [23]) offshore wind farms are designed to produce during 25 years. Starting at year 0 until year 24, the 25 years is the years of decommissioning. This aspect of the life cycle of a FOW project has not be discussed in this work, it will nevertheless be taken in consideration in LCOE calculation. In [57] and [59] the decommissioning expenditures (DECEX) for a FOW project is discussed and put in perspective with the DECEX for fixed-bottom offshore wind. As expected, due to smaller seabed impact and the ability to easily disconnect and tow back structures to shore, the DECEX of FOW is expected to be significantly lower than fixed bottom one. According to [23] the decommissioning typically represents 1.40% of CAPEX of a fixed-bottom offshore wind project. In our model, a reasonable value of 1% of CAPEX will thus be considered for FOW DECEX. Then, due to construction time, cash flows exist before the commissioning of the plant which impact the LCOE. Considering the size of the plants, two years of construction will be assumed. This factor could heavily change from one project to another but will have actually a low impact on the final LCOE cost. The CAPEX distribution will be assumed equal between the two years of construction.

Let's head up to financial hypothesis. The LCOE and the NPV (net present value) of a power plant project take in consideration the future cash flows for an investment project. Inflation mechanism have thus to be taken in consideration [106]. Inflation has a tremendous impact on every financial aspect of a project and in society in general, and its exact evolution is impacted that many potential factors that will be not detailed here. For a Power plant project, a positive inflation rate must be seen as beneficial for investors: to

put it very simply, the major part part of investment (CAPEX) is invested before year 0 and the assets will gain value year after year thanks to inflation. To remain conservative, relatively low values of inflation rate will be made: it will be assumed that the inflation rate j (cf equation 3.8) will be j=1.5%.

The most critical decision variable in calculation of the net present value - and thus the calculation of the LCOE - of a plant is the selection of an appropriate discount rate d (cf equation 3.8). Typically either the weighted average cost of capital (WACC) for the company or the rate of return on alternative investments. For power plants, the first option is usually the most accurate one and WACC are used (cf IEA [5]). As a rule the higher the discount rate the lower the net present value with everything else being equal. The WACC value used as a discount rate will be the post-tax WACC since post tax cash flows and thus LCOE is calculated. Taxes on benefits are usually considered in this kind of projects and enters in the LCOE calculation by decreasing the positive values of cash flows each years. In Italy, as get from discussion from A2A renewable project developers, the tax rate to take in consideration is 28%. Similar values are used all over Europe but could drastically change in other zones of the world.

Interest rates can be expressed in nominal or real terms. A nominal interest rate equals the real interest rate plus a projected rate of inflation as explains on picture 3.25. A real interest rate reflects the true cost of funds to the borrower (project leader) and the real yield to the lender or to an investor. The two approaches are valid and give different information. Since in our study, the LCOE is as previously explained more a tool used to evaluate the viability of a project and more generally of FOW in comparison with other sectors, it is important to keep this distinction in mind and not compare the real LCOE of a project with the nominal one of another. Usually, in the energy field, technologies are compared to a LCOE calculated in real term (BNEF [29], IEA [5], Catapult [23] etc...). Eventough the LCOE calculator presented model described here after gave us both nominal and real results, the outputs discussed in subsection 3.3.3 will thus be in real terms. For A2A project developers expert in renewable projects, the classical value use as real WACC in early stafe planing phase to model the financial aspect of a project is $WACC_{real} = 5.4\%$.

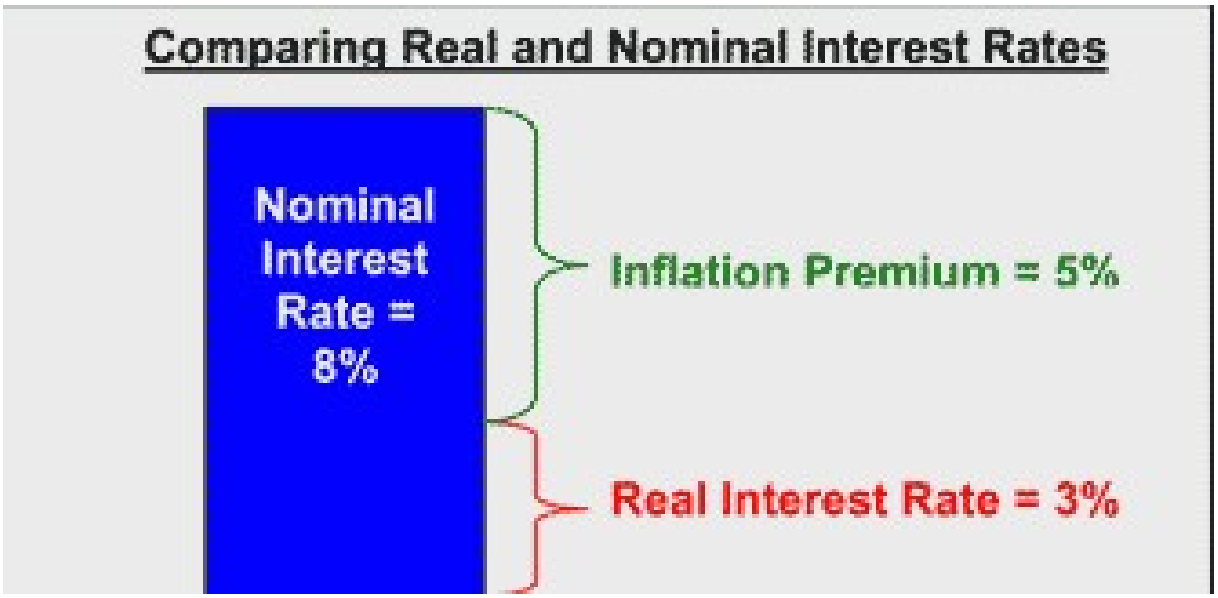

Figure 3.25: Real and nominal discount rate

Plus, it is required to apply a risk element in establishing the discount rate: riskier investments should have a higher discount rate than a safe investment [106]: in simple terms, the less mature a technology is (small proven record) the more risky an investment is and the bigger the return on investment for investors will be required to convince investors. This is the case for FOW that is a young field, and still we be (to a lower extent) in 2030 when first hypothetical projects considered in our study will be commissioned. To take in consideration this reality, a additional discount rate component will be added to the WACC of reference equal to 5.4%. With the years, the FOW market is expected to gain momentum and the financial risk shall decrease, this additional discount rate component will thus be assumed to decrease as well. It will be assumed an addition discount rate of 3% for 2030 projects, 1.5% for 2035 projects and 0% for late 2040 projects when the sector will be mature.
In the end, in real terms, we will get for the discount rate d in the LCOE calculation (cf equation 3.8):

- d = 8.4% in 2030
- d = 6.9% in 2035
- d = 5.4% in 2040

To effectively calculate the LCOE for every project of interest, a dedicated Excel file used in A2A for the early evaluation of renewables projects file will be adapts and extends to our cases (inputs and outputs have notably been re-worked to be more easily manipulated

and analysed). This Excel calculator is based on targeting optimisation method made on Earnings Before Interest, Taxes, Depreciation, and Amortisation (EBITDA) where the target function is the NPV that must be put to zero. The inputs of this calculator, described and discussed previously, are summarised here:

- CAPEX of the project: This input comprehends the whole site related impacts parameters (depth, distance from shore, meteorological conditions etc...) as well as the technological ones (floaters type, turbine size, layout etc...).
- OPEX of the project: cf section dedicated 3.2.
- DECEX: percentage of CAPEX.
- Lifetime on the plant.
- Construction time.
- Tax rate.
- Inflation rate.
- Discount rate.
- Net annual electricity production (AEP_{net}), that is assumed to remain the same during every year of production. The impact of turbine class considered is comprehends here, as well as wind resource of the zone obviously.

3.3.3. Results for sites of interest

LCOE calculation have been performed for 2030, 2035 and 2040 projects in 6 selected sites of interest among the 12 presented in section 3.1. A deeper analysis of the 12 sites would have burden the discourse and the 6 selected present features various enough to be insightful. First, N Sardinia have been selected for being the most promising Italian site identified in section 3.1. Then, S Sardinia have also been chosen since as seen on figures 3.17 and 3.18 this zone is targeted by many industrial for potential future projects. Then, another very promising Italian site, in terms of bathymetry this time (cf table from picture 3.16) has been selected: W Sicily. The last Italian site for which LCOE calculation have been performed is the Puglie one, since it was located in mainland and featured less good potential: a wider range of LCOE achievable over Italy will then be get. Plus, GDL and Scotwind sites have also been inserted to represent what are the FOW potential in even better conditions than the Italian ones. Finally, for sake of comparison, a typical 2022 Italian onshore wind project have been added to the model. The summary of inputs for every of these 18*3+1=19 projects alongside main projects features assumed

(cf hypothesis in subsection 3.3.2) are summarised on the following table displayed on figure 3.26. The two last rows of this table are the results for these inputs if the LCOE calculator in real and nominal terms.

	N Sardinia			S Sardinia			W Sicily			Puglie			Golfe du Lyon			Scotwind			Onshore
	Config. 1 : N Sardinia 2030	Config. 2 : N Sardinia 2035	Config. 3 : N Sardinia 2040	Config. 4 : S Sardinia 2025	Config. 5 : S Sardinia 2030	Config. 6 : S Sardinia 2050	Config. 7 : Sicilia 2025	Config. 8 : Sicilia 2030	Config. 9 : Sicilia 2050	Config. 10 : Puglie 2025	Config. 11 : Puglie 2030	Config. 12 : Puglie 2050	Config. 13 : GDL 2025	Config. 14 : GDL 2030	Config. 15 : GDL 2050	Config. 16 : Scotwind 2025	Config. 17 : Scotwind 2030	Config. 18 : Scotwind 2050	Config. Onshore attuale
year	2030	2035	2040	2030	2035	2040	2030	2035	2040	2030	2035	2040	2030	2035	2040	2030	2035	2040	2022
Installed power (MW)	450	960	2100	450	960	2100	450	960	2100	450	960	2100	450	960	2100	450	960	2100	200
turbine power (MW)	15	20	35	15	20	35	15	20	35	15	20	35	15	20	35	15	20	35	4
machine height (m)	287	312	413	287	312	413	287	312	413	287	312	413	287	312	413	287	312	413	
turbine mean height (m)	170	190	250	170	190	250	170	190	250	170	190	250	170	190	250	170	190	250	
expected class	I	II	II	I	II	II	I	II	II	I	II	II	I	I	I	I	I	I	II
distance from shore (km)	65	68	77	32	32	67	65	68	77	32	32	63	22	23,7	30,3	65	68	77	
pourcentage visibility	0%	0%	0%	80%	85%	10%	0%	0%	0%	80%	85%	15%	0%	0%	0%	0%	0%	0%	
depth (m)	1000	1000	1000	500	500	1000	200	500	500	200	200	1000	100	100	200	200	200	200	
ocean/med	med	med	med	med	med	med	med	med	med	med	med	med	med	med	med	ocean	ocean	ocean	
h eq	3840,64	4200,77	4264,05	3268	3714,13	3832,58	3194,72	3581	3671	3263	3677,4	3800,54	5080,4	5962	5707	5501	5962	6041,3	
wake losses	10,00%	10,00%	10,00%	10,00%	10,00%	10,00%	10,00%	10,00%	10,00%	10,00%	10,00%	10,00%	10,00%	10,00%	10,00%	10,00%	10,00%	10,00%	
transmission losses	1,30%	1,36%	1,54%	0,47%	0,64%	1,34%	0,95%	1,36%	1,54%	0,47%	0,64%	1,26%	0,59%	0,79%	1,01%	2,17%	2,27%	2,57%	
availabilty	98%	98,50%	99%	98%	98,50%	99%	98%	98,50%	99%	98%	98,50%	99%	98%	98,50%	99%	98%	98,50%	99%	
h eq after losses	3343,408	3673,336	3740,76	2868,91	3271,504	3369,07	2791,003	3131,38	3220,49	2864,52	3239,151	3343,61	4454,69	5243,476	5033,476	4746,548	5165,273	5244,363	1900
LF	38,17%	41,93%	42,70%	32,75%	37,35%	38,46%	31,86%	35,75%	36,76%	32,70%	36,98%	38,17%	50,85%	59,86%	57,46%	54,18%	58,96%	59,87%	21,69%
Capex (M$/MW)	3,81	3,15	2,67	2,77	2,423	2,38	3,19	2,88	2,46	2,59	2,28	2,36	3,19	2,71	2,33	3,04	3,06	2,34	1,2
Opex ($/kW)	80	60	50	80	60	50	80	60	50	80	60	50	80	60	50	80	60	50	40
LCOE reale	167,9791	109,3359	78,8219	149,9371	98,66476	79,6241	173,145	118,908	85,57569	142,2235	94,8623	79,6818	108,4808	67,49497	52,38406	97,81566	75,86566	50,45245	80,49764
LCOE Nominale	190,9132	125,5939	91,4464	169,3688	112,7065	92,11891	196,1477	136,345	99,08633	160,4203	108,2073	92,1659	122,8926	77,29362	60,57154	110,7054	80,93056	58,34442	90,09263

Figure 3.26: Inputs to the LCOE calculator and characteristics of selected sites of interest

For each configuration, these results are displayed an histogram graph on figure 3.27, bars being clustered by sites and by years. The first insight is that, as expected, important LCOE drops are witnessed with increasing years for every sites. These drops are particularly significant for Italian sites in absolute values since the Scotwind and GDL sites starts from way lower LCOE values even in 2030. In the end, the relative drops witnessed between 2030 - that represent a first of kind commercial scale project - and 2040 - that represent a fully mature commercial scale project - ranges 44% in Puglie to 53% in N Sardinia.

These first results give an idea of of what the Mediterranean FOW market could look like and how it could evolve with years. Yet, the parameters were not exactly the same for every sites, leading to different visual impacts on landscapes from one configuration to another, highlighted by green to red colours on figure 3.27. In this first iteration the idea was to re-transcript the industrial ambitions disclosed by the study on Italian planned projects led in subsection 3.1.6, and particularly from map displayed on figure 3.17 where visible impact on projects is described. Thus in these inputs the projects considered in S Sardinia and Puglie did not reached the 1000 m line (for 2030 and 2035 projects) where distance could allow to reduce the visual impact. For Puglie, it as for example been assumed that project developers would take advantage of the interesting bathymetry profile where the 200 meters lines is quite far from shore (cf picture 3.16) to install Semi-submersibles floating turbines at low depth reducing the CAPEX while re-

maining in the accepting visual zone defined earlier with picture 3.13. For S Sardinia case, it has been assumed that while turbines where "small" enough (until 20 MW) projects would remain within the 500 m line, resulting in an important visual impact on landscape. For 2040 projects and thus huge 35 MW, at these distance the visual impact would have overpass the acceptable framework on picture 3.13, and the 1000 meters line is thus assumed to be reached, explaining the greener bar for 2040 projects in these two zones on figure 3.27. Let's precise that the visibility impact scale used in this representation is fully based on the two barriers lines of picture 3.13: a 0 visual impact corresponds to points located on or higher than the higher line, then this criteria linearly grows to 1 when point are approaching the lower line, 1 being achieved for projects on the limit. With these outputs, this criteria reaches 0.85 for S Sardinia and Puglie with 2040 projects.

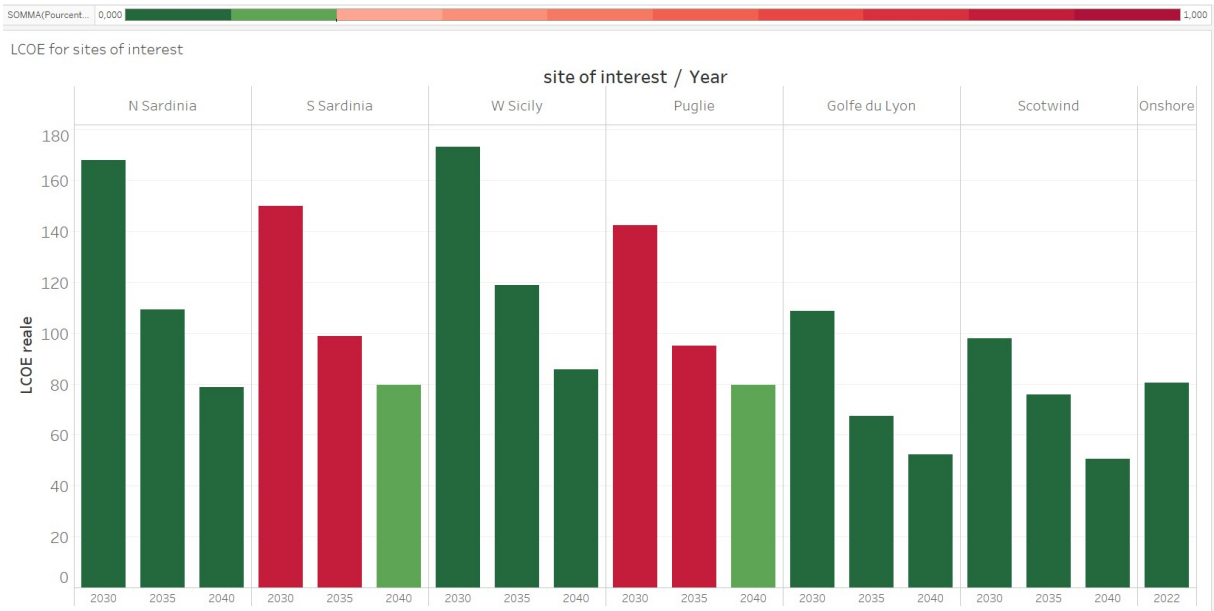

Figure 3.27: LCOE values for selected sites of interest alongside visual impacts

The previous set of inputs and outputs highlighted the impact of accepted visual impact on the LCOE, and thus the viability of Italian projects. Indeed, the red bars on chart 3.27 shows lower values of LCOE than other Italian sites eventough Puglie and S Sardinia lower wind resource related potential than N Sardinia for example. Finding compromises on visual impact on landscape could thus be useful or even mandatory for some projects and more globally for the Italian FOW sector to become as competitive and viable as possible and thus foster an faster development.

To further assess this tremendous impact on LCOE, a sensibility analysis on the visual impact on landscapes - and particularly in the Mediterranean where many sites are touristic zones - has been performed for 3 different sites presenting different characteristics: first N

Sardinia that features interesting wind resources but present a harsh bathymetry profile, then W Sicily where wind resources are a little less promising but where bathymetry allow shallower projects to be developed and finally GDL that represent the optimum Mediterranean site with important wind resources and relatively low depths even far from shore. In this study, both technologies of floaters (TLP and SS), independently of depth considerations described in section 2.4, have been considered. The results of this study are summarised on three graphs, one per site, displaying on figure 3.28 the LCOE evolution with turbine power and thus commissioning year (assumed strictly linked here). The green curves representing "invisible" conditions correspond to the higher barrier where turbines start to be fully hidden by earth curvature and the red ones represent "visible" conditions corresponding to the lower visual barrier and leading to a visual impact similar to the one displayed on figure 3.12.

AS expected, for every site and for both technologies, important LCOE drops are generated when going from the invisible frontier to the visible one from chart 3.13. These drops are heavily linked to bathymetry profiles. Indeed, the drops are more important for N Sardinia than for W Sicily, it self more impacted than GDL site. And while the GDL seabed depth profile remains for long distance from shore more or less constant to 200 meters, for W Sicily and even more N Sardinia going further from shore to decrease the visual impact implies to development of projects in deeper water that will be more costly. When bathymetry is not flat, the diminution have a double detrimental impact on CAPEX and then LCOE: from distance from shore and from depth point of view. The harsher the seabed depth profile of site will be, the more the developers will be encouraged to neglect the visual impact of their projects: it's "easier" from an economic to respect landscapes in Western Sicilian sites than in Northern Sardinia ones (or than Puglie ones for example).

The impact of floater technology used, less important than landscape preservation one, is also highlighted by charts on figure 3.28. Similar insights can be obtained from this charts tough. Indeed, when the visual impact in non negligible (red curves) the projects considered feature relatively low depths (200 meters) and thus TLP and SS globally presents similar costs (cf figure 2.114). On the contrary, when harsh seabed depth profile are considered, the preservation of visual impact (green curves) make industrial players developing projects in deep waters where TLP offers interesting drops in CAPEX over SS solutions (cf figure 2.114), which lead to LCOE reduction for TLP invisible witnessed in West Sicily and even more in North Sardinia. Landscape visual preservation and use of Tension leg platforms could thus be seen as dependant issues for Italian FOW development.

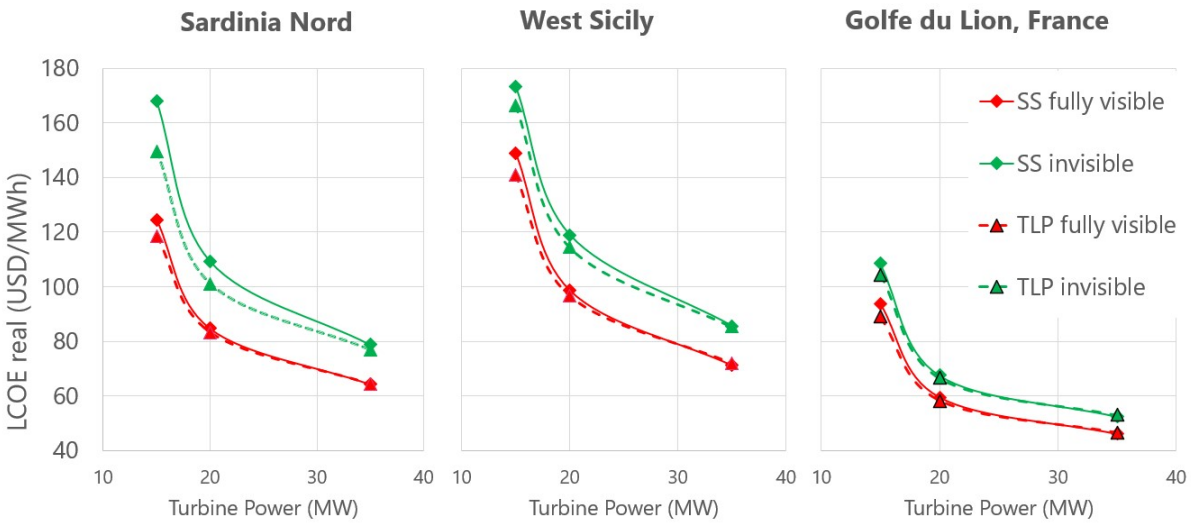

Figure 3.28: LCOE evolution in terms of turbine power and thus commissioning year that are here assumed to be coupled for different floater typologies and visual impact levels

As explained multiple times along this work, trends and mutual evolution are here more insightful than absolute values obtained. Yet, since LCOE can be used as a tool for comparing different types of power plants in economical terms, let's do so in these last lines. First to have have the more coherent comparison possible, as seen on picture 3.26, a 19th configuration has been added to our first LCOE investigations: an onshore wind configuration. The inputs for this onshore wind hypothetical project have been representative of what a good Italian site could offer, accordingly to previous comparison made with onshore wind previously in subsection 3.6. Let's precise that onshore has been considered as a non risky investment in comparison FOW and that no additional WACC have been added for the discount rate d. Plus, O&M were considered lower and a 40 USD/kW yearly value has been adopted. In these conditions, a 80.5 USD/MWh LCOE is obtained for a typical onshore wind project in Italy. It can be seen on previous graphs that, even while diminishing at its maximum the visual impact on coastal landscapes (not the case for onshore wind), FOW can break even with onshore wind in terms of LCOE by 2040 in Italy. If a small visual impact is accepted, this concurrence can be reached as soon as 2035, and could become about 25% more competitive (in terms of LCOE) than onshore wind by 2040. Let's that the amazing potential of FOW outside of Italy (Scotwind and GDL) is evidenced by this comparative analysis and that the development of FOW, at least out of Italy, should happen according to the results of this LCOE assessment.
If we try to perform such kind of comparison out of our LCOE input framework, i.e. comparing our results with ones disclosed by other sources, results must be analysed with caution. Indeed, it is sometimes hard to find the hypothesis used for the LCOE estimation

- especially the financial ones - which can make the comparison less insightful. Yet, DNV [29] led an holistic LCOE assessment for main energy sources and integrated wide margins in their results as shown on figure 3.29. This margins especially take in consideration local requirements and issues, and financial hypothesis are not detailed. In comparison with this study, FOW is set to overcome classical fossil fuel based power plants in Italy (and even more in zones like Scotwind or GDL). Then, it matches the higher margins of renewables sources as solar PV and Onshore wind and the trend displayed for FOW is similar to the one we obtained. A focus on onshore wind shows that their LCOE results are better than the one obtained for onshore i our model. This could mean than our hypothesis are more conservative than theirs, making the results of this comparison even more satisfying.

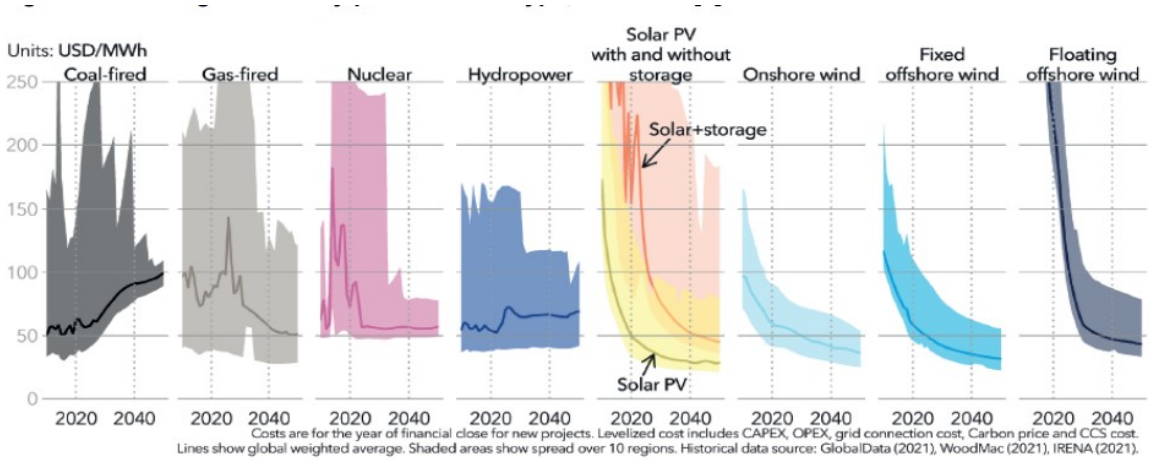

Figure 3.29: LCOE evolution of different energy sources from DNV [29]

Even in a case where FOW in Italy did not break even with solar PV or onshore wind (main renewables sources) in the years to come, the difference in term of LCOE would probably be small enough to justify the development of the floating wind sector in Italy. Indeed, as explained in chapter 1, offshore wind (of which floating wind is the only possible representative in Italy in regards of depth) offers various non LCOE related comparative advantages. For example, it offers way better stability in production and has a seasonal behaviour that tends to compensate the Solar PV one (OW tends to produce more in winter, cf figure 1.15). Its characteristics in terms of grid inertia is also better since big rotating parts are considered. This technology is thus way more grid friendly than onshore wind and especially Solar PV and could be an asset for the green transition on grid side. Then, the use of big turbines offers a way lower footprint per MW, a tremendous issue for a country as Italy that lack suited place for renewables power plants installation (dense and mountainous country). Finally going offshore is good solution for saturation phenomenon discussed in chapter 1 for onshore wind, and might suffer less local protests

in terms of landscape impact.

Then comparison can also be made with LCOE predictions of offshore wind in general (thus mainly with fixed bottom offshore wind), in this case the comparison will be interesting since FOW and fixed bottom OW offer similar performances in terms of grid friendliness and footprint. It has been chosen to compare our results to data disclosed by IEA in their 2019 offshore wind report [5] since IEA made a focus on EU and clearly stated what the WACC used in their model was. These forecasts on offshore LCOE evolution for a WACC of 8%, a smaller one of 4% and without transmission are displayed on figure 3.30. Similar trends are witnessed between IEA predictions and the results from our model and, for a "standard" WACC of 8%, the IEA LCOE of fixed bottom projects by 2040 would range between 50 and 75 USD/MWh. By 2040, our predictions would almost match this range even without damaging the visual impact for Italian costs, confirming the possibility for FOW to fill the gap with more advanced fixed-bottom technologies. This comparison is thus encouraging for FOW eventough as previously explained these comparative results have to be analysed with caution. Plus let's recall that in general and even more in Italy, fixed-bottom and floating offshore wind can hardly be put in competition since the zones of interest are diverse.
The main insight to get from this comparative analyses, more than absolute values, is that the predictions made are coherent with expected market trends and that even in Italian seas that could not appear as the number one spot for offshore wind development, this technology has a lot to offer in could become an important asset for the country to effectuate the decarbonation of its energy sector since it could an excellent complement to Onshore wind and Solar PV that will anyway lead the transition in Italy (cf IEA data on Italy [32]) in the years to come.

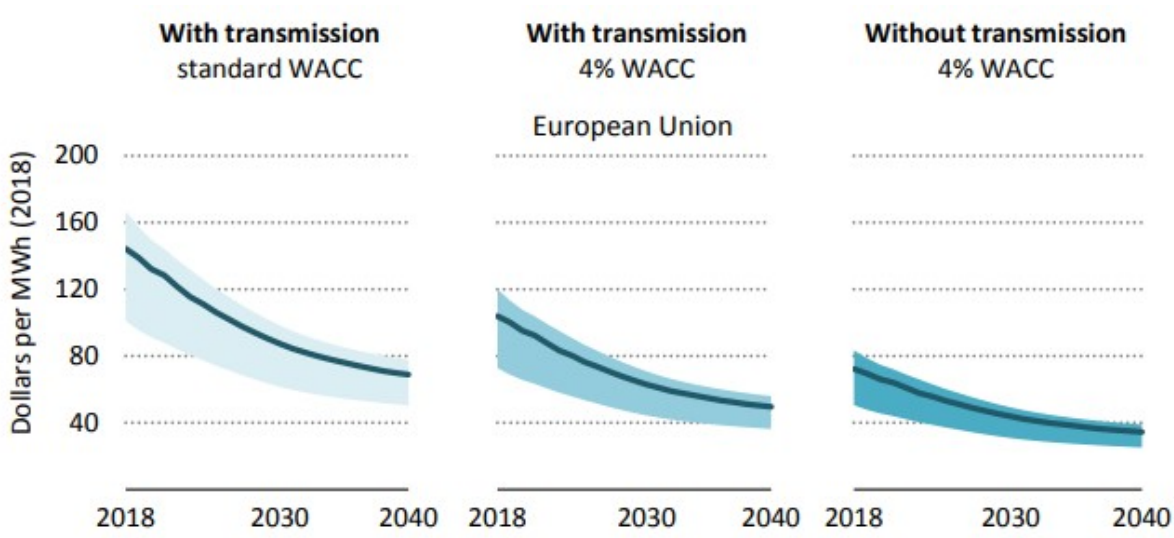

Figure 3.30: LCOE evolution of fixed-bottom offshore wind from IEA [5]

To close this discussion, let's add a little argument to the discussion on the visual impact on landscape of FOW and to what extent this issue may affect the cost of the sector. Indeed it has been seen that with our assumptions, developers might have to go further from shore when introducing bigger turbines to mitigate the visual impact of even bigger turbines on landscapes (cf graphs on figures 3.27 and 3.28). Until now, it has always been considered that, to foster economies of scale (cf chapter 2), developers would automatically use the bigger turbine available each year for their projects: 2040 projects have thus been automatically considered to be using huge 35 MW turbines. Yet, as shown on visibility graph from picture 3.13, to obtain a given visual impact for an observer on the shore, bigger turbines will have to be place further from shore which will lead to over costs. Let's try to assess these over costs in various sites and see to what extent the use of bigger turbines may always have to be advised. To do so, our CAPEX model described in chapter 2 has been adapted and 20 MW turbines instead of 35MW have been considered for 2040 projects. Yet, the improvements in terms of specific turbine price (cf section 2.2), manufacturing complexity factors (MCF) for floaters (cf section 2.3) and the technological breakthroughs (110 kV dynamic cables for examples) are conserved. Since the visual impact on landscape is the root of this analysis, the this CAPEX adaptation have been performed for the two limit configuration defined on figure 3.13: no visual impact and Low visual impact (higher accepted). Then results have been clustered according on floater typology used and obviously on the site considered. The table on figure 3.31 summarised the results of every CAPEX comparison for 2040 projects using 20 MW or 35 MW. The 20 MW CAPEX results are highlighted in red when the use of smaller turbines induces

a clear bigger CAPEX, in yellow when when the use of smaller turbines induces a higher but CAPEX value (relative increase lower than 2.5%) and in green when when the use of smaller turbines induces a lower CAPEX value.
The analyse from these results proves that mainly for TLP technologies, and for sites with fast depth descent as North Sardinia, the use of smaller turbines can be beneficial. The results in green or in yellow, are interesting. Knowing the difficulties of going deeper for installation and maintenance, these solutions can be preferred for the Mediterranean case. For SS solutions, the economies of scale fostered by introduction of bigger turbines on platform side are too important to be compensated by the development in closer from shore and less deep sites. In zone as West Sicily where seabed profile is softer, the few kilometres gained by the use of smaller turbines does not change significantly the project depth and thus its CAPEX.

Capex in USD M/MW		Capex comparison 2040: 20 MW or 35 MW turbines			
		SS		TLP	
		Low visual impact	No visual impact	Low visual impact	No visual impact
Nord Sardinia	35 MW	2,1	2,67	2,1	2,59
	20 MW	2,16	2,94	2,09	2,63
West Sicily	35 MW	1,98	2,46	2,01	2,45
	20 MW	2,14	2,67	2,06	2,51

Figure 3.31: Potential advantage of using smaller turbines for different sites

In the end the FOW sector remains promising in Italy eventough its domestic is nowadays lagging behind the one from France for example in the Mediterranean that will benefits from its experience in fixed-bottom offshore wind as well as the excellent conditions offered by GDL site to become pioneers of offshore win in the Mediterranean. Optimising relation between distance from shore, depth (both impacting the CAPEX of a project) and the visual impact on coastal landscapes will be the key, alongside wind resource of course, to identify sites of interest and develop the viable and competitive floating projects. The LCOE is expected to drastically decrease in the years to come and once commercial scale will be reached FOW could be a strong asset of Italian green transition since no other

renewables sources could offer similar performances in terms of productivity, seasonal and daily constancy, power density (footprint per MW) and grid friendliness.

Conclusion

The objective of this thesis has been to carry out an analysis of current offshore wind market and which role the floating wind field could play in the offshore wind development and more generally in the green transition of electricity production sector. After having described the main actors of this evolution and studied FOW from a technological and economic aspect, the focus has been put on the Mediterranean zone and more specifically on Italy to see to what extent this sector could have a future there.

In the first chapter, after a contextual setting of offshore wind within the global carbon reduction policies led by governments around the world, the potential of wind power to support this transition and most of all the advantages of going offshore have been widely described. Then, a first global overview of the offshore wind market have been performed and logically has been concentrated on fixed-bottom technologies since the existing field is nowadays almost exclusively composed by such kind of projects that are set to keep dominating the offshore wind sector in the decade to come. Yet, the FOW market has then be put under scrutiny and the global development trends (in terms of project pipelines) as well as the main industrial players and domestic markets have been identified and presented. To do so, an holistic count down of announced pipeline have been performed and clustered in terms of project owners, project developers, expected commissioning years and countries. To get an idea of the pipeline counted down, 98 projects have been listed for a global pipeline of about 55 GW until 2034. Yet, the real commercial transition is only expected by 2025 or 2026, 87% of the pipeline in terms of installed power still being constituted of projects in early planning stage.

In the second chapter, a CAPEX model have been designed for FOW projects with the idea of predicting the cost evolution of a floating project - nowadays very expensive since the field is not mature yet - in the years to come. Six main cost drivers have identified and their impact on CAPEX have been holistically assessed: Turbines, floating platforms, moorings and anchors, connection to grid, inner array cables and installation. Alongside technological improvements and the market development of the field fostered by crescent industrial feedbacks, the introduction of bigger turbines in offshore wind is set to trigger important economies of scale. Many input parameters can influence the CAPEX of a

FOW projects, yet it can be take home that the introduction of bigger turbines (from 15MW to 35MW) can generate CAPEX drops between 24% and 36%. These drops in specific CAPEX mainly concern the two specific and more critical cost drivers of a FOW project: floaters and moorings and anchors. To predict the specific cost [$/MW] evolution of these elements with the introduction of bigger turbines, a static physical model was developed based on the capacity of the floating structures to mitigate the external loads actions. To widen the framework of the work and to anticipate the following chapter as well, two types of external conditions were considered: a harsher one representative of classical oceanic or northern sea condition (where the majority of FOW projects will be located) and a softer one representative of Mediterranean conditions. Other parameters as depth, distance from shore and most of all floater typology - semi-submersibles or tension leg platforms - have been included in the CAPEX model and their impact have been widely analysed.

Finally, in the third and last chapter, the estimation of the LCOE and thus the appreciation of the viability of FOW projects has been the main objective. To reached it diverse sites, mainly in Italy, have been identified as potential interesting sites for FOW projects implementation based firstly on their resources in wind. The potential annual electricity potential of these sites was estimated and various important features as the vicinity to industrial ports and most of all the bathymetry of the selected zones have been studied and then inserted in our LCOE calculation model. Besides, a particular attention has been put on the visual impact on coastal landscape that FOW project may have and how this detrimental impact could drive the distance from shore and depth of a project, and by extension its CAPEX. Then, these considerations on site impact assessment have been confronted to the reality of the disclosed Italian floating projects currently in early planning stage. Then, a word on operation and maintenance has been said. To complete the LCOE calculation model, further losses and financial and construction related hypothesis have been discussed and interesting outputs have been then obtained and analysed. Many parameters could influence the LCOE that have been computed for various zones. To get an idea of the values obtained in output of our LCOE model in real terms, let's focus on an hypothetical project commissioned in 2035, a year at which the first Italian projects should start operate. Respecting the minimum criteria in terms of visual impact, the real LCOE of Italian would range between 80 and 120 USD/MWh in 2035. These values, still higher than the ones around 65 USD/MWh for exceptional sites as GDL or Scotwind typical ones, are however acceptable from a competitive point of view for Italy.

The driving problematic of this thesis was the potentialities of the floating offshore wind market in the Mediterranean. It end up that, eventough the bathymetry as well as the wind resources in the Mediterranean, and more specifically in Italy, are not always as well

suited to offshore wind as in the North sea for example, regarding the important depth of the Mediterranean FOW appears as the only solution for Mediterranean countries to unlock their offshore wind potentialities. Plus the combination of economies of scale expected generated by the introduction of bigger turbines, technological breakthroughs, supply chain optimisation and diminution of the risk related to FOW investments is set to enhance important LCOE drops making FOW competitive by the mid 2035's in the Mediterranean. This economic viability coupled to the excellent comparative features of offshore wind in terms of power density, land occupation and grid friendliness regarding other fatal renewables sources could make FOW plants strong assets for Mediterranean governments yearning for decarbonation of their energy mixes.

Alongside this work, many assumptions have been made to evaluate the CAPEX of FOW and then the LCOE of hypothetical projects. Eventough these hypothesis have always been supported by scientific sources and argumentative reasoning, when forecast are at stake absolute results must be analysed with caution. Instead, the trends, relative importance of various cost drivers and technological insights as for example the huge potential of TLPs for Mediterranean applications or the importance of visual impact in project design will be regarded as the main take away information from this thesis work. This thematic is wide and the ambition here have been to discuss every angle of an techno-economical assessment of FOW potentials. Yet, some issues had to be let out of the scope of the study or has not been deeply analysed. Indeed, the idea here was to remain global and to deliver general insights, but if a given FOW is under study, deeper and more precise considerations on the wind resource of the site, the platform technologies and dimensions (dynamical behaviour in particular would have to be further assess), external loads, supply chain and local content use as well as environmental impact would have to be performed. Plus, some aspects as the supporting policies from EU or countries (Feed in tariff, financial incentives etc...) or the potential revolution of offshore electrical grid composed of various hubs have not been integrated to the discourse. The results from this work are solid and the discourse has been led in a way to coherently and logically argument one part with another. The FOW is still a young but very promising market and many results of this study will be sharpened thanks to the industrial feedbacks to come.

Bibliography

[1] Mohammad Ebrahimpour. Numerical investigation of the savonius vertical axis wind turbine and evaluation of the effect of the overlap parameter in both horizontal and vertical directions on its performance. *Symmetry*, 2019.

[2] Imogen Brown. 35 mw wind turbines to lower material demand. *Bloomberg NEF for a2a s.p.a*, 2020.

[3] Paolo Silva. Politecnico di milano m2 course: Wind, hydro and geothermal power generation. *Politecnico di Milano, Energy department*, 2021.

[4] P Lynn. *Onshore and Offshore Wind Energy: An Introduction*. John Wiley & Sons, Ltd., 2011.

[5] Fatih Birol. Iea ofshore wind outlook 2019. *IEA: World Energy Outlook Special Report*, 2019.

[6] Jean-Michel Chelsea. The offshore wind auction boom. *Bloomberg NEF for a2a s.p.a*, 2021.

[7] Olivier Metcalfe. 1h 2022 offshore wind market outlook. *Bloomberg NEF for a2a s.p.a*, 2022.

[8] Crown estate Scotland. Crown estate scotland, 2023. URL `https://www.crownestatescotland.com/`.

[9] French ministry of ecologic transition. Parcs et projets éoliens en france, 2023. URL `https://www.eoliennesenmer.fr/parcs-et-projets-eoliens-en-france?f%5B0%5D=c%3A16`.

[10] CrownEstate. Japan & south korea floating offshore wind 2019. *iuk-ktn*, 2019.

[11] Provincia di Trento. valutazione d'impatto ambientale, 2023. URL `http://www.valutazioneambientale.provincia.tn.it/valutazioni_ambientali/VIA/-DCI/`.

[12] Study tips youtube channel. Morison equation - wave loads on structures - youtube videos, 2023. URL `https://www.youtube.com/watch?v=R3OgfZ21lGo&t=17s`.

[13] Emilio Farragiana. A review of numerical modelling and optimisation of the floating support structure for offshore wind turbines. *Springer*, 2022.

[14] Atul Agarwal. The assessment of extreme wave analysis methods applied to potential marine energy sites using numerical model data. *ResearchGate Renewable and Sustainable Energy Reviews*, 2013.

[15] Emre Uzunoglu. Hydrodynamic design of a free-float capable tension leg platform for a 10 mw wind turbine. *Elsevier*, 2019.

[16] A Ioannou. A preliminary parametric techno-economic study of offshore wind floater concepts. *Elsevier*, 2020.

[17] Sanjeet Sanghera. Tommorow's cost of floating wind. *Bloomberg NEF for a2a s.p.a*, 2021.

[18] Wei-Wua Huang. Water depth variation influence on the mooring line design for fowt within shallow water region. *MDPI*, 2021.

[19] Bridon-Bekaert company. Moorline polyester parallel laid, polyester sub-ropes encased in polyester jacket with an integrated particle filter system, 2022. URL `https://www.bridon-bekaert.com/en-gb/steel-and-synthetic-ropes/offshore-construction/mooring/anchoring-lines/moorline-polyester`.

[20] Maria Ikhennicheu. Review of the state of the art of dynamic cable system design. *Corewind reports*, 2020.

[21] Stiesdal. Tetra floating wind floater, 2023. URL `https://www.stiesdal.com/offshore/the-vital-role-of-floating-wind/`.

[22] Ocean Winds. Windfloat atlantic, 2023. URL `https://www.windfloat-atlantic.com/`.

[23] ORE Catapult. guide to an offshore wind farm, 2022. URL `guidetoanoffshorewindfarm.com`.

[24] Denmark technical institue. Global wind atlas, 2022. URL `https://globalwindatlas.info/fr`.

[25] Stefan Pfenninger. Renewable ninja, 2022. URL `https://www.renewables.ninja/`.

[26] Karin J. Van der Reijden. Beyond connecting the dots: A multi-scale, multi-resolution approach to marine habitat mapping. *Elsevier*, 2021.

[27] Minesterio Italiano dell'ambiante. Geoportale nazionale, 2023. URL `http://www.pcn.minambiente.it/viewer/`.

[28] Ren Zhengru. Offshore wind turbine operations and maintenance: A state-of-the-art review. *Elsevier*, 2021.

[29] DNV. State of the offshore wind industry, today through 2050. *State of Maine Governor's Energy Office*, 2021.

[30] COP 21. The paris agreement, 2015. URL `https://unfccc.int/process-and-meetings/the-paris-agreement/the-paris-agreement`.

[31] James Rhodri. Floating offshore wind: Market and technology review. *IEA: World Energy Outlook Special Report*, 2019.

[32] IEA. world energy data, 2022. URL `https://www.iea.org/world`.

[33] CFI : corporate finance institute. Levelized cost of energy (lcoe), 2022. URL `https://corporatefinanceinstitute.com/resources/valuation/levelized-cost-of-energy-lcoe/`.

[34] M Ragheb. Wind turbines theory - the betz equation and optimal rotor tip speed ratio. *IntechOpen*, 2017.

[35] Anne Schwenkenbecher. What is wrong with nimbys? renewable energy, landscape impacts and incommensurable values. *Environmental Values Published by White Horse Press*, 2017.

[36] oceanconference. Factsheet: People and oceans / united nation ocean conference. *The Ocean Conference*, 2017.

[37] T Wizelius. 2.13 design and implementation of a wind power project. *Elsevier Ltd*, 2012.

[38] NASA. Earth observatory / global ocean wind energy potential, 2008. URL `https://earthobservatory.nasa.gov/images/8916/global-ocean-wind-energy-potential`.

[39] RTE. Earth observatory / global ocean wind energy potential, 2022. URL `OptimiserlepilotagedurÃľseau`.

[40] encyclopeadie universalis. Éolien offshore, bref historique, 2022. URL https://www.universalis.fr/encyclopedie/eolien-offshore/1-bref-historique/.

[41] Market prospects. Offshore wind power will become the driving force for green energy development, 2023. URL https://www.market-prospects.com/articles/offshore-wind-power-will-become-the-driving-force-for-green-energy-development#:~:text=The%20development%20of%20offshore%20wind%20power%20began%20in,United%20Kingdom%20were%20the%20first%20countries%20to%20invest.

[42] 4cOffshore. Global offshore renewable map, 2022. URL https://map.4coffshore.com/offshorewind/.

[43] Walter Musial. Offshore wind market report: 2022 edition. *US department of energy, NREL*, 2022.

[44] Tyler Shetly. 2019 cost of wind energy review. *National Renewable Energy Laboratory*, 2019.

[45] Siemens Gamesa. Siemens gamesa offshore services, 2023. URL https://www.siemensgamesa.com/products-and-services/offshore.

[46] Vestas. Vestas offshore services, 2023. URL https://www.vestas.com/en/products/offshore.

[47] General electric. Ge offshore services, 2023. URL https://www.ge.com/renewableenergy/wind-energy/offshore-wind.

[48] Ivan Komusanac. Wind energy in europe in 2018. *Wind Europe*, 2019.

[49] Navingo Media Group. offshorewind.biz, 2023. URL https://www.offshorewind.biz/.

[50] US international trade administration. United kingdom offshore wind market intelligence, 2022. URL https://www.trade.gov/market-intelligence/united-kingdom-offshore-wind#:~:text=Offshore%20wind%20currently%20contributes%20about,installations%20in%20Europe%20that%20year.

[51] CrownEstate. scotwind-leasing-offer-document-april-2021. *Scotwind*, 2021.

[52] ecological transition french ministry. French offshore wind, 2022. URL https://www.ecologie.gouv.fr/parcs-eoliens-en-mer-mediterranee-gouvernement-annonce-selection-13-candidats-part

[53] TERNA. Connection requests to italian tso terna for offshore projects, 2023. URL https://www.terna.it/it/media/comunicati-stampa/dettaglio/soluzioni-connessione-nuovi-impianti-eolici-offshore#:~:text=Entro%20la%20fine%20del%202022,complessiva%20di%20circa%2095%20GW.

[54] ministero italiano della transizione energetica. Definizione contenuti sia (pniec-pnrr), 2023. URL https://va.mite.gov.it/it-IT/Procedure/ViaElenco/26/13?pagina=1.

[55] Lucas Bauer. wind turbines models database, 2023. URL https://fr.wind-turbine-models.com/.

[56] Leo Wang. 2h 2021 wind turbine price index. *Bloomberg NEF for a2a s.p.a*, 2021.

[57] Carmela Maienza. A life cycle cost model for floating offshore wind farms. *Department of Engineering, University of Campania*, 2020.

[58] Laura Causi. Iea world energy outlook 2022. *Scotish Governement*, 2015.

[59] Luke Eatough. Floating offshore wind technology and operations review. *SCatapult FOW latest reports*, 2021.

[60] PrinciplePower. The wind float adavantage, 2023. URL https://www.principlepower.com/windfloat/the-windfloat-advantage.

[61] BW Ideol. Damping pool, 2023. URL https://www.bw-ideol.com/fr/technologie.

[62] Equinor. Hywind scotland, 2023. URL https://www.equinor.com/energy/hywind-scotland.

[63] SBM offshore. Float4windtm, 2023. URL https://www.sbmoffshore.com/creating-value/new-energies.

[64] Franck Lemmer. Multibody modeling for concept-level floating offshore wind turbine design. *Springer*, 2018.

[65] Zhao Zhixin. Analysis of dynamic characteristics of an ultra-large semi-submersible floating wind turbine. *Journal of marine science and engineering*, 2018.

[66] Arany Lazlo. Simplified load estimation and sizing of suction anchors for spar buoy type floating offshore wind turbines. *Elsevier*, 2018.

[67] Martin O.L Hansen. Basic rotor aerodynamics applied to wind turbines. *Osti*, 1998.

[68] Tristan Revas. Numerical framework for aerodynamic characterization of wind turbine airfoils: Application to miniature wind turbine wire-01. *MPDI*, 2020.

[69] Giancarlo Bruschi. Drag coefficient of a cylinder. *MPDI*, 2003.

[70] Zeki Demirbilek. Water wave mechanics. *Marine meteorological center*, 2018.

[71] Alagan Chella Mayilvahanan. An overview of wave impact forces on offshore wind turbine substructures. *Elsevier*, 2012.

[72] Karim Raed. Uncertainty modelling of wave loads acting on semisubmersible floating support structure for offshore wind turbine. *Research Gate*, 2015.

[73] Brittanica. Archimedes' principle, 2022. URL `https://www.britannica.com/science/Archimedes-principle`.

[74] Erin Bachynski. Design considerations for tension leg platform wind turbines. *Elsevier*, 2012.

[75] JOHANNESSEN MARKUS. Concept study and design of floating offshore wind turbine support structure. *University of KTH*, 2018.

[76] Fernando Vigara. Floating offshore design basis. *Corewind outputs*, 2019.

[77] Arthur Erich Haas. *Introduction to Theoretical Physics volume I*. Van Nostrand, 1928.

[78] Shin Hyunkyoung. Model test of new floating offshore wind turbine platforms. *School of Naval Architecture and Ocean Engineering, University of Ulsan*, 2013.

[79] A Robertson. Definition of the semisubmersible floating system for phase ii of oc4. *National Renewable Energy Laboratory*, 2014.

[80] Arash E. Samani. The impact of pitch-to-stall and pitch-to-feather control on the structural loads and the pitch mechanism of a wind turbine. *MDPI*, 2020.

[81] George Johannes. Windfloat design for different turbine sizes. *Centre for Marine Technology and Ocean Engineering (CENTEC), Instituto Superior Tecnico, Universidade de Lisboa*, 2014.

[82] Michael Borg. Technical definition of the tetraspar demonstrator floating wind turbine foundation. *MDPI*, 2020.

[83] Eolink. Eolink cost-effective floating wind farms, 2023. URL `http://eolink.fr/fr/`.

[84] X1wind. Hexicon's patented twinwind, 2023. URL https://www.x1wind.com/.

[85] Hexicon. X1 wind, disruptive offshore wind, 2023. URL https://www.hexicongroup.com/twinwind/.

[86] Kai-tung Ma. *Mooring System Engineering for Offshore Structures*. Gulf Professional Publishing, 2019.

[87] Floatation Energy. Green volt offshore windfarm - offshore environmental impact assessment. *Offshore Environmental Impact Assessment*, 2021.

[88] Dynamica ropes. Floating offshore wind turbines (fowt) mooring systems, 2023. URL https://www.rivieramm.com/news-content-hub/news-content-hub/will-floating-wind-farms-be-the-saviour-of-the-ahts-market-61248.

[89] Amran Nur Aireen. A review on types of mooring material for deep water offshore structure. *Journal of Subsea and Offshore*, 2016.

[90] huyuanrope. Polyester mixed mooring rope for ship, 2022. URL https://www.huyuanrope.com/sale-7693749-64mm-x-220-mtr-white-12-strand-polypropylene-and-polyester-mixed-html.

[91] Gicon. Gicon-sof tlp concept, 2023. URL http://www.gicon-sof.de/en/sof1.html.

[92] Gazelle. Gazelle wind power, 2023. URL https://gazellewindpower.com/technology/#light.

[93] Saitec. Sath barge technology, 2023. URL https://saitec-offshore.com/en/sath/.

[94] N Barberis Negra. Loss evaluation of hvac and hvdc transmission solutions for large offshore wind farms. *Elsevier*, 2005.

[95] Joanna Bauer. The offshore wind farm array cable layout problem: a planar open vehicle routing problem. *Journal of the Operational Research Society Taylor & Francis*, 2015.

[96] Franck Adam. Design optimization of dynamic inter-array cable systems for floating offshore wind turbines. *Elsevier*, 2019.

[97] John Snyder. Will floating windfarms be the saviour of the ahts market? *Riviera*, 2020.

[98] L Moraes Jr. Comparison of long-term wind and photovoltaic power capacity factor datasets with open-license. *Elsevier*, 2018.

[99] Miguel Munoz Ortiz. Evaluation of open photovoltaic and wind production time series for norwegian locations. *Elsevier*, 2021.

[100] The Wind Power. Vestas > v164/9500, 2022. URL `https://www.thewindpower.net/turbine_en_1476_mhi-vestas-offshore_v164-9500.php`.

[101] GSE. Il punto sull'eolico. *Gestore Servizi energetici reports*, 2017.

[102] COMMISSION TO THE EUROPEAN PARLIAMENT. Report from the commission to the european parliament and the council on the implementation of the marine strategy framework directive (directive 2008/56/ec). *EUROPEAN COMMISSION*, 2020.

[103] Eiffage Metal. Sur le site de fos-sur-mer (13), les trois flotteurs du projet "provence grand large" prennent forme, 2022. URL `https://www.eiffagemetal.com/actualites/sur-le-site-de-fos-sur-mer-13-les-trois-flotteurs-du-projet-provence-grand-large-p`

[104] N Moskalenko. Study of wake effects for offshore wind farm planning. *Research Gate*, 2010.

[105] P Argyle. Offshore turbine wake power losses: Is turbine separation significant? *Elsevier*, 2017.

[106] Strategic CFO. Net present value method, 2023. URL `https://strategiccfo.com/articles/accounting/net-present-value-method/`.